

**The Pathophysiology of Renal Failure in a Shiga Toxin plus Lipopolysaccharide
Induced Murine Model of Hemolytic Uremic Syndrome**

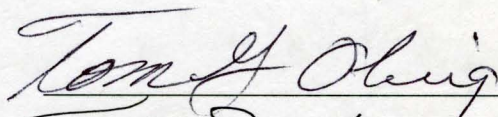
Mitchell Adam Psotka
Rockville, Maryland

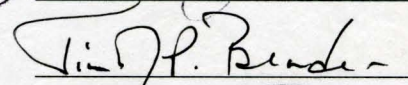
B.A., Biology, Brown University
M.S., Biological and Physical Sciences, University of Virginia

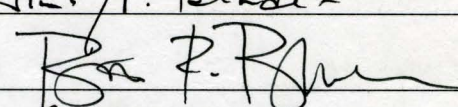
A Dissertation presented to the Graduate Faculty
of the University of Virginia in Candidacy for the Degree of
Doctor of Philosophy

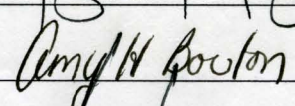
Department of Microbiology

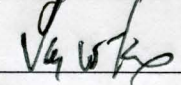
University of Virginia
August, 2008











Abstract

Hemolytic uremic syndrome (HUS) is the primary cause of worldwide pediatric acute renal failure. The vast majority of HUS is due to gastrointestinal infection with Shiga toxin producing *Escherichia coli* (STEC), bacteria that produce the ribosomal protein synthesis inhibitor Shiga toxin (Stx). During the diarrheal prodrome, virulence factors lipopolysaccharide (LPS) and Stx cross into the systemic circulation and cause inflammation and apoptosis in many tissues. The multi-organ pathology that results from toxemia consists of microvascular thrombosis and tissue ischemia with parenchymal destruction. The clinical syndrome of HUS typically comprises microangiopathic hemolytic anemia, thrombocytopenia, acute renal failure, a complex inflammatory response, and neurologic dysfunction. The prognosis is variable; however death or significant lasting renal impairment occurs in up to half of cases. Current treatment consists only of supportive care with intravenous fluids and dialysis, and therapeutic advances have been unforthcoming.

Due to the infrequent and sporadic nature of HUS, clinical and therapeutic advancement require an appropriate model system that will allow the underlying mechanisms of this disease to be elucidated. Thus far, only expensive and cumbersome large animal models mimic the human disease, and small animal models of HUS are either incomplete or inadequate. This work fully describes the renal failure that occurs in the mouse model of Shiga toxin mediated HUS. Intraperitoneal injection of Shiga toxin 2 (Stx2) plus LPS into mice causes systemic toxemia and results in death over 96 hours. Acute renal failure, thrombocytopenia, inflammation and neurologic dysfunction develop

as well. Nevertheless, although many of the findings correspond with human disease, the etiology of Shiga toxin induced renal failure in the mouse is distinct from that in humans. Human renal glomerular and tubular cell types are rich in Gb₃, while the mouse only produces Gb₃ in renal tubular cells. For this reason, Stx causes only tubular dysfunction in the mouse, and the renal failure is not due to microvascular thrombosis. Therefore, although the mouse model provides a means to evaluate therapeutics that block Shiga toxin mediated cellular toxicity, it does not appropriately recapitulate human HUS.

Acknowledgements

Thank you to my nurturing family and my gracious friends who have shown me tremendous support throughout this long and grueling process. They have been instrumental in my success. Without their mental fortitude, emotional brawn, and generosity this work would not have been accomplished. Thank you also to my mentor Tom O'Brig and the members of my committee, Amy Bouton, Tim Bender, Brett Blackman, and Jay Fox, for hope and optimism in the face of failure and frustration, and of course for granting me this honor. I received tremendous scientific help from Tiffany Keepers, Fumiko Obata, Glynis Kolling, Lisa Gross, Matthew Stone and Matt Lindner, and I am indebted to their efforts on my behalf. I also received expert technical advice and generous assistance from Sanford Feldman, Yongde Bao, Nikki Hastings, Kailo Schlegel, Marek Marcinkiewicz, Ken Tung, Michael Rouse, Amandeep Bajwa, Alaa Awad, Mark Hoofnagle and James Thomas.

Table of Contents

Title Page.....	i
Abstract.....	ii
Acknowledgements.....	iv
Table of Contents.....	v
List of Figures.....	viii
List of Tables.....	xi
Abbreviations.....	xii
Chapter 1: Introduction.....	1
Renal Physiology and Acute Renal Failure.....	1
Shiga Toxin and Shiga Toxin Producing <i>Escherichia coli</i>	12
Evaluation of the Hemolytic Uremic Syndrome Literature.....	24
Clinical Aspects of the Hemolytic of Uremic Syndrome.....	26
Vascular Endothelial Physiology.....	44
Theories Regarding Hemolytic Uremic Syndrome Pathophysiology.....	48
Inflammation in the Hemolytic Uremic Syndrome.....	51
Coagulation in the Hemolytic Uremic Syndrome.....	62
Consensus Pathophysiology of the Hemolytic Uremic Syndrome.....	80
Treatment for the Hemolytic Uremic Syndrome.....	95
Animal Models of the Hemolytic Uremic Syndrome.....	102
Goals of the Current Research.....	121

Chapter 2: A Murine Model of HUS: Shiga Toxin with Lipopolysaccharide Mimics the Renal Damage and Physiologic Response of Human Disease	122
Abstract.....	122
Introduction.....	123
Methods	124
Results.....	128
Discussion.....	161
Supplemental Data.....	165
Chapter 3: Shiga Toxin 2 Induced Collecting Duct Apoptosis Causes Renal Failure in the Murine Model of the Hemolytic Uremic Syndrome.....	173
Abstract.....	173
Introduction.....	173
Methods	175
Results.....	181
Discussion.....	208
Supplemental Data.....	214
Chapter 4: Conclusions and Perspectives	224
The Future of the Mouse Model of Hemolytic Uremic Syndrome.....	224
Ribotoxic Stress and Apoptosis	235
Shiga Toxin Targets: Vascular and Parenchymal Cells.....	238
A Current Model of Shiga Toxin Mediated Hemolytic Uremic Syndrome	245
Hemolytic Uremic Syndrome: Current Problems and Future Investigations	247
References.....	255

	vii
Appendix I: Direct Interactions of Platelets with Stx2 and LPS	329
Background.....	329
Methods	330
Results.....	332
Discussion.....	332
Appendix II: The Role of Cyr61 in Stx2 Mediated Cell Death	336
Background.....	336
Methods	338
Results.....	339
Discussion.....	347
Appendix III: The Role of p38 and JNK MAP Kinases in Stx2 Mediated Apoptosis ...	348
Background.....	348
Methods	348
Results.....	348
Appendix IV: The Therapeutic Role of p38 and JNK MAP Kinase Inhibitors SB203580 and SP600125 in the Mouse Model of HUS.....	354
Background.....	354
Methods	354
Results.....	355

List of Figures

Figure 1. Schematic of a typical nephron.	4
Figure 2. Ultrastructure of the glomerular filtration barrier.	6
Figure 3. Glycosyltransferases responsible for Gb ₃ metabolism.	20
Figure 4. Typical timeline of STEC infection and progression to HUS.	37
Figure 5. Light micrograph of schistocytes.	39
Figure 6. Light micrograph of glomerular thrombotic microangiopathy.	41
Figure 7. Electron micrograph of HUS associated endothelial damage.	43
Figure 8. Schematic of the intravascular coagulation cascade.	67
Figure 9. Electron micrographs of normal fibrin clots.	69
Figure 10. Light micrographs of renal cortical apoptosis from HUS patients.	87
Figure 11. Survival and weight loss of mice challenged with Stx2 plus LPS.	131
Figure 12. Serum creatinine and BUN of mice challenged with Stx2 plus LPS.	136
Figure 13. Peripheral blood cell changes in mice challenged with Stx2 plus LPS.	141
Figure 14. Peripheral and renal platelets in Stx2 plus LPS injected mice.	144
Figure 15. Fibrin and erythrocyte congestion in Stx2 plus LPS injected mice.	147
Figure 16. Glomerular electron micrographs from Stx2 plus LPS injected mice.	150
Figure 17. Venn diagram of mouse renal genes altered by Stx2 or LPS challenge.	153
Figure 18. Patterns of renal genes altered by Stx2 or LPS challenge in mice.	157
Figure 19. Human and murine glomerular cell SV40 and Gb ₃ <i>in vitro</i>	184
Figure 20. Western blots for p38 from human and murine glomerular cells.	190
Figure 21. Caspase 3 activity and apoptosis inhibition in human glomerular cells.	196
Figure 22. Immunohistochemistry of Gb ₃ in mouse kidney.	199

Figure 23. Immunofluorescence of Gb ₃ and aquaporin-2 in mouse kidney.	201
Figure 24. Renal apoptosis in Stx2 plus LPS challenged mice.	204
Figure 25. Timeline of renal dysfunction in Stx2 plus LPS challenged mice.	207
Figure 26. Caspase inhibition and renal dysfunction in Stx2 and LPS injected mice. ..	211
Figure 27. Electron micrographs of murine renal tubular damage.	217
Figure 28. Light micrograph of murine renal caspase 3 activation.	219
Figure 29. Immunofluorescence of Gb ₃ and aquaporin-1 in mouse kidney.	221
Figure 30. Human kidney Gb ₃ and Aquaporin-2.	223
Figure 31. Aggregometry of platelets incubated with LPS and ADP.	334
Figure 32. Aggregometry of platelets incubated with LPS and ADP without CD14.	335
Figure 33. Heatmap of murine renal transcripts altered by Stx2 injection.	341
Figure 34. RPTEC 24 hour Stx2 mediated cytotoxicity.	343
Figure 35. Cyr61 siRNA effect on Stx2 mediated RPTEC cytotoxicity.	344
Figure 36. Recombinant Cyr61 effect on Stx2 mediated RPTEC cytotoxicity.	345
Figure 37. Cyr61 overexpression effect on Stx2 mediated RPTEC cytotoxicity.	346
Figure 38. Effect of p38 inhibition on glomerular endothelial cytotoxicity.	350
Figure 39. Effect of JNK inhibition on glomerular endothelial cytotoxicity.	351
Figure 40. Effect of p38 inhibition on glomerular podocyte cytotoxicity.	352
Figure 41. Effect of JNK inhibition on glomerular podocyte cytotoxicity.	353
Figure 42. Effect of p38 inhibition on Stx2 plus LPS mouse lethality.	356
Figure 43. Effect of JNK inhibition on Stx2 plus LPS mouse lethality.	357
Figure 44. Effect of p38 and JNK inhibition on Stx2 plus LPS mouse lethality.	358

List of Tables

Table 1. Features of Stx induced small animal models of human HUS.	119
Table 2. Summary of pathological conditions induced by Stx2 plus LPS in mice.....	133
Table 3. Gene ontology clusters altered by Stx2 or LPS challenge in mice.....	160
Table 4. Murine renal genes altered by Stx2 or LPS challenge.....	165
Table 5. The 24 hour LD ₅₀ for human and murine cell types.....	187
Table 6. Extracellular signaling molecules altered by Stx2 or LPS <i>in vitro</i>	192
Table 7. Murine renal transcripts rapidly upregulated by Stx2 challenge.	342

Abbreviations

A/E	Attaching and Effacing
ACE	Angiotensin Converting Enzyme
ADP	Adenosine Diphosphate
AKI	Acute Kidney Injury
ARF	Acute Renal Failure
β -TG	β -Thromboglobulin
BUN	Blood Urea Nitrogen
CBC	Complete Blood Count
CCL2	C-C Chemokine Ligand 2 (MCP-1)
CCL4	C-C Chemokine Ligand 4 (MIP-1 β)
Cer	Ceramide
CD ₅₀	50% Cytotoxic Dose
CDH	Ceramide Dihexoside
CMH	Ceramide Monohexoside
CNS	Central Nervous System
CXCL1	C-X-C Chemokine Ligand 1 (Gro- α)
CXCL5	C-X-C Chemokine Ligand 5 (ENA-78)
D+HUS	Diarrhea associated Hemolytic Uremic Syndrome
DAF	Delay Accelerating Factor
DB	Dutch Belted (Rabbit)

dCHIP	DNA-Chip Analyzer
DIC	Disseminated Intravascular Coagulation
DNA	Deoxyribonucleic Acid
EHEC	Enterohemorrhagic <i>Escherichia coli</i>
ELISA	Enzyme Linked Immunosorbant Assay
ENA-78	Endothelial-derived Neutrophil Attractant-78
EPEC	Enteropathogenic <i>Escherichia coli</i>
ER	Endoplasmic Reticulum
FSGS	Focal Segmental Glomerulosclerosis
GADD	Growth Arrest and DNA Damage
Gal	Galactose
GalNAc	<i>N</i> -acetylgalactosamine
Gb ₃	Globotriaosylceramide
Gb ₄	Globotetraosylceramide
G-CSF	Granulocyte Colony-Stimulating Factor
Glc	Glucose
GM-CSF	Granulocyte-Macrophage Colony Stimulating Factor
Gro- α	Growth Related Oncogene- α
HeLa	Henrietta Lacks Cervical Carcinoma Cells
HGEC	Human Glomerular Endothelial Cells
HMEC	Human Microvascular Endothelial Cells
HUS	Hemolytic Uremic Syndrome

HuSAP	Human Serum Amyloid P
HUVEC	Human Umbilical Vein Endothelial Cells
IFN- α	Interferon- α
IFN- γ	Interferon- γ
IL-1 β	Interleukin 1 β
IL-1Ra	Interleukin 1 Receptor Antagonist
IL-2	Interleukin 2
IL-4	Interleukin 4
IL-6	Interleukin 6
IL-8	Interleukin 8
IL-10	Interleukin 10
i.p.	intraperitoneal
i.v.	intravenous
KO	Knock Out
LBP	Lipopolysaccharide Binding Protein
LD ₅₀	50% Lethal Dose
LEE	Locus of Enterocyte Effacement
LPS	Lipopolysaccharide
MAPK	Mitogen Activated Protein Kinase
MCP	Membrane Cofactor Protein
MCP-1	Monocyte Chemoattractant Protein 1
MIP-1 α	Macrophage Inflammatory Protein 1 α

MIP-1 β	Macrophage Inflammatory Protein 1 β
MMP-9	Matrix Metalloproteinase 9
mOsm	Milliosmole
MPGN	Mesangioproliferative Glomerulonephritis
mRNA	Messenger Ribonucleic Acid
MSB	Martius Yellow-Brilliant Crystal Scarlet-Aniline Blue
NO	Nitric Oxide
PAF	Platelet Activating Factor
PAI-1	Plasminogen Activator Inhibitor 1
PAS	Periodic Acid Schiff
PCM	Protein Calorie Malnutrition
PF ₄	Platelet Factor 4
PLIER	Probe Logarithmic Intensity Error
RANTES	Regulated upon Activation Normal cell Expressed and Secreted
RBC	Red Blood Cell
RPTEC	Renal Proximal Tubule Epithelial Cell
RNA	Ribonucleic Acid
rRNA	Ribosomal Ribonucleic Acid
SAM	Significance Analysis of Microarrays
SAPK	Stress-Activated Protein Kinase
SD	Standard Deviation
SLE	Systemic Lupus Erythematosus

SOM	Self Organizing Map
STEC	Shiga Toxin producing <i>Escherichia coli</i>
Stx	Shiga toxin
Stx1	Shiga toxin 1
Stx2	Shiga toxin 2
TAFI	Thrombin Activatable Fibrinolysis Inhibitor
TF	Tissue Factor
TFPI	Tissue Factor Pathway Inhibitor
TIMP-1	Tissue Inhibitor of Metalloproteinase 1
Tir	Translocated Intimin Receptor
TLR4	Toll-Like Receptor 4
TLR5	Toll-Like Receptor 5
TMA	Thrombotic Microangiopathy
TNF- α	Tumor Necrosis Factor α
tPA	Tissue Plasminogen Activator
TTP	Thrombotic Thrombocytopenic Purpura
uPA	Urokinase Plasminogen Activator
vWF	von-Willebrand Factor
VTEC	Verotoxigenic <i>Escherichia coli</i>
WBC	White Blood Cell

Chapter 1: Introduction

Renal Physiology and Acute Renal Failure

The kidney precisely regulates mammalian extracellular fluid volume, acid-base balance, waste disposal, and plasma osmolality¹. Constant fluid volume and salt content maintain blood pressure and tissue perfusion during normal physiological states. Changes in blood volume and plasma osmolality are sensed centrally by the hypothalamus and peripherally by the kidney itself. To sustain homeostasis, the kidney responds to extrinsic (hypothalamic) and intrinsic extracellular signaling initiated by these changes and alters the concentration of salt and water excreted¹. Excess bodily salt and water in addition to aqueous waste products are eliminated in urine.

The basic functional unit of the kidney is the nephron: a blood-filtering glomerulus followed by a tubular system that drains into the renal pelvis (Figure 1)². Each human kidney contains approximately one million nephrons, while each murine kidney contains about thirty thousand². The glomerulus is composed of three primary cell types, the vascular glomerular endothelium, the glomerular epithelial cells called podocytes, and the regulatory and structural mesangial cells. The subsequent tubular system is extensive and diverse, with four primary parts and numerous specific cell types that display unique function and protein expression. Vascular endothelial growth factor (VEGF) signaling from the podocytes to the glomerular endothelium is known to maintain the normal structure and function of the adjacent endothelial layer². The endothelial cells and podocytes create a mutual basement membrane matrix composed

primarily of collagen IV, and together this trilaminar structure forms the glomerular filtration barrier (Figure 2)².

The filtration barrier prevents circulating cells from entering the tubular system, and blocks the passage of many proteins larger than 60-70 kDa, though the extent of this latter inhibition is the subject of significant debate³⁻¹². The barrier is morphologically intricate (Figure 2), with highly fenestrated endothelial cells and podocytes that form specialized foot processes from which they derive their name². Blood plasma that passes through the filtration barrier enters the tubular system formed primarily of four sections: the proximal tubule (PT), the loop of Henle, the distal tubule (DT), and the collecting duct (CD). The glomerulus controls the glomerular filtration rate (GFR), a measure of the amount of plasma that enters the tubular system. Relative afferent and efferent arteriole vasodilation or constriction, total renal blood flow through the renal arteries, the pressure in the glomerular capillaries, and the relative glomerular versus tubular protein concentration predominantly determine the GFR. The tubular system is responsible for the modifying the filtered plasma and controlling the systemic water balance by regulating the excretion of free water¹¹. The tubules perform their function either by leaving the luminal fluid filtered by the glomerulus isotonic with plasma, or by concentrating it far beyond normal plasma osmolality of 300 mOsm/kg H₂O. A normal glomerular filtration rate for an adult human with two functioning kidneys is 120 mL/min.

3

Figure 1. Schematic of a typical nephron.

Schematic of the typical renal nephron in yellow (Adapted from: http://msjensen.cehd.umn.edu/Webanatomy/image_database/Urinary). The associated renal vasculature is colored red. Plasma is initially filtered by the glomerulus, and after modification in the tubular system, exits the terminal collecting duct as urine. Glomeruli are only present in the cortex, while the tubular system extends throughout the three morphologically distinct regions of the kidney: the cortex, medulla, and papilla.

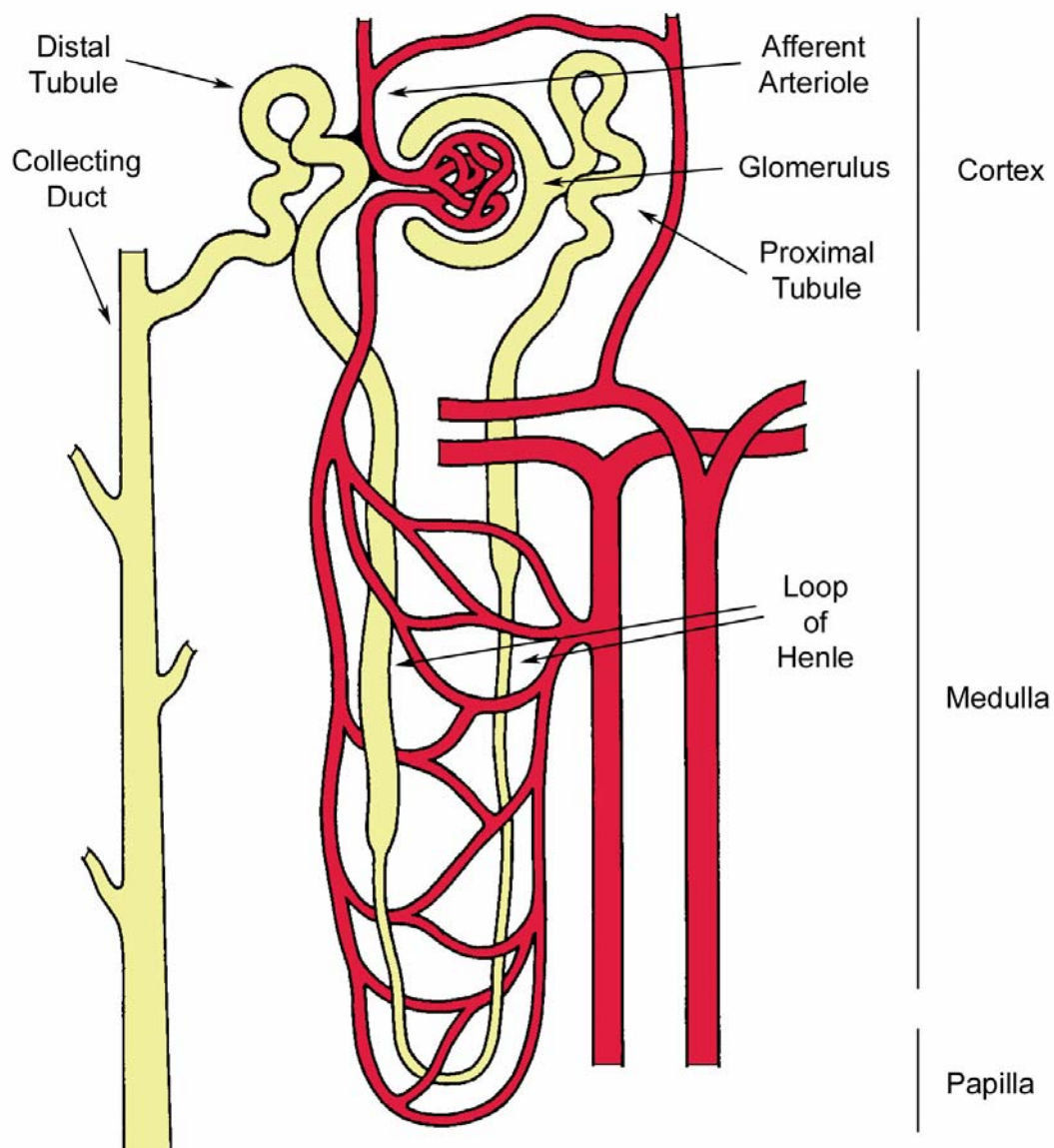


Figure 1. Schematic of a typical nephron.

Figure 2. Ultrastructure of the glomerular filtration barrier.

An electron micrograph demonstrates the normal ultrastructure of the glomerular filtration barrier (Taken from *The New England Journal of Medicine* 2008. **358**:1129-1136¹³). In this figure, the upper layer consists of podocyte foot processes with their connecting slit diaphragms, the middle is the glomerular basement membrane, and the bottom is the fenestrated glomerular endothelium. Podocytes produce VEGF while endothelial cells express both VEGF receptors. Arrowheads indicate endothelial fenestrations and the arrow indicates a slit diaphragm. The direction of plasma flow through the filtration barrier is shown to the right.

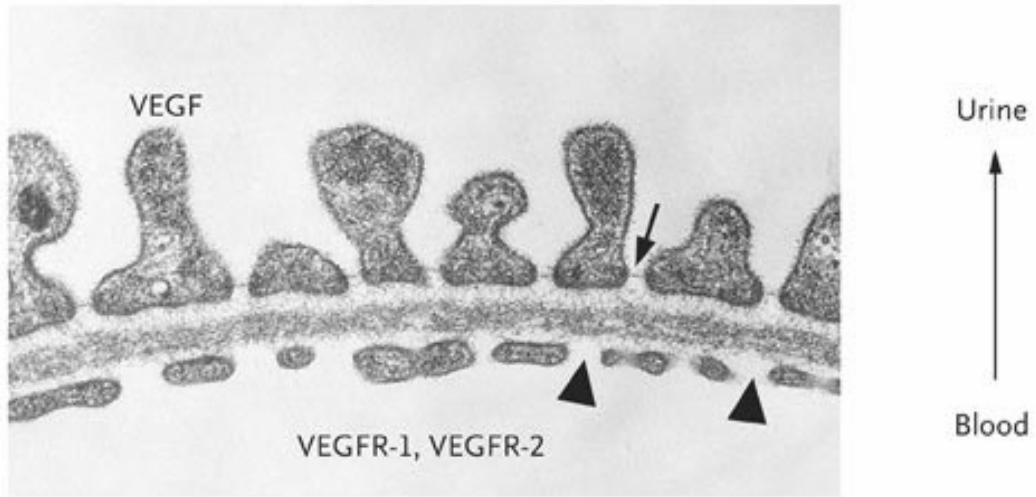


Figure 2. Ultrastructure of the glomerular filtration barrier.

Although the kidney receives and filters 20% of the total cardiac output, amounting to a glomerular filtrate volume equal to all bodily extracellular fluid every two hours, 99% of this filtrate is reabsorbed by the tubular system each day¹⁴⁻¹⁶. The majority of this reabsorption occurs through cell-type specific solute and water transporters¹⁷. For this reason, the renal tubules use approximately 10% of total body energy¹⁶. Of the total plasma filtered at the glomerulus, 60% is immediately reabsorbed by the proximal tubule¹⁸. Subsequently, salt transport into the medullary interstitium during fluid passage through the loop of Henle establishes an interstitial osmolality gradient, which can reach 1200 mOsm/kg H₂O at the tip of the loop in the papilla. However, upon completion of the loop of Henle, and passage through the salt-modifying thick ascending limb and distal tubule, where another 35% total solutes and water are reabsorbed, the luminal fluid is approximately isotonic with plasma¹⁸. Thus it is at the final tubular segment, the collecting duct, that the relative osmolality of urine is determined.

Hypothalamically-controlled pituitary-released arginine vasopressin (AVP) is the principal extracellular agent that controls urine concentration¹. In dehydrated states, AVP is released and binds to receptors on the collecting duct cells causing insertion of the water channel aquaporin-2 into the luminal membrane¹⁸. Using the medullary osmolality gradient established by the loop of Henle, the collecting duct then reabsorbs luminal free water and causes production of concentrated (yellow) urine. When well hydrated, no AVP is released from the hypothalamus so the collecting duct lacks luminal aquaporin-2, is impermeable to water, and thus produces low osmolality (clear) urine.

Acute disorders of kidney function manifest in a variety of ways, though the most prominent is an alteration in the volume of urine produced¹⁹. Increased urine output is

called polyuria, decreased output is oliguria, and complete lack of urine output is anuria. Oliguria can be defined as urine output of less than 0.5 mL/kg body weight per hour for 24 consecutive hours²⁰. Because 90% of nitrogenous waste is normally excreted by the kidney as urea, increased urea is found in the blood when production of urine is diminished¹¹. This serum urea is called blood urea nitrogen (BUN). Creatinine is also normally eliminated by the kidney and serum creatinine is used as another measure of renal function. Nevertheless, these values only measure renal waste elimination, and do not allow determination of the mechanism of the dysfunction. Specifically, renal failure can be caused by both intrinsic renal damage, and changes extrinsic to the kidney. The two primary extrinsic mechanisms of renal failure are decreased renal blood flow, called pre-renal failure, and decreased urine output due to post-tubular obstruction, called post-renal failure^{19,21}. Pre-renal failure is most often caused^{19,21} by conditions that decrease blood pressure, including dehydration, heart failure, and volume depletion, while post-renal failure can often be due to congenital malformations or insoluble deposits in the renal pelvis or ureter²¹. In contrast to oliguria induced by intrinsic renal injury, pre-renal decreased urine production is a normal and appropriate maintenance response to decreased circulating blood volume, and thus oliguria itself is only a sign of renal dysfunction in some contexts²².

Intrinsic renal damage generally comes in two forms as well: damage to the glomeruli or damage to tubules, though both aspects are injured in many disease states, and interstitial insult can occur as well²³. Diseases that demonstrate glomerular injury typically result in abnormal glomerular appearance by light or electron microscopy^{19,21,24}. Tubular damage is more commonly associated with inflammatory infiltrates and

sloughing of cells into the tubular lumen^{19,23}. Nonetheless, damage to any of the many parts of the nephron by a myriad of distinct mechanisms can disrupt the efficient production of urine and proper control of salt and water balance. Thus, in cases of demonstrated renal failure by measure of serum waste markers and urine output, all four steps: renal blood flow, glomerular filtration, tubular modification, and urine outflow, must be appropriately evaluated to distinguish the relevant mechanism²⁴. Furthermore, because low renal perfusion can cause prerenal failure, and some types of intrinsic renal injury can decrease blood volume and thus renal perfusion, the time course is important in determining the inciting event leading to renal failure, and renal hypoperfusion may coexist with most types of intrinsic renal injury²⁵.

Acute renal failure (ARF) also called azotemia or uremia can be due to myriad types of acute kidney injury (AKI), and is defined as an abrupt decline in kidney function over hours or days^{19,22}. Most ARF is at least partially reversible in that the kidney can recover lost function with only some residual defect²¹. For patients that lose all renal function, renal replacement therapy by mechanical and chemical removal of serum solutes and waste products also called dialysis, is the only option²¹. Overall up to 50% of patients with ARF die, though the mortality observed spans a wide spectrum, is dependent on the cause of ARF, and is lower in children²¹. In addition to increased serum creatinine and BUN, other laboratory results can help to distinguish the degree and cause of acute renal failure. Urinalysis involves the inspection of urine for color, salt content, volume, and molecules and cells not normally present²⁴. Concentrated urine is often yellow, while dilute urine is clear. Urine osmolality is a measure of the salt content of urine, and the concentrating or diluting capacity of the functioning nephrons. Protein

levels in urine are usually low, and increased proteinuria can be found in states of glomerular or tubular damage²⁴. Renal biopsy is considered to be the gold standard to diagnose the underlying cause of ARF, however because of the risk of bleeding, it is only performed in cases where the treatment would be significantly altered by the outcome of the biopsy^{24,26}. The lack of renal biopsy specimens in most cases of acute renal injury allows only indirect assessment of renal damage and pathogenesis by the previously described methods²⁶.

The two most common causes of adult ARF are pre-renal azotemia and intrinsic renal damage caused by ischemia or toxins, which make up 55% and 40% of all ARF, respectively²¹. 5% of ARF is due to post-renal obstruction. Pre-renal azotemia is usually rapidly corrected by restoration of renal perfusion, unless sufficient hypoperfusion occurred to cause intrinsic renal damage²⁵. Because it is correctable by extrinsic manipulation, pre-renal ARF does not truly represent renal injury, but rather an inability of the kidney to function given systemic failure²⁵. Severe sustained hypoperfusion can result in renal ischemia and tubular damage however, so the degree and duration of the perfusion defect is important^{23,25}. Urine output is decreased during pre-renal azotemia, however the urine osmolality remains high, the concentrating mechanism intact, most urine sodium is reabsorbed leading to fractional excretion of sodium less than 1%, and the urine does not contain significant debris^{21,23}. In cases of acute intrinsic renal damage, the changes in renal function are less rapidly reversible, with peak renal dysfunction after 3-5 days, and return to normal within 7-14 days given an isolated acute incident²¹. Overt tubular necrosis only occurs in some cases, and the most common finding is loss of individual cells from the tubular epithelium²¹. Findings during intrinsic renal damage

include vascular congestion, glomerular deformity, inflammatory cell infiltration, loss of tubular concentrating capacity, abnormally increased fractional excretion of sodium, and visible tubular regeneration²¹. Tubular regeneration is associated with a de-differentiation and repair response whereby undamaged tubular cells stop expressing specific proteins so they can undergo mitosis and repair the denuded epithelium²⁷⁻²⁹. Once they have multiplied, these cells then re-differentiate and produce normal cell-type specific molecules²⁷.

In contrast to adult ARF, pediatric ARF is most commonly associated with a specific disease, the hemolytic uremic syndrome (HUS) that follows gastrointestinal infection with Shiga toxin producing *Escherichia coli* (STEC)^{30,31}. This post-diarrheal HUS (D+HUS) consists of the clinical triad of hemolytic anemia, thrombocytopenia and acute renal failure, although additional findings described below are also typical. The renal insufficiency that occurs in HUS can be prolonged in some cases, causing months of hospitalization and acute care³². Nevertheless, even though HUS is classically thought of as a disease of young children, outbreaks of the disease have occurred in adult populations^{33,34}. Most significantly, cases of HUS in the elderly cause significant morbidity and mortality above that for the pediatric population^{31,33-38}. Finally, as treatment of the acute phase of HUS has improved and acute mortality has declined, the incidence of HUS mediated chronic renal disease has risen significantly, such that in some parts of the world it is a prominent cause of chronic renal failure^{39,40}.

Shiga Toxin and Shiga Toxin Producing *Escherichia coli*

Shiga toxin producing *E. coli* (STEC) cause gastrointestinal infection and illness in 75,000 people per year in the United States, and cause greater than 90% of worldwide pediatric hemolytic uremic syndrome^{35,36}. There are over 200 serotypes capable of Shiga toxin production, though only 50 have so far been associated with human disease^{41,42}. O157:H7 is the most common STEC serotype in North American, Japanese, and British patients, responsible for greater than 80% of STEC infections in the United States and Europe^{35,41-48}. Non-O157 subtypes such as O26, O111, O103, and O145 cause prominent disease in other countries, and additional bacterial types can undergo transient conversion to become Stx producers during STEC infection of the human gut^{34,35,41-49}. The O-antigen designates the specific subtype of lipopolysaccharide (LPS) produced, while the H-antigen marks the type of flagellum⁵⁰. HUS has an average yearly incidence of 2.65 cases per 100,000 children under age 5 in the United States, and in Buenos Aires, Argentina, the country with the highest burden of HUS in the world, the incidence is 21.7 cases per 100,000 children per year^{31,35,43}. Other countries with significant STEC disease burden, and thus where much valuable research has been performed, include South Africa and the Netherlands⁵¹. Overall, STEC induced HUS is most common in temperate climates during the summer months^{47,49,51}. Although large epidemic outbreaks have been the most publicized, most disease caused by STEC consist of sporadic infections^{31,41}.

Escherichia coli is a dominant member of the common human intestinal flora, usually involved in the mutually beneficial breakdown of food products, and harmlessly contained within the gastrointestinal tract^{41,42}. STEC pathogenic to humans normally transiently inhabit the intestinal tract of ruminants like cattle, sheep, goats, buffalo, and

deer, and human infection initiates from the spread of manure from cow pastures and improper bovine slaughter^{34,49,52,53}. In light of this, the high incidence of STEC infection in Argentina probably derives from pervasive cattle farming and beef consumption. Furthermore, increased summertime incidence of STEC infection correlates with increased bovine fecal STEC shedding during warmer weather⁴⁹. To cause disease these toxin-producing bacteria make their way into consumable items, either in the beef directly, or onto related products⁵⁴. A sample of farm animals revealed that in the United States, 3.6% of beef cattle, 3.4% of dairy cattle, 0.9% of chicken, 7.5% of turkey, and 8.9% of swine rectal farm samples tested positive for O157:H7⁵³. STEC is a worldwide pest and also infects cattle in Australia, Brazil, Norway, Italy, Germany, Spain, and France⁴⁹. Spread of the bacteria is augmented by the low infectious dose of less than 100 bacteria required for human colonization, and the national and global food supply chain that combines and then disperses food products^{41,42,55,56}. When food is repackaged and distributed, contamination is doled out as well^{41,42,55,56}.

In twenty years of outbreaks in the United States, 52% of cases were due to food contamination, 21% were unknown, 14% were from person to person transmission, and 9% were waterborne⁵². Between 1982 and 2002 in the United States, 41% of outbreak infections were associated with ground beef, 21% with produce, and 4% with milk products or other beef preparations⁵². Most prominent have been outbreaks of STEC mediated disease in ground beef from fast food restaurants, although numerous other items have transmitted infection including home-cooked beef, raw milk, gouda cheese, mayonnaise, lettuce, potatoes, salami, grapes, apple juice, apple cider, cantaloupe, alfalfa sprouts, radish sprouts, swimming pools, and spinach^{34,41,52,54,56-75}. Unpasteurized liquids

including milk and juice are especially prone to contamination, even when processed with the most modern equipment not involving pasteurization, and the organism can survive refrigerated for weeks in food products^{64,71,72}. A common mechanism of crop infection is fecal contamination due to water flow from cow pastures, as the organism can survive for months in water or feces^{34,49,54,76}. Furthermore, outbreaks demonstrate that STEC can survive the processes of fermentation and drying, and thus cooking is the only way to safely prepare infected food items⁴⁹. Although only responsible for a minority of cases, person to person transmission has been liable for outbreaks at day care facilities and institutions, as patients are known to shed STEC for 2-3 weeks following gastrointestinal infection^{38,63,77,78}. Furthermore, early during the course of illness children infected with STEC excrete 10^6 - 10^7 bacteria per gram of stool and have multiple bowel movements per day⁷⁹. Because proximity determines most risk for person to person spread, siblings of infected children have an especially large chance of contracting STEC⁸⁰. Asymptomatic STEC carriage can occur in humans, although the prevalence of this finding in the general population is unknown^{49,81-83}.

After oral ingestion, STEC intestinal and colonic colonization is supported by an array of bacterial virulence factors, though these *E. coli* do not produce either heat-labile or heat-stable enterotoxins made by some other intestinal *E. coli* pathogens^{82,84}. STEC form unique histopathological attaching and effacing (A/E) lesions that help maintain epithelial adherence, a trait presumably maintained as STEC evolved from enteropathogenic *E. coli* (EPEC)^{41,42,49,85}. These A/E lesions are characterized by localized intestinal epithelial effacement with loss of normal microvilli, and the formation of pedestals of polymerized actin on which sit the bacteria. The genes that encode the

bacterial products necessary for this host cell subversion are located on the locus of enterocyte effacement (LEE) pathogenicity island^{41,42,85}. The LEE encodes a type III secretion system that injects the attachment molecule Tir (translocated intimin receptor) into adjacent epithelial cells. STEC bind to Tir with their membrane protein Intimin to mediate adherence and A/E lesion formation^{41,42,85}. The presence of these adherence factors is associated with disease pathogenesis in animal models and epidemiologically with disease in infected humans^{42,85}. Nevertheless, A/E lesions have not been observed in biopsy specimens from human STEC patients, and LEE negative strains exist and cause HUS in humans, suggesting that the components of the LEE pathogenicity island are not the crucial virulence factors necessary for HUS development^{41,42,49}.

Shiga toxin (Stx) is considered to be the primary necessary virulence factor produced by STEC responsible for HUS in humans, though the bacterial membrane component lipopolysaccharide (LPS) may also play a role^{41,49,86,87}. In contrast to *Shigella* species that invade the intestinal mucosa, STEC do not normally invade or cause bacteremia, and thus significantly lower relative levels of LPS enter the bloodstream during STEC infection⁸⁸⁻⁹⁰. Stx is encoded by chromosomal DNA from an incorporated lysogenic bacteriophage in STEC, and the active protein was originally discovered as toxic to African Green Monkey Kidney cells called Vero cells^{41,42,49}. Hence, an alternative and equivalent term for Stx is verotoxin, and STEC can also be called Verotoxigenic *E. coli* (VTEC)^{41,42}. Of *E. coli* that produce Stx, those that produce the Shiga toxin 2 (Stx2) subtype are more prevalent in cases of human disease, and are especially connected to HUS and bloody diarrhea^{31,35,44,91-93}. Furthermore, Stx2 shows greater toxicity in animal model systems, with the dose required to kill 50% of the

animals in a group (LD₅₀) approximately 400 times smaller than Shiga toxin 1 (Stx1)^{94,95}. In the United Kingdom 92% of O157 and 80% of non-O157 STEC produce Stx2 alone or with Stx1⁴³. However, HUS patients frequently develop antibodies specifically against O157 LPS following infection, and produce increased levels of lipopolysaccharide binding protein (LBP), suggesting that it may be important as well^{47,50,87,96-101}. LPS is abundant in the outer membrane of gram negative bacteria like *E. coli*, and mediates cellular inflammation and endothelial apoptosis by binding to toll-like receptor 4 (TLR4) on the mammalian cell surface¹⁰²⁻¹⁰⁴. Currently, the relative roles and importance of each of the bacterial toxins Stx and LPS in mediating human HUS are incompletely characterized.

Shiga toxin is a 70 kDa subunit toxin composed of one active (A) subunit and five binding (B) subunits in a pentameric ring^{31,35,82,105}. Stx1 is completely identical to Shiga toxin from *Shigella dysenteriae* I that was first isolated in 1898, while Stx2 is only 56% identical though with similar functional activity^{41,90,106}. Other functional variants of Stx exist, but are relatively minor compared to Stx1 and Stx2 subtypes⁴⁴. In this report, Stx will be used to refer to both Stx1 and Stx2, though if necessary the toxins will be named specifically. The B subunits of Stx bind to the cell surface glycosphingolipid globotriaosylceramide (Gb₃) present on some types of mammalian cells^{31,107-109}. Upon binding, the holotoxin is endocytosed into the endosomal recycling pathway whereby it makes its way through the endoplasmic reticulum (ER) to the cytosol^{41,90,110,111}. The activated A subunit is an *N*-glycosidase that specifically depurinates the 28S rRNA and thereby inhibits nascent peptide elongation, ribosomal activity, and general protein synthesis^{35,82,112}. While Stx1 has a greater affinity for Gb₃ and cells that express it, Stx2

is more toxic *in vitro* than equivalent quantities of Stx1¹¹³. Protein synthesis inhibition by Stx1 and Stx2 causes the initiation of a ribotoxic stress response consisting of MAP kinase activation and inflammation, and initiates apoptosis in some cell types^{114,115}.

Synthesis of the glycosphingolipid Gb₃ is performed by a sequential series of catabolic and anabolic enzymes, though the endogenous role of the Gb₃ molecule remains uncharacterized. Other names for Gb₃ include the P^k antigen of the P blood group system, and CD77¹¹⁶. The base molecule for all of the glycosphingolipids is the sphingolipid ceramide, to which glycosyltransferases add sugars to create more complicated molecules¹¹⁶. Gb₃ is made by specifically adding one glucose and two galactose residues to ceramide in sequence, mediated by glucosylceramide synthase, lactosylceramide synthase, and Gb₃ synthase, respectively (Figure 3)¹¹⁶⁻¹¹⁸. Gb₃ can also be made by removing a sugar residue from the more complex glycosphingolipid globotetraosylceramide (Gb₄), a process catalyzed by β -hexosaminidase^{116,117}. Gb₄ is created by Gb₄ synthase from Gb₃ by adding an *N*-acetylgalactosamine residue. Degradation of Gb₃ to its constituent sugars and ceramide occurs by the action of α -galactosidase, β -galactosidase, and β -glucosidase, respectively¹¹⁷. However, the reasons certain cell types express Gb₃ and others do not, as well as the reasons for species specific patterns of expression are unknown¹¹⁶.

Of special note is the human lysosomal storage disorder called Fabry disease, an X-linked recessive genetic illness that eliminates the production of α -galactosidase (Figure 3)¹¹⁹⁻¹²¹. Lack of this enzyme allows the accumulation of excess glycosphingolipids in various tissues, the most prominent being the neutral glycolipid Gb₃. In humans, Gb₃ collects in the walls of the microvasculature, nerves, renal

glomerular and tubular cells, and cardiomyocytes, causing complex multi-organ system dysfunction¹²⁰. Clinically, the syndrome consists of chronic pain, gastrointestinal changes, dermal angiokeratomata, progressive renal impairment, cardiomyopathy and stroke¹²⁰. These manifestations of Gb₃ overproduction identify the gastrointestinal tract, nervous system, kidney, heart and skin as locations of human Gb₃ production, and thus targets of Stx. Specifically, the renal glomerular endothelial cells, mesangial cells, podocytes, tubular cells of the loop of Henle, and distal tubular cells accumulate Gb₃, and renal impairment can include deficient renal concentrating ability, proteinuria, glycosuria, and acidosis¹²¹. As well as can be ascertained, no person with Fabry disease has ever been reported to develop HUS, probably because they are both rare diseases, though presumably also because increased Stx receptor would dilute out the effectiveness of a normal Stx dose caused by STEC infection. Fabry disease is treated in patients by administration of recombinant α -galactosidase intravenously, which appropriately improves symptoms and Gb₃ levels¹²⁰. Fabry disease can be produced in mice by targeted genetic deletion of the α -galactosidase gene^{119,122}. Though these mice are clinically normal unlike their human counterparts, they do produce excess ceramidetrihexosides in multiple tissues including the liver and kidney^{119,122}.

19

Figure 3. Glycosyltransferases responsible for Gb3 metabolism.

The globoside metabolic pathway. Anabolic enzymes are on the left in blue, while catabolic enzymes are on the right in orange.

Cer = ceramide; Glc = glucose; Gal = galactose; GalNAc = N-acetylgalactosamine;

Gb3 = globotriaosylceramide; Gb4 = globotetraosylceramide.

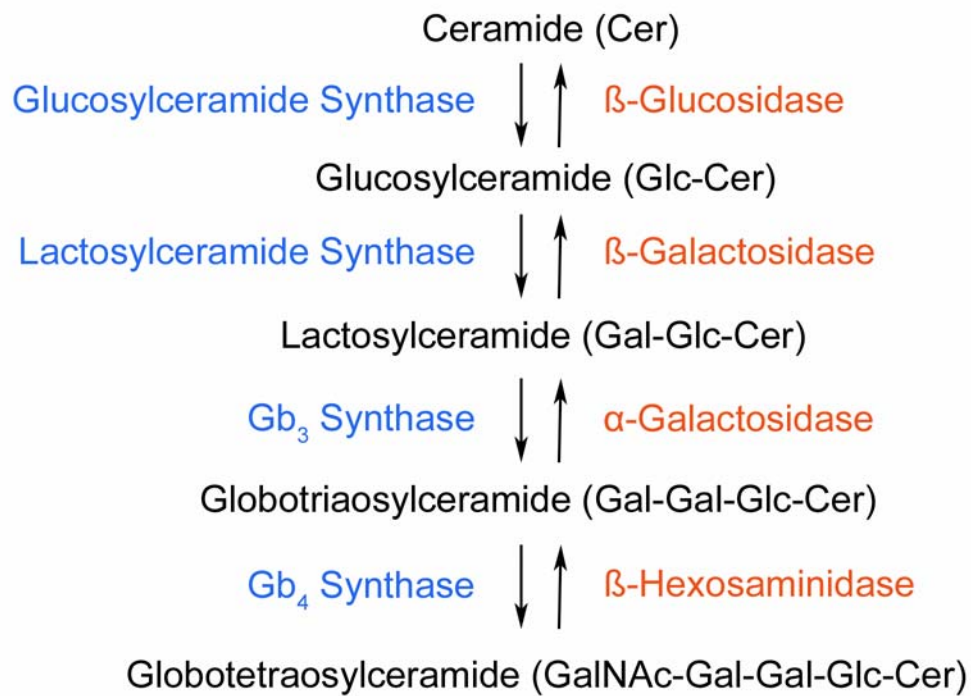


Figure 3. Glycosyltransferases responsible for Gb₃ metabolism.

The mechanism of Shiga toxin induced cellular dysfunction and death, though known to extend from ribosomal inhibition after Gb₃ mediated cell entry, is incompletely characterized^{114,123,124}. Although they vary in sensitivity, cells that abundantly express Gb₃ die after 24 hours when incubated with picomolar concentrations of Stx¹²⁵. These cells undergo apoptotic programmed cell death induced by Stx, in contrast to uncontrolled necrotic cell death in response to situations of ischemia or other toxic insult¹²⁶. While both processes end with non-viable cells, necrosis is a passive process characterized by cell swelling, rupture, and release of inflammatory contents into the surrounding tissue. On the contrary, apoptosis is an active process with morphological cell shrinkage, cytoplasmic and chromatin condensation, and membrane blebbing to form non-inflammatory apoptotic bodies that are ingested by nearby phagocytic cells¹¹⁴. Apoptosis can be initiated by either intrinsic cell damage or extrinsic extracellular signaling molecules, though the process typically channels through a cascade of cytoplasmic cysteine proteases called caspases¹²⁷. When upstream caspases 8 or 9 are activated by extrinsic or intrinsic cell damage signaling respectively, they cause the cleavage and activation of the downstream effector caspase 3¹¹⁴. Caspase 3 initiates the steps that take the cell through the final stages of programmed cell death, with DNA cleavage, chromatin condensation, and cytoplasmic blebbing^{114,128}.

Although programmed cell death is observed in a variety of cells in response to Stx challenge, portions of the signaling cascades responsible differ between cell types¹¹⁴. Studies in numerous cell lineages have demonstrated that Stx induced apoptosis progresses through caspase activation, and that inhibition of caspases often rescues cells from the lethal effects of Stx^{114,124,128,129}. Upstream of terminal caspase activation, the

mechanism of Stx apoptosis is usually dependent on Bcl-2 molecule regulation^{114,124}.

The Bcl-2 family consists of pro-apoptotic members Bid, Bax, Bak, and Bok, and anti-apoptotic members Bcl-2, Bcl-x_L, Bcl-w, and Mcl-1 that control the intrinsic apoptosis pathway localized around mitochondria¹²⁷. In response to pro-apoptotic signaling the ratio of these proteins swings, changing the normally equivalent pro and anti-apoptotic heterodimer population into pro-apoptotic multimers. This shift mediates mitochondrial changes and activation of caspases 9 and 3¹²⁷. A pentapeptide sequence of the Stx A-subunit is similar to Bcl-2, and can directly activate the pro-apoptotic Bcl-2 switch in human liver cells¹³⁰. Alternatively, Stx treatment of some cells increases Bax levels and overexpression of Bcl-2 can protect these cells from apoptosis^{128,129,131}. Bak activity is necessary for renal proximal tubule epithelial cell (RPTEC) apoptosis, while Bid activity is increased by Stx in human cervical carcinoma (HeLa) cell lines and in intestinal epithelial cells, and Stx decreases the expression of the anti-apoptotic proteins Mcl-1 and FLIP in human microvascular endothelial cells (HMEC)^{128,129,131-133}. However, Stx increases the expression of the growth arrest and DNA damage (GADD) family of molecules in colonic cells, which can contribute to apoptosis as well¹³⁴. Direct DNA depurination followed by a DNA repair response may also play a role in Stx mediated cell damage, as well as being a consequence of ribosomal stress mediated apoptosis induction¹³⁵⁻¹³⁷. Thus, although caspase activation is necessary for Stx mediated apoptosis, and Bcl-2 molecules are involved in many cell types, the upstream signaling events that lead to increased caspase activity are complex and cell type dependent.

While some cell types undergo non-inflammatory apoptosis in response to Shiga toxin, others release increased inflammatory mediators coincident with activation of

mitogen-activated protein kinase (MAPK) signaling. MAPKs phosphorylate serine and threonine residues on a host of cellular proteins in response to numerous stimuli. Often these signaling molecules function in cascades of kinases beginning with MAPK kinase kinases (MAPKKK) followed by MAPK kinases (MAPKK) and then leading to the MAPK itself. Activation of these kinase cascades is usually modulated by scaffolding proteins that bind multiple kinases into a signaling complex and give them specificity depending on the stimulus¹²⁷. There are three main families of MAPKs, the extracellular signal-regulated kinases (ERK), the stress-activated protein kinases (SAPK or JNK), and the p38 mitogen activated protein kinases. Once activated, these MAPKs can translocate into the nucleus and phosphorylate transcription factors directly to regulate gene expression. Traditionally, ERK signaling is implicated in cell survival, growth and proliferation, while JNK and p38 are associated with inflammatory and apoptotic signaling. However, in some cases, ERK has been shown to activate both JNK and p38 without inducing apoptosis¹²⁷.

The MAPK activation that occurs in response to Shiga toxin challenge derives from ribosomal inhibition and has been termed the ribotoxic stress response¹³⁸. Ribotoxic stress from Stx activates JNK and p38 by sequence specific rRNA damage to the 28S rRNA^{105,115,135,139-141}. Unlike genotoxic, osmotic or inflammatory stress, ribotoxic stress requires the presence of translationally activated ribosomes at the time of toxin insult, and these rapidly activate JNK and p38, usually within minutes^{105,138}. Challenge of the same cells with enzymatically inactive Stx fails to increase inflammatory signaling and protein release, indicating that active toxin is necessary for this response¹⁴⁰⁻¹⁴². These signaling pathways typically cause the *in vitro* release of the

inflammatory extracellular signaling molecules IL-6, IL-8, granulocyte-macrophage colony stimulating factor (GM-CSF), MCP-1, MIP-1 β and TNF- α ^{113,135,140-147}.

Paradoxically, these proteins are usually highly expressed and released in spite of strong protein synthesis inhibition mediated by Stx that decreases the production of other proteins^{113,142,146}. It is hypothesized that the overproduction of inflammatory mediator mRNA and ribotoxic stress mediated prolongation of mRNA lifespan allows this phenomenon to occur^{142,144,146,148}. Thus, increased inflammatory signaling as well as tissue damage caused by cellular apoptosis are the common effects of cellular Shiga toxin exposure.

Evaluation of the Hemolytic Uremic Syndrome Literature

A literature search for “hemolytic uremic syndrome” (HUS) or the Spanish “síndrome urémico hemolítico” (SHU) generates a list of almost 5000 published articles, however many of these refer to syndromes that are pathologically but not necessarily etiologically related to STEC derived HUS. Syndromes called the thrombotic microangiopathies (TMA) are associated with similar histopathologic lesions, and include post-diarrheal STEC induced HUS, familial genetic HUS, thrombotic thrombocytopenic purpura (TTP), systemic lupus erythematosus (SLE), and conditions resulting from non-STEC infection, renal transplantation, malignancy, and various medication usages¹⁴⁹. However, the etiology, prognosis, modern clinical presentation, and treatment for each of these diseases are distinct. Much of the problem in classification is historical, as post-diarrheal HUS was discussed interchangeably with TTP from the time when HUS was first described by

Conrad Gasser at the Zurich Kinderspital in 1951¹⁵⁰⁻¹⁵³. TTP had been previously characterized by Eli Moschcowitz in New York in 1924^{151,154}.

Not until March 1983 was it published that the constellation of findings termed post-diarrheal HUS was most likely due to infection with Shiga toxin producing *E. coli*, the single most important discovery in the field of HUS^{86,155,156}. Prior speculation had asserted that the responsible agent was most likely viral or multifactorial in nature, as numerous trials had been unsuccessful in finding a consistent bacterial agent^{32,157,158}. Subsequent purification and testing of Stx, further clinical trials on an outbreak from contaminated beef patties in Oregon and Michigan in 1982, and careful pathological characterization solidified the role of STEC in mediating the typical post-diarrheal form of HUS^{84,151,153,159,160}. However, many clinical investigations into the etiology of HUS were performed prior to the recognition that D+HUS was a specific syndrome distinct from TTP, familial HUS, and others, and often patients with TTP, post-diarrheal HUS, familial HUS, and other thrombotic microangiopathies were grouped together in clinical studies. For these reasons, evaluations of HUS pathophysiology based on findings that were not made with pure D+HUS patient populations are therefore considered flawed.

Only recently have the various thrombotic microangiopathies been separated as distinct disease forms in the literature, though in some cases TTP and HUS are still aberrantly discussed synonymously^{153,161}. They are not identical and constitute distinct syndromes that can be etiologically, pathologically, and epidemiologically identified and separated, in spite of a small body of literature that seeks to unify them mechanistically^{153,161-165}. Furthermore, the term HUS represents a category of diseases, and the disorder of post-diarrheal HUS caused by Shiga toxin producing *Escherichia coli*

is distinguished from other rare types of HUS by numerous criteria^{153,161}. Contained in this report are clinical and scientific studies that appropriately test for and properly acknowledge the role of Shiga toxin producing *E. coli* in the pathogenesis of D+HUS, or older papers that by virtue of their study of renal failure, inflammation, coagulation abnormalities, or acknowledgement of details that necessarily distinguish their cases as being due to STEC infection, still offer valuable scientific insight into the pathogenesis of D+HUS. For instance, because *Shigella dysenteriae* type I has not been isolated for decades from Argentinian patients, diarrhea associated HUS in Argentinian children can be reliably attributed to STEC even without specific serologic testing¹⁶⁶. In this document, D+HUS, STEC mediated HUS, Stx induced HUS, and HUS will be used interchangeably to refer to HUS resulting from gastrointestinal infection with Shiga toxin producing *E. coli*. Atypical familial genetic HUS, TTP and other thrombotic microangiopathies not due to STEC will be specifically acknowledged as such at each reference.

Clinical Aspects of the Hemolytic of Uremic Syndrome

The clinical diagnostic triad of HUS includes hemolytic anemia with a hematocrit (percent packed erythrocyte volume in blood) of less than 30, acute renal failure assessed by abnormally increased serum creatinine and BUN, and thrombocytopenia with a platelet count less than 150,000 per μL of blood^{31,35,167}. The classic post-diarrheal HUS (D+HUS) prodrome begins with watery diarrhea that becomes bloody and painful in 95% of cases after a few days, though HUS can rarely occur without any diarrhea (Figure 4)^{31,32,36,43,60,152,158,168-174}. Diarrhea is associated with cramping abdominal pain, a

distended and tender abdomen, increased stool number with greater than 6 each day, and vomiting^{158,173}. The hemorrhagic colitis is what propels many patients to present to the hospital, where their stool is cultured for STEC or tested for Stx production^{45-47,175}. Over the following 7 days most people clear the STEC intestinal infection and the colitis resolves, though the gastrointestinal bleeding may be profuse^{31,171,175,176}. Bacteria are usually not found in the bloodstream, demonstrating that this disease is not a sepsis³¹. It is after diarrheal resolution that the 15% minority of patients develop HUS and the other 85% resolve without any other complications³¹.

Although various clinical and pathological findings can be correlated with HUS development following the prodromal hemorrhagic colitis, the factors that determine which people progress to HUS or clear the STEC infection without further disease are unknown. Those patients with hemorrhagic colitis and higher levels of leukocytosis at presentation, clinical dehydration, age less than 5 years, or age greater than 65 years are at greatest risk for subsequently developing complete HUS, though additional factors probably participate in this process^{31,33,36,177-180}. Of those who develop HUS the current acute mortality rate is less than 1%, though it may be significantly higher in the frail and immunocompromised elderly population^{31,34,39,41,172,180}. The acute HUS period is typically brief, with 95% of children recovering from most non-permanent damage within a matter of weeks¹⁸¹. Unfortunately, a historical decrease in acute mortality has increased chronic morbidity and 30-50% of people demonstrate lasting renal dysfunction or progress to end stage renal failure^{31,39,41,172,180}.

Those patients who develop the HUS clinical diagnostic triad of hemolytic anemia, thrombocytopenia, and renal failure elicit specific findings upon laboratory and

clinical examination. The hemolysis and thrombocytopenia usually precede the renal failure, last for 10-14 days following the diagnosis of HUS, and are not autoimmune mediated^{31,32,157,182,183}. From the decreased hematocrit these patients often appear pale, and the hemolysis can persist the longest during normal resolution of the syndrome^{31,152}. In addition to the decreased hematocrit, peripheral blood smears demonstrate the presence of fragmented red blood cells called schistocytes (Figure 5), and increased newly synthesized red blood cells called reticulocytes^{31,32,158,184,185}. Erythrocyte lysis releases free hemoglobin into the circulation, decreasing both the detectable red blood cell hemoglobin levels, and binding and diminishing the levels of the plasma hemoglobin scavenger haptoglobin¹⁵⁸. The platelet and erythrocyte consuming process may persist for the duration of the acute phase, as some children given blood and platelet transfusions maintain decreased hematocrits and thrombocytopenia¹⁵². The renal failure is oligoanuric, and the severity of the renal failure correlates with the long term morbidity and mortality of the patient^{31,39,186}. Neither the degrees of anemia nor thrombocytopenia correlate with the severity of acute renal failure in these patients, and can occur in the absence of any renal failure^{31,187-189}. Oliguria may be a sign of tubular as well as glomerular damage and often persists for up to one week^{20,190}. Urinalysis shows proteinuria and hematuria (blood in the urine) in almost all cases, and signs of both tubular and glomerular dysfunction^{36,152,158,190-193}. Diagnosis relies on both the described clinical signs and symptoms of HUS, and positive stool testing for STEC or Stx, which is definitively positive in 75% of cases¹⁶⁹.

Rare renal biopsies obtained from HUS patients, or pathologic specimens taken from autopsies, show glomerular vascular thrombosis with clots in both the afferent

arterioles and the glomerular capillaries (Figure 6) along with variable tubular damage^{31,32,37,151,152,194,195}. Tubular dilation, necrosis, and apoptosis is more typical from biopsies of patients with worse disease, though often hemorrhagic necrosis in the medulla is not associated with connected arteriolar thrombosis^{32,37,152,195}. Renal tubular epithelial damage includes tubular dilation, degeneration, and intraluminal cell sloughing^{37,195}. The vascular clots are rich in fibrin and red blood cells similar to those found in septic disseminated intravascular coagulation (DIC), however they are distinct from the platelet and von-Willebrand Factor rich clots found in thrombotic thrombocytopenic purpura (TTP)^{162,196}. Along with fibrin, platelets can often be detected in the thrombosed glomerular capillaries of D+HUS patients¹⁵¹. The pathologic lesion is called thrombotic microangiopathy (TMA), and glomerular TMA is the pathologic finding that most represents this disease state^{31,194}. Specifically, in D+HUS patients these clots typically form in the glomeruli and can extend into the afferent arteriole^{32,161,163,170,194,196}. In contrast, other types of TMA including TTP and atypical familial HUS demonstrate clots centered around the afferent glomerular arterioles and small arteries; these can extend into the glomeruli^{32,161,163,170,194,196}. Features observed in other types of thrombotic microangiopathy but not D+HUS also include mesangial hypercellularity, duplication or thickening of the basement membrane, mucoid intimal thickening of small arteries, and sclerosis of small arterioles^{161,193,194}.

Affected glomeruli in Stx mediated HUS are enlarged and demonstrate thickened capillary walls by light microscopy¹⁵¹. The glomerular capillaries often have a ‘double-contour’ appearance created by endothelial detachment from the glomerular basement membrane compared to the single contour appearance of the trilaminar glomerular

filtration barrier under normal conditions¹⁵¹. Typically the glomerular basement membrane itself appears normal^{151,194}. Endothelial cell swelling with increased intracytoplasmic organelles and detachment obstructs the capillary lumen in capillaries that are not thrombosed, and podocytes are often swollen with hyaline droplets (Figure 7)^{151,194}. Mesangial cells sometimes swell as well, though without proliferation or mesangiolysis, suggesting that the primary lesion concerns the filtration barrier¹⁵¹. The space between the detached endothelial cells and the basement membrane may be filled with pale 'fluffy' material considered to be cellular debris (Figure 7)^{151,194}. Immunofluorescence microscopy supports the morphological conclusion of fibrin deposition in these capillaries and arterioles, and deposition of other plasma factors including immune complexes, IgM, or complement protein C3 are rare^{32,151,194}. Overall, the vascular lesions do not resemble vasculitic diseases, and pathologically define themselves as a unique form of vascular injury typical only for the thrombotic microangiopathies, and by glomerular placement specific for D+HUS^{152,194}.

Stx induced HUS is associated with multiple findings in addition to the clinical diagnostic triad, as extrarenal abnormalities affecting multiple organ systems are exceedingly common in these patients^{62,173,180}. Fever is found during the diarrheal prodrome, however it is rare upon the initiation of fulminant HUS or during the renal failure^{31,32,36,60,84,158,197}. Metabolic disturbances including increased serum potassium concentration (hyperkalemia), increased serum glucose (hyperglycemia), decreased serum sodium (hyponatremia), increased serum phosphate (hyperphosphatemia), decreased serum calcium (hypocalcemia), and metabolic acidosis manifested by decreased serum bicarbonate, occur in the acute phase of HUS as well^{32,176,186,190,198}.

Because of decreased renal function, arterial hypertension with increased diastolic blood pressure and edema with pleural effusion from volume overload may also result during anuria^{38,152,157,158,176,186,199}. Peripheral white blood cell counts are usually increased (leukocytosis), often consisting of high numbers of neutrophils (neutrophilia), and the degree of elevation correlates with the development and severity of HUS in some studies^{31,36,178-180}. However, the metabolic, anemic and hypertensive disturbances do not correlate well with disease outcome or prognosis, probably because they are treatable with supportive measures and are not reflective of the extent of the underlying pathology³².

In general, the presence of extrarenal abnormalities correlates with more severe disease and higher mortality, and these include peritonitis, dermal petechiae, skin necrosis, rectal prolapse, pancreatic TMA, and damage to the lungs and heart^{152,158,170,180,186,197,200,201}. Microvascular thrombosis is observed in these numerous other organ systems, specifically in the cerebral vasculature, intestines, colon, skin, pancreatic insulin-producing islets of Langerhans, spleen, myocardium, adrenal glands, thyroid gland, thymus, liver, and lungs^{32,152,162,170,171,173,180,194,198,201,202}. In order of symptomatic appearance, the extrarenal organs most affected are the colon, central nervous system (CNS), heart and pancreas¹⁷¹. The colon is the primary site of TMA in the human gastrointestinal tract, with close to 100% of patients demonstrating colitis and denuded friable mucosa often covered by a pseudomembrane on examination; less than 10% present with small intestine damage¹⁷³. Cardiac injury may manifest as increased serum concentrations of troponin I, and occurs in 10% of patients^{31,173,203}. Clinical presentations of the cardiac and systemic abnormalities can present as myocarditis,

cardiomyopathy, or congestive heart failure¹⁹⁰. Pancreatic injury causes diabetes onset with hyperglycemia in 5-10% of patients during the acute phase, or afterwards during the recovery period. Some of these children remain permanently diabetic and require lifelong insulin^{173,190,198,204,205}. Although lung and liver damage, manifested respectively by pulmonary thrombi with edema and hepatomegaly with elevated transaminases, are common they rarely cause severe dysfunction and are not associated with organ failure^{83,173}.

Central nervous system (CNS) disorders are frequent, with 15-30% of patients demonstrating some degree of significant neurologic dysfunction, often lethargy, seizures, coma, convulsions, or blindness^{32,43,47,59,171,173,176,180,197,200,206,207}. Minor neurologic symptoms consist of irritability, tremor, somnolence, and disorientation, while the major CNS disorders include convulsions, coma, and paralysis^{32,207}. Minor CNS manifestations are extremely common and present in up to 90% of cases, though they may be due to uremic waste accumulation as well as direct CNS damage and toxicity^{32,171}. Severe CNS complications most highly associate with mortality in HUS patients even though CNS examinations at autopsy only reveal edema and microscopic hemorrhages consistent with ischemia in most cases^{32,35,152,173,180,207,208}. However, some studies have demonstrated pervasive cerebrovascular changes in severely affected patients, with major intracranial hemorrhages, subdural hematomas, and hemorrhagic infarctions of the cerebrum, suggesting that CNS damage can be pathologically brutal^{171,180,209}.

Mortality during the acute stage of HUS best correlates with the presence of oligoanuria, dehydration, leukocytosis, increased (though still decreased) hematocrit, and

major CNS dysfunction such as seizures¹⁸⁰. Although many patients used to die of complications of renal failure, central nervous system involvement is the current most common cause of death in these patients, responsible for approximately 60% of mortality, with fewer fatalities due to heart failure, pulmonary hemorrhage, or hyperkalemia¹⁸⁰. Severe renal failure and inflammation have been long associated with worse prognosis in this disease, however increased lethality coinciding with dehydration and slightly raised hematocrits are a recent discovery^{180,210}. The reason for the association with increased hematocrit could be that in those destined to die there is complete as opposed to partial vascular thrombosis, such that less erythrocyte shearing occurs and the hematocrit remains higher, or the higher hematocrit may reflect greater degrees of dehydration and consequently higher circulating toxin concentrations¹⁸⁰.

Of those that survive the acute phase of HUS, lasting kidney damage occurs in 30-50%, with renal dysfunction manifested by persistently decreased glomerular filtration rate being the most prominent finding^{32,40,169,200,206,208,211-220}. In contrast, patients with STEC colitis without renal symptoms do not develop any long term dysfunction²²¹. Recurrence of D+HUS is very uncommon, though some children never recover normal renal function and can progress to end stage renal disease even after apparent complete recovery from the acute phase^{32,39,170,206}. These children demonstrate unremitting proteinuria and sometimes hypertension, signs of continuing glomerular and tubular dysfunction, and decreased urine concentrating capacity^{39,40,200,206,213,215-217,219,220,222,223}. Persistent oligoanuria and worse proteinuria during the acute phase of HUS correlates with worse long term prognosis, as do severe gastrointestinal complications like gangrene or rectal prolapse, severe neurological symptoms like coma, and initially high neutrophil

levels^{157,170,215-217,220,222-224}. Even so, up to 36% of children without any oliguria present with sequelae after the resolution of the acute phase, demonstrating the loss of urine production is unnecessary for irreparable renal damage²²⁰. A persistent decrease in GFR as well as urine concentrating defects over long-term follow-up are signs of loss of normal functioning glomeruli, findings that normally occur with increasing age but can be accelerated by the acute renal insult of HUS^{32,39,219,223}.

The rapid loss of functional glomeruli during the acute disease causes surviving patients to be at greater risk for future renal failure, and at abnormally younger ages, because of lack of substantial renal functional reserve^{32,211,217,219,222,224}. Biopsies taken within two months following the acute period of HUS demonstrate focal glomerular damage with segmental glomerular necrosis, hyaline thrombi, and cellular crescents^{39,152}. These biopsies do not show characteristic features of TMA, rather they demonstrate various types of glomerulosclerosis (dysfunctional scarring of the glomerular capillaries)^{39,193}. Biopsies taken 6-30 months following the acute HUS incident show obliteration of isolated glomeruli, up to 30% in severe cases, though rare interstitial changes are also evident^{39,152}. Disintegrating scarred glomeruli do not repair and represent lost functional reserve capacity²¹⁶. Those patients with greater than 50% of glomeruli pathologically involved demonstrate worse prognosis²¹⁶. Tubular sections demonstrate injury at these time points, however increased tubular pathology correlates most with increased glomerular scarring indicating that lack of glomerular repair causes new onset ongoing tubular damage¹⁵². There is no evidence of lasting fibrin deposition or ongoing vascular damage similar to that which occurs during the acute phase of the

syndrome, and no biopsies demonstrate autoimmune injury with complement or antibody deposition^{39,152}.

Damage during the acute stage of HUS can thus cause long term morbidity in the kidney, as well as other organs including the brain and pancreas, which may lead to the development of diabetes mellitus^{171,200}. Although rare overall, because the TMA of the pancreas is frequently restricted to the islets of Langerhans, pancreatic damage results in glucose intolerance and permanent insulin dependent diabetes in 3% of cases^{171,225}. Central nervous system dysfunction may persist long past the acute phase, with visual and intellectual disturbances²⁰⁹. Severe renal damage can evolve into other typical forms of renal glomerular abnormalities including focal segmental glomerulosclerosis (FSGS), or less commonly diffuse mesangioproliferative glomerulonephritis (MPGN) or diffuse glomerulosclerosis^{39,170,222}. Glomerular injury is progressive after the acute stage due to renal glomerular hyperfiltration injury^{211,215,217,224}. Loss of some functional glomeruli causes increased blood flow to the remaining glomeruli, hyperperfusing them and damaging them from hyperfiltration, leading to visible enlargement^{39,216,217,222}. The glomerulosclerosis blocks plasma filtrate flow into the tubular system and causes resultant tubular atrophy and interstitial scarring^{39,216,217,222}. In some patients, the glomerulosclerosis causes chronic renal failure with glomerulonephritis and hypertension because not enough viable glomeruli remain to provide adequate renal function^{39,219}.

36

Figure 4. Typical timeline of STEC infection and progression to HUS.

Progression of *E. coli* O157:H7 infection through the diarrheal prodrome to HUS.

(Taken from *The Lancet* 2005. **365**:1073-1086.³¹) Numbers refer to time in days.

Percents refer to percent of cases positive for the indicated condition.

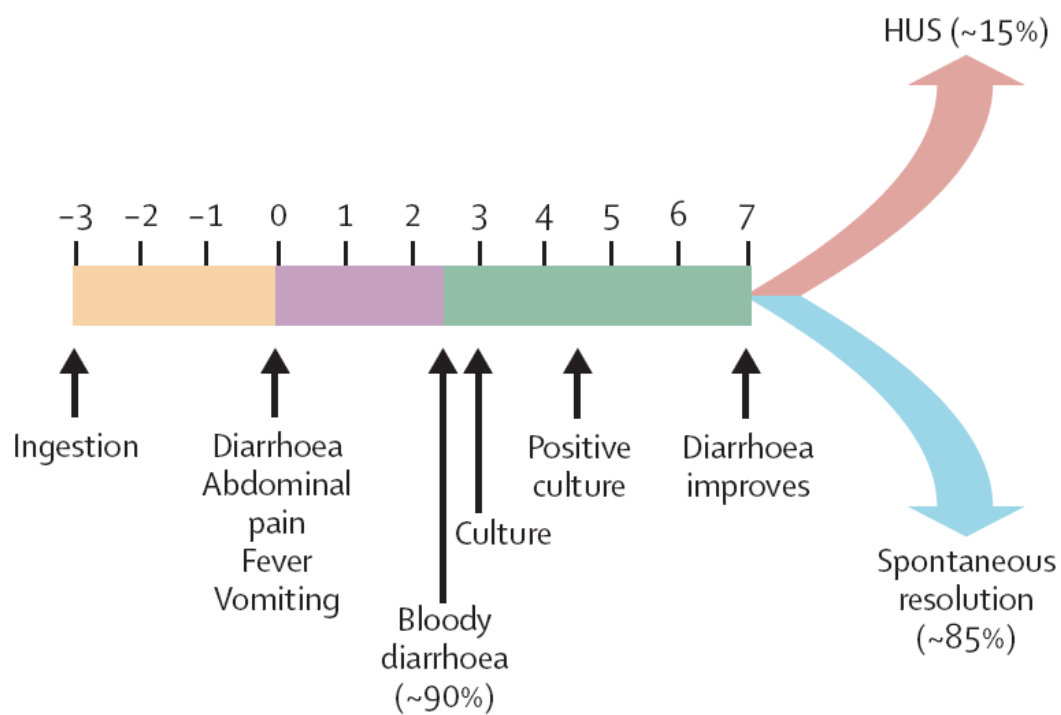


Figure 4. Typical timeline of STEC infection and progression to HUS.

38

Figure 5. Light micrograph of schistocytes.

Schistocytes on a human peripheral blood smear. (Taken from *Am Fam Physician* 2004.

69:2599-606.¹⁸⁴) Schistocytes indicated by arrows are fragmented red blood cells that appear much smaller and abnormal compared to normal round red blood cells.

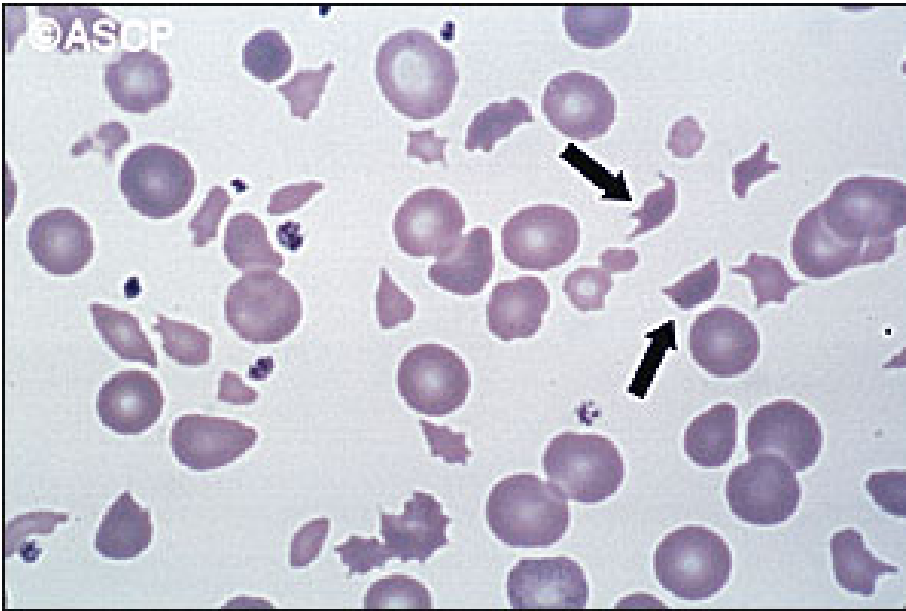


Figure 5. Light micrograph of schistocytes.

40

Figure 6. Light micrograph of glomerular thrombotic microangiopathy.

The typical glomerular pathologic lesion of HUS: a fibrin-rich thrombus (arrow) in a glomerular arteriole from a child who died of HUS. (Taken from *The Lancet* 2005.

365:1073-1086.³¹)

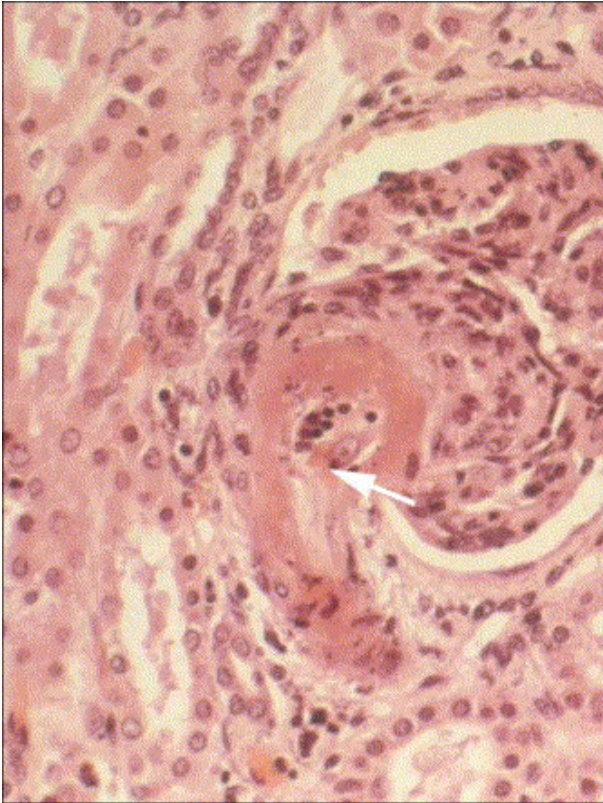


Figure 6. Light micrograph of glomerular thrombotic microangiopathy.

Figure 7. Electron micrograph of HUS associated endothelial damage.

Electron micrograph of typical HUS associated endothelial detachment from the basement membrane with subendothelial amorphous material in a renal glomerular capillary. (Taken from *Am J Pathol.* 1969 **57**: 627–647.¹⁹³) The subendothelial space is widened and the capillary lumen is almost completely filled with the detached endothelial cell. The glomerular podocyte foot processes are abnormal and fused. E = glomerular endothelial cell (E labels the nucleus); L = capillary lumen; M = mesangial cell (M labels the nucleus). Magnification at 6075x.

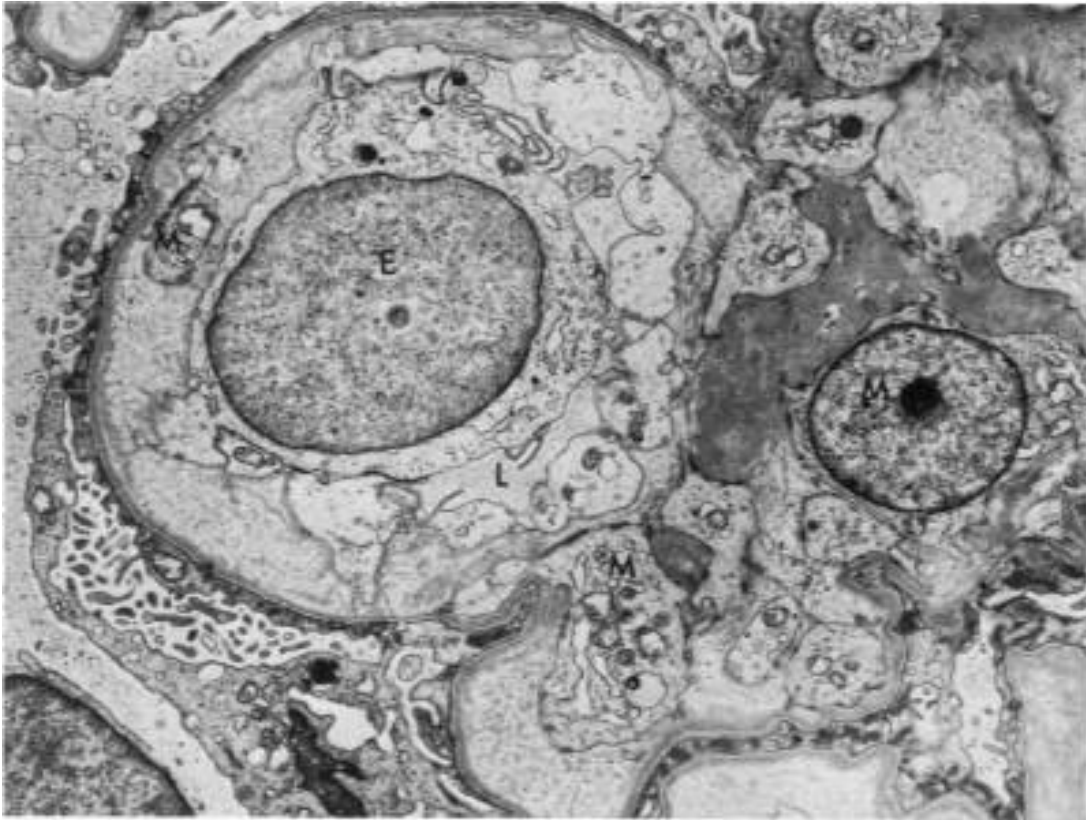


Figure 7. Electron micrograph of HUS associated endothelial damage.

Vascular Endothelial Physiology

The vascular endothelium produces an array of functionally active regulators of systemic inflammation and hemostasis, and thus serves as a key control to prevent coagulopathy and vascular dysfunction^{226,227}. The role of the vascular endothelium in mediating these functions has primarily been studied in the context of atherosclerosis, but the data are applicable in the setting of acute endothelial damage and inflammation as well.

Dysfunction of the vascular endothelium is thought to be crucial to the pathogenesis of the Stx mediated hemolytic uremic syndrome and all forms of thrombotic microangiopathy (TMA) because of the characteristic endothelial damage visible on biopsy specimens^{151,170}. The presumed role of the vascular endothelium in HUS also derives from its known activity regulating primary hemostasis and blood coagulation, interacting with circulating leukocytes, controlling vasoconstriction by producing vasoactive mediators, and its involvement in the maintenance of systemic blood pressure^{226,227}.

The vascular endothelium forms a continuous monolayer spanning greater than 1,000 square meters in an adult human, with 80% of vascular endothelial cells located in capillaries²²⁶. Tissue perfusion and exchange of molecules between the circulation and the interstitial fluid occur in these capillary beds, usually at relatively low pressure. Because of the coagulation-prone low pressure, and the large endothelial surface in the capillary beds needed to perform macromolecular exchanges, endothelial cells actively prevent abnormal coagulation initiation at these sites. These cells produce anti-thrombotic heparin-like glycosaminoglycans that serve as receptors for thrombin-

inhibitory thrombomodulin, and also make the coagulation pathway inhibitors protein S and tissue factor pathway inhibitor (TFPI)^{226,228}. To further increase the anticoagulant properties of the endothelial surface, the heparan sulfate proteoglycans bind antithrombin III and urokinase, and if bound to thrombin the thrombomodulin-thrombin complex activates the anticoagulant protein C to degrade circulating and surface associated coagulation factors^{226,228}. Finally, the endothelium is the primary source of vascular tissue plasminogen activator (tPA), a key fibrinolytic enzyme responsible for clot lysis and prevention of significant vascular surface clot construction²²⁶.

Nevertheless, the vascular endothelium also produces a number of molecules necessary for normal coagulation. The endothelium secretes von-Willebrand Factor (vWF), fibronectin, and thrombospondin, proteins used in initial platelet activation and clot formation, fibrin clot stabilization, and platelet aggregate stabilization, respectively²²⁶. Besides interacting with thrombomodulin, endothelial cells also produce thrombin receptors that help localize active thrombin mediated coagulation, and when bound by activated thrombin coordinate increased coagulation²²⁶. However, normal endothelial cells produce these procoagulant proteins not to increase non-specific coagulation, but to control the location of an activated coagulation process.

In these ways, the normal vascular endothelium both helps prevent unwarranted initiation of coagulation and thrombosis, and prevents spreading of activated coagulation into undamaged vasculature adjacent to hemostatic sites. Processes such as direct endothelial damage and systemic inflammation can disrupt this normal vascular endothelial homeostasis and cause significant dysfunction of the coagulation pathway. Sepsis, the response to intravascular growth of typically gram negative bacteria

(bacteremia) with concomitant release of large amounts of LPS, is the prototypical mechanism of generalized endothelial dysfunction and coagulopathy. Sepsis involves severe systemic inflammation due to activated endothelial toll-like receptor 4 (TLR4) that stimulates inflammatory cytokine release. Sepsis induces disseminated intravascular coagulation (DIC) by increasing vascular tissue factor expression and activity²²⁹. Bacteremic sepsis is a subcategory of vasculitis, vascular endothelial pathology due to inflammatory damage to blood vessels²²⁷. Vasculitis occurs in response to numerous drugs, autoimmune insults, and infectious agents, and is characterized by endothelial activation and injury with altered shape, increased permeability, necrosis, and thrombotic vascular occlusion^{227,230}. Although in some cases endothelial cell damage is discussed in the literature interchangeably with activation, activation will here be used to describe endothelial production of proinflammatory and procoagulant products, while endothelial damage will refer to toxic effects on endothelial cells. Importantly neither of these effects occurs in a vacuum, and it is likely that in all cases of vascular endothelial dysfunction, endothelial activation and damage occur concurrently though to unequal degrees²³⁰.

Severe sepsis causes unrestrained activation of the vascular endothelium in multiple modalities, and if sustained can be followed by endothelial injury and apoptosis²²⁹. The endothelial response depletes anticoagulant molecules and causes impaired fibrinolysis²²⁹. Inflammatory molecules including LPS, interleukin-1 (IL-1), tumor necrosis factor- α (TNF- α), and others increase the endothelial release of plasminogen activator inhibitor-1 (PAI-1)²²⁶. Furthermore, upon endothelial damage thrombomodulin is released into the circulation²²⁶. Depressed membrane

thrombomodulin allows augmented thrombin activity on the endothelial surface, and increased PAI-1 blocks the fibrinolytic pathway allowing clot formation and impairing normal thrombus elimination. Circulating thrombomodulin is thus also a sign of endothelial damage and most likely an indication of increased endothelial pathogenesis²³¹. Endothelial injury releases numerous other procoagulant molecules including coagulation factors IX, X and tissue factor, P-selectin, and platelet activating factor (PAF), along with proteins that encourage leukocyte attraction including E-selectin, intercellular adhesion molecule-1 (ICAM-1), vascular cell adhesion molecule-1 (VCAM-1), PAF, interleukin-8 (IL-8), and C-C chemokine ligand 2 (CCL2)^{226,227}.

Conversely, isolated advanced coagulation and partial vascular thrombosis can increase endothelial shear stress enough to also cause endothelial inflammation²²⁷. Although normal levels of shear stress serve as a differentiation signal to vascular endothelial cells, increased abnormal turbulent flow perturbs the endothelial surface and stimulates release of cytokines and growth factors^{227,232}. In this process, endothelial damage usually results from an imbalance in vasoconstrictor and vasodilator properties of the vasculature, and extreme arterial vasodilation or increases in regional blood flow recreated by drug treatment cause vascular endothelial lesions²²⁷. Although the normal endothelium releases some vasodilatory nitric oxide (NO), during inflammation inducible NO synthase (NOS) precipitates the release of excessive amounts of NO from leukocytes that produces oxygen radicals and causes endothelial injury²²⁷. In this way, direct activated coagulation or coagulation following from endothelial activation can mediate endothelial injury and pathologic lesions. Thus the presence of visible endothelial

damage does not necessarily imply that it is the cause rather than the result of dysregulated coagulation or inflammation.

Because of the significant pleiotropic roles of normal vascular endothelium, endothelial activation and damage is accompanied by detectable changes in circulating endothelial molecules. These include markers of endothelial cell activation like vWF, ICAM-1, VCAM-1, E-selectin, interleukins, CCL2, TNF- α , fibrinogen, and VEGF²²⁷. In contrast, other molecular markers are associated with endothelial injury, including increased numbers of circulating endothelial cells, and fibrinolytic factors thrombomodulin, PAI-1, and tissue plasminogen activator (tPA)²²⁷. However despite general classifications, the distinction between endothelial activation and injury based on circulating biomarkers is unclear, and cannot currently be made based on these plasma constituents²²⁷. Furthermore, little correlation has been found between the levels of circulating inflammatory mediators and the severity of endothelial dysfunction, thus indicating that although endothelial dysfunction is a grave disorder characterized by widespread detectable pathologic alterations, the currently used physiological markers cannot determine the type or manner of endothelial change²²⁷.

Theories Regarding Hemolytic Uremic Syndrome Pathophysiology

The TMA lesion typically found on biopsy of HUS vasculature is thought to cause the renal failure, thrombocytopenia and hemolytic anemia (Figure 5)^{167,170}. As previously discussed, ultrastructural examination of these lesions show glomerular endothelial cell swelling, basement membrane detachment (Figure 7), and the formation of fibrin and platelet rich thrombi in the capillary lumen (Figure 6). This occurs in virtually all

patients with HUS for whom pathologic specimens are available^{167,233}. It is hypothesized that STEC produced Shiga toxin and LPS create these lesions by entering the systemic circulation during the hemorrhagic colitis and causing a systemic toxemia^{31,35}. The thrombosis is hypothesized to inhibit glomerular filtration and urine production, thus causing the acute renal failure, and the fibrin strands of the clots are hypothesized to cause shearing of red blood cells as they try to pass by, forming schistocytes³¹. The microvascular thrombosis is believed to be widespread and involve a majority of the circulating platelet population, thus depleting them from whole blood^{31,35}.

The initiating event in the HUS process, how coagulation is begun, is currently incompletely determined. The coagulopathy could result from initial endothelial death, detachment exposing the pro-coagulant basement membrane, decreased endothelial production of anticoagulant or anti-inflammatory molecules, direct coagulation activation with secondary endothelial disruption, or some as yet undescribed pathologic process. Direct triggering of coagulation could result from a process similar to thrombotic thrombocytopenic purpura (TTP), where altered activity of a circulating protease allows formation of thrombogenic mediators. Alternatively toxins could directly interact with and stimulate the primary thrombogenic circulating cell type, platelets. Human endothelial cells are known among other cell types to express the Stx and LPS receptors Gb₃ and TLR4, and thus most theories propose that Stx or LPS mediated endothelial damage initiates the process that leads to activation of coagulation and thrombosis in the glomerulus^{35,107,234}. Either LPS or Shiga toxin could contribute to the endothelial detachment and pro-coagulant basement membrane exposure followed by coagulation, or these same factors could primarily cause a vasculitis, with endothelial inflammation

causing coagulation and endothelial damage occurring as a secondary process.

Although there is some weak evidence for the presence of circulating factors that directly activate coagulation, and increased inflammation can correlate with severe disease, investigations characterizing the histopathology and coagulation derangements in HUS patients strongly advocate that endothelial damage rather than vasculitis is the predominant etiology of post-diarrheal HUS^{31,152}.

Shiga toxin and LPS have been detected in the tissue and circulating blood cells of STEC mediated HUS patients, though the concentration they reach in the blood is currently unknown^{77,170,235-238}. Case reports demonstrate renal glomerular and tubular deposition of Stx1 and Stx2, however the dose and duration of this association is unclear^{37,239}. Because most patients demonstrate specific IgM responses to Stx and LPS, it is well agreed that significant levels of these toxins enter the bloodstream^{47,50,96-101}. Greater than 90% of patients demonstrate new antibody responses to specific STEC LPS following the acute phase⁵⁰. Stx cannot be detected directly presumably because of its relatively low serum concentration, and although the levels of LPS in these patients can be measured directly, significant serum LPS concentrations have not been reported^{89,240}. Septic patients demonstrate circulating LPS while HUS patients have less than 100 pg/mL LPS, the lower detection limit of the *Limulus* test used⁸⁹. Thus, the evidence for circulating Stx and LPS in HUS comes from the acute phase HUS immunologic responses to these toxins, tissue and vascular damage consistent with their known pathologic functions, and the presence of Stx in tissue samples and on blood cells from affected patients.

Unfortunately, because the clinical signs typically facilitate the diagnosis of HUS, and no treatment other than supportive care is available, renal biopsies from these patients are rare^{24,26,152}. Biopsy of the kidney may cause bleeding and kidney loss, and is only justifiable in cases where it would change the clinical outcome²⁶. This lack of pathologic tissue from patients throughout the course of the disease leaves open to debate the precise nature and timing of the changes seen on the few biopsies taken acutely, or after the fact in autopsy specimens. This is not only a problem in the field of HUS, as the pathogenesis of human acute renal failure is poorly understood in general due to this paucity of histopathologic data²⁶. To overcome this problem the field of nephrology has turned to animal models that appropriately mimic human disease. These model systems allow invasive and advanced measurements that can discern the underlying cause and potential treatments of various renal injuries²⁶. Overall, the HUS theories described above have not been validated because no appropriate animal model exists that can be used to robustly determine the mechanism of HUS and relate it to thrombotic microangiopathy.

Inflammation in the Hemolytic Uremic Syndrome

Cytokines and chemokines released by damaged and inflamed cells attract circulating white blood cells to sites of injury and modulate their activity^{241,242}. These extracellular signaling molecules regulate the immune response to a wide variety of host cell damage, and are responsible for the edema and leukocyte infiltration that is called inflammation²⁴¹. The hallmarks of systemic inflammation include fever, vascular dilation

with decreased blood pressure, increased numbers of circulating white blood cells (leukocytosis), and increased serum inflammatory mediators, while local tissue inflammation is characterized by white blood cell infiltration, increased blood flow, edema, and often damage. Cytokines are normally present at only very low levels, but when upregulated by specific stimuli they are rapidly though transiently produced and released by a large number of cell types²⁴¹. These molecules mediate their activity by binding to specific cell surface G-protein coupled receptors on target cells, and from there determine target cell gene expression and activity^{241,242}. Often, cytokine receptor binding causes endocytosis of the receptor-ligand complex and consequent downregulation of the receptor, thus making the cellular response transient. Cytokines are involved in the pathology of numerous inflammatory ailments including autoimmune disease and tumorigenesis as well as in the development of fever and systemic shock, and may play a role in the development of HUS^{241,242}.

Increased inflammatory mediators and leukocytes have been found in the serum and urine of HUS patients, though their role in mediating the disease remains unclear^{78,180}. The leukocytosis of HUS is not due to abnormal bone marrow white blood cell production, as bone marrow aspirations in these patients only reveal erythroid hyperplasia, consistent with the production of new red blood cells¹⁵². The leukocytosis typically consists of increased numbers of neutrophils, however subtypes of B-lymphocytes, natural killer T cells (NKT) are decreased^{163,179,206,243-245}. Not only are they more populous, but these inflammatory cell types especially neutrophils also demonstrate augmented activity and adjusted inflammatory molecule and cell surface marker expression in the acute phase compared to controls^{206,246}. Monocytes and neutrophils are

found in increased numbers in the glomeruli of the few children biopsied during the acute phase of HUS, however this may only be a result of raised total circulating numbers^{163,193,194,200,243}. Additionally, after the acute phase, circulating monocytes expressing the receptor for fractalkine (CX₃CR1) are depleted in HUS patient blood samples²⁴³. Although fractalkine itself is not reliably changed in HUS patients compared to controls, the degree of CX₃CR1 positive monocyte depletion inversely correlates with the severity of renal failure^{168,243}. The monocytes from these patients also downregulate L-selectin (CD62L) and increase CD16, signs of general deactivation that may be due to tissue targeting and removal from the circulation²⁴³. Generally, leukocytes appear to be activated early in HUS and deactivated later, presumably after they have homed to target tissues. Nevertheless, whether these inflammatory cells are attracted by damage or cooperate in causing some of the renal vascular injury is currently unresolved.

Because the levels of inflammatory cytokines correlate with the degree of leukocytosis in patients, which in turn correlates with worse prognosis in STEC infected patients, the inflammation is hypothesized by some to be integral to syndrome development^{31,33,36,78,177-180}. Leukocytes may mediate direct tissue damage or help to spread the circulating toxins to target tissues^{206,231,247}. Leukocytosis during STEC colitis that progresses to HUS is significantly increased compared to STEC colitis that does not progress to HUS, and compared to non-STEC hemorrhagic colitis^{179,231,244,245,248}. Thus, there is additional inflammation in those patients that progress to HUS compared to those with uncomplicated gastrointestinal infection. The only caveat to these data is that often patients who progress to HUS present to the hospital later in the course of infection, and their serum leukocyte counts are sampled later^{245,248}. Although not reported in every

case, controlling for time delay by using controls time-matched to the beginning of hemorrhagic colitis as day 1 shows that leukocytosis and increased inflammation still correlate with worse patient outcome²⁴⁸.

Nonetheless the primary confounding factor in all measurements of serum parameters in patients with STEC hemorrhagic colitis or complete HUS is time. The concentration and activity of many of these cells and molecules change over the course of the STEC infection and development of HUS, sometimes in complex patterns. Therefore values for these serum markers can vary widely depending on the relative time of sample collection^{168,197,200,249,250}. For instance, granulocyte colony stimulating factor (G-CSF) levels are increased upon admission with STEC hemorrhagic colitis, but decrease over the following week, whereas the levels of C-C chemokine ligand 2 (CCL2) are normal on admission, but increase over the following week^{168,200}. Thus, to properly characterize the inflammatory response to STEC infection during the progression to HUS, multiple serum measurements should be performed that include time points during the diarrheal prodrome, the resolution of the hemorrhagic colitis, the onset of HUS, during HUS, and after HUS resolution³¹. However, recording values at all these times is extraordinarily difficult because of the variability in time of patient presentation to the hospital, and the variability in onset of HUS after the hemorrhagic colitis. For these reasons, the best way to study the inflammatory response would be to use a reproducible model system.

Despite the caveats, significant differences in the levels of many inflammatory factors have been detected in patient serum during the distinct stages of D+HUS progression. These include adhesion molecules like intercellular adhesion molecule-1 (ICAM-1), macrophage chemoattractants like the C-C family chemokines, neutrophil

chemoattractants like the C-X-C family of chemokines, leukocyte growth factors like G-CSF, interleukins, and a host of additional thrombotic and vasoactive compounds²⁴². Also, LPS stimulation of whole blood from patients who have recovered from HUS causes release of significantly increased inflammatory mediators compared to blood from control patients, suggesting that an underlying preexisting propensity for inflammation participates in deciding which patients develop HUS and which do not²⁵¹.

During the hemorrhagic colitis phase, approximately three days after the beginning of bloody diarrhea, patients display increased serum interleukin-6 (IL-6), soluble tumor necrosis factor receptor-1 (TNFR1), matrix metalloproteinase-9 (MMP-9), tissue inhibitor of metalloproteinases-1 (TIMP-1), soluble ICAM-1, CCL4, and soluble Fas^{231,248,250,252}. These same patients demonstrate no significant changes in IL-8, IL-10, interferon- γ (IFN- γ), IL-2, IL-4, soluble P-selectin, interleukin-1 receptor antagonist (IL-1Ra), IL-13, C-X-C chemokine ligand 5 (CXCL5), G-CSF, CXCL1, CCL2, or soluble Fas-ligand^{168,191,231,248,250,252}. The reported levels of tumor necrosis factor- α (TNF- α) and soluble E-selectin during the prodromal colitis conflict among different studies, though have been found increased in some^{248,252,253}. Finally, some inflammatory markers including soluble L-selectin, transforming growth factor- β 1 (TGF- β 1), and CCL4 have been found increased in STEC hemorrhagic colitis compared to acute HUS^{168,248}. In these patients with STEC hemorrhagic colitis who do not progress to HUS, the inflammation is most likely produced by a combination of intestinal damage and LPS toxemia that is less than what occurs in overt bacterial sepsis or fulminant HUS¹⁰⁴.

During the acute phase of HUS, approximately 1-2 days after achievement of HUS case definition, patients display increased IL-6, G-CSF, endothelin-1,

thrombomodulin, soluble TNFR1, MMP-9, TIMP-1, and IL-1Ra, over the levels produced during STEC hemorrhagic colitis alone^{168,231,248,252}. These same patients demonstrate no changes in IFN- γ , IL-2, IL-4, IL-13, soluble ICAM-1, soluble vascular cell adhesion molecule-1 (VCAM-1), CXCL1, CCL2, soluble Fas, and soluble Fas-ligand compared to those with colitis alone^{168,191,248,252}. Decreased levels of CXCL5 and CCL4 compared to STEC hemorrhagic colitis patients are found during the acute phase of HUS¹⁶⁸. HUS patients with encephalopathy have even further increased levels of IL-6, IL-10, soluble TNFR1, MMP-9, and TIMP-1 compared to HUS patients without CNS disorders, and in individual HUS patients, increased IL-10 and endothelin-1 levels plateau prior to the peak in serum creatinine^{191,231,252}. Finally, the reported levels of TNF- α , soluble E-selectin, IL-8, and IL-10 during acute HUS conflict among the studies that are properly controlled, though have been found increased in some trials^{231,248,252,253}. Notably, upon the resolution of HUS and patient release from the hospital the serum levels of IL-6, TNF- α , G-CSF, CCL4, but not CXCL5 return to normal^{168,197}.

Unfortunately, many studies of inflammation during the acute phase of D+HUS do not include the proper control patients with hemorrhagic colitis alone. Although vascular endothelial growth factor (VEGF), IL-6, IL-8, IL-10, CCL2, G-CSF, TNF- α , IL-1 β , IL-1Ra, IFN- α , soluble TNF receptor 55, soluble TNF receptor 75, soluble IL-2 receptor, and soluble VCAM-1 are found upregulated, with soluble ICAM-1 downregulated in these HUS patients compared to normal controls, they cannot be concluded to be specific to HUS rather than the colitis^{169,189,247,254-256}. Increased urine levels of IL-6, IL-8, CCL2 and sometimes TNF- α have also been found in HUS cases, though these do not correlate with serum levels, and again because of a lack of controls

with colitis, these urine cytokines cannot be specifically attributed to HUS^{197,200,249}.

Notwithstanding conflicting reports of specific cytokines, inflammatory mediators are substantially increased during the diarrheal prodrome of patients who progress to HUS.

Although healthy children have low levels of all the cytokines and chemokines mentioned above, many of the individual inflammatory mediators found increased as well as their patterns of upregulation are not specific to HUS^{168,169,247,248,252}. Children with non-HUS renal failure demonstrate increased serum IL-1 β , IL-6, IL-8, CCL2, TNF- α , C reactive protein (CRP), soluble TNF receptor 55, soluble TNF receptor 75, and IL-10^{200,247,257}. These children with non-HUS renal failure also release IL-6 and TNF- α into their urine during the acute phase of illness¹⁹⁷. Children with chronic renal failure on dialysis also demonstrate cytokine abnormalities, with increased serum CCL2, soluble VCAM-1, soluble tissue factor (TF), and soluble thrombomodulin^{168,233}. Children with non-STEC infection or hemorrhagic colitis demonstrate increased IL-6, soluble E-selectin, soluble ICAM-1, and IL-1Ra²⁴⁸. Furthermore, many of the HUS-associated cytokines are elevated in the serum of volunteers given LPS injection alone and in patients with bacterial sepsis. These include IL-1 β , IL-6, IL-8, IL-10, ICAM-1, TNF- α , IFN- γ , CCL2, G-CSF, soluble E-selectin, soluble L-selectin, VCAM-1, soluble TNF receptors, and others^{191,258-260}. Thus, although inflammatory changes are visible in HUS patients before and during the syndrome, many of these same inflammatory mediators are consistently altered by other related disease states.

Although systemic inflammation with leukocyte response occurs in prodromal and fulminant HUS patients, the cause of these effects is unclear. Multiple factors could contribute to the inflammation, including intestinal tissue damage, renal tissue damage,

renal dysfunction, LPS toxemia, and Stx toxemia, however the contributions of these agents has not been determined. It is likely that Stx mediated protein synthesis inhibition is responsible for at least the decline in plasma CXCL5, as previous studies have shown that the protein synthesis inhibitor cycloheximide causes similar effects in cell culture²⁶¹. However most STEC related cytokines are probably due to LPS rather than Stx, as the plasma cytokines often correlate with increased levels of lipopolysaccharide binding protein (LBP), a protein specifically induced in response to LPS⁸⁷. Additionally, intravenous administration of low dose LPS is known to cause increased serum TNF- α , IL-6, IL-8, IL-1Ra, G-CSF, GM-CSF, and soluble E-selectin in normal volunteers²⁶². Compared to Stx, STEC H7 flagellin also strongly increases inflammatory cytokine production by human colonic epithelium *in vivo* by binding to TLR5²⁶³. Alternatively, the increased serum cytokines detected during the acute phase may be partially attributable to decreased renal clearance because of lack of kidney function, as has been shown for IL-10 and IL-1Ra^{200,264,265}. However, the STEC colitis best associates with the production of detectable serum cytokines even though some inflammatory molecules are further increased in HUS compared to colitis patients, as the inflammation usually peaks before the renal failure develops^{168,266}. These data suggest that the inflammation is primarily due to the colitis, and possibly LPS, though Stx and renal dysfunction may contribute as well^{168,263}.

The role these inflammatory mediators and leukocytes play in the pathogenesis of HUS is equally unclear despite overwhelming *in vitro* evidence that inflammation can increase target cell sensitivity to Stx^{144,148,267-280}. Human endothelial cells pre-treated with inflammatory molecules LPS, IL-1 β , TNF- α and others prior to Stx challenge

demonstrate increased cytotoxicity^{148,267-269}. This effect is created in at least some cell types by signaling through p38 MAPK and subsequent upregulation of Gb₃ production^{148,267-269}. Furthermore, many cell types exposed to LPS or Stx *in vitro* release loads of inflammatory proteins, thus initiating their own increased sensitivity to Stx^{144,270}. Besides augmenting the sensitivity of target cells to Stx, inflammation may also cause direct tissue damage, further inflammation, and infiltration by damaging leukocytes. Leukocyte adhesion molecules may help target white blood cells to organs causing tissue damage, and the levels of ICAM, VCAM, and E-selectin all decrease with increasing age, suggesting that they may determine why HUS primarily occurs in young children²⁸¹. Nonetheless, despite strong *in vitro* data, the ability of inflammatory mediators to increase Stx cytotoxicity in patients has yet to be demonstrated.

While it is clear that increased cytokine levels and leukocytosis correlate with worse disease, the effects of these mediators are undefined^{168,169,197,200,206,231,245,247,249,250,256}. Increased inflammation occurs with leukocytosis, increased lactate dehydrogenase (LDH), raised BUN, elevated serum creatinine, oligoanuria, and the need for dialysis, and negatively correlates with the GFR one year later, erythrocyte, and platelet counts^{168,169,197,231,250}. Furthermore, the levels of increased G-CSF and decreased CXCL5 correlate with the need for dialysis in these patients¹⁶⁸. Finally, plasma cytokine levels predict mortality in patients with non-HUS associated acute renal failure, suggesting either that systemic inflammation has a significant effect on the kidney or that when the kidney is damaged it releases significant inflammatory mediators²⁵⁷. LDH is released by damaged tissue, and is thus a measure of organ injury. Secreted IL-8 specifically is known to attract activated neutrophils, and IL-

6 and IL-8 levels correlate with increased leukocyte counts^{197,231,248}. Soluble Fas is an inhibitor of apoptosis. It may be produced to antagonize circulating pro-apoptotic circulating mediators, and can extend the life of tissue damaging neutrophils^{250,282,283}. Cytokine treatment upregulates leukocyte adhesion molecules on the surface of endothelial cells *in vitro*, however these adhesion molecules are not specifically increased in HUS²⁸⁴. IL-10 performs primarily anti-inflammatory effects, specifically blocking the production of IFN- γ , and it may either be a response to other pro-inflammatory molecules, or it may encourage STEC gastrointestinal persistence by limiting the antibacterial host response²³¹. Increased TGF- β 1 probably represents normal intestinal healing in those STEC colitis patients that do not progress to HUS¹⁹¹. The absence of significant changes in T-cell cytokines suggests a lack of T lymphocyte involvement in HUS pathogenesis¹⁹¹. Altogether, though the mechanism is speculative, the increased inflammation in HUS patients may play a causative role in the disease etiology, or instead may be a product or marker of increased tissue damage and pathology in sicker patients²⁰⁰.

The complement cascade is a specialized non-cellular portion of the innate immune system that can mediate inflammatory tissue injury. Complement deserves mention in this discussion of inflammation because its dysregulation causes atypical familial HUS²⁸⁵. Complement factors constitute 15% of circulating plasma proteins and consist of at least 30 peptides that are activated by foreign or inflammatory membrane surfaces²⁸⁵. Complement proteins are present as inactive zymogens in plasma and are activated by a proteolytic cascade. They proceed from C1 to C2 and C4, then through the crucial activator C3, followed by the final membrane destructive C5-C9 membrane attack

complex²⁸⁵. These zymogens are typically cleaved into two pieces, the active protease that catalyzes the cleavage of the next step in the pathway, and a smaller inflammatory fragment that signals to specific cellular receptors. The inflammatory fragments from C3 and C5 are called anaphylatoxins^{230,285}. Complement activation is clinically detectable by decreased circulating levels of the complement factors. Although multiple mechanisms can initiate the complement cascade, these converge on C3 which is normally critically regulated by a host of anti-complement molecules²⁸⁵. Deactivating mutation of any of a number of these C3 inhibiting enzymes causes abnormal complement deposition on the vascular endothelial surface, and results in familial or atypical HUS, a syndrome of adult patients usually unrelated to STEC infection²⁸⁶⁻²⁹¹.

Patient data are unclear as to the role of complement activation in STEC mediated HUS. Complement C3 and C4 levels are decreased in only 30% of Shiga toxin induced HUS acute phase cases, though the cause of this change is unknown^{292,293}. Intriguingly, although complement is activated only in some cases, its activation can correlate with observed leukocytosis and worse prognosis, and might be a sign of more severe disease^{292,293}. However, pathologic evidence does not support complement activation in HUS, as immunoglobulins and complement components are rarely found in glomerular thromboses or associated with endothelial damage in these patients¹⁵¹. Despite the measured complement activity in these cases, the role of complement in STEC mediated HUS remains incompletely assessed. Complement may be activated either as a result of endothelial damage, by circulating toxins, or it may directly contribute to the pathogenesis of D+HUS.

Coagulation in the Hemolytic Uremic Syndrome

Hemostasis consists of three processes: platelet aggregation, extracellular coagulation, and fibrinolysis, that work in tandem to appropriately regulate clot formation²⁹⁴. Clots composed of platelets and coagulation factors normally form in response to vascular injury to prevent bleeding²⁹⁴. Initiation of hemostasis is normally inhibited because tissue factor (TF, Factor III), von-Willebrand factor (vWF), and activated coagulation factors are kept physically separated from circulating unactivated platelets²⁹⁵. vWF is normally stored by endothelial cells and platelets, and when released is thrombogenic by binding to platelet glycoprotein receptors IIb/IIIa²⁹⁶. Platelets are inactive until they either adhere to exposed subendothelial matrix or are stimulated by soluble adenosine diphosphate (ADP) or activated thrombin (coagulation factor II)²⁹⁷. Vascular damage exposes sub-endothelial collagen and vWF to which circulating platelets bind, and in turn expose low levels of active TF²⁹⁴. Platelet receptor adhesion partially activates the platelets, and they adhere to fibrinogen which allows platelet-platelet aggregation and formation of a platelet plug²⁹⁴. Platelet activation coincides with platelet spreading and the release of various granules containing pro-coagulant and inflammatory molecules²⁹⁸. These activated platelets facilitate vascular coagulation by exposing activated coagulation factors and necessary phospholipids for the coagulation cascade²⁹⁸. Downstream effects of TF also feed back and activate platelets, linking the entire pro-coagulant process²⁹⁵.

Coagulation is mediated by a host of circulating protein clotting factors, the pro-coagulant surface on activated platelets, and exposed TF bearing cells (Figure 8)²⁹⁵. TF is at the heart of the initiation process, also previously called the extrinsic pathway of coagulation^{294,295,299}. TF is expressed by cells of the vascular wall and not found on cells

in direct contact with the bloodstream²⁹⁹. When exposed to clotting factors in the systemic circulation, TF bearing cells form TF-factor VII activated complexes (TF/VIIa) that activate Factor X. Xa and Va combine to activate thrombin (factor II), however this process only produces minute amounts of thrombin before it is inhibited by the circulating tissue factor pathway inhibitor (TFPI)²⁹⁹. This low thrombin level is insufficient to cleave enough fibrinogen into fibrin to create a clot^{295,299}. Propagation of the original TF-generated thrombin requires the small amount of thrombin to activate Factors V and VIII of the classical intrinsic pathway on the platelet surface, and thus only happens if platelets are close^{295,299}. Factors Va, VIIIa, IXa, and Xa then combine to produce enough active thrombin to substantially cleave fibrinogen and mediate clot formation²⁹⁹. Thrombin cleavage releases prothrombin fragments 1 and 2, which can be used as markers for thrombin activation³⁰⁰. Because TF and Factor VII from the extrinsic pathway and Factors IX and VIII from the intrinsic pathway are both needed for proper coagulation, it is appropriate to conceive of them as initiation and amplification steps of the same process^{295,299}. Importantly, substantial abnormal bleeding occurs with defects in either pathway, supporting the view of a unified mechanism in which neither side can completely substitute for the other²⁹⁵.

The initial platelet aggregation and coagulation steps of hemostasis run in parallel²⁹⁵. Once thrombin is generated on the surface of TF bearing cells, and the platelets are attracted by exposed vWF and collagen, the small dose of activated thrombin can be moved to the surface of the nearby platelets²⁹⁵. Decreasing the distance and limiting the exposure to circulating TFPI allows binding of thrombin to its high affinity platelet receptor GPIb²⁹⁵. This then creates the appropriate situation for large scale

amplification of the coagulation cascade by allowing thrombin activation of Factors V and VIII to generate more thrombin. This secondary thrombin produces the stable hemostatic clot by stabilizing the platelet plug with a fibrin meshwork²⁹⁵. The initial platelet adhesion and thrombin binding can each moderately activate the platelets directly, however in combination the effect is synergized to fully activate the present platelets²⁹⁵. Finally, localization of the pro-coagulant surface to the site of injury serves to partially limit the extent of the coagulation²⁹⁵.

Nevertheless, coagulation must be further regulated so that while vascular damage is stopped by an appropriate level of hemostasis, complete thrombosis of the vessel does not occur²⁹⁵. Plasma protease inhibitors including TFPI serve this function by inactivating activated coagulant proteases when they diffuse away from the central clot^{294,295}. Secondly, endothelial associated antithrombotic molecules protect the adjacent uninjured endothelium. These molecules include endothelial TFPI, antithrombin, thrombomodulin, protein C, and protein S (Figure 8)^{294,295}. As the amount of thrombin generated most directly governs the stability of the clot, thrombin is the key positive modulator of clot expansion²⁹⁵. Low rates of thrombin generation produce loosely packed clots of thick fibrin fibers whereas robust thrombin generation causes formation of tightly packed rigid structures²⁹⁵. Clot extension is also negatively regulated by fibrinolytic factors that dismantle the fibrin network. Endothelial tissue plasminogen activator (tPA) and urokinase (uPA) convert circulating plasminogen to plasmin, which directly degrades fibrin²⁹⁴. Plasmin can be inhibited by thrombin-activatable fibrinolysis inhibitor (TAFI) and plasminogen activator inhibitor 1 (PAI-1), among others²⁹⁴. However, not all PAI-1 is active, as platelet derived PAI-1 is mostly latent while normal

circulating plasma PAI-1 is active³⁰¹. Plasmin cleaves fibrin into detectable D-dimers and fibrin degradation fragment E, both of which can be used to evaluate plasmin activity²⁹⁷.

Fibrin is thus the final and crucial outcome of the coagulation pathway, and both its formation and destruction are highly regulated (Figures 8, 9)^{297,300}. Fibrin is formed from fibrinogen, a 45 nm molecule comprised of three proteins called A α , B β , and γ linked by disulfide bonds³⁰⁰. Fibrinogen is an acute phase protein, meaning that it is upregulated by cellular stress including LPS and IL-6 signaling, primarily in the liver²⁹⁷. Thrombin binds and activates fibrinogen by cleaving off fibrinogen peptide A (FPA) and fibrinogen peptide B (FPB), turning the plasma soluble fibrinogen into the insoluble fibrin^{297,300}. Fibrinopeptide removal exposes intermolecular binding motifs that allow half-staggered fibrin oligomers to lengthen into protofibrils²⁹⁷. Protofibrils aggregate laterally to make fibers, which branch to create the meshwork of the hemostatic fibrin clot (Figure 9)²⁹⁷. Once formed, the transglutaminase coagulation factor XIII covalently crosslinks the molecules together to stabilize the clot²⁹⁷. Normally, only small amounts of crosslinked fibrin or fibrinogen are present in human plasma³⁰⁰. The fibrin clot is a scaffold for fibroblast and macrophage migration, allowing collagen deposition and clot degradation respectively, and is stabilized by fibronectin, albumin, thrombospondin, and vWF²⁹⁷. In addition to serving as a frame for hemostatic platelets and inflammatory white blood cells, crosslinked fibrin also increases the ability of growth factors like FGF and VEGF to mediate endothelial proliferation and healing^{297,300}.

Figure 8. Schematic of the intravascular coagulation cascade.

The intravascular coagulation cascade to form crosslinked fibrin and a stable clot. (Taken from <http://www.biocrawler.com/encyclopedia/Coagulation>). The cellular injury pathway has been previously called the extrinsic pathway, while the contact system has been previously called the intrinsic pathway. Legend: HWMK = High molecular weight kininogen, PK = Prekallikrein, TFPI = Tissue factor pathway inhibitor. Black arrow = conversion/activation of factor. Red arrows = action of inhibitors. Blue arrows = reactions catalysed by activated factor. Grey arrow = functions of thrombin.

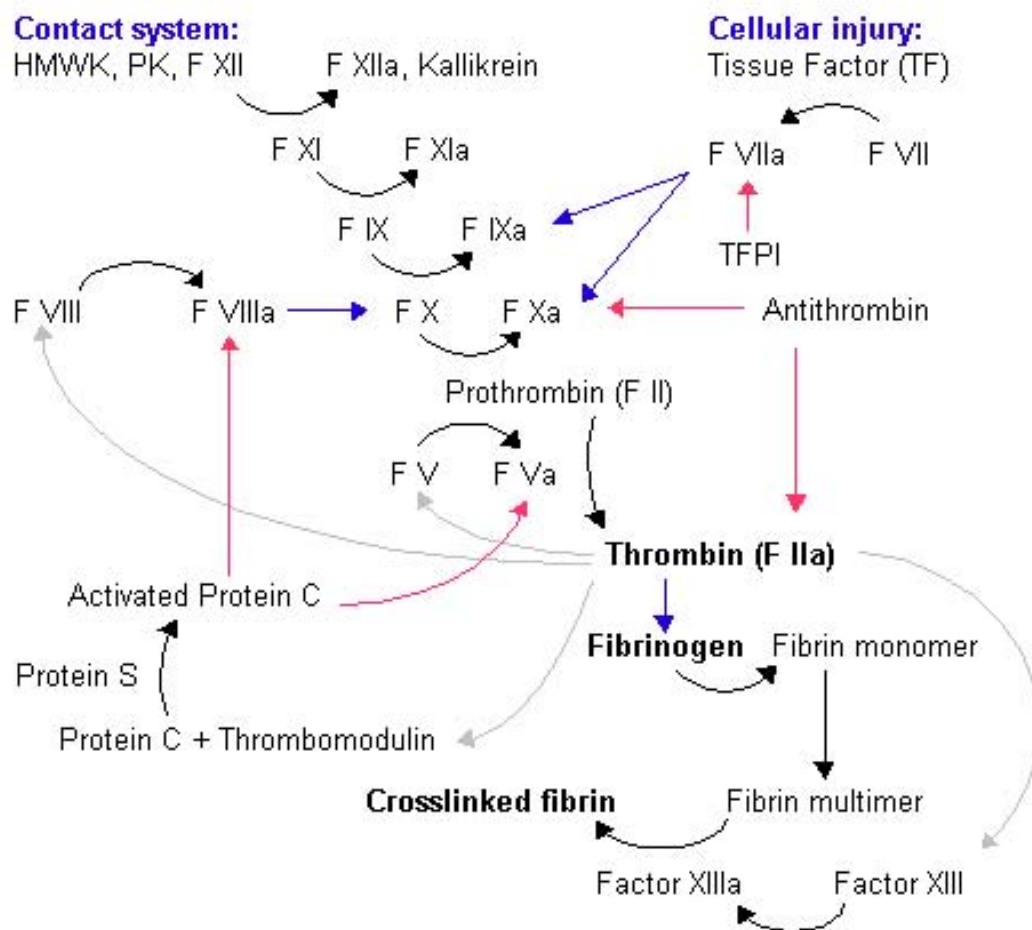


Figure 8. Schematic of the intravascular coagulation cascade.

Figure 9. Electron micrographs of normal fibrin clots.

Scanning electron micrographs of fibrin clots. (Taken from *Advances in Protein Chemistry* 2005. 70: 247-299.) (A) Micrograph of clot formed by addition of thrombin to purified fibrinogen. Magnification bar is 5 μm . (B) Micrograph of whole blood clot from fresh blood with no additional factors. Fibrin fibers often originate from platelet aggregates (small round cells), while erythrocytes (large doughnut cells) and leukocytes are trapped in the fibrin meshwork. Magnification bar is 10 μm .

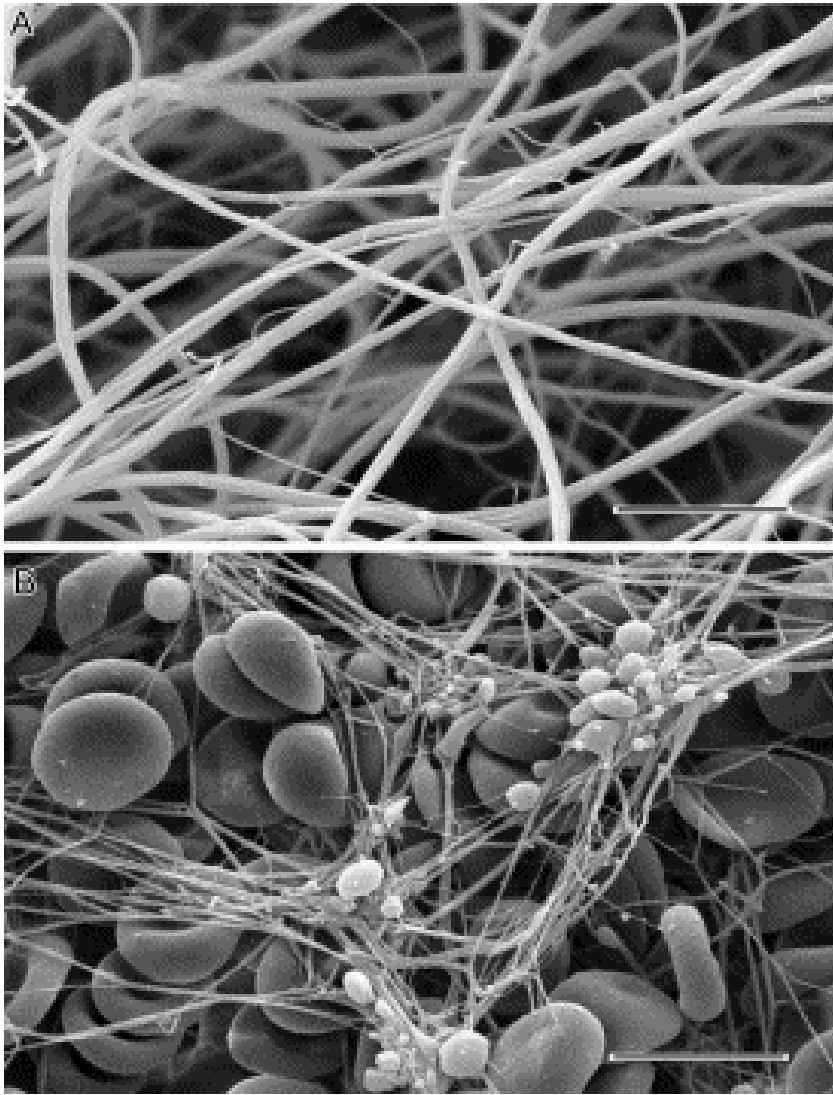


Figure 9. Electron micrographs of normal fibrin clots.

Coagulation factor activity and whole blood clotting ability are clinically examined using three blood tests in addition to measuring the serum levels of specific coagulation factors^{294,295,302,303}. Activated partial thromboplastin time (PTT) is performed on whole blood in a glass tube, sometimes with additional phospholipid. The glass or the phospholipid creates a negatively charged surface to which coagulation factor XII associates, and activates the contact based coagulation system, also known as the intrinsic pathway. Proper activation of the PTT measures factors XI, X, VIII, V and thrombin, though importantly, not all of these factors are necessary for normal hemostasis. In contrast, the prothrombin time (PT) is induced in whole blood by the exogenous addition of excess tissue factor. This TF overcomes the TFPI normally present in serum and allows significant activation of thrombin using the pathway usually initiated by cellular injury, also called the extrinsic pathway. Proper activation of the PT requires factors VII, X, V, and thrombin. However, neither the PT nor the PTT actually represents physiologic hemostasis, rather they are manners to test the activity and presence of various coagulation factors. The final test is the thrombin time (TT), in which purified exogenous thrombin is added to plasma. The TT is a direct measure of fibrinogen function, and in hypofibrinogenemic states the TT is increased. These three tests are used to evaluate numerous coagulation disorders in the clinical setting, although normal clotting times for the PT, PTT, and TT do not exclude dysregulated coagulation³⁰³.

The generalized Shwartzman reaction deserves special mention as a red herring, as it displays many of the features of HUS but is due to a distinct though often underappreciated mechanism³⁰⁴⁻³⁰⁷. The Shwartzman reaction occurs solely because of LPS exposure, and is used as a model for sepsis induced disseminated intravascular

coagulation (DIC). The response can either be local, with only local LPS contamination, or general, with systemic LPS infiltration. The general Shwartzman reaction due to two intravenous doses of LPS 24 hours apart causes a syndrome that appears similar to the coagulopathy of HUS, with petechial hemorrhages, microvascular thrombi, and decreased numbers of circulating platelets^{304,308}. This multi-system disorder does not occur with single dose LPS challenge, though can occur with continuously infused LPS over 6-12 hours^{307,308}. Typically, other inflammatory mediators can substitute for the initial inflammatory insult, with TNF- α or IL-1 followed 24 hours later by LPS also able to initiate the Shwartzman pathology^{304,305}. The etiology of the reaction is thought to consist of initial LPS activation of endothelial cells, with upregulation of leukocyte and platelet adhesion molecules, followed by activation of leukocytes and platelets with the second dose of LPS, resulting in thrombosis and microthrombi^{304,305}. This reaction recapitulates the coagulopathy of sepsis, but can occur in experimental settings without bacteria if reagents are contaminated with LPS, or if LPS is administered multiple times³⁰⁸.

As stated above, the coagulation changes that occur in the Shwartzman reaction are comparable to those that occur in DIC with sepsis, and though the pathology may appear similar to HUS, the coagulation measurements demonstrate that the Shwartzman reaction and sepsis are distinct from HUS³⁰⁷. Septic DIC derived from LPS intoxication is associated with fever, leukocytosis, platelet consumption, decreased fibronectin levels, and acute renal failure, but also with increased PT and PTT^{259,309,310}. Coagulation activation in sepsis proceeds from LPS induced endothelial damage and TF mediated thrombin activation³⁰³. Overzealous thrombin generation consumes the anticoagulant

molecules protein C, protein S, and antithrombin, and liver dysfunction probably contributes with decreased production of these proteins as well³⁰³. Patients with DIC also demonstrate increased D-dimers and characteristic decreases in plasma fibrinogen and factor VIII and V levels that distinguish it from other coagulopathies³⁰³.

In contrast to DIC or the Schwartzman reaction, HUS patients typically demonstrate no increases in PT or PTT, and have normal or increased circulating fibrinogen, factor VIII, and factor V concentrations, even though they may have decreased fibronectin levels and increased thrombin and bleeding times^{32,176,182,185,306,310-312}. The thrombocytopenia due to the Schwartzman reaction is transient, and in experimental models usually recovers within 24 hours after the administration of LPS³⁰⁷. In contrast, the thrombocytopenia of HUS is persistent for days or weeks. Finally, the relative lack of LPS in HUS compared to sepsis argues that LPS is not the sole cause of the coagulopathy in HUS⁸⁹. Though not similar to DIC, the crucial unresolved problem regarding the coagulopathy of D+HUS concerns whether the platelets or coagulation factors are primary causes of the defect. Arguing for the role of the coagulation factors, they are found to be abnormal before the onset of fulminant HUS during the colitis prodrome. Arguing for the role of the platelets, they are found to acutely activate early in the course of HUS, and maintain a relatively deactivated state for much of the latter portion of the disease³².

Despite the obvious thrombocytopenia that develops during HUS, the role platelets play in the pathophysiology of the disease has been poorly investigated. Clinically, children in the acute phase of HUS demonstrate abrupt thrombocytopenia and a functional decrease in directly measured platelet activity^{182,306,313,314}. Platelets from

acute phase HUS patients produce a diminished aggregation response to agonists, have drained intracellular molecular stores, and have decreased surface markers compared to platelets isolated from normal children and children in renal failure^{182,313-315}. This may be due to splenic sequestration of normal circulating platelets or prior activation and clotting of most platelets, with only those that are hyporesponsive left in the systemic circulation during the acute renal failure^{182,313,314}. As evidence for prior platelet activation, and platelet exhaustion during acute HUS, the phenotype of platelet hyporesponsiveness can be recapitulated by activating normal platelets *in vitro* and then attempting a second activation³¹⁴. Unfortunately, similar changes in platelet functionality occur in other types of renal failure and during dialysis. Nonetheless, the HUS platelet changes are believed to be independent of renal failure, as they resolve even before the renal failure as a sign of impending improvement³¹⁴. The numbers of circulating platelets in these patients recover gradually following the acute phase, suggestive of normal replenishment following their acute destruction or usage, and platelet producing megakaryocytes are normal in the bone marrow^{182,306}.

HUS patients evidence additional signs of significant platelet activation, with increased plasma levels of platelet specific molecules serotonin, β -thromboglobulin (β -TG), platelet factor 4, P-selectin, and platelet-derived microvesicles, although some increased β -TG is found in other types of renal failure^{199,314,316-318}. Prior to HUS case definition, those who do develop HUS and those that only develop colitis both have increased levels of platelet activating factor (PAF), a platelet activating phospholipid synthesized by endothelial cells, platelets, and leukocytes³¹⁹. Interestingly, PAF is also found increased in urine during acute HUS, and the level of this mediator falls back to

normal during the acute phase of HUS, suggesting renal specific endothelial and platelet activation followed by resolution^{319,320}. Platelet activation in this way except for PAF correlates with renal dysfunction, and suggests that platelets activate and release their granules early or prior to HUS attainment¹⁹⁹. Thus platelets appear to be activated early in the course of acute HUS, and during renal failure the remaining platelets are degranulated and dysfunctional, though their relation to circulating toxins or endothelial damage remains only correlation and conjecture.

In vitro work on human platelets is as unsatisfactory as clinical platelet studies in HUS patients. Three publications report that platelets do not bind Stx, while one group shows that Gb₃ presence on human platelets and Stx binding is widely variable, and a separate group that Stx only binds to platelets that are already activated³²¹⁻³²⁵. Four articles have investigated whether Stx has a direct effect on platelet function, with three concluding that Stx has no direct action on platelet activation, granule release, or shape change, though one disagrees on all counts^{321,323,324,326}. Each of these reports is associated with technical problems including the use of improper controls, however the controversial consensus at this point is that Stx interaction with platelets has no functional consequence. Additionally, the inflammatory mediators generated in HUS patients do not directly stimulate platelet activity, though they may act as co-activators in some cases³²⁷⁻³²⁹. These data therefore suggest that the coagulation findings present in HUS derive from somewhere other than the platelets and by a mechanism that acts directly on a distinct cell type.

Besides the thrombocytopenia, laboratory measured changes in coagulation and fibrinolytic factors measured prior to HUS onset argue that hematologic abnormalities in

HUS patients follow from dysregulated coagulation^{306,330,331}. Pathologically, HUS microvascular injury is characterized by the deposition of fibrin rich and von-Willebrand factor (vWF) poor clots with fibronectin and platelets^{310,311}. Although early investigations had difficulty demonstrating active coagulation increases in the acute phase of D+HUS, with quicker admission to hospitals earlier in the disease process, and better techniques for monitoring coagulation, activation of both coagulation and fibrinolysis has been demonstrated in fulminant HUS patients¹⁸⁵. Changes early in the disorder suggest the presence of a hypercoagulable state, while later studies of the acute phase demonstrate an impaired coagulation system, similar to that observed for platelets³⁰⁶.

Although many clinical studies lack proper control groups: patients with only STEC colitis who do not progress to HUS, patients with non-HUS renal failure, and normal controls to compare to the acute phase of HUS, one prospective coagulation study includes them³³⁰. Thrombin activity is elevated before the onset of HUS, as measured by increased prothrombin fragments above those present in normal controls or children with colitis that do not progress to HUS³³⁰. Patient plasma prior to HUS also demonstrates increased levels of plasminogen activator inhibitor 1 (PAI-1), D-dimers, and tPA^{35,312,330}. Overall fibrinolysis appears to be inhibited in these patients because the tPA is complexed to the PAI-1, blocking its activity^{312,330}. Unlike DIC following sepsis, fibrinogen concentrations are not decreased in HUS patients, and the prothrombin measure of coagulation time is only slightly elevated^{31,182,311,312,332}. Finally, each of the factors found increased prior to HUS onset are increased to a lesser extent in patients

with STEC colitis that do not develop HUS, and further increased in patients during the acute episode of HUS itself³³⁰.

Numerous additional properly controlled studies from the acute phase demonstrate changes in coagulation factors during HUS consistent with activated coagulation. During fulminant HUS patients display increased serum levels of thrombin-antithrombin complexes, raised thrombin activity, prothrombin fragments, fibrinopeptide A, and fibrin degradation products compared to those that only develop STEC colitis or those with non-HUS acute renal failure^{182,185,192,301}. These findings correlate with disease severity^{182,185,192,301}. Fibrin degradation products are specifically low in STEC colitis patients that do not progress to HUS compared to acute phase patients, suggesting that a crucial aspect of HUS development is the increased coagulation and fibrinolysis¹⁹². Elevated fibrinolytic activity is evidenced by increased D-dimers, plasma tPA, and uPA^{182,301}. Although levels of vWF, fibrinogen, α 2-antiplasmin, and PAI-1 activity are significantly increased in acute HUS compared to normal controls, their responses to STEC colitis alone are unknown, and chronic renal failure independently upregulates these factors, making them nonspecific for HUS^{256,301}. Plasma fibronectin is found decreased in HUS patients compared to children with renal failure alone, though again this has not been compared to patients with STEC colitis alone³¹⁰. Furthermore, even though some investigators have found increased total PAI-1 in HUS patient plasma, approximately 90% of plasma PAI-1 is in the latent form released by platelets, thus making the measure of activity more accurate and relevant³⁰¹. Patients with HUS, STEC colitis that does not progress to HUS, acute renal failure, and control patients all have

similar PT, PTT, factor VIII, plasminogen, C1-esterase inhibitor, soluble tissue factor (sTF), thrombomodulin, and active unbound PAI-1^{233,301}.

In contrast to TTP, in which abnormal activity of the ADAMTS13 protease allows high levels of ultra-large vWF to exist in the circulation, there is no change in ADAMTS13 activity either during acute D+HUS or in the diarrheal prodrome^{181,196}. ADAMTS13 protease normally cleaves vWF into a series of plasma multimers, and in TTP no lower weight molecules are present¹⁹⁶. This defect in ADAMTS13 makes TTP treatable by plasma exchange that removes any inhibitor of the protease, as well as provides additional normal protease¹⁸¹. The abnormal ultra-large vWF induces formation of vWF and platelet rich clots that cause a similar syndrome to D+HUS involving microangiopathic hemolytic anemia, thrombocytopenia, renal failure, and neurologic dysfunction¹⁹⁶. Although there is not ultra-large vWF, the plasma levels of vWF are modified in HUS patients compared to normal. Normally low but detectable vWF is present in glomerular endothelial cells from HUS patients, and the total level of plasma vWF is increased in HUS^{182,196,333}. vWF multimers also have decreased average size in HUS plasma and are shortened to a lesser extent during STEC colitis in the same patients^{196,333,334}. The distribution of vWF multimers is normal in other types of renal failure¹⁹⁶. The decrease in large vWF multimers in HUS plasma only partially correlates with thrombocytopenia observed in these patients, suggesting that vWF consumption in this disease is only involved indirectly with the consumption of platelets¹⁹⁶. It has been proposed that this decrease in large vWF multimers is due to increased proteolytic activity in the HUS circulation due to elevated shear stress, that vWF may be consumed as part of HUS development, and that increased total vWF in HUS occurs because of

endothelial damage or stress^{196,333}. However these theories have not been definitively proven¹⁹⁶. Despite the lack of understanding, vWF multimers are consumed during HUS, demonstrating again that HUS is a coagulopathy and that it is distinct from TTP.

Though significant data support activated coagulation and fibrinolysis in HUS patient vasculature, substantial uncertainties persist in what these changes are, their underlying cause, and how they determine the visible thrombotic microangiopathy, thrombocytopenia, and hemolytic anemia³³⁵. Despite the crucial proposed role dysregulated coagulation plays in HUS patients, how it is activated during the disease course is currently unknown. The coagulation abnormalities may depend on endothelial death and exposure of the hemostatic basement membrane, they may derive from modified products released by the endothelium, or they may be spurred by other cell types or plasma factors. Measurements of clotting factor levels in HUS patients are difficult to interpret because these plasma factors vary wildly in normal individuals, with significant functional changes only when they are decreased below 20% of normal²⁹⁵. Furthermore, activated partial thromboplastin time (PTT) and prothrombin time (PT) are normally elevated in children for the first six months and 16 years of life, respectively³⁰². Renal failure alone has been shown to increase the circulating levels of PAI-1 and fibrin degradation products, confounding the argument for their roles specifically in HUS^{301,335,336}. Although patients that proceed to HUS have elevated levels of pro-coagulant factors, those infected with *E. coli* O157:H7 also demonstrate a coagulation disorder, though to a lesser degree³³⁰. Finally, weak data suggest that circulating STEC derived toxins can directly activate coagulation in HUS patients, which may occur in addition to the coagulopathy derived from endothelial dysfunction³³⁷.

It may be that the degree of coagulation activation determines whether there is progression to HUS or resolution without significant microvascular or renal disease. Because the rate of thrombin generation can determine the structure of the clot, the coagulation changes in HUS may be due to abnormal levels of thrombin generation^{295,297}. Low thrombin levels could cause the formation of loose fibrin rich clots leading to erythrocyte shearing and subsequent anemia, as well as less precise localization of the clotting process and overabundant platelet use causing thrombocytopenia. In contrast, high thrombin levels may overzealously generate thrombin without a supportive cellular network, thus creating a mesh through which erythrocytes become sheared into schistocytes when they pass. These theories remain untested.

HUS dogma proposes that vascular endothelial damage mediated directly by Shiga toxin initiates the dysregulation of coagulation, however other factors likely participate as well. Stx causes endothelial cell death *in vitro*, and in most cases does not alter the coagulation factors released by these endothelial cells in a pro-coagulant way, instead blocking protein synthesis of all factors²⁷⁷. Inflammatory mediators found increased in the serum of HUS patients may play a role in mediating abnormal coagulation in HUS. Endogenous TNF- α , IL-1 β , EGF, VEGF, and interferons, as well as exogenous substances including LPS can upregulate TF, PAI-1 and uPA expression on vascular endothelial cells^{277,338,339}. In general the upregulation of TF is part of a general endothelial response to inflammation that includes increased production of various adhesion molecules to locally limit inflammation and coagulation^{233,338}. Furthermore, activated platelet or thrombin binding to the endothelium can increase TF production as well, so even if increased tissue factor is found in tissue it may be either a direct or

indirect cause of abnormal coagulation³³⁸. Apoptotic cells release tissue factor associated with the activating phospholipids phosphatidylserine, and the apoptosis mediated by Stx may thus contribute to the coagulation in HUS²⁹⁹. Thus observed HUS coagulation is likely a multifactorial process, and though the initiating events are currently undescribed they deserve research attention as crucial aspects in the development of the syndrome.

Consensus Pathophysiology of the Hemolytic Uremic Syndrome

Shiga toxin is hypothesized to cause the unique tissue damage and cellular dysfunction profile that takes place during the hemolytic uremic syndrome by acting on cell types that produce its glycosphingolipid receptor. Human cell types known to express Gb₃ and be sensitive to Stx *in vitro* include glomerular endothelial cells, glomerular epithelial cells (podocytes), renal tubular cells, mesangial cells, non-glomerular renal microvascular endothelial cells, non-renal microvascular endothelial cells, and some intestinal cell types^{113,125,239,263,268,330,340-353}. The principal unresolved questions in the HUS field concern how Stx and LPS circumvent the intestinal epithelial barrier, which of the inflammatory, cytotoxic, or procoagulant effects are most responsible for syndrome development, and whether some currently undescribed STEC mechanism initiates HUS.

STEC pathogenesis begins with gastrointestinal epithelial adherence, probably characterized by A/E lesions, and the initial release of cytotoxic virulence factors. The intimin produced by most STEC mainly facilitates interaction only with follicle-associated epithelial cells of Peyer patches, intestinal aggregations of lymphoid tissue⁴⁹.

D+HUS begins when bacteria dying from host immunity and other causes release Stx into the intestinal lumen and initiate intestinal damage. Pathological specimens of STEC infected intestinal tissue appear hemorrhagic and edematous, with focal necrosis and infiltration of inflammatory cells including neutrophils^{41,42}. Stx is toxic to some of the intestinal epithelium, and may cause both inflammatory mediator release and cell death^{41,354}. While bacterial adherence with A/E lesions is thought to promote the production of watery diarrhea, Stx seems critical for the evolution of bloody diarrhea and hemorrhagic colitis⁴¹.

There are multiple epithelial cell types that make up the luminal intestinal wall, however only some of these express Gb₃ and are sensitive to Stx^{263,344-348}. The intestinal mucosa forms contiguous villi and crypts, undulations of both the epithelial and mesenchymal layers that increase the surface area of the luminal face³⁴⁴. Physical landmarks on the villi or crypts separate multiple cell types by their respective locations. Intestinal cells responsible for absorption of luminal contents, enterocytes, further increase the absorptive surface area of the intestine by forming microvilli, undulations of their cell membrane. The villi measure approximately 1 mm in length, while the microvilli are about 1 μ m in length³⁴⁴. Three types of epithelial cells compose the villi: enterocytes that absorb nutrients, goblet cells that secrete the protective mucus barrier, and enteroendocrine cells that release hormones³⁴⁴. The intestinal crypts contain mainly immature undifferentiated cells that terminally differentiate into the three villus cell types as they migrate up the villi, and Paneth cells that produce and release antimicrobial peptides lysozyme and α -defensins into the crypt lumen^{344,345}. Though similar, the colon lacks the villi and Paneth cells of the small intestine³⁴⁴.

Of the major cell types that comprise the human intestinal surface, only Paneth cells have been demonstrated to express Gb₃ *in vivo*^{263,345-348}. When pediatric intestinal tissue is cultured and challenged with Stx2 for 24 hours, cells are extruded from the intestinal crypts³⁴⁶. Although Stx1 is unable to mediate significant crypt cytotoxicity in this organ culture system, both Stx1 and Stx2 bind to Paneth cells on human small intestine biopsies, with binding both in the cytoplasm and on the membrane^{345,346}. However, no increased Gb₃ expression or Stx binding is observed in inflamed intestinal biopsies compared to controls, suggesting that the intestinal epithelial interaction with Stx does not change in states of infection^{263,345}. Also, only 30-50% of individuals express Gb₃ and show Stx binding to Paneth cells, intimating that Paneth cell Gb₃ expression may determine whether STEC gastrointestinal infection progresses to colitis or HUS³⁴⁵.

The effect of Stx binding on Paneth cell physiology and function remains uncharacterized, and it is unclear if this interaction initiates the colitis that occurs in these patients, or whether it simply mediates Stx passage into the intestinal stroma. Additionally, intestinal epithelial cells including those that lack Gb₃ expression have been demonstrated capable of transmitting Stx across the intestinal barrier, and this may allow systemic Stx entry *in vivo* without significant epithelial disruption^{346,348,355,356}. Overall, significant pathological breakdown of both small and large intestines occur, with resultant hemorrhagic colitis and microangiopathy¹⁹⁴. Although it is unclear precisely how the breakdown of the intestinal barrier occurs, and numerous pathogenic mechanisms may be at play, the end result is entry of bacterial virulence factors from the luminal intestinal contents into the systemic circulation.

Once the intestinal barrier is compromised by the luminal action of STEC and their pathogenic products, Shiga toxin and LPS can enter and cause further pathology. Surprisingly, the amount of Stx detected in stools of patients with only STEC induced colitis is not significantly different from the amount in stool samples from those patients that progress to HUS³⁵⁷. One explanatory model of this phenomenon argues that as more Stx is released into the intestinal lumen, more is absorbed by the permeable or susceptible epithelial cell types, thus leaving equal Stx levels in the forming stool of the colon. This may be evidence that the primary absorption of Stx from STEC colonization occurs in the small intestine where Peyer's patches and Paneth cells are present, with the associated colitis occurring because of microvascular insult from circulating Stx rather than luminal attack by STEC³⁵⁷. The first Gb₃ expressing target encountered by Stx and LPS when absorbed is the human intestinal microvasculature, where endothelial cells highly express Gb₃³⁴⁶. Stx also binds to stromal cells and fibroblasts adjacent to the intestinal epithelium, providing a variety of additional targets^{345,346}. Interestingly, although cattle do have some intestinal epithelial Gb₃, their intestinal microvasculature is devoid of the Stx receptor, and this may explain their tolerance to gastrointestinal colonization by STEC³⁴⁶. It is believed that the direct Stx cytotoxic action on the intestinal epithelial cells, the secondary direct action of other bacterial products, and the thrombotic microangiopathy that develops in the intestinal microvasculature following barrier function breakdown, all contribute to the hemorrhagic colitis present in these patients.

Shiga toxin probably circulates in the bloodstream bound to both blood cells and plasma proteins, and it is likely that the delay between bloody diarrhea and HUS development is partially due to this circulation time. Human serum amyloid P (HuSAP),

a normal component of human blood, has been demonstrated to bind Stx2, though it is likely that other molecules participate as well^{358,359}. HuSAP binds weakly to Stx2 though not Stx1, and over a few days the Stx2 gradually released from the protein complex is capable of killing target cells³⁵⁸⁻³⁶¹. The concentration of serum HuSAP increases in inflammatory conditions, though no relative increase is present in patients with STEC infection that develop HUS compared with those that do not^{360,361}. In patients with HUS, Stx1 and Stx2 can be detected bound to all leukocytes by flow cytometry, and remain detectable for up to 5 days after resolution of diarrhea^{77,235-238}. Much of this binding may be due to non-specific adherence following activation of the leukocytes and platelets, or may be facilitated by HuSAP interaction with Stx^{238,325,362,363}. Stx can also bind to the P blood group antigen on erythrocytes³⁶⁴. The five day time period of Stx persistence in the circulation correlates with the lag time between initiation of patient bloody diarrhea and development of HUS, and increased neutrophil lifespan in these patients may extend the Stx circulation time^{31,178,236}. Nevertheless, the relative amounts of Stx bound to circulating leukocytes and plasma proteins has not been determined, and the mechanistic details of Stx plasma transport remain to be explained.

The Shiga toxin and LPS in the bloodstream circulate to tissues that express Gb₃. The non-intestinal human tissues that express Gb₃ on one or more cell types display varying degrees of pathology in these patients. Renal glomerular and tubular injury occurs *in vivo*, and is often the cardinal sign of HUS development. Urine levels of the tubular protein *N*-acetyl glucosaminidase and β_2 -microglobulin, a protein normally reabsorbed by the proximal tubule, are increased both during the prodrome and during HUS^{330,365}. Glomerular and tubular apoptosis occurs in HUS patients (Figure 10), likely

causing the renal and vascular dysfunction^{195,341}. Furthermore, Shiga toxin binding to these Gb₃ expressing renal elements has been demonstrated in small studies, connecting the toxin with the observed pathology²³⁹. Stx binding and Gb₃ expression in the human kidney appears on subsets of renal tubules, the glomerular endothelium, and the non-glomerular vascular endothelium²³⁹.

Figure 10. Light micrographs of renal cortical apoptosis from HUS patients.

Light microscopy (A-C) and TUNEL staining (D, E) of D+HUS (A, B, D) and normal renal biopsies (C, E). HUS samples have glomerular thrombi (arrow, A) and interstitial inflammatory cells (arrow, B). HUS patients demonstrate apoptotic TUNEL positive cells in glomerular and tubular structures (D). Magnification $\times 392$ (all panels). (Taken from *Infect Immun.* 1998. **66**: 636-644.¹⁹⁵)

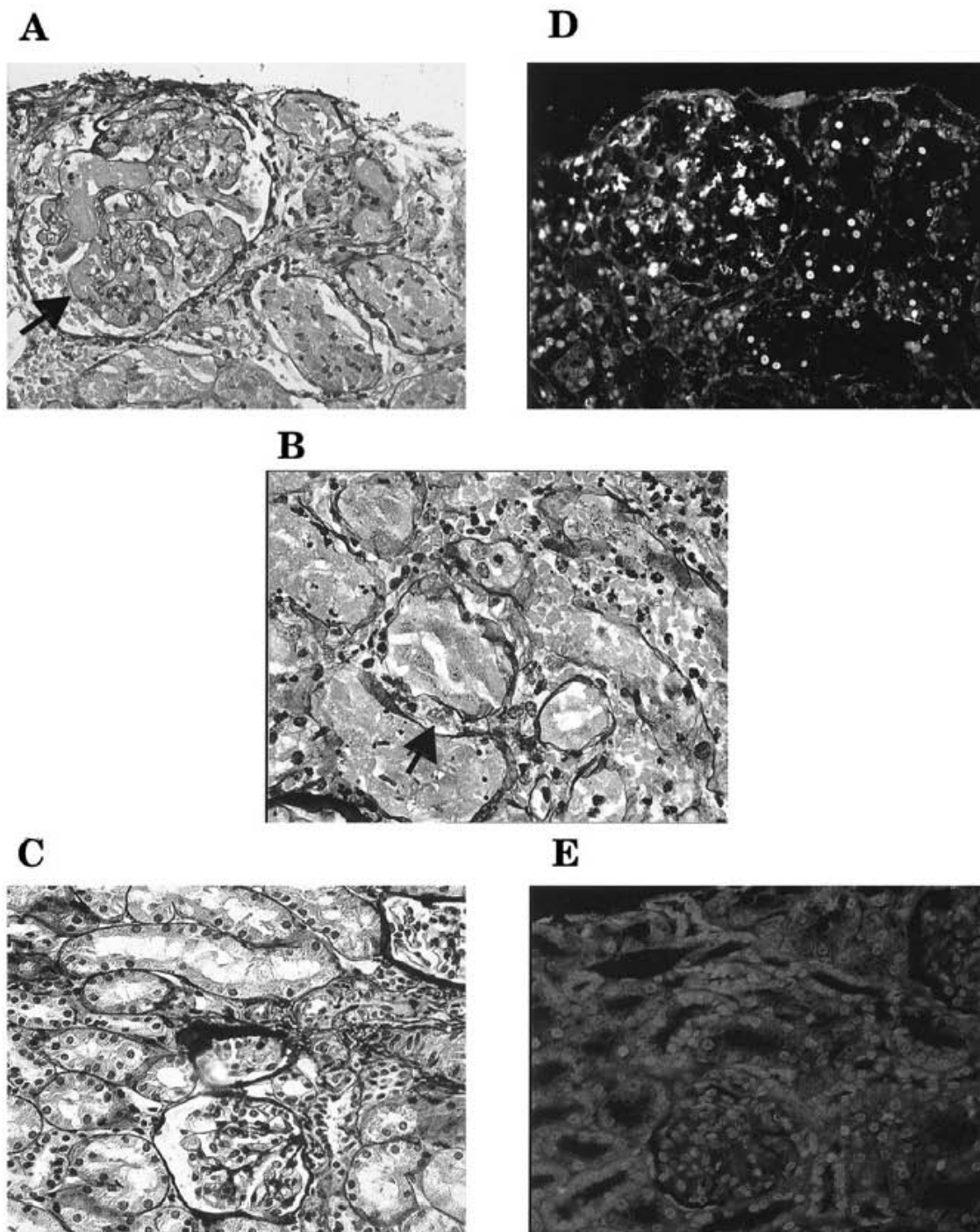


Figure 10. Light micrographs of renal cortical apoptosis from HUS patients.

There are various theories as to why the kidney appears to be specifically affected by circulating toxins in HUS. First and foremost, the human kidney expresses the Stx receptor Gb₃ on both glomerular and tubular cell types^{107,234}. Because the kidneys receive 20% of the cardiac output, besides the lungs and heart they likely encounter the largest dose of circulating toxins¹⁵. The renal blood flow is far greater than in other vascular beds, and additionally, so is the energy consumption needed to process this tremendous volume into only a relatively tiny proportion of urine¹⁵. Thus, renal insult may be magnified by the large metabolic need of the tissue. Furthermore, the solute concentrating mechanism of the medullary interstitium is prone to collect nephrotoxins as well as solutes, and may accumulate toxin concentrations above those present in plasma¹⁸. Pro-coagulant ability may also predispose the kidney to excessive thrombosis once initial endothelial damage occurs, as the renal glomerular podocytes produce high levels of tissue factor^{366,367}.

Even though it is generally accepted that the renal vasculature is the primary site of toxic damage in D+HUS, the precise location of Gb₃ in the human kidney is the subject of some controversy. *In situ* binding of Shiga toxin to human renal sections demonstrates that the renal binding profiles of Stx1, Stx2, and the rat IgM against Gb₃ are not identical¹⁰⁷. Stx1 binds only some adult human glomeruli, while Stx2 and anti-Gb₃ antibody stain all glomeruli, and all three stain many tubules including collecting ducts and loops of Henle^{107,368}. However all these human studies have been performed with sections dehydrated in ethanol, a reagent that is known to remove Gb₃ from some tissues and create falsely positive staining in others^{107,369}. Another caveat that may cast dubious light on the location of Gb₃ in the human kidney is that some studies allow Stx binding at

4°C as compared to 37°C. 4°C binding displays 10-fold increased staining of all tissues and is more likely non-specific and non-physiological^{107,234}. Additionally, Stx1 and Stx2 have different binding kinetics and bind different pools of probably slightly altered Gb₃¹⁰⁷. Stx1 interacts with a select and distinct group of synthetic monodeoxy Gb₃ analogs assayed by TLC than does the rat IgM or Stx2. Finally, FITC labeling of the B subunit is commonly used to follow Stx, however the FITC alters the binding of Stx1B to Gb₃¹⁰⁷. Nevertheless, as stated above, even though not all glomeruli bind Stx1, all glomeruli are labeled by Stx2 and the rat IgM anti-Gb₃¹⁰⁷. Thus, the consensus human renal targets of Stx include multiple tubular epithelial cell types as well as glomerular endothelial cells and podocytes of some patients under some conditions, and all studies agree that significant Gb₃ is present in the human kidney.

Irrespective of Gb₃ localization, the pathophysiology of renal failure in HUS is distinct from that which develops in *E. coli* induced and endotoxin mediated sepsis. Septic renal failure is associated with high cardiac output, increased renal blood flow, and decreased renal vascular resistance in contrast with the hypertension that develops in HUS²⁶. It is the renal vascular vasodilation that causes decreased GFR in sepsis because the plasma is not pushed across the filtration barrier into the tubular system²⁶. Normally post-glomerular efferent arteriole constriction increases the post-glomerular vascular resistance, and causes increased filtration of plasma into the lower pressure tubular system²⁶. In sepsis, the afferent and efferent glomerular arterioles both dilate, increasing the renal blood flow but decreasing the GFR²⁶. Thus, in septic renal failure, the serum creatinine and BUN rise because of decreased filtration, and the role of primary intrinsic damage to the renal parenchyma is controversial²⁶.

Although the primary effect of Shiga toxin likely stems from its interaction with endothelial and parenchymal cells, it is known to directly affect some circulating cell types as well. In mice, cattle, and humans Stx is cytotoxic to circulating lymphocytes, though the susceptible subsets vary between species¹¹⁶. Erythrocyte binding by Stx may be accompanied by direct red blood cell cytotoxicity, though oxidative damage from other vascular complications may also weaken erythrocyte membranes to shear stress^{116,364,370}. Neutrophil apoptosis is inhibited but other functions are not affected by either Stx1 or Stx2, and the neutrophilia and subsequent neutrophil deactivation in acute HUS is probably due to colitis derived cytokine production and inflammation^{178,362,363,371-373}. In spite of these described interactions, a causative role for direct Stx interaction with circulating cell types in HUS patients remains to be demonstrated.

Neurologic dysfunction in HUS patients probably derives from a combination of direct cerebrovascular insult by circulating bacterial toxins and metabolic wastes present because of decreased or absent renal function^{31,32}. Typical metabolic abnormalities present in states of renal failure include plasma hypotonicity, metabolic acidosis, hyperosmolality, hypoglycemia, hypocalcemia, and hypermagnesemia, however even when properly dialyzed many patients with severe renal disease still express virulent central nervous system disorders^{31,32}. HUS associated encephalopathy and neurologic dysfunction are most strongly correlated with HUS mortality, however the etiology and related factors are relatively unexplored¹⁸⁰. Those HUS patients who do develop neurologic symptoms have increased serum levels of some inflammatory mediators including IL-6, IL-10, soluble TNFR1, and TIMP-1²⁵². However, there are no significant

differences between encephalopathic patients and those without neurologic dysfunction in terms of leukocyte counts, thrombocytopenia, BUN, serum creatinine, or other markers of disease progression, even though encephalopathy generally occurs in those patients who are qualitatively more diseased²⁵². Because of its strong correlation with poor outcomes and the paucity of relevant etiological and therapeutic data, the pathogenesis and treatment of CNS dysfunction in Stx mediated HUS represents a necessary focus of future research.

Metabolic disorders in HUS derive from the renal dysfunction, the acute hemolysis that releases normal erythrocyte contents into the systemic circulation, and tissue hypoxia. Hyperkalemia (increased extracellular potassium) occurs in this disease from aberrant renal potassium regulation due to hypofiltration, tissue catabolism, and from intravascular hemolysis^{19,176,190}. Hyperkalemia is common in oliguric ARF, and HUS patients are at increased risk because of the concurrent intravascular hemolysis²¹. Potassium is the most abundant intracellular cation, and only 2% of bodily potassium is normally extracellular³⁷⁴. In situations of hemolysis, this potassium is released into the extracellular space, and a release of only 1% of bodily potassium can double the plasma concentration³⁷⁴. Without a means to effectively remove excess intravascular potassium, hyperkalemia ensues. Lactate dehydrogenase (LDH) is also released by red blood cell lysis, and contributes to the lactic acidosis, though tissue hypoxia probably significantly mediates increased lactic acid production as well. Other metabolic disturbances including hyperphosphatemia, hypocalcemia, and hyponatremia result from renal failure or the resulting intravascular volume dilution¹⁹⁰.

Insight into the pathophysiology of HUS can be found in the development of Shiga toxin independent thrombotic microangiopathy. The thrombotic microangiopathies have been proposed to result from a similar histopathologic lesion, and can occur during post-diarrheal HUS, familial genetic HUS, thrombotic thrombocytopenic purpura (TTP), systemic lupus erythematosus (SLE), infection with *Streptococcus pneumoniae*, renal transplantation with immunosuppression, malignancy, various medication usage, and after pregnancy associated with preeclampsia^{83,149}. As mentioned previously, atypical familial HUS occurs in patients who have genetic mutations in endothelial-protecting complement genes including Factor H, Factor I, membrane cofactor protein (MCP), and delay accelerating factor (DAF)^{83,375}. Mutations in these complement inactivating proteins cause abnormal activation of complement component C3 resulting in microvascular endothelial damage⁸³. Also as discussed previously, TMA in TTP occurs following the abnormal formation of extra-large vWF that activates intravascular coagulation. In pneumococcal infection, TMA is caused by the bacterial neuraminidase exposure of the normally cryptic Thomson-Friedenreich antigen, and subsequent autoimmune endothelial damage similar to that found in SLE^{83,149}. Finally, post-transplantation TMA results from endothelial dysfunction due to immunomodulatory drugs¹⁴⁹. Although the pathological details of these diseases are distinct, and the composition of the glomerular thrombi differ between the diseases, the common pathway is hypothesized to occur because of disruption of the normal platelet-endothelial cell interaction¹⁴⁹.

Evidence for a similar endothelial etiology among the thrombotic microangiopathies comes from case reports of individuals with confirmed STEC

mediated HUS who also have underlying defects in ADAMTS13 activity. One patient with concurrent STEC induced HUS and decreased ADAMTS13 activity demonstrated more severe disease and clinical features more like TTP¹⁸¹. Specifically, this patient displayed the typical HUS findings of anemia, thrombocytopenia, and acute renal failure, but also fluctuating neurological signs, fever, and abnormal liver function¹⁸¹. These data suggest that the distinct modes of endothelial damage that normally mediate TMA may be able to synergize in some patients, and cause mixed forms of TMA that utilize the pathophysiology of both syndromes.

Long lasting renal dysfunction in HUS patients follows from initial glomerular destruction and subsequent hyperfiltration and hyperperfusion injury²²⁴. Generally in cases of renal glomerular damage, glomeruli that are not destroyed in the acute phase of disease have to compensate by processing comparatively more blood than they had to previously when more functional glomeruli existed²¹¹. These remaining glomeruli are thus hyperperfused and this hyperfiltration causes injury^{211,224}. Specifically, remaining glomeruli exhibit increased urinary albumin excretion and decreased ability to appropriately deal with systemic protein loading. These patients also more rapidly lose additional function than patients without an initial acute glomerular insult²²⁴. Thus initial loss of functional nephrons both decreases the ability of the kidneys to perform their tasks normally and increases the future rate of glomerular loss, overall leading to early onset chronic renal failure^{211,224}.

By synthesizing the data from multiple clinical studies of HUS patients in the acute state and during other related diseases, it seems that the two major observable pathophysiologic changes aside from overt pathology, the inflammation and coagulation,

have distinct roles in this disease. The inflammation usually takes place concurrently with the gastrointestinal infection prior to HUS development, and many of the mediators found circulating in HUS patient plasma are not different from those found in patients who only develop STEC colitis, except in their levels⁷⁸. As discussed above, the increased inflammatory mediators may correlate with worse disease because they serve as a marker for intestinal breakdown, leukocyte trafficking of Shiga toxin, and total toxin dose entering the body, and may have no causal role in the syndrome⁷⁸. Although the inflammation may contribute to the Stx mediated target tissue damage by upregulating the Gb₃ receptor, weakening the immune system, providing an initial insult to various tissues, and perhaps altering parts of the coagulation cascade, there is little evidence that the inflammation is the lynchpin to disease development⁷⁸.

In contrast, the pathology of microangiopathic hemolytic anemia clearly involves dysregulated coagulation, endothelial damage, and overall activation of pro-coagulant and fibrinolytic activity. The changes in coagulation factors are not similar to inflammatory DIC. Not only do the changes in coagulation precede the development of HUS, they continue during the acute disease when most inflammation in these patients has subsided¹⁹⁹. The coagulation changes typically occur just prior to and during the acute phase, with a spike in platelet consumption followed by prolonged thrombocytopenia. Furthermore, the resolution of renal failure usually follows normalization of hematologic abnormalities¹⁹⁹. Thus it seems that though the inflammation may serve to augment the damaging and hemostatic influences of Shiga toxin mediated HUS, and though the inflammation may directly cause part of the

coagulopathy, the primary pathologic alterations center around coagulation and fibrinolysis. Thus these are the areas where increased research effort is warranted.

If the crucial pathologic mechanism is the coagulation, and the coagulation abnormalities definitively occur before patients meet the case definition of HUS, then the time for therapeutic intervention in these patients occurs before they meet the case definition of HUS. In agreement, because the platelets, leukocytes, and coagulation system are in a post-activated state during acute HUS, it follows that activation of these systems occurred before the onset of fulminant HUS. Therefore it seems likely that once the threshold of damage has been breached and HUS occurs, treatment options beyond supportive therapy are not useful. This assessment of the data has been borne out by trials of therapeutics in HUS patients: only supportive therapy has demonstrated any beneficial effect. The failures of numerous anticoagulant, antiplatelet, and anti-inflammatory therapies to preempt morbidity and mortality during the acute phase of HUS are explained by this interpretation of the disease process, and suggest that the only time to attempt novel therapeutics is during the hemorrhagic colitis before the onset of significant signs or symptoms of extraintestinal tissue dysfunction.

Treatment for the Hemolytic Uremic Syndrome

Treatment for post-infectious Shiga toxin mediated HUS is currently entirely limited to basic supportive care including intravenous saline and dialysis^{31,32,35,157,186,376}. Dialysis is required because of persistent renal failure in up to 60% of HUS cases, and although patients with other forms of TMA may benefit from plasmapheresis, plasma infusions, or

platelet infusions, there is no role for these treatments during D+ HUS^{149,168,196,215}.

Dialysis effectively maintains these patients during renal failure, as evidenced by complete recovery of some even after months of dialysis¹⁸⁶. Furthermore, aggressive dialysis started within 24-48 hours of oliguria correlates with better outcome, consistent with data showing that prompt hospitalization allows better care and improved prognosis in these patients^{186,376}. Indications for dialysis include anuria, hyperkalemia, volume overload, and severe acidosis, though those patients with severe renal failure manifested by increased BUN and creatinine who still produce urine may do well without renal replacement therapy³⁷⁶. The acute mortality rate in HUS patients has declined from greater than 45% to less than 1% over the past 50 years, and improvements in supportive care are primarily responsible for this change^{31,32,157,170,180,377}. Prior to the use of early dialysis, many children with HUS died of fluid overload, metabolic abnormalities including hyperkalemia and acidosis, hypervolemia, and uremia during the oligoanuric phase^{32,170,377}.

Besides dialysis, other commonly used treatment procedures for patients in the acute phase of HUS include red blood cell transfusions and general maintenance of normal extracellular volume in spite of vomiting, diarrhea, declining oral intake, hypoalbuminemia, and oliguria³¹. During the prodrome, renal perfusion should be sustained by increasing blood volume with intravenous fluid; however once HUS begins the primary effect of oliguria is volume overload with edema and lung compromise and intravenous fluids should be restricted³¹. For these reasons diligent monitoring of intravascular volume during the course of disease development is crucial³¹. Up to 80% of patients require one or more erythrocyte transfusions because of anemia during the acute

phase of HUS, though these can also contribute to hypertension if administered too rapidly^{31,378}. Blood products should thus be volume reduced and depleted of leukocytes to counteract any possible inflammatory aspect to the syndrome³¹. Oliguric and anuric patients with or without hemolysis may also necessitate potassium restriction to prevent hyperkalemia and phosphate binders to prevent hyperphosphatemia³¹. If hypertension or cardiopulmonary overload occurs fluids are rapidly restricted and patients are treated with vasodilators like calcium channel blockers along with dialysis^{31,190}. Angiotensin converting enzyme (ACE) inhibitors are only used after the acute stage of HUS has passed. These patients must be hospital admitted and carefully monitored³¹. The average hospitalization lasts 23 days though it can continue for months before resolution of renal function⁵⁹.

Although direct support for aggressive intravenous volume expansion to treat HUS without volume overload comes from only one clinical trial, additional data suggest that volume depletion correlates with worse outcome^{20,31,33,36,177-180}. Specifically, higher hemoglobin levels on admission are associated with poor prognosis²⁴⁴. Even though the increased hemoglobin is paradoxical considering the disease consists of microangiopathic hemolytic anemia, the most likely cause of the increased hemoglobin is dehydration and hemoconcentration from the diarrheal prodrome. This diarrheal fluid loss occurs before the onset of HUS and hemolysis, explaining why both early increased hematocrit and later decreased hematocrit are compatible. Though unresolved, hemoconcentration and volume depletion could cause worse disease by increasing the relative concentration of systemic toxins, by causing microvascular sludging with increased shear stress followed by coagulation and hemolysis, or by augmenting vessel occlusion and decreasing

appropriate tissue perfusion thus adding secondary ischemic insult to the tissue²⁰.

Despite the lack of mechanism for the therapeutic effect, isotonic saline volume expansion is nephroprotective during STEC infection and should be used, with the primary potential side effect being fluid overload with lung edema and effusion^{20,31}.

Currently, new treatment regimens focus on blocking Stx access to the systemic circulation, however little progress has been made. Antibiotics increase the intestinal release of Stx upon bacterial lysis and are contraindicated, oral administration of Stx-binding agents does not prevent HUS in human studies, and Stx blocking antibodies have not yet progressed through clinical trials^{31,35,38,379-381}. Treatment with antibiotics increases the risk of progression from hemorrhagic colitis to HUS up to 50% in retrospective studies, and thus current recommendations prohibit the use of antibiotics in these patients^{20,33,35,38,78,379,380}. However, these studies typically used sulfa-containing, β -lactam, or fluoroquinolone antibiotics, so other classes may still prove clinically useful^{33,78,379}. Though still not in use, anti-Stx blocking humanized antibodies are in advanced clinical trials, and represent the most likely novel improvement coming to the field in future years³⁸²⁻³⁸⁵. Administration of these inhibitory antibodies may be able to limit the extent and duration of Stx damage, and lessen the probability of developing HUS in STEC infected patients. Nonetheless, in spite of novel treatments in the pipeline, the current regimen still primarily consists of aggressive intravenous rehydration and saline volume expansion upon diagnosis of STEC positive bloody diarrhea^{20,31,381}.

Therapeutics without any beneficial effect also include corticosteroids, diuretics, plasmapheresis, and fibrinolytics including urokinase and streptokinase^{31,170}.

Contraindicated are antimotility agents, narcotics, and nonsteroidal agents, although only

antimotility agents have been associated with increased risk of developing HUS and subsequent neurological complications^{31,35}. Methylprednisone does not modify acute HUS hematological, neurological, or nephrological outcomes in low-power placebo controlled patient trials³⁷⁸. Non-steroidal anti-inflammatory drugs can decrease what may be already diminished renal blood flow by blocking afferent glomerular arteriole vasodilation^{23,31}. Diuretics have the theoretical ability to decrease medullary tubular energy consumption and oxygen demand, but have shown no consistent ability to improve outcomes in any type of acute renal failure^{31,386}. Unlike TTP, in which abnormal or inhibited ADAMTS13 can be replaced by plasmapheresis, no single plasma enzymatic disturbance occurs in HUS^{170,181}. Though thrombin activation is thought to be a critical aspect of the pathogenesis of HUS, pharmacologic inhibition of thrombin activity with heparin lacks effectiveness and increases lethal hemorrhage in trials^{32,176,185,186,306,387-389}. Anticoagulants are most likely ineffective during the acute phase because the acute pro-coagulant incident has already passed, with these patients then in a hypocoagulant state and no longer in need of further anticoagulation³⁰⁶. Thrombolytic efficacy is difficult to evaluate and streptokinase demonstrates little positive effect in small older trials while also being associated with deadly hemorrhages³⁸⁸. Finally, the sporadic nature and rural association of most cases of the disease, and the need to often initiate therapy before diagnosis is confirmed, makes performing randomized controlled trials on any new therapeutic regimens extraordinarily difficult³⁸⁷. For this reason, significant advances must be made in model systems before the effort and resources can be gathered to perform the painstaking studies in HUS patients.

Treatments for HUS patients who progress to long term renal dysfunction have little option other than standard care for renal decline²¹¹. Diligent observation of patients after resolution of the acute stage of HUS is necessary yearly for the first decade, dropping off to every other year afterwards²²⁰. Hyperfiltration injury manifest by microalbuminuria, increased serum creatinine, and rising blood pressure is the primary concern²²⁰. Pharmacologic therapy in these patients includes angiotensin-converting enzyme (ACE) inhibitors in cases of lasting proteinuria or hypertension^{170,211,390}. Protein restriction to reduce the filterable protein load encountered by the kidney is also advised, and its combination with ACE inhibition is associated with improved long term renal outcome^{211,390}. For more severe and persistent renal failure, renal transplant is available, and D+HUS patients have very low risk of recurrence^{170,212,391}. This is in contrast to patients with end stage renal disease due to other forms of thrombotic microangiopathy, like atypical familial HUS, for which there is a high incidence of recurrence in the transplanted kidney³⁹¹. Overall, good outcome from long term renal dysfunction following acute STEC mediated HUS is determined by prompt and proper treatment of declining renal parameters, making appropriate observation and routine testing for renal decline vital²⁰⁶.

Given the lack of therapeutics, the most effective strategy to prevent HUS is to prevent infection with Shiga toxin producing *Escherichia coli*^{55,73,80,170}. However, creation of environments and raw food products completely free from STEC is not practically possible, and thus infection is best averted by implementing superb levels of hygiene throughout the food production chain⁴⁹. Awareness of the signs and symptoms of STEC gastrointestinal infection are necessary for when preventative measures fail.

Early recognition of STEC infection allows prompt intravenous volume expansion, and may in the future allow treatment with new and potent therapeutic regimens.

Furthermore, in general those patients who develop HUS present to the hospital up to three days later than those children with uncomplicated hemorrhagic colitis, suggesting that earlier presentation allows better treatment²⁴⁸. Thus, children with bloody diarrhea should be immediately initiated on intravenous fluids and have their stool tested for Stx or STEC. To ensure proper management of the patient, continuous careful monitoring for signs of volume overload and deterioration to fulminant HUS should continue past resolution of the hemorrhagic colitis in cases of STEC positivity. Careful supportive care has improved the mortality of children in the acute stage of HUS from 45% to less than 1% in the most current epidemic forms, mostly due to modern fluid administration and dialysis techniques^{170,186}.

After the acute phase, patients should be closely monitored for signs of renal decline, specifically for microalbuminuria or hypertension, and aggressively treated with dietary protein restriction and ACE inhibition at the first signal of declining GFR^{40,211,215,219}. Those patients who maintain a GFR above 80 mL/min without dipstick measured proteinuria above 0.3 g/L and without hypertension have very good prognosis²¹⁶. Other progressive organ dysfunction associated with HUS should also be watched, with particular attention to hyperglycemia and decreased insulin production secondary to pancreatic insult²⁰⁵. The best way to prevent long term complications is to decrease the renal damage that occurs in the acute phase because despite that most patients recover well with only supportive care, long term severe morbidity remains significant and correlates with the severity in the acute phase. Therefore novel treatment

modalities to prevent dire outcomes are still needed for HUS, and can probably best be developed and studied in animal model systems.

Animal Models of the Hemolytic Uremic Syndrome

Although large animal models of Shiga toxin mediated HUS appropriately recapitulate the human syndrome, they are expensive and difficult to manipulate³⁹²⁻³⁹⁷. Nevertheless, these models serve as proof of principle that the crucial etiologic agent is Shiga toxin. Both the dog and the baboon models demonstrate hemolytic anemia with schistocytes, acute renal failure with thrombotic microangiopathy, thrombocytopenia, and coagulation disorders found in human patients, however their hefty requirements only allow the use of small numbers with little repetition of experiments³⁹⁵⁻³⁹⁷. The robust investigation of pathologic mechanisms and new therapeutics requires a model that is more easily altered and can be studied in a variety of precise and large scale manners. To this end, many groups have attempted to use rodents and rabbits to study the pathophysiology and treatment of Shiga toxin induced HUS. Unfortunately, descriptions of these model systems remain incomplete or do not accurately recapitulate the human disease (Table 1).

In general, recapitulation of HUS may be theoretically accomplished by either gastrointestinal infection with STEC or direct administration of Shiga toxin to create systemic toxemia^{85,94,116,119,392-394,398-427}. Though mimicking the route of toxin absorption in HUS patients, models utilizing gastrointestinal infection are more variable and less reproducible than the controlled administration of specific Stx doses at particular times³⁸⁷. Most of this unpredictability probably derives from the inconsistent absorption

of Stx into the enteric circulation. Gastrointestinal administration of STEC also has the added limitation of providing an unrestricted source of LPS and bacteria to the model system, which may cause DIC or the Shwartzman reaction, conditions difficult to discriminate from the pathophysiology of HUS. The limitation of direct administration of Stx is that this parenteral route does not occur in human disease³⁸⁷. For the following discussion of relevant animal models, systems utilizing both oral STEC infection and direct Stx injection are included and compared.

LPS is a difficult confounding element in all these studies, as all Stx isolations are purified from LPS containing bacterial cultures, because it can cause a host of effects even at low doses^{398,402,405}. There is some conflict as to whether LPS sensitizes animals to the effects of Stx, whether Stx sensitizes animals to the lethal effects of LPS, or whether LPS can desensitize animals to Stx^{402,403,405,406,408}. These conflicts have been borne out in many studies, and thus the relative roles of intentionally or unintentionally given LPS and Stx in these models is confusing and complicated. In most cases LPS appears to increase Stx mediated animal toxicity when given concurrently, and can desensitize animals by increasing endogenous corticosteroids if given prior to Stx^{403,405,406,408}. Though the most effective way to ensure that outcomes observed *in vivo* are due to Stx and not LPS is to employ LPS resistant TLR4 knockout mice, few reports have used these animals^{401-403,412}.

Because it is the most complete and physiologically relevant system, the baboon (*Papio anubis*) model of Shiga toxin induced HUS serves as the gold standard for animal modeling of this disease. Baboons possess Gb₃ in kidney cortex, kidney medulla, and colon, but not in the brain, and where present, Gb₃ exists in similar amounts compared to

human tissues⁴²⁸. Intravenous injection of 0.05-2.0 µg/kg Stx1 or 25 ng/kg Stx2 into the baboon femoral vein in a single bolus causes the clinical and laboratory features of human HUS, with hemorrhagic colitis, acute renal failure, thrombocytopenia, hemolytic anemia and death after 36-72 hours⁴²⁹⁻⁴³¹. Injection of the same relative amount of toxin in four divided doses over 48 hours causes no pathological change, though injection of this sub-pathological Stx1 dose concurrent with 1 mg/kg LPS results in HUS features^{430,432}. There are no differences between the effects of Stx1 and Stx2 except for relative potency; the induced pathology is identical⁴³¹. Parenteral administration of LPS alone causes thrombocytopenia after 24 hours, some schistocytosis, mild anemia, increased serum and urine cytokines, and some proteinuria, but no renal failure or evidence of thrombotic microangiopathy⁴³². Serum vWF is increased by LPS in the baboon, but not by Stx, and vWF levels are independent of disease progression or outcome²⁹⁶. LPS likely increases baboon sensitivity by increasing the expression of tissue Gb₃⁴³³. Although LPS alone causes some hematologic and renal findings reminiscent of HUS, there is no associated thrombotic pathology and single LPS injection does not cause true HUS features in the baboon model⁴³².

Stx1 and Stx2 cause some inflammation of the baboon adrenal glands, lungs and liver, however the major pathologic findings are hemorrhage, microvascular fibrin-rich thrombosis, vascular congestion, endothelial and podocyte swelling, and epithelial necrosis, each observed in the gastrointestinal tract, adrenal glands, kidney and lungs^{429,430}. Very little leukocytosis is observed with Stx administration alone⁴²⁹. The symptoms of renal dysfunction include proteinuria, hematuria, increased serum creatinine and BUN, hyperkalemia, and oligoanuria after 12-24 hours⁴²⁹⁻⁴³¹. Hematologic disorders

include increased fibrinogen concentrations, fibrin split products, and tissue plasminogen activator, anemia with some schistocytes and thrombocytopenia after 24 hours⁴²⁹⁻⁴³¹. Coagulation times including PT and PTT are normal⁴²⁹. Neurologically, these animals exhibit brain edema, demyelinated nerve fibers, and seizures but little overt pathology and no microvascular thrombosis, consistent with low cerebral Gb₃ expression⁴²⁸⁻⁴³⁰. While little increased serum inflammatory mediators are detected, IL-6 and TNF- α are found in the urine within 2-6 hours after Stx1 administration^{429,430}. Chronologically, increased urine cytokines precede the initial signs of renal damage (proteinuria, at 24 hours), which is followed by further hematologic and renal injury (hematuria, schistocytosis, thrombocytopenia, at 36 hours), and then by complete renal failure (oligoanuria) and death (seizures) after 60 hours^{430,431}. No amelioration of signs, symptoms or pathology occurs if baboons are given prophylactic heparinization prior to Stx challenge⁴³⁴.

The paradoxical finding in the baboon is that increased Stx1 administration (2.0 $\mu\text{g}/\text{kg}$) is associated with augmented gastrointestinal damage, cerebral damage, renal tubular necrosis, serum markers of renal failure, and faster death, but also with diminished renal glomerular and hematologic pathology compared to low dose Stx1 (100 ng/kg)⁴²⁹. Thus, formation of the critical renal lesion of fibrin-rich thrombotic microangiopathy with anemia positive for schistocytes is increased by injecting less Stx1 to baboons, however decreased renal function, urine output and survival is associated with high dose Stx1⁴²⁹. These data may suggest that the systemic dysfunction described by renal failure and survival is unrelated to the unique glomerular and microvascular pathology present in these animals and HUS patients, though this contention has not been

investigated by any other manner. The baboon also differs from observations made in human HUS patients in that the hematologic abnormalities, such as decreased factor VII, increased tPA, and raised fibrin degradation products do not occur until the animals enter renal failure and satisfy the case definition of HUS⁴²⁹. This is in contrast the coagulation disorder manifest during the diarrheal prodrome in humans before the onset of HUS^{330,429}. Furthermore, no decrease in coagulation factor VII is observed in humans⁴²⁹. Although the cause of these interesting observations in the baboon might be explained after repetition of these experiments with a broader range of toxin concentrations and controlled manipulation of the model system, the prohibitive cost and difficulty in using this system have discouraged those investigations.

Nonetheless, the baboon model lays the groundwork for other animal model systems by demonstrating that injection of the toxins known to be involved in HUS can cause a similar syndrome in the absence of STEC gastrointestinal infection. The baboon experiments also suggest that cerebral damage is not necessary to cause animal death, as the cerebral pathology in these animals is relatively minor, even though human HUS fatalities are most correlated with neurological dysfunction^{180,429,430}. In this case, it may be the renal failure or hematologic abnormalities that lead to the eventual demise of these animals, and this could be proved by additional experiments treating them with dialysis. Work with the baboon demonstrates that there is a threshold for development of HUS in response to Stx1 dose, specifically that 50 ng/kg causes HUS features, while 25 ng/kg does not without LPS co-administration^{429,430,432}. Finally, these data implicate Stx alone as being the crucial agent in human HUS, as LPS is not needed for HUS development in this system, though it can intensify the effects of sublethal Stx1 doses^{429,430,432}. However

the lack of neurologic damage in these animals suggests that there are crucial differences between the human and baboon in this disease context. The seizures observed in these animals may be due to Stx damage, though more likely are due to the renal failure and resulting uremia. Additional differences include the changes in coagulation factor VII, and the timing of coagulation changes. In conclusion, the baboon model appears best able to recapitulate the renal and hematologic changes of human HUS, with unclear relation to the neurologic changes and coagulation disorders that occur in humans.

New Zealand White rabbits develop diarrhea and neurologic complications when exposed to oral STEC infection or Shiga toxin by injection^{85,392,393,417-419,421,422,425}. Rabbits given 2×10^8 STEC or 0.2-20 $\mu\text{g}/\text{kg}$ Stx1 or Stx2 intravenously develop anorexia, dehydration, diarrhea, weight loss, paresis, and decreased urine output starting 24 hours post-injection, and die in 3 days^{392,393,418,419,422,425}. Co-infusion of 30 $\mu\text{g}/\text{kg}$ LPS increases the Stx mediated lethality, diarrhea, and dehydration, though this enhancement only occurs when LPS is given 8-24 hours after Stx2⁴⁰³. The diarrhea and flaccid paralysis in these rabbits is progressive, with edema and hemorrhage as well as thrombotic microangiopathy with fibrin thrombi of the intestinal and cerebral vasculature^{392,420}. These changes correlate with Gb₃ presence on both intestinal and cerebral vascular endothelial, epithelial, and neuronal cell types³⁹⁴. However, the rabbits do not develop anemia, thrombocytopenia, leukocytosis, or schistocytes^{392,393}. Though renal function indicators rise slightly, these rabbits lack renal Gb₃ on glomerular and tubular cells, and have no renal damage when observed pathologically^{392-394,419}. The anuria and weight loss are due to a combination of diarrheal dehydration, adipsia (lack of

drinking), and anorexia (lack of eating)³⁹². The rabbit model demonstrates that Stx alone can cause the bloody diarrhea, neurological complications, and some vascular lesions of HUS in the absence of gastrointestinal bacterial infection. Nevertheless, although the rabbit model provides a valid means to evaluate intestinal and neuronal damage in Stx mediated TMA, it is insufficient for the study of renal and hematologic changes because it fails to replicate human HUS^{392,393}.

The Dutch Belted (DB) strain of rabbit infected with STEC develops more complete HUS compared to the New Zealand White strain, although not when given Stx2 alone⁴²⁶. Though lacking total leukocytosis, Dutch Belted rabbits inoculated with 5×10^8 bacteria develop neutrophilia, very mild anemia, mild thrombocytopenia, mildly increased BUN, rare increased serum creatinine, and hyperkalemia^{423,424}. Mimicking other rabbits, the Dutch Belted develop watery and bloody diarrhea with transmural intestinal edema and hemorrhage⁴²⁶. Fibrin thrombi are found to occlude the microvascular glomerular capillaries, along with peripheral blood schistocytes, tubular necrosis, and endothelial swelling in some Dutch Belted rabbits given STEC^{423,424}. However, the increased BUN without significantly increased serum creatinine suggests a pre-renal failure as opposed to renal dysfunction from an intrinsic process, even with associated renal lesions^{423,424}. Because the model utilizes STEC gastrointestinal infection, the visible renal lesions may be due to either septic DIC or the LPS induced Schwartzman reaction^{423,424}. Dutch Belted rabbits given 1200 ng/kg Stx2 alone develop only diarrhea, neutrophilia, increased fibrinogen concentration, increased IL-8, tPA, PAI-1, and TNF- α mRNA, glomerular erythrocyte congestion, and some paralysis, with no thrombocytopenia or glomerular fibrin thrombi⁴²⁶. Although these authors describe thin

layer chromatography visualization of Gb₃ isolated from the cortices of these rabbits, the data are not shown⁴²⁴. Additionally, these authors claim that New Zealand White rabbits also have renal Gb₃ identified by mass spectrometry, a finding that has previously been clearly demonstrated not to be true, thus shedding doubt on their method of Gb₃ detection³⁹³. Until Gb₃ can be sufficiently demonstrated in the renal glomerular vascular cells of Dutch Belted rabbits, because appropriate pathology does not develop after administration of Stx alone, the value of this model will remain in doubt.

In contrast to rabbits, mice and rats given Stx or STEC do not consistently develop diarrhea, colitis or A/E lesions, however they do demonstrate some renal and neurologic pathology^{85,412}. Numerous mouse strains have been tested, including C57BL6, CD-1, C3H/HeN, C3H, HeJ, and BALB/c, and the results are comparable between strains^{94,116,119,394,398-413,427}. Rat strains used include Sprague-Dawley and Wistar, and again the results are relatively equivalent between strains^{394,414-416}. Nevertheless, the responses of mice and rats to Stx or STEC are incomplete in either the renal or hematologic aspect of the syndrome, and the relative timing of various findings has not been well documented. Intraperitoneal (i.p.) and intravenous (i.v.) administration of Stx appear to only differ in the timing of disease onset, with intravenous administration causing symptoms and pathology earlier than intraperitoneal injection, but both routes yielding equal calculations for the LD₅₀⁹⁴.

Stx1 and Stx2 administration to rats at between 10-200 ng/kg is lethal over an approximately 72 hour time course, though the time to death is extended with lower doses of Stx⁴¹⁴. In general Stx2 causes more severe damage than Stx1⁴¹⁴. When given to rats i.v., Stx2 travels to and binds the renal collecting duct epithelium within 3 hours,

though there is also weak binding to glomeruli⁴¹⁴. The glomerular binding is increased with higher doses of Stx at 200 ng/kg, and significantly diminished at 10 ng/kg, whereas the tubular binding is observed at all of these dosages⁴¹⁴. The collecting ducts display altered morphology over time, and these rats become polyuric 24-48 hours after Stx administration, with dehydration and weight loss⁴¹⁴. Increased aquaporin-2 is found in the urine of the polyuric rats, and the levels of aquaporin-2 in the urine better correlate with the renal histopathology than the levels of the proximal tubule damage markers *N*-acetyl glucosaminidase and β 2-microglobulin⁴¹⁴. Furthermore, these rats are unable to concentrate their urine in response to water restriction or exogenous vasopressin administration, and during polyuria the urine is abnormally dilute⁴¹⁴. These data imply that the primary damage to the rat occurs at the renal tubular system, specifically at the collecting duct, without any major sequelae in other organ systems. Thus, the rat only appropriately mimics the renal tubular damage of human HUS, and does not appropriately resemble the neurologic, gastrointestinal, hematologic, or renal glomerular damage in human patients.

The rat response to Stx has been further investigated by injecting Stx1 directly into the renal vasculature, and thus solely perfusing the kidney with toxin^{415,416}. Direct perfusion of 2 μ g/mL Stx1 at 2 mL/min (28 nM, for 6 μ g total Stx1 in 1.5 minutes), or 10 pM Stx1, followed by normal vascular reperfusion removes the role of any circulating inflammatory mediators or cells activated by toxin interaction with non-renal cell types. Specifically those consequences in response to Stx or LPS acting on other organs are eliminated, allowing pathological comparison to the contralateral unchallenged kidney of the same animal as a control⁴¹⁵. In these animals renal function can be assessed by

removing the contralateral normal kidney, and this demonstrates increased BUN, serum creatinine, and fractional excretion of sodium three days after perfusion^{415,416}. No pathologic change is visible in Stx perfused kidneys until the first day after perfusion, and on day 3 extensive tubular injury is apparent with vacuolation, pyknosis, nuclear loss, and sloughed epithelial cells^{415,416}. TUNEL stained apoptotic figures are only present in tubules and not in glomeruli, and mainly in the medulla but rarely in the cortex. The histopathology of tubular degeneration continues through the 9 days following Stx perfusion, however no glomerular changes are observed throughout the same time course⁴¹⁵. TNF- α mRNA is specifically upregulated in the medulla of these kidneys, with no change in cortical levels, though macrophage infiltration is seen in the medullary interstitium as well as the glomeruli⁴¹⁵. Finally, platelet aggregation increases in both the glomeruli and interstitial vasculature as measured by platelet specific immunohistochemistry and computed densitometry. These findings suggest that solely tubular injury can increase glomerular platelet aggregation⁴¹⁵. Unfortunately, high power images are not provided, so it is unclear if the glomerular platelets are singlets or true platelet clumps and thrombi⁴¹⁵. Overall, Stx perfusion of isolated rat kidneys demonstrates that Stx causes direct tubular injury without significant glomerular pathology in the rat, though glomerular changes in cell infiltration do occur. While it seems intuitively likely that changes similar to the rat take place in the mouse, the published murine studies are conflicting.

Labeled Stx2 has a short half life in mouse serum, and when given i.v. rapidly travels to the kidney within 1 hour of injection⁴³⁵. However, the exact cell types bound by Stx in the murine kidney have been conflictingly reported, as has the localization of

murine renal Gb₃ expression. Targeted knockout of the Gb₃ synthase gene eliminates the susceptibility of mice to all effects of Stx, demonstrating that Gb₃ is the sole Stx receptor³⁹⁸. In addition, the Fabry disease mouse model with approximately 100 fold increased tissue Gb₃ levels requires 20 times the dose of injected Stx or oral STEC to cause disease than in their wild type littermates¹¹⁹. The injection of recombinant α -galactosidase to the Fabry mice prior to Stx or STEC challenge reduces the levels of Gb₃ and resensitizes them to the effects of Stx¹¹⁹. Grossly, Gb₃ staining and Stx targeting is seen in all three main murine renal compartments, the cortex medulla and papilla, however the specific cellular localization is disagreed upon^{94,116}. One group of reports describe toxin binding to and Gb₃ expression on subsets of proximal, distal, and collecting duct tubular cells within the renal parenchyma^{94,116,408,410,414,427,435}. Other publications demonstrate Stx interaction with or Gb₃ expression on glomeruli, the renal vasculature, and other vascular cells³⁹⁸⁻⁴⁰⁰. Thus the exact localization of the injected toxin and its receptor in the murine kidney is controversial and in need of further characterization. Additional sites of published murine Gb₃ expression include the spleen, lung, skin, neurons, and endothelial cells of the cerebrum, though the endothelial expression is controversial here as in the kidney^{116,410}. Notably, the mouse intestine lacks Gb₃ production and Stx binding capabilities^{116,410}.

Mice injected with Stx develop a host of systemic and organ specific signs and symptoms of disease. Distinguishing the systemic and renal consequences of Stx administration to mice is difficult, as isolated kidney perfusion has not been performed because of the technical trouble cannulating the small mouse renal vasculature. Systemic findings in Stx injected mice include lethality after 72-96 hours post administration,

anorexia, lethargy, glycemia, thrombocytopenia in some cases, neutrophilia with lymphopenia, and increased serum cytokines including TNF- α and IL-1 β in some studies^{94,398,400-402,405,406,408,427}. However, cytokine levels from these Stx injected mice are relatively close to baseline and far lower than in those given LPS alone or in combination. Macrophage elimination from the mouse moderately decreases the lethal effect of Stx, perhaps due to the consequent decline in inflammation after toxin challenge⁴⁰⁴. However, though macrophages have been subsequently demonstrated to infiltrate the renal tissue in Stx plus LPS challenged mice, systemic macrophage reduction does not alter the Stx plus LPS induced renal pathology (T.R. Keepers, unpublished observations)¹⁸⁸. Treatment of nude mice lacking the T-cell compartment demonstrates no change from wild type mice, indicating that T-cells are unimportant in this model system⁴⁰⁴. Finally, the cytokine TNF- α appears to have little role in the pathogenesis of Stx mediated murine toxicity. Even though specific renal upregulation of TNF- α mRNA has been reported in response to Stx, anti-TNF- α blocking antibody co-administration and the use of TNF- α knockout mice do not alter Stx1 mediated cytotoxicity^{402,427}. Furthermore, little TNF- α appears in the serum or urine of Stx challenged mice^{402,427}.

Some coagulation markers increase in Stx challenged mice including the formation of thrombin-antithrombin III complexes, PAI-1 release, tissue factor activity, and fibrinogen levels, though the primary driving factor in these studies is LPS rather than Stx⁴⁰⁰. No decreases in hematocrit have been observed even though glomerular platelet clumping does occur in some cases^{406,407}. Urinary dysfunction in some studies is characterized by excess glucose in the urine (glucosuria) and proteinuria, which can be

signs of glomerular, proximal tubular, or distal tubular dysfunction^{94,435}. Some hematuria has also been observed⁴⁰⁷. BUN increases in a dose and time dependent manner, and though a urinary concentrating defect has been suggested, it has not been demonstrated^{94,405-407,435}. Rather, anuria develops after about 3 days of most Stx administration to mice⁴⁰⁶.

Renal pathology in Stx1 or Stx2 injected mice consists of tubular dilation and flattening, tubular cell death labeled as tubular necrosis, and renal interstitial hemorrhage^{94,427,435}. Also visible in Stx challenged mice are signs of tubular cell regeneration including epithelial hypertrophy, mitotic figures, and hyperplasia⁹⁴. More often those mice that are also exposed to LPS in one or more doses develop glomerular pathological changes characterized by endothelial damage and fibrin deposition, though endothelial swelling, sloughing, and cell loss have been described in studies that purportedly utilized solely pure Stx^{398-400,407}. Neurologic abnormalities develop within a similar 72 hour time course, consisting of seizures, lethargy, anorexia, and paralysis, and some reports contend that murine brain microvascular endothelial cells express Gb₃³⁹⁸. Pathology is not limited to the kidney and brain, as increased splenic phagocytosis and splenic iron deposition from erythrocyte turnover are observed⁴³⁵. The murine response to Stx injection is thus a complex and imprecisely described multi-system disease. Careful delineation of the etiology of organ system dysfunction during the acute time course of disease progression requires more precise measurements, and must take into account any contaminating effect of low dose LPS. Only once further Stx injected experiments are performed will the suitability of the mouse model to improve the understanding of human HUS be decided.

Mice orally inoculated with STEC display a wider range of findings than those given Stx alone, though the etiology of some pathology remains unclear. Oral infection in mice is more difficult than rabbits because the murine gastrointestinal tract has to be modified, either by streptomycin treatment or maintenance in a pathogen free environment with additional protein calorie malnutrition (PCM), to allow proper STEC colonization⁴⁰⁹⁻⁴¹³. Gastrointestinal symptoms are inconsistent, and may consist of watery diarrhea with colonic dilation or vascular congestion⁴¹². Stx can be demonstrated by dubious enzyme linked immunoabsorbant assay (ELISA) to enter the circulation of mice challenged with 2×10^6 STEC from the intestinal luminal infection. Stx ostensibly reaches a serum concentration of about 30 pg/mL, and the bacteria cause a host of circulating inflammatory signaling including increased TNF- α , IL-10 and IL-1 β ^{409,410}. In some cases the bacteria can be shown to invade some intestinal epithelial cells, though this has not been demonstrated in humans⁴¹¹. These mice demonstrate central nervous system (CNS) dysfunction with seizures and paralysis, and pathology consisting of inflammation, neuronal apoptosis, and occasionally vessel thrombosis^{409,410}. The increase in TNF- α is initial, and appears to coincide most with the intestinal absorption of LPS, while IL-10 levels increase days later⁴⁰⁹. Hematologic changes in these mice are variable, and appear to depend on the dose of STEC and thus the amount of Stx and LPS in the circulation. Lower STEC inoculations do not affect platelet levels while increased STEC or LPS doses induce thrombocytopenia and in some cases mild schistocyte formation^{410,412}. Renal pathology in infected mice is also inconsistent. Most mouse models of STEC infection report primarily tubular damage in response to STEC inoculation, though models that utilize particularly high doses of STEC inoculum or

additional LPS injection demonstrate glomerular damage as well^{399,412}. Though glomerular damage can resemble HUS fibrin rich clotting, it only occurs in mice given either a large initial or second separate dose of LPS³⁹⁹.

A final murine model of HUS utilizes the plant toxin ricin instead of Stx to mediate target cell damage⁴³⁶⁻⁴³⁸. Ricin is an enzymatically similar subunit toxin in that it is an *N*-glycosidase, however the binding subunit of ricin is far more promiscuous than Stx⁴³⁶. Ricin binds all terminal galactose residues, and does not require the terminal digalactose bound by Stx⁴³⁶. In this way, ricin attacks virtually all mammalian cell types⁴³⁶. However, ricin depurinates the identical site on the 28S rRNA as Stx, and causes identical protein synthesis inhibition and ribotoxic stress response in target cells⁴³⁶. The drawback to ricin administration in the whole animal model is the widespread tissue action which lacks the specificity of Stx. Nevertheless, 0.6-100 µg/kg ricin administration i.v. with or without LPS to mice and rats causes some renal thrombotic microangiopathy, with oliguric renal failure, proteinuria, endothelial apoptosis, neutrophilia, anemia, and thrombocytopenia similar to human HUS⁴³⁶⁻⁴³⁸. These ricin injected animals demonstrate ricin binding to glomerular and tubular structures, and though there are no schistocytes, decreased erythrocyte numbers and hemoglobinuria suggest ongoing hemolysis⁴³⁶. The glomerular damage is pervasive, with greater than 95% of glomeruli from ricin challenged animals demonstrating thrombotic changes. These animals also show increased serum levels of inflammatory molecules including MCP-1, TNF- α , IL-1 β , IL-6 and IFN- γ as well as the typical ribotoxic stress response demonstrated for ribosomal inhibitors *in vitro*^{436,438}. Interestingly, although ricin can affect most mammalian cells, significant pathology following intravenous

administration is only observed in the kidney, and absent from the brain, liver, spleen, pancreas, lung, colon, and intestine⁴³⁷. Although ricin affects all the cells of the kidney and the rest of the body, whereas in human HUS Stx is known to only bind to some cell types, these models prove that thrombotic microangiopathy can be developed in the murine systems, and can be clinically informative if the additional effects of ricin can be distinguished.

Table 1. Features of Stx induced small animal models of human HUS.

Positive (+), negative (-), contradictory or equivocal (\pm), or unknown (?) findings in small animal models of Stx mediated HUS. STEC = Shiga toxin producing *E. coli*; DB = Dutch Belted rabbit only; PCD = programmed cell death (apoptosis).

Table 1. Features of Stx induced small animal models of human HUS.

Finding	MOUSE		RAT		RABBIT	
	Stx Injection	STEC Infection	Stx Injection	Stx Perfusion	Stx Injection	STEC Infection
Dose	0.04-10 µg/kg	10 ⁵ -10 ⁹ STEC	0.01-0.2 µg/kg	0.01-28 nM	0.2-20 µg/kg	2-5x10 ⁸ STEC
Lethality	+	+	+	-	+	- (+DB)
<u>Intestinal</u>						
Diarrhea	-	±	-	-	+	+
Gb ₃	-	-	-	-	+	+
Pathology	-	±	-	-	TMA, PCD	Colitis, A/E
<u>Neurologic</u>						
Paralysis	+	+	?	-	+	-
Neuronal Gb ₃	+	+	-	-	+	+
Endothelial Gb ₃	±	±	-	-	+	+
Cerebral TMA	±	±	?	-	+	-
Neuron Apoptosis	±	+	?	-	+	-
<u>Hematologic</u>						
Leukocytosis	± (LPS?)	+	?	?	- (+DB)	-
Serum Cytokines	± (LPS?)	+	?	?	? (+DB)	?
↓ Platelets	± (LPS?)	-	?	?	-	- (±DB)
Anemia (↓ Hct)	-	?	?	?	-	- (+DB)
Reticulocytosis	-	?	?	?	-	-
Schistocytosis	-	±	?	?	-	- (+DB)
Dehydration	+	+	+	?	transient	- (+DB)
<u>Renal</u>						
↑ BUN,Creatinine	+	↑BUN	+	+	transient	- (±DB)
Oligoanuria	+	±	-	+	transient	-
Proteinuria	+	?	+	+	-	- (+DB)
Glomerular Gb ₃	-	-	±	?	- (DB?)	- (DB?)
Tubular Gb ₃	+	+	+	+	- (DB?)	- (DB?)
Fibrin Deposits	± (+LPS)	±	?	-	-	- (+DB)
Glomerular Pathology	± (+LPS)	± (+LPS)	↑RBC	±	-	- (+DB)
Tubular Pathology	+	+	+	+	-	- (+DB)
Tubular Apoptosis	+	+	?	+	-	- (DB?)
References	94,116,119,3 94,398- 408,427	119,399,409- 413	394,414	415,416	392- 394,403,417- 421,426	85,422-425

The current literature describing the mouse model of Shiga toxin mediated HUS contains some consistent results, other contradictory information, and a few clues to the underlying mechanism of disease in these animals. Although the mouse does not consistently manifest gastrointestinal disease, renal and neurologic dysfunction are common. Even though the cause of death in mice given STEC or Stx is unknown, it seems likely that it results from either the neuronal or renal damage, or a combination of the two. The neurologic changes include hind limb paralysis along with anorexia and decreased activity⁴¹². The renal pathology varies between the murine models reported. However, often only those mice exposed to and sensitive to LPS or whole bacteria appear to develop glomerular lesions, while Stx alone seems to target tubules for damage^{399,401-403,412}. Furthermore, in at least one case of STEC oral inoculation with significant systemic damage, blood cultures were positive for growing bacteria, indicating a bacteremic sepsis as opposed to a non-septic toxemia found in HUS patients⁴¹⁵. Gb₃ is reliably present in murine renal tubular cell types. However it is less consistently detected in the murine vasculature, and undetectable in the murine glomerulus. Often it is stated that the murine glomerular cells produce far reduced levels of Gb₃ than the humans, however whether these cells produce Gb₃ at all has not been adequately assessed¹⁸⁷. Hematologic and inflammatory changes also vary between the models, and those without any exposure to LPS more often fail to mediate a decrease in circulating platelet numbers or increased cytokine levels⁴⁰⁸. These data suggest that thrombocytopenia in this model may be due to the effects of LPS and is independent of Stx.

Goals of the Current Research

The above data indicate that in the mouse LPS is needed in addition to Stx to cause the full triad of clinical findings typically associated with STEC induced HUS, and that the underlying mechanism of disease may significantly differ between the human and mouse⁴⁰⁷. Care has to be taken to not induce the Shwartzman reaction in these experimental situations, and to account for the effects of LPS when given alone in the model system. Given the reported incompletely described small animal models of Shiga toxin mediated HUS, the lack of appropriate therapeutic modalities, and the failure to discern the pathophysiological details of HUS, this current work explains the mouse model of Stx and LPS toxemia and its implications. These data seek to explicate the discrepancies reported regarding murine models of HUS, and to further characterize the ability of the mouse to appropriately mimic humans in this disease state. To this end, the LPS plus Stx2 murine model of HUS is fully described by utilizing whole-mouse, serum, blood, urine, immunohistochemical, and electron micrographic measurements. While the data argue that the mouse is not a productive model of Shiga toxin induced human renal failure, the complete description contained in this manuscript provides groundwork for powerful experiments to prove the etiology of Stx mediated renal failure.

Chapter 2: A Murine Model of HUS: Shiga Toxin with Lipopolysaccharide Mimics the Renal Damage and Physiologic Response of Human Disease

This chapter was originally published as a co-authorship with Tiffany R. Keepers.

Keepers, T.R., Psofka, M.A., Gross, L.K., and Obrig, T.G. A Murine Model of HUS: Shiga Toxin with Lipopolysaccharide Mimics the Renal Damage and Physiologic Response of Human Disease. J Am Soc Nephrol, 2006. 17(12): p. 3404-14^{31,83,439}.

Abstract

Hemolytic uremic syndrome (HUS) caused by Shiga toxin-producing *Escherichia coli* (STEC) infection is the leading cause of acute renal failure in children. At present, there is no complete small animal model of this disease. We have investigated a mouse model using intraperitoneal co-injection of purified Shiga toxin 2 (Stx2) plus lipopolysaccharide (LPS). Through microarray, biochemical, and histological analysis we have found this to be a valid model of the human disease. Biochemical and microarray analysis of mouse kidneys revealed the Stx2 plus LPS challenge to be distinct from the effects of either agent alone. Microarrays identified differentially expressed genes previously demonstrated to play a role in this disease. Blood and serum analysis of these mice showed neutrophilia, thrombocytopenia, red cell hemolysis, and increased serum creatinine and blood urea nitrogen. In addition, histological analysis and electron microscopy of mouse kidneys demonstrated glomerular fibrin deposition, red cell congestion, microthrombi formation, and glomerular ultrastructural changes. We have

established that this C57BL/6 mouse is a complete model of HUS that includes the thrombocytopenia, hemolytic anemia, and renal failure that define the human disease. Additionally, we describe a time course of HUS disease progression that will be useful for identification of therapeutic targets and development of new treatments for HUS.

Introduction

Shiga toxin-producing *E. coli* (STEC), also known as enterohemorrhagic *E. coli* (EHEC), is the primary cause of diarrhea-associated hemolytic uremic syndrome (D+ HUS)⁴⁴⁰. This pathogen is also the major cause of acute renal failure in young children^{31,47,83,439,441}. It is generally accepted that systemic toxemia and subsequent renal disease is due to a combined action of Shiga toxins (Stx1, Stx2) that are the primary virulence factors of STEC, and bacterial lipopolysaccharide (LPS)⁴⁴². The series of events preceding acute renal failure in D+ HUS and the respective roles of Stx and LPS in the disease remain to be elucidated. A complete understanding of these events is essential for identification of new drug targets and development of therapeutics for D+ HUS, as the latter do not currently exist. It is hopeful that such therapeutics may be employed in the clinical setting where a three to five day “window of opportunity” generally exists prior to acute renal failure. Towards this goal, in the present study we report on the temporal series of host response events, including renal gene activation, in a small animal model that exhibits the hallmarks of HUS, thrombocytopenia, microangiopathic hemolytic anemia, and acute renal failure. We also demonstrate that both virulence factors of STEC, Stx and LPS, are required to elicit the triad of HUS symptoms.

Methods

Shiga toxin purification

Stx2 was purified by immunoaffinity chromatography from cell lysates (kindly provided by Alison O'Brien) of *E. coli* DH5 α containing the Stx2 producing pJES120 plasmid⁴⁴³. Briefly, Stx2 was purified using 11E10 antibody^{93,444} immobilized using an AminoLink Plus Kit (Pierce Biotechnology, Inc., Rockford, IL) according to manufacturer's instructions. Endotoxin was removed using De-toxi-Gel (Pierce Biotechnology) as per the manufacturer's instructions. Stx2 purity was assessed by SDS-PAGE, determined to be endotoxin free, and activity was measured in a Vero cell cytotoxicity assay. Stx2 was chosen because it is far more frequently associated with HUS clinical isolates than Stx1⁴⁴⁵.

Animal studies

C57BL/6 male mice weighing 22-24 grams were purchased from Charles River Laboratories (Wilmington, MA). Mice were injected intraperitoneally (i.p.) with a low sublethal dose of LPS at 300 μ g/kg (O55:B5, Sigma-Aldrich, St. Louis, MO), 225 ng/kg Stx2 (2 times the LD50), or both. Saline injection was used for control mice. At 0, 2, 4, 6, 8, 12, 24, 48, and 72 hours after injection, 2 mice per time point were euthanized and kidneys were processed as described below. These experiments were repeated 3 times. In separate experiments, blood samples were obtained from mice at 0, 4, 8, 12, 24, 36, 48, 60, and 72 hours after injection. Mice were weighed every 12 hours for 3 days to

determine percent weight loss. All animal procedures were done in accordance with University of Virginia Animal Care and Use Committee policies.

Blood Analysis

Blood was collected from mice with EDTA treated or with non-EDTA treated capillary tubes via retroorbital bleed. Blood collected without anticoagulant was either smeared on microscope slides or allowed to clot for 30 minutes at room temperature. Dried blood smears were flooded with Wright-Giemsa stain (Sigma-Aldrich) for 1 minute and rinsed with distilled water for 2 minutes. After clotting, blood was centrifuged at 2,000 x g for 15 minutes at 4°C. The serum layer was removed and stored at -80°C until analysis.

Creatinine was determined using Cayman Chemical Creatinine Assay Kit (Ann Arbor, MI) as per the manufacturer's instructions. BUN was determined spectrophotometrically with VetScan (Idexx Corporation, Westbrook, ME). For reticulocyte counts, three drops of EDTA treated blood was mixed with two drops Reticulocyte Stain (Sigma-Aldrich) for 10 minutes at room temperature. Mixtures were then smeared on a microscope slide, dried, and coverslipped. Percentage of reticulocytes was determined by counting the number of reticulocytes per 1000 red blood cells. Complete blood count (CBC) was performed on 20µl of the EDTA treated blood using MASCOT HEMAVET 850 (CDC Technologies Inc., Oxford, CT) according to the manufacturer's instructions.

Immunohistochemistry

One-half mouse kidney was fixed in 4% paraformaldehyde for 24 hours, processed, and embedded in paraffin. Three micron thick sections were cut and placed onto charged

slides. Martius Yellow-Brilliant Crystal Scarlet-Aniline Blue (MSB) differential staining procedure was performed as previously described⁴⁴⁶. Martius yellow and phosphotungstic acid in alcoholic solution stain red cells, brilliant crystal scarlet stains muscle and mature fibrin, and aniline blue stains collagen. Glomeruli positive for fibrin staining were quantified by counting 3 sets of 20 glomeruli per slide and averaging the percent positive for fibrin at each time point. Immunohistochemistry for platelets was performed using polyclonal goat anti-human integrin- β 3 antibody that cross-reacts with the mouse protein (Santa Cruz Biotechnology, Inc., Santa Cruz, CA)⁴⁴⁷. Primary antibody was detected using an avidin/biotin horseradish peroxidase system (Vector Laboratories, Burlingame, CA) and DAB. Sections were then counterstained in hematoxylin, dehydrated and mounted.

Electron Microscopy

Kidneys were harvested from euthanized mice 0, 24, 48, and 72 hours after Stx2 plus LPS challenge, cut into blocks approximately 1-2mm³, and fixed overnight at 4°C in 4% paraformaldehyde and 2.5% glutaraldehyde in 1X PBS. The fixed tissue was subsequently processed by the University of Virginia Advanced Microscopy Facility. The tissue blocks were washed with PBS at 24°C and post-fixed for one hour in 1.0% osmium tetroxide. The blocks were then washed in distilled water, dehydrated employing a graded acetone series, embedded in epoxy resin (EMBED 812, Electron Microscopy Sciences, Inc.), and polymerized for two days at 60°C. Ultrathin sections approximately 70 nm in thickness, obtained with a diamond knife (Diatome, Inc.) on a Leica Ultracut UCT ultramicrotome, were collected on 200 mesh copper grids, contrast

stained with uranyl acetate and lead citrate according to routine procedures, and examined in a JEOL 1230 transmission electron microscope. Digital images were acquired using an SIA L3-C digital camera (Scientific Instruments and Applications, Inc.). At least four glomeruli from each of three mice were examined per time point.

cRNA Synthesis and Microarray Hybridization

One-half mouse kidney was stored in 2ml RNALater (Ambion, Austin, TX) at 4°C until RNA extraction. Total RNA was isolated using the RNeasy Midi Kit (Qiagen, Santa Clarita, CA) according to the manufacturer's instructions. Total kidney RNA from saline and treated mice was compared with GeneChip® Expression Analysis using Mouse Genome 430A 2.0 Arrays (Affymetrix, Santa Clara, CA) by the Biomolecular Research Core Facility (University of Virginia, <http://www.healthsystem.virginia.edu/internet/biomolec/>).

Microarray Analysis and Quantitative RT-PCR

Microarray probe level determinations were made by the Probe Logarithmic Intensity Error (PLIER) estimation method, part of the ArrayAssist Lite software package (Stratagene, La Jolla, CA). DNA-Chip Analyzer (dChip)⁴⁴⁸ model based estimation was used to normalize the signal levels to the median arrays for each series of experiments. Multi-class significance analysis across the time course was performed with the Significance Analysis of Microarrays (SAM) software⁴⁴⁹. Genes with q-values (False Discovery Rate or FDR) of less than 5% were determined to be significantly altered by challenge. From this set, only those genes which were altered 2.0-fold or greater at any

time point compared to controls were used for further analysis. Cluster analysis was performed on this data set with GeneCluster 2.0 software⁴⁴⁷, and dChip was used for gene ontology analysis of the clusters^{168,450}. Expression patterns of select genes from each cluster were verified by quantitative real-time PCR using the iScript cDNA Synthesis Kit, iQ SYBR Green Supermix and iCycler Thermal Cycler (BioRad, Hercules, CA).

Statistics

All statistics (excluding those used for microarray analysis) were performed using single factor ANOVA followed by two sample Student's t-test, and $p < 0.05$ was considered significant.

Results

Stx2 plus LPS causes diminished renal function.

Mice were injected i.p. with either a low sub-lethal dose of LPS (300 $\mu\text{g}/\text{kg}$), or 225 ng/kg Stx2, or both agents. The dose of Stx2 chosen is the minimum 100% lethal dose resulting in lethality within 4 $\frac{1}{2}$ days (Figure 11). When this dose of Stx2 was combined with the sub-lethal dose of LPS, the time to death was decreased by 1 day. Mice were weighed every 12 hours to determine percent weight loss caused by the toxins (Figure 11). LPS induced weight loss early in the time course, while Stx2 induced weight loss late in the time course. Stx2 plus LPS caused weight loss both early and late in the time course. Mice were evaluated for kidney function, peripheral cell count

abnormalities, and structural kidney changes. These results are summarized in Table

2. We determined that only mice injected with both Stx2 plus LPS exhibited all the signs of clinical HUS. Therefore, we have chosen to present those data relevant to the complete Stx2 plus LPS mouse model of HUS. Stx2 plus LPS co-administration i.p. at these doses was used for all subsequent experiments except where noted.

Figure 11. Survival and weight loss of mice challenged with Stx2 plus LPS.

Survival and weight loss of Stx2, LPS, and Stx2 plus LPS challenged mice. Mice were injected with 225 ng/kg Stx2, 300 μ g/kg LPS, or both. (A) Survival curve representative of 3 experiments. Data contain 6 mice per group. (B) Mice were weighed every 12 hours after injection for 72 hours. Data contain 10-12 mice per group. * $p < 0.002$ significantly decreased from weight at time 0hr and # $p < 0.002$ significantly increased from weight at time 0hr evaluated by ANOVA and Student's t-test.

Figure in collaboration with T.R. Keepers.

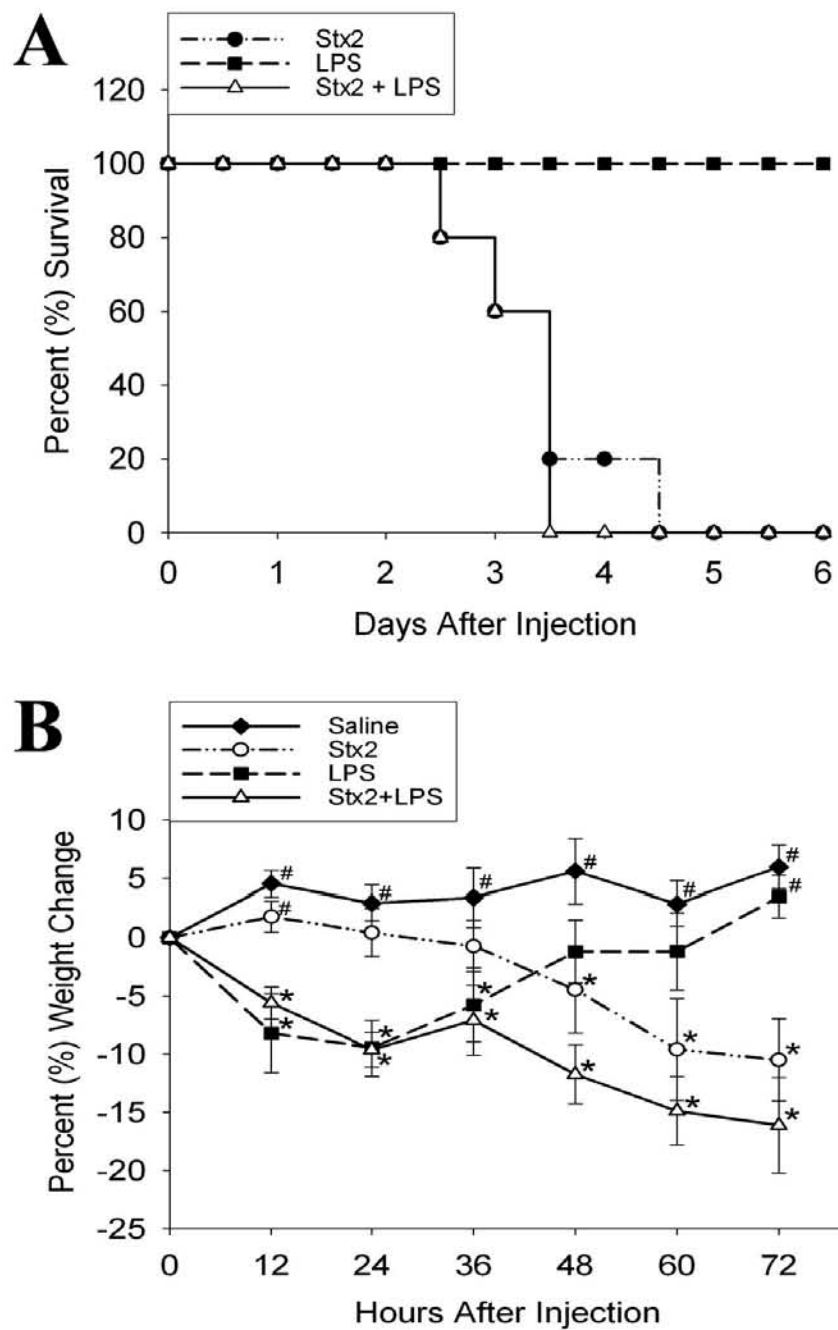


Figure 11. Survival and weight loss of mice challenged with Stx2 plus LPS.

Table 2. Summary of pathological conditions induced by Stx2 plus LPS in mice.

Summary of pathological conditions induced by Stx2, LPS, or Stx2 plus LPS injection.

Mice were injected with 225 ng/kg Stx2, 300 µg/kg LPS, or both and evaluated for the conditions listed throughout the 72 hour time course as described in materials and methods. A “+” indicates relative severity of the condition, with each additional “+” indicating greater change from normal. Temporally, changes occurring from 0-12 hours were designated ‘early,’ 12-36 hours ‘mid,’ and 36-72 hours ‘late.’

Table in collaboration with T.R. Keepers.

Condition	Treatment								
	Stx2			LPS			Stx2+LPS		
	Time Course of Condition Expression								
	Early	Mid	Late	Early	Mid	Late	Early	Mid	Late
Neutrophilia		+	++	++			+++	++	+
Lymphocytopenia			++	++			++	++	+
Monocytosis	+	+		+	+		++	++	+
Renal Platelet Aggregation	++	+	++	++	+	++	+++	++	+++
Thrombocytopenia				+	++	+	+	+++	+
Fibrin Deposition	++	+	+	+	+	+	+	++	+++
Reticulocytosis	+	++	+++				+	+	++
Increased Serum Creatinine	+	+	++				+	+	++
Weight Loss			+	+	+		+	+	++

Table 2. Summary of pathological conditions induced by Stx2 plus LPS in mice.

Increases in serum levels of creatinine and blood urea nitrogen (BUN) imply decreased glomerular filtration, and were used as indicators of abnormal renal function (Figure 12). After administration of Stx2 plus LPS, creatinine levels were significantly increased compared to saline at 12 hours, and continued to rise with a maximal average concentration of 0.92 mg/dL at 72 hours. Similarly, BUN levels were increased in mice injected with Stx2 plus LPS in a time-dependent manner. BUN was significantly elevated at 8 hours post-injection and continued to increase until death with a maximal average BUN concentration of 114.33 mg/dL by 72 hours.

Figure 12. Serum creatinine and BUN of mice challenged with Stx2 plus LPS.

Serum creatinine and BUN analysis. Serum from mice injected with Stx2 plus LPS was analyzed for (A) creatinine and (B) BUN concentration. Each circle represents one mouse and data represent 3 separate experiments. Black bars are the average of all mouse samples. * $p < 0.05$ significantly increased over saline by ANOVA and Student's t-test.

Figure courtesy of T.R. Keepers.

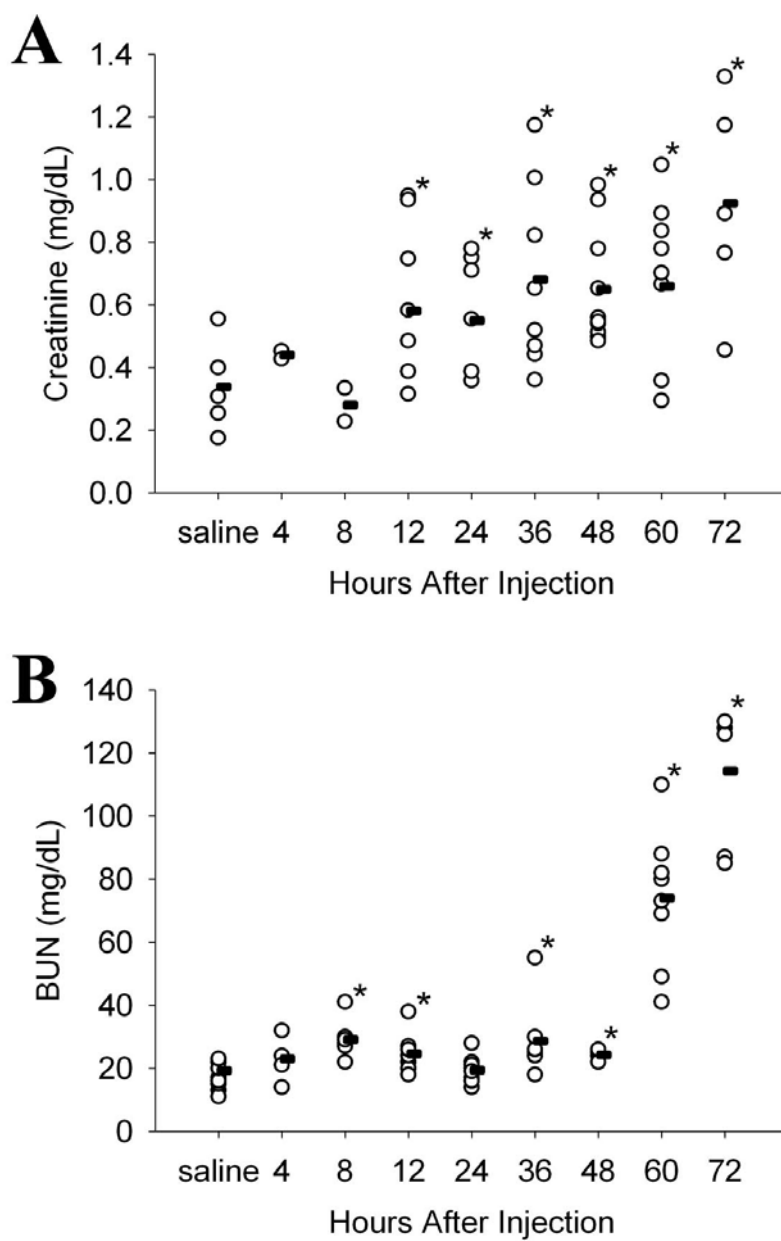


Figure 12. Serum creatinine and BUN of mice challenged with Stx2 plus LPS.

Stx2 plus LPS alters white blood cells.

A complete blood cell count was performed on Stx2 plus LPS injected mice throughout the 72 hour time course (Figure 13A-D). Mice exhibited neutrophilia, lymphocytopenia, and mild monocytosis. Rise in peripheral neutrophil levels was significant at 4 hours and maximal at 8 hours following Stx2 plus LPS injection, after which levels gradually returned to normal at 72 hours (Figure 13A). Neutrophils expanded from 0.67 ± 0.17 to 2.09 ± 0.48 K/ μ l, and increased from $12.4 \pm 2.1\%$ of the total white blood cell (WBC) population to $56.8 \pm 8.9\%$. Consequently, the lymphocyte population decreased from $82.9 \pm 4.7\%$ of total WBC with saline injection to $37.7 \pm 5.8\%$ at 8 hours post Stx2 plus LPS injection (Figure 13B). Similarly, total lymphocyte levels were minimal at 4-8 hours post-injection with a significant drop from 4.69 ± 0.92 to 1.30 ± 0.28 K/ μ l. Lymphocyte levels then gradually increased throughout the time course with a recovery at 72 hours to about half the normal level. The monocyte cell population expanded with respect to the other white cell populations as reflected by the increase in the percent monocytes of total WBC throughout the time course. While the total number of monocytes was not significantly altered after Stx2 plus LPS injection, the percent monocytes increased from $3.17 \pm 1.0\%$ with saline injection to $5.92 \pm 2.8\%$ 8 hours following Stx2 plus LPS injection (Figure 13C).

Blood smears from mice at various time points after Stx2 plus LPS administration demonstrated changes in white blood cell morphology. Figure 13F is a blood smear taken 24 hours following Stx2 plus LPS injection, and depicts a segmented neutrophil as well as an activated monocyte. Monocytes and neutrophils increased in smears beginning at 12 hours post-injection and were thereafter present throughout the time

course. Monocytes displayed evidence of activation including, increased cell size, linearized chromatin, granules, and pseudopod formation. Neutrophil activation was indicated by increased cell size, granules, and segmentation as well as hypersegmentation. Plasmacytoid lymphocytes were also present in blood smears.

Stx2 plus LPS causes signs of hemolytic anemia.

Although a complete blood count of Stx2 plus LPS mice over the 72 hour time course showed moderately increased hematocrit and hemoglobin levels (data not shown), blood smears demonstrated signs of anemia and hemolysis. Hematocrit reached a plateau at 36 hours post injection of $52.0 \pm 2.6\%$ compared to the saline injected of $44.3 \pm 4.3\%$. However, manual peripheral reticulocyte counts were increased at 12 hours following Stx2 plus LPS injection and remained elevated throughout the time course (Figure 13D,G). Reticulocytes are newly developed immature red blood cells (RBCs) that appear blue/purple and are a sign of anemia. It was also noted that serum collected from mice injected with Stx2 plus LPS had a red discoloration, presumably from hemoglobin due to RBC hemolysis.

Additionally, blood smears revealed several RBC morphological abnormalities (Figure 13G,H) compared to normal (Figure 13E). Howell-Jolly bodies are nuclear fragmentations of DNA that appear as small round blue structures in erythrocytes in anemic states. These were found in smears beginning at 8 hours (Figure 13G arrow head), were more numerous at 12 hours (Figure 13H arrows), and continued to increase through 72 hours following Stx2 plus LPS injection. Echinocytes are a morphological

change in which the RBC has uniform spikes or burrs on its surface, indicating uremia. At 24 hours after Stx2 plus LPS injection, echinocytes were evident in blood smears.

Figure 13. Peripheral blood cell changes in mice challenged with Stx2 plus LPS.

Peripheral blood cells in Stx2 plus LPS injected mice. (A) Total neutrophil counts (closed circles) and percent neutrophils of total WBC (open squares). * $p < 0.01$ significantly increased compared to saline. (B) Total lymphocyte counts (closed circles) and percent lymphocytes of total WBC (open squares). * $p < 0.0001$ and # $p < 0.05$ significantly decreased compared to saline. (C) Total monocyte counts (closed circles) and percent monocytes of total WBC (open squares). * $p < 0.05$ significantly increased compared to saline. (D) Percent peripheral reticulocytes. * $p < 0.05$ significantly increased compared to saline. Data are the average of 7-18 mice and 3 separate experiments. All data are the average \pm SD and all statistical analysis was performed using ANOVA and Student's t-test. Blood smears of mice administered Stx2 plus LPS at different times following injection: (E) 0 hour control shows no irregularities. (F) 24 hours post-injection increased neutrophils (arrow head) and monocytes (arrow). (G) 8 hours after injection appearance of reticulocytes as indicated by arrows. (H) 12 hours following injection appearance of red blood cells with Howell-Jolly bodies as indicated by arrows. All pictures were taken under oil immersion at 1000X and (H) was enlarged 2 fold.

Figure in collaboration with T.R. Keepers.

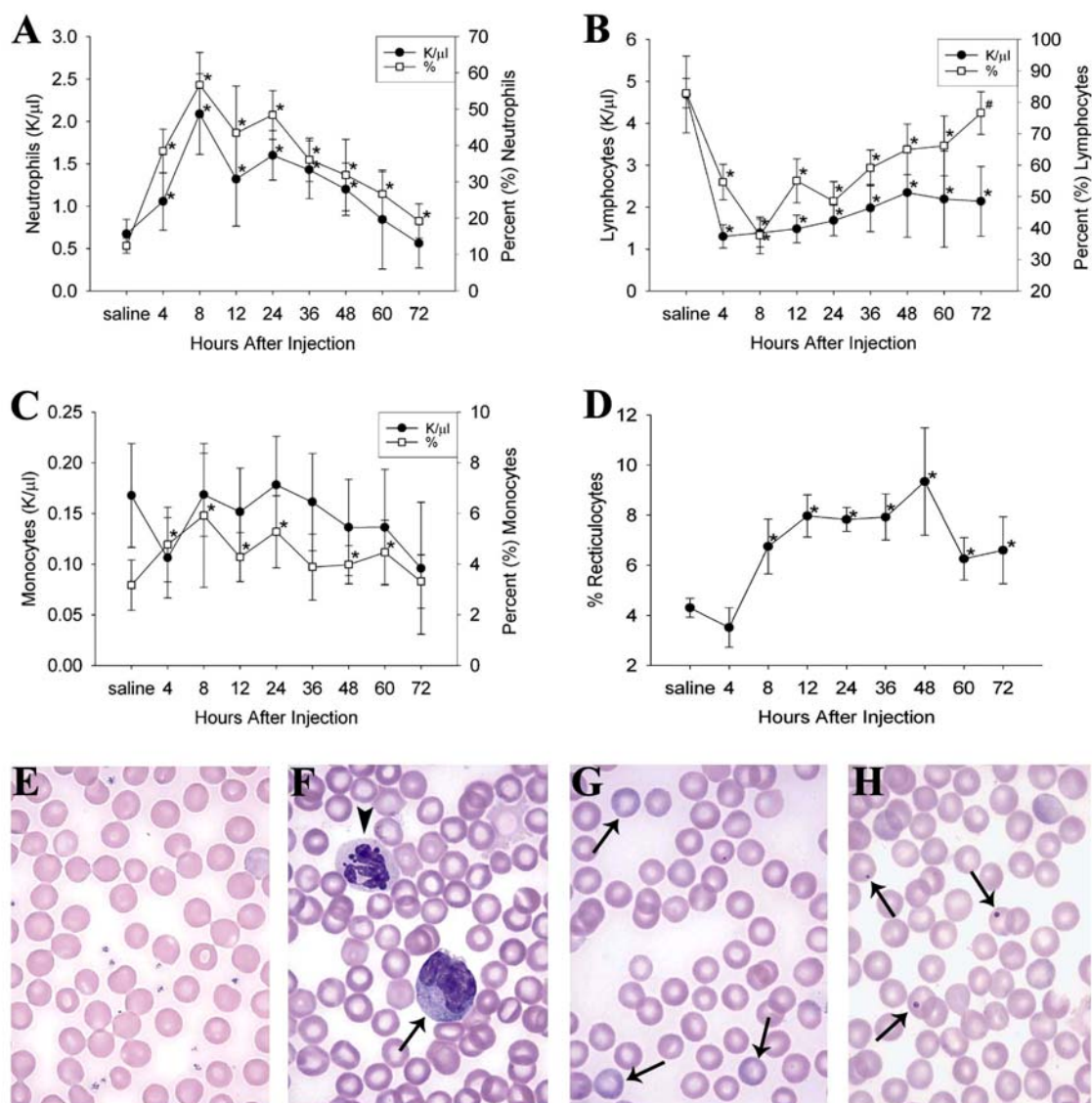


Figure 13. Peripheral blood cell changes in mice challenged with Stx2 plus LPS.

Stx2 plus LPS causes thrombocytopenia in mice.

Platelet levels significantly decreased in mice administered Stx2 plus LPS beginning at 4 hours after injection and continued to decline through the time course (Figure 14A). The minimal platelet level was 392.7 ± 104.9 K/ μ l at 36 hours post-injection compared to 820.8 ± 134.6 K/ μ l with saline injection. In addition, platelet clumping in blood smears was most apparent at 72 hours after Stx2 plus LPS injection. In the kidney, glomerular platelet aggregation was increased at 2 hours after Stx2 plus LPS injection (Figure 14B). After a slight decline at 12 hours, platelet clumping began to increase again until the end of the time course (Figure 14B-D).

Figure 14. Peripheral and renal platelets in Stx2 plus LPS injected mice.

Peripheral and kidney platelets in Stx2 plus LPS injected mice. (A) Peripheral platelet levels indicate thrombocytopenia. Data are the average of 9-14 mice and 3 separate experiments, and * $p < 0.005$ significantly decreased compared to saline. (B) Glomeruli positive for platelet clumping in kidney. * $p < 0.05$ significantly decreased compared to control. Three sets of 20 glomeruli were counted for platelet clumps per time point at 400X. Immunohistochemistry demonstrating platelet clumping in the kidney at (C) 0 hour and (D) 2 hours after injection. Platelets are stained brown and arrows indicate platelet clumping. All pictures were taken at 400X magnification, data are the average \pm SD, and statistics performed using ANOVA and Student's t-test.

Figure courtesy of T.R. Keepers.

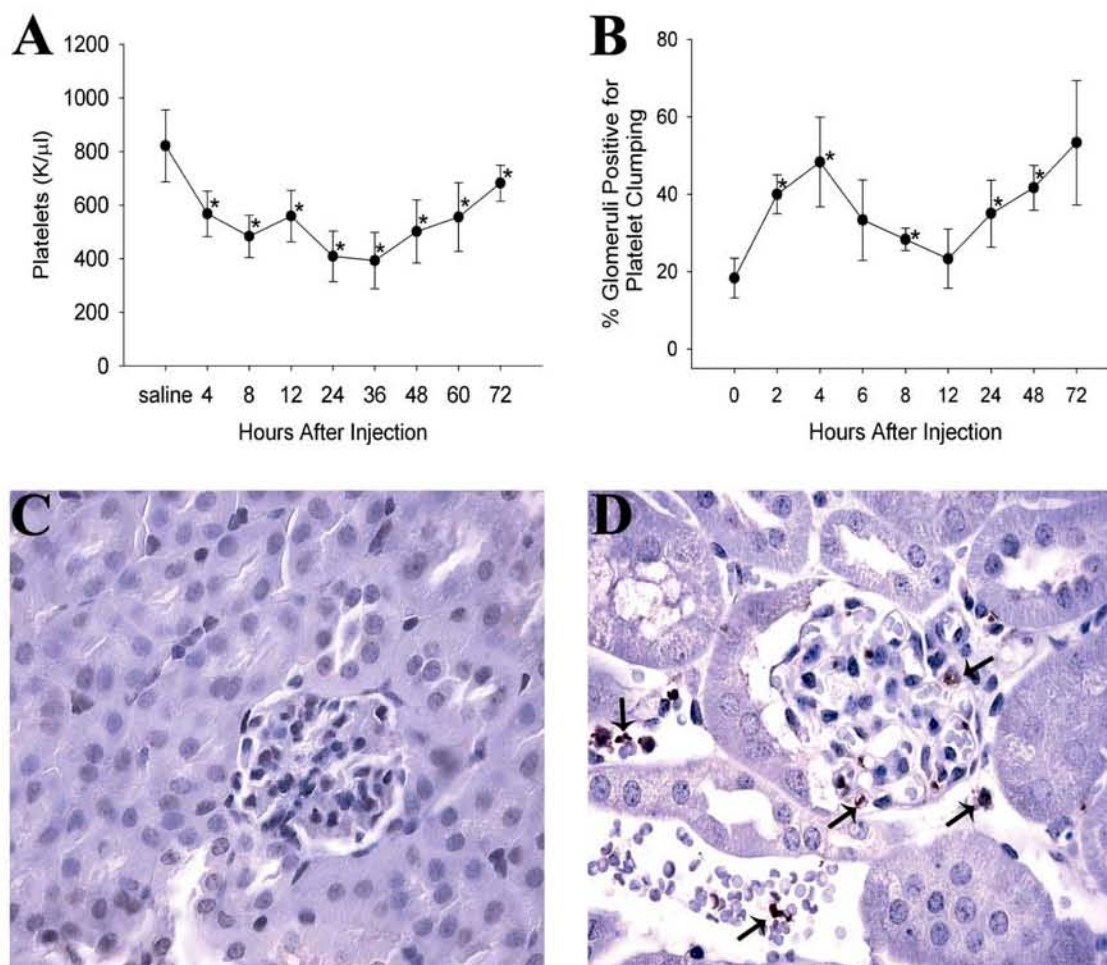


Figure 14. Peripheral and renal platelets in Stx2 plus LPS injected mice.

Stx2 plus LPS causes changes in the mouse kidney.

The MSB differential stain for red blood cells, fibrin, and collagen was performed on fixed mouse kidney tissue during the time course (Figure 15). In normal kidney tissue (Figure 15A), collagen was distributed throughout the inner tubules of the cortex, medulla and papilla as indicated by light blue staining. There was no significant change in collagen levels after Stx2 plus LPS injection.

Red blood cells (RBCs), stained yellow, were widely dispersed throughout the normal kidney in small numbers. There was a general increase in RBCs in the entire kidney and red cell clustering in the cortex beginning at 4 hours following Stx2 plus LPS injection (Figure 15B). RBC congestion in glomeruli, capillaries, and intertubular spaces continued to increase during the time course. Specifically, RBCs began to accumulate in the medulla at 6 hours post-injection, glomerular RBC congestion was evident at 8 hours post-injection, and at 24, 48, and 72 hours post-injection large areas of RBC congestion and clumping were evident throughout the cortex.

Significant changes in fibrin staining were evident at 8 hours after Stx2 plus LPS injection. Fibrin was increased in the cortex of the kidney in the intertubular spaces, glomeruli, and capillaries. It was dispersed throughout the papilla and medulla. Glomeruli positive for fibrin also increased at this time point from 23.3% positive at 0 hour to 75.0% positive for fibrin at 8 hours post-injection. Fibrin continued to accumulate with maximal staining at 48 hours after Stx2 plus LPS challenge (Figure 15C). At this time, the medulla and cortex showed a rise in the number and in the size of concentrated areas of fibrin deposition, and 93.3% of glomeruli were positive for fibrin.

Figure 15. Fibrin and erythrocyte congestion in Stx2 plus LPS injected mice.

Fibrin deposition and red blood cell congestion accumulates over time in mice administered Stx2 plus LPS. Martius Yellow-Brilliant Crystal Scarlet-Aniline Blue staining of mouse kidneys at (A) 0 hours, (B) 4 hours, (C) 48 hours, and (D) 72 hours following injection (arrow indicates thrombi in arteriole). Bright red staining is fibrin deposition, red blood cells are stained yellow, nuclei are stained dark blue/purple, and collagen is stained blue. A-C are 200X magnification and D is 400X magnification.

Figure in collaboration with T.R. Keepers.

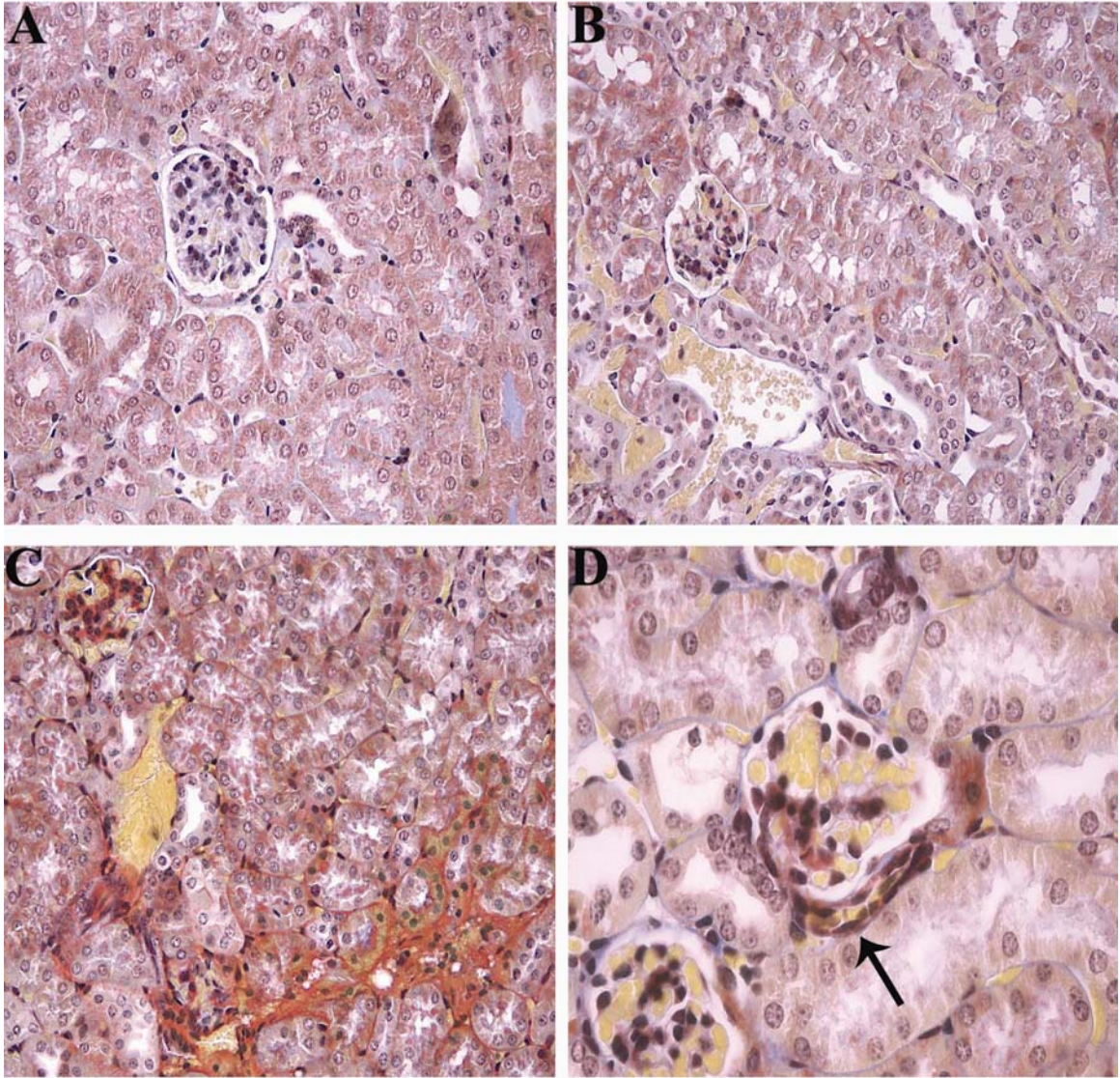


Figure 15. Fibrin and erythrocyte congestion in Stx2 plus LPS injected mice.

Additionally, thrombi of RBCs and fibrin were seen in the glomerular arterioles (Figure 15D).

Transmission electron microscopy of glomeruli from Stx2 plus LPS challenged mice demonstrated significant ultrastructural change to the capillary loops, endothelial cells, and podocytes compared to controls (Figure 16). RBC congestion and electron dense flocculent material, which is likely a combination of collected serum proteins and fibrin, was present from 24-72 hours (Figure 16,C). Increasingly large extranuclear endothelial inclusions were observed beginning at 24 hours and extending through 72 hours post challenge (Figure 16B). These inclusions are bounded by two membranes and are anuclear, which suggests that they are remnants of endocytosed RBCs, platelets or other cellular debris. Furthermore, endothelial cell fenestrations were irregular and occasionally partially detached from the glomerular basement membrane (Figure 16C). Podocytes appeared swollen, diminishing the urinary space, and some contained extensive vacuoles of unknown significance (Figure 16D). None of the pathological findings were observed in control mouse kidneys (Figure 16A).

Figure 16. Glomerular electron micrographs from Stx2 plus LPS injected mice.

Stx2 plus LPS administration causes glomerular ultrastructural changes in mice.

Representative transmission electron micrographs of mouse glomeruli from control (A), and 72 hour post challenge (B-D). (B) Endothelial cell with arrows indicating extranuclear inclusions. (C) Glomerular capillary loop with endothelial detachment (arrow). (D) Abnormal podocyte with cytoplasmic vacuolation (arrows). A is 5000X magnification and B-D are 10,000X magnification, white bar is 2 μm . Abbreviations: E, endothelial cell; P, podocyte; R, red blood cell.

Figure in collaboration with T.R. Keepers.

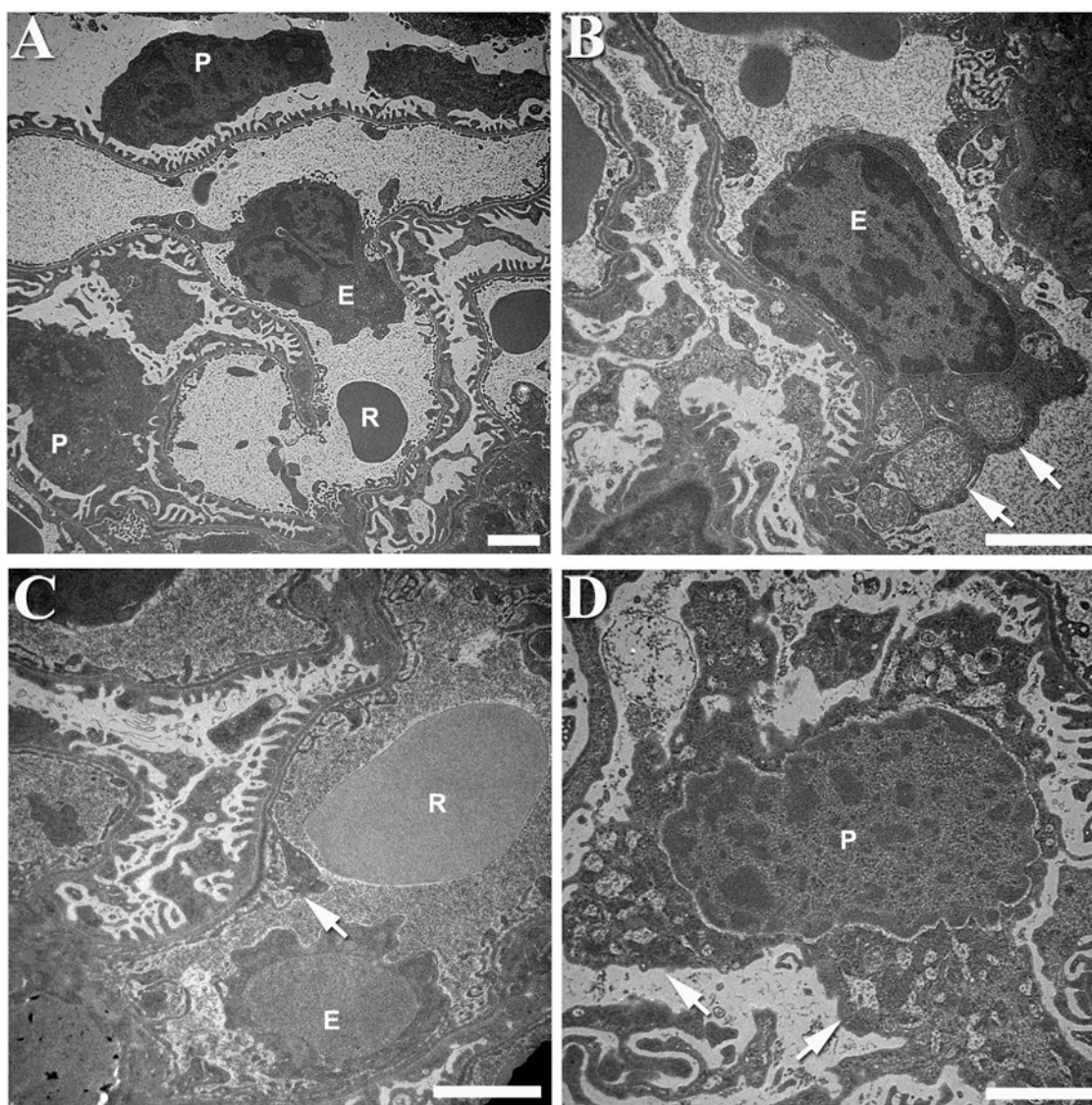


Figure 16. Glomerular electron micrographs from Stx2 plus LPS injected mice.

Stx2, LPS and Stx2 plus LPS challenges alter renal gene expression.

Microarrays were used to analyze gene expression in the whole mouse kidney in response to Stx2, LPS, or Stx2 plus LPS challenges. Analysis of the data revealed 136, 737, and 722 significant differentially expressed genes for the Stx2, LPS, and Stx2 plus LPS challenges, respectively (Figure 17). These genes represented approximately 1% (Stx2) and 5% (LPS and Stx2 plus LPS) of the 14,000 genes included on the array. The Venn diagram in Figure 10 demonstrates that, while many of the genes whose expression was altered by each challenge were affected by the other challenges, there was also a distinct set of genes that was uniquely significant for each challenge. For example, of the 136 genes differentially expressed in response to Stx2 alone, 74 were also differentially expressed in response to LPS alone, 75 also in response to Stx2 plus LPS, and 57 were also differentially regulated by both LPS and Stx2 plus LPS while 44 were unique to Stx2 alone.

Figure 17. Venn diagram of mouse renal genes altered by Stx2 or LPS challenge.

Venn diagram of genes altered 2.0 fold or greater by each challenge with a q-value < 5% in multi-class ANOVA analysis. The total genes used from each challenge are outside of the circles. Each challenge alters both an overlapping set of genes and a distinct gene set, compared to the other challenges.

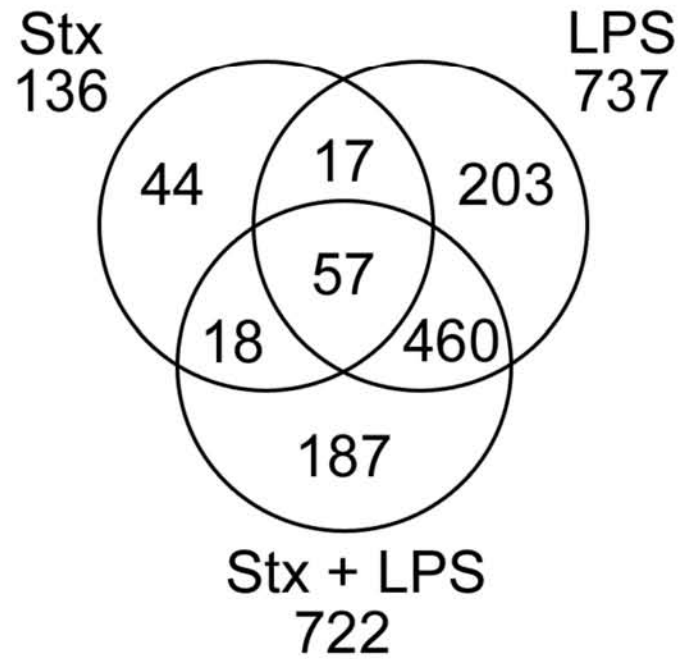


Figure 17. Venn diagram of mouse renal genes altered by Stx2 or LPS challenge.

Stx2, LPS and combination challenges provoke distinct renal expression patterns.

The Stx2, LPS and Stx2 plus LPS challenges exhibited distinct temporal alterations in gene expression over the time course. Figure 18A is a plot of the number of genes whose transcription was altered, either increased or decreased, at each time point by each challenge. LPS affected a rapid early change in gene expression, while Stx2 caused a later gradual change. The differentially expressed genes from Stx2 plus LPS challenge created a pattern that shared the respective temporally early and late changes in gene expression from the individual agents. To discover classes of genes with similar expression patterns, self organizing map (SOM) clustering, an unsupervised learning method, was performed with the GeneCluster program. Within each challenge, genes were grouped together based on the similarity of their expression patterns within the 72 hour time course (Figure 18B). These groups were labeled based on the time point of maximum expression change over the course of the pattern. Six major gene expression patterns were observed for LPS challenge. Genes whose maximum differential expression occurred at 2-4 hours post injection were termed ‘immediate,’ those at 6-8 hours were termed ‘early,’ and those at 12-24 hours were termed ‘late.’ In contrast, Stx2 challenge created only an upregulated and downregulated pattern, each reaching maximum differential expression at 48-72 hours. These clusters were thus termed ‘very late’ to contextualize them in light of the LPS expression patterns. The Stx2 plus LPS challenge creates an arrangement of gene expression patterns that combines each of the Stx2 plus LPS patterns together (data not shown). Supplemental Table 4 contains a list of the most differentially expressed genes in each cluster from Figure 18B. Many of these

gene products are upregulated in HUS patients, most notably IL-6 and MCP-1, thus adding validity to the HUS mouse model^{31,83,439}.

Figure 18. Patterns of renal genes altered by Stx2 or LPS challenge in mice.

(A) The total number of genes altered at each time point by each challenge. Temporal changes in gene expression due to LPS and Stx2 are distinct, and the Stx2 plus LPS time course incorporates both of these alterations (time course to scale). (B) Temporal clusters created by GeneCluster for LPS and Stx2 challenges. The average expression pattern for each cluster across the 72 hour time course is shown (time course not to scale). Inset is the number of significant 2.0 fold changed genes in each cluster. LPS and Stx2 cause distinct alterations in patterns of gene expression.

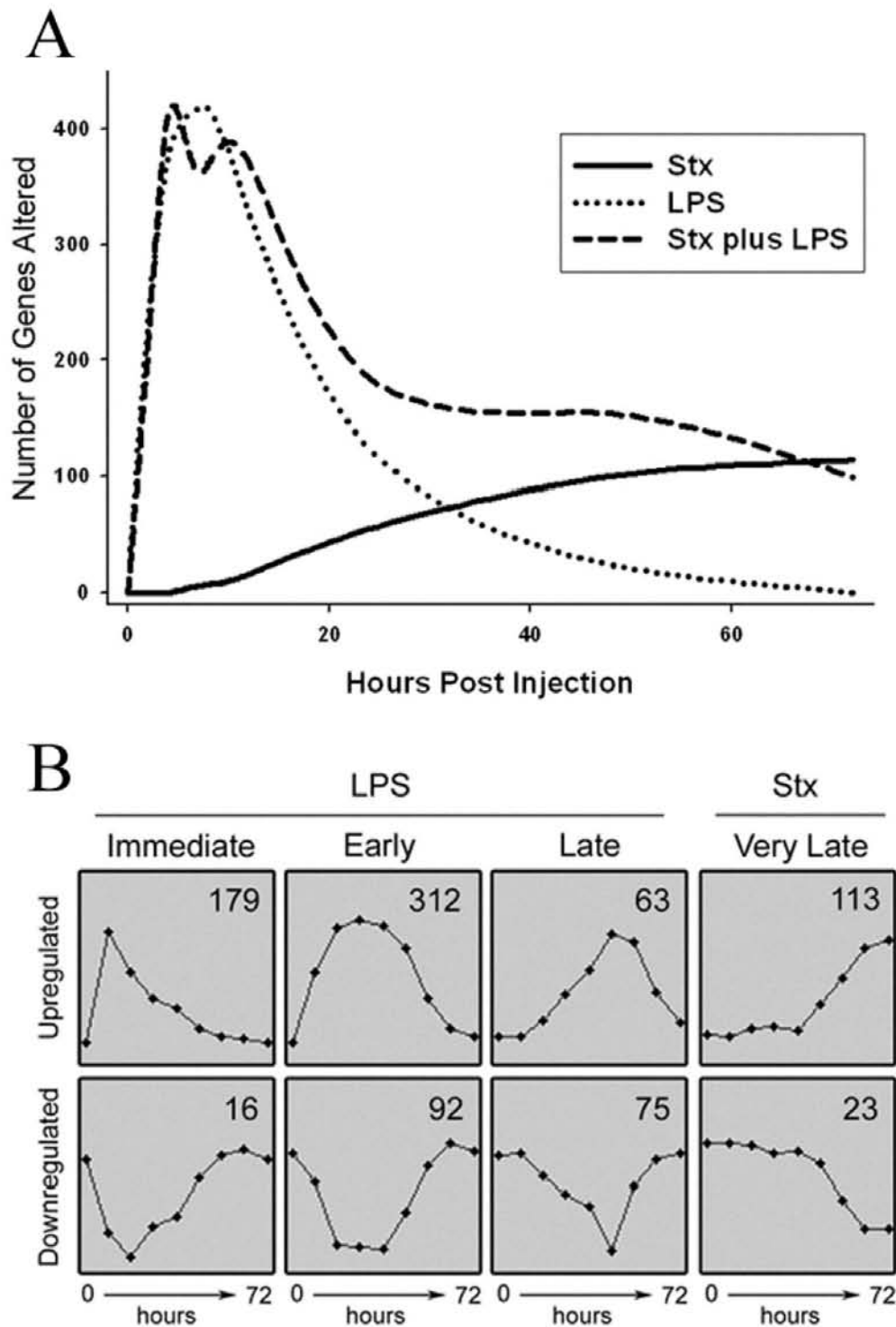


Figure 18. Patterns of renal genes altered by Stx2 or LPS challenge in mice.

Stx2 and LPS alter overlapping and unique groups of genes.

To discern the functions of those genes differentially expressed in response to challenge, each cluster described in Figure 18B was subjected to gene ontology analysis (Table 3). dChip categorizes genes based on molecular function, biological process and cellular component using GeneOntology (<http://www.geneontology.org/>) terms and information from the NCBI LocusLink database, and calculates a p-value for overrepresentation of that cluster in the gene set. The LPS upregulated gene clusters contained significantly large alterations in genes involved in the following biological processes: inflammatory response, immune response, and regulation of transcription, with more minor changes of genes involved in apoptosis, cell differentiation, proliferation, and regulation of cell cycle. Molecular function analysis of the LPS upregulated genes identified numerous cytokines, transcription factors, cell surface ligands, and complement components. In contrast, those gene biological processes upregulated by Stx2 did not include the inflammatory and immune responses, though Stx2 did cause an upregulation of genes involved in cell proliferation, differentiation, and regulation of cell cycle and transcription. Molecular function analysis of the Stx2 upregulated genes included some cytokines and transcription factors, but not any complement components. Downregulated by both challenges were solute and macromolecule transporters necessary for normal renal function. The Stx2 plus LPS challenge altered the combined functional groups from each of the individual challenges (data not shown).

Table 3. Gene ontology clusters altered by Stx2 or LPS challenge in mice.

Significant gene ontology clusters as identified by dChip for each gene expression cluster described in Figure 11. LPS and Stx induce both distinct and overlapping gene expression responses in the mouse kidney. LPS induces a large inflammatory and defense response not affected by Stx2, while they share many other aspects including increased apoptosis and proliferation, cell cycle regulation and transcription factor changes. * indicates p-value < 0.05 as described in methods.

Biological Process	LPS						Stx2		Total Genes in Pathway
	Up			Down			Up	Down	
	Immediate	Early	Late	Immediate	Early	Late	Very Late	Very Late	
Apoptosis	10*	8*	1	0	0	3	5*	1	147
Cell Differentiation	3	3	0	0	2	0	4*	0	101
Cell Proliferation	2	10	5*	0	1	2	13*	0	332
Chemotaxis	8*	4	1	0	1	0	1	0	55
Cholesterol Metabolism	1	1	2*	0	1	1	3*	1	23
Defense Response	24*	44*	12*	0	4	1	1	0	338
Immune Response	22*	37*	10*	0	4	1	2	0	251
Inflammatory Response	14*	6*	1	0	1	0	2	0	69
Lipid Metabolism	2	5	3	0	1	7*	5	1	199
Regulation of Cell Cycle	9*	4	4*	0	1	2	10*	0	123
Regulation of Transcription	22*	19	2	2	4	3	20*	0	720
Response to Stress	16*	15*	7*	0	3	1	4	0	208
Response to Wounding	15*	8*	1	0	1	1	3	0	89
Molecular Function									
Complement Activity	0	3*	3*	2	2*	0	0	0	29
Chemokine Activity	9*	3	1	0	1	0	3*	0	35
Cytokine Activity	13*	9*	1	0	2	0	5*	0	160
DNA Binding Activity	29*	22	2	4	5	6	25*	0	1095
Receptor Binding Activity	15*	11	1	1	2	0	5	0	289
Transcription Regulator Activity	12	15	2	2	3	2	12*	0	575
Transporter Activity	2	14	3	0	11*	10	1	6*	761

Table 3. Gene ontology clusters altered by Stx2 or LPS challenge in mice.

Discussion

This Stx2 plus LPS mouse model of HUS recapitulates the human disease in both its signs and symptoms, including the clinical diagnostic triad of renal failure, thrombocytopenia, and hemolytic anemia^{438,451,452}. Increased serum creatinine and BUN in these mice demonstrate kidney dysfunction. Low platelet counts found in our model are the definition of thrombocytopenia. Reticulocytes and Howell-Jolly bodies found in the blood smears, an increase in the percent reticulocytes, and red discoloration of the serum caused by free hemoglobin are evidence of hemolytic anemia. Although no schistocytes were seen in the blood smears, we found that, for unknown reasons, in published mouse models of hemolytic anemia, schistocytes are an uncommon finding⁷⁸. The mice also exhibited the neutrophilia and monocytosis found clinically¹⁶², and fibrin and red cell staining of kidneys show thrombus formation in the microvasculature, as seen in HUS patients^{47,453}. Furthermore, electron microscopy showed ultrastructural changes in the glomeruli that are consistent with HUS. As indicated in Table 2, neither Stx2 nor LPS alone was able to mimic HUS in the mouse; however, injection of both agents together elicited the diagnostic triad as well as the other associated clinical signs. This reinforces evidence from human patients that both Stx and LPS are involved in the development of HUS³¹.

Microarray expression analysis reinforces the mouse as a model for human disease, and provides new insight into the details of HUS pathogenesis. Specific gene products known to be increased in HUS patients are upregulated in these mice, such as IL-6 and MCP-1, and these were shown to be part of a general inflammatory response by

evaluation of gene expression clusters. Furthermore, global expression analysis demonstrates that there are temporal waves of transcriptional response for distinct types of genes. A closer look at the specific differentially expressed genes allows formation of multiple testable hypotheses that should be useful to the scientific community, such as that the formation of the fibrin-rich clots typical of HUS may be heavily impacted by the upregulation of all three types of fibrinogen in the kidney (data not shown). Although these gene clusters were formed in an unbiased manner by grouping similar expression patterns, it is noteworthy that the quoted classifications of these clusters do not necessarily describe the complete functional potential of these genes. Nevertheless, the classifications cited in Table 3 do provide insight into what a transcript or group of transcripts does. It is also important to note that the numbers of genes altered by each challenge does not reflect the importance of those genes nor of the challenge. For instance, even though Stx2 alters fewer transcripts than LPS in this model (Figure 17), much of the HUS pathology in Table 2 can be attributed to Stx2. Additionally, this leads to the hypothesis that pharmacological or other alteration of relatively few gene products may be able to significantly alter the course of this disease. Overall, the gene expression analysis should serve as a starting point for numerous avenues of future research.

This model may be complicated by dehydration of the mice, a consequence that does not occur in the human disease²⁷. Although HUS patients normally have decreased hematocrit, the Stx2 plus LPS injected mice display moderately increased hematocrit and hemoglobin. In the mouse, this is likely hemoconcentration due to dehydration, as suggested by the weight loss sustained after injection (Figure 11). We contend that all our significant findings are evidence of HUS as caused by Stx2 plus LPS, and are distinct

from the vascular volume depletion. Specifically, even though the mice challenged with LPS alone lose as much initial weight as the Stx2 plus LPS mice, they exhibit no increased serum creatinine and no signs of hemolytic anemia (Table 2). Furthermore, the mice given Stx2 alone develop increased serum creatinine and reticulocytosis at 4-12 hours post injection, but do not lose weight until 48 hours post injection. Because LPS induces early weight loss without a rise in creatinine, and Stx2 causes a rise in creatinine and reticulocytosis 36 hours before weight loss, we conclude that the dehydration resulting from combinatorial challenge with Stx2 and LPS is distinct from the signs of HUS.

Based on our model, we propose a time course of disease progression in the mouse. Two hours after Stx2 plus LPS injection, platelet levels rise in the kidney followed by peripheral thrombocytopenia that persists throughout the time course. After the rise in renal platelets, red blood cells infiltrate the kidney, form clumps, and congest the glomeruli and vasculature of the kidney. Fibrin deposition follows RBC infiltration and leads to thrombus formation in the renal microvasculature. This thrombosis likely causes glomerular filtration failure, uremia, and eventual death of the mouse. During this time course, we have also ascertained the progression of gene expression in the affected kidney tissue. Inflammatory signaling induced primarily by LPS and cellular damage and repair pathways induced by both Stx2 and LPS are activated in these model HUS kidneys. Furthermore, the downregulation of genes necessary for normal renal function is evidence for activation of a de-differentiation and repair pathway that has been described in response to other renal insults⁴²⁹. Modulation of upregulated genes involved in cell proliferation, apoptosis, the cell cycle, and repair could be able to alter

this disease course. This precise establishment of the physiologic and molecular progression of HUS in the mouse model will allow identification of novel therapeutic strategies to treat this disease.

While other animal models have been reported, this mouse model of HUS is the most economical, practical, and complete model of HUS so far described. Although the baboon³⁹⁵ and canine^{400,407,412,435,436,454} models of HUS mimic the human disease, these large animal models are expensive and impractical for the common researcher. Other rodent models of HUS have been described⁴¹³, but none have completely investigated the full pathophysiology of the disease. Mouse models utilizing oral bacterial inoculation require antibiotic pretreatment and do not result in a one hundred percent rate of infection³¹. Hence these models can be inefficient and impractical. Additionally, HUS is a toxemia and not a bacteremia and thus a model does not require live bacteria^{31,83,439}. In summary, we have shown that concurrent intraperitoneal injection of both Stx2 and LPS is sufficient to reproduce HUS in the C57BL/6 mouse. The data indicate this and offer a reproducible model with which to study HUS, to identify potential therapeutic targets, and for testing of new therapies.

Supplemental Data**Table 4. Murine renal genes altered by Stx2 or LPS challenge.**

For each cluster in Figure 14B, the 20 most differentially expressed genes are listed. The expression values are given in fold change, and represent the greatest deviation from control at any time point during the 72 hour time course. Positive fold change indicates upregulation, while negative indicates downregulation.

Immediate Upregulated		
Gene	Accession	Max Fold Change
chemokine (C-X-C motif) ligand 10	NM_021274	96.2
chemokine (C-X-C motif) ligand 1	NM_008176	51.6
chemokine (C-C motif) ligand 2	AF065933	35.8
2'-5' oligoadenylate synthetase-like 1	AB067533	31.5
ubiquitin specific protease 18	NM_011909	23.9
chemokine (C-X-C motif) ligand 9	NM_008599	22.9
pyruvate dehydrogenase kinase, isoenzyme 4	NM_013743	20.8
FBJ osteosarcoma oncogene	AV026617	20.5
interferon activated gene 205	AI481797	20.3
vascular cell adhesion molecule 1	NM_011693	19.5
intercellular adhesion molecule	BC008626	19.3
early growth response 1	NM_007913	18.8
serine (or cysteine) proteinase inhibitor, clade E, member 1	NM_008871	18.6
thymidylate kinase family LPS-inducible member	AK004595	17.6
cholesterol 25-hydroxylase	NM_009890	17.0
CCAAT/enhancer binding protein (C/EBP), delta	BB831146	15.8
interleukin 6	NM_031168	13.7
suppressor of cytokine signaling 3	BB241535	13.4
colony stimulating factor 1 (macrophage)	NM_007778	13.4

Early Upregulated		
Gene	Accession	Max Fold Change
interferon-induced protein with tetratricopeptide repeats 1	NM_008331	76.8
fibrinogen, gamma polypeptide	NM_133862	55.1
interferon-induced protein with tetratricopeptide repeats 2	NM_008332	50.0
lipocalin 2	X14607	40.4
guanylate nucleotide binding protein 2	NM_010260	39.9
interferon-induced protein with tetratricopeptide repeats 3	NM_010501	36.5
T-cell specific GTPase	NM_011579	30.7
interferon-inducible GTPase	BM239828	29.1
guanylate nucleotide binding protein 3	NM_018734	26.1
interferon-stimulated protein (15 kDa)	AK019325	24.5
fibrinogen, alpha polypeptide	BC005467	22.9
complement component 3	K02782	22.3
serum amyloid A 3	NM_011315	20.0
chemokine (C-C motif) ligand 5	NM_013653	19.0
2'-5' oligoadenylate synthetase-like 2	BQ033138	18.8
interferon gamma induced GTPase	NM_018738	18.3
interferon gamma inducible protein	NM_008330	17.4
tripartite motif protein 30	BM240719	15.2
viral hemorrhagic septicemia virus(VHSV) induced gene 1	BB132493	14.3
interferon regulatory factor 7	NM_016850	14.0

Late Upregulated		
Gene	Accession	Max Fold Change
serum amyloid A 2	NM_011314	26.2
fibrinogen, B beta polypeptide	AK011118	19.7
serum amyloid A 1	NM_009117	16.1
similar to interferon-inducible GTPase	BC023105	11.5
ceruloplasmin	BB009037	8.2
tissue inhibitor of metalloproteinase 1	BC008107	6.1
ubiquitin D	NM_023137	6.0
3-hydroxy-3-methylglutaryl-Coenzyme A synthase 2	BC014714	5.8
interleukin 18 binding protein	AF110803	5.2
leucine-rich alpha-2-glycoprotein	NM_029796	4.8
chemokine (C-X-C motif) ligand 13	NM_018866	4.7
aldehyde dehydrogenase family 1, subfamily A2	NM_009022	4.7
interferon, alpha-inducible protein 27	AY090098	4.5
arginase type II	NM_009705	4.5
histocompatibility 2, class II, locus DMA	NM_010386	3.9
apolipoprotein H	NM_013475	3.7
serum amyloid A 4	BC019212	3.6
histocompatibility 2, class II, locus Mb2	NM_010388	3.4
lipopolysaccharide binding protein	NM_008489	3.3
complement component 1, r subcomponent	NM_023143	3.1

Very Late Upregulated		
Gene	Accession	Max Fold Change
growth arrest and DNA-damage-inducible 45 beta	AI323528	16.4
tumor necrosis factor receptor superfamily, member 12a	NM_013749	11.5
activating transcription factor 3	BC019946	11.1
interferon-related developmental regulator 1	NM_013562	10.6
chemokine (C-X-C motif) ligand 10	NM_021274	9.4
growth differentiation factor 15	NM_011819	8.9
cyclin-dependent kinase inhibitor 1A (P21)	AK007630	7.2
serum-inducible kinase	BM234765	6.9
myeloid differentiation primary response gene 116	NM_008654	6.8
avian reticuloendotheliosis viral (v-rel) oncogene related B	NM_009046	6.5
early growth response 1	NM_007913	6.3
v-maf	BC022952	4.9
plasmacytoma variant translocation 1	BE956863	4.8
chemokine (C-X-C motif) ligand 1	NM_008176	4.7
FBJ osteosarcoma oncogene	AV026617	4.3
core promoter element binding protein	AV025472	4.3
H4 histone family, member A	BC028550	4.3
Jun oncogene	BC002081	4.2
pyruvate dehydrogenase kinase, isoenzyme 4	NM_013743	4.2
histone 1, H3a	NM_013550	4.1

Immediate Downregulated		
Gene	Accession	Max Fold Change
insulin-like growth factor binding protein 5	NM_010518	-4.3
SRY-box containing gene 18	NM_009236	-3.8
vascular endothelial zinc finger 1	BC024610	-3.4
endothelial-specific receptor tyrosine kinase	NM_013690	-2.9
ETL1	NM_133222	-2.8
transcription factor 21	NM_011545	-2.8
solute carrier family 9, isoform 3 regulator 2 (Na/H exchanger)	BF468098	-2.7
serum deprivation response	NM_138741	-2.4
RAS-like, family 11, member B	BC008101	-2.4
paralemmin	NM_023128	-2.2
secreted frizzled-related sequence protein 1	BC024495	-2.2
centromere autoantigen B	BC006628	-2.1
cask-interacting protein 2	NM_080643	-2.1
SPRY domain-containing SOCS box 4	BC023083	-2.1
phosphatidylcholine transfer protein	NM_008796	-2.0
matrix-remodelling associated 8	BB765827	-2.0

Early Downregulated		
Gene	Accession	Max Fold Change
carbonic anhydrase 14	NM_011797	-3.8
angiopoietin-like 2	BF681826	-3.3
creatine kinase, brain	BG967663	-3.2
cholecystokinin	NM_031161	-3.2
transcription factor 2	AB008174	-2.9
insulin-like growth factor 1	BG075165	-2.9
plasmalemma vesicle associated protein	NM_032398	-2.8
endomucin	AB034693	-2.7
ubiquitin-like 1	AK002312	-2.7
transmembrane 7 superfamily member 1	BB325447	-2.6
complement component 1, q subcomponent, alpha	NM_007572	-2.6
thioesterase, adipose associated	NM_025590	-2.5
ATPase, Na ⁺ /K ⁺ transporting, beta 2 polypeptide	BG261955	-2.5
C-type lectin domain family 14, member a	BC019452	-2.5
solute carrier family 4 (anion exchanger), member 1	NM_011403	-2.4
osteoglycin	BC021939	-2.4
protein phosphatase 1, regulatory (inhibitor) subunit 1B	BC026568	-2.4
semaphorin 4D	NM_013660	-2.4
activating signal cointegrator 1 complex subunit 1	AK007519	-2.4
septin 4	NM_011129	-2.4

Late Downregulated		
Gene	Accession	Max Fold Change
D site albumin promoter binding protein	BB550183	-8.2
hydroxysteroid dehydrogenase-2, delta<5>-3-beta	BC026757	-6.5
hydroxysteroid dehydrogenase-6, delta<5>-3-beta	NM_013821	-5.7
solute carrier family 9, member 8 (Na/H exchanger)	BB408147	-5.2
carbonic anhydrase 3	AK003671	-4.7
transferrin receptor	NM_011638	-4.2
mitogen activated protein kinase 10	BB313689	-3.7
glycine amidinotransferase	AW108522	-3.5
G protein-coupled receptor 91	NM_032400	-3.4
cholecystokinin A receptor	BC020534	-3.3
branched chain aminotransferase 1, cytosolic	X17502	-3.3
similar to Isopentenyl-diphosphate delta-isomerase	BC004801	-3.3
cytochrome P450, 24	D89669	-3.2
C-type lectin 1	AK017207	-3.2
myosin Va	AK002362	-3.1
nuclear receptor subfamily 1, group D, member 1	W13191	-3.1
profilin 3	BC019455	-3.1
elastase 1, pancreatic	BC011218	-3.1
growth arrest specific 2	NM_008087	-2.8
solute carrier family 5, member 11 (Na/glucose transporter)	AK008219	-2.6

Very Late Downregulated		
Gene	Accession	Max Fold Change
mitogen activated protein kinase 10	BB313689	-6.5
hydroxysteroid 11-beta dehydrogenase 2	BC014753	-6.1
calbindin-28K	BB246032	-4.4
arginine vasopressin receptor 2	NM_019404	-3.9
aquaporin 2	BC019966	-3.8
5' nucleotidase, ecto	NM_011851	-3.2
sodium channel, nonvoltage-gated 1 gamma	NM_011326	-2.8
Rhesus blood group-associated C glycoprotein	NM_019799	-2.6
transferrin receptor	NM_011638	-2.5
nucleoplasmin 3	BB811478	-2.5
FXFD domain-containing ion transport regulator 4	NM_033648	-2.4
carbonic anhydrase 3	NM_007606	-2.3
sodium channel, nonvoltage-gated 1 beta	NM_011325	-2.3
similar to Isopentenyl-diphosphate delta-isomerase	BC004801	-2.1
aldo-keto reductase family 1, member B3	BB469763	-2.1
clusterin	BB433678	-2.1
cholecystokinin A receptor	BC020534	-2.1
procollagen, type III, alpha 1	AW550625	-2.0
protein related to DAN and cerberus	NM_011825	-2.0
calbindin-D9K	NM_009789	-2.0

Chapter 3: Shiga Toxin 2 Induced Collecting Duct Apoptosis Causes Renal Failure in the Murine Model of the Hemolytic Uremic Syndrome

Abstract

Hemolytic uremic syndrome (HUS) caused by Shiga toxin producing *Escherichia coli* infection is a leading cause of pediatric acute renal failure. Bacterial toxins produced in the gut enter the circulation and cause a systemic toxemia and targeted cell damage. It had been previously shown that injection of Shiga toxin 2 (Stx2) and lipopolysaccharide (LPS) caused signs and symptoms of HUS in mice, but the mechanism leading to renal failure remained uncharacterized. The current study elucidated that murine cells of the glomerular filtration barrier were unresponsive to Stx2 because they lacked the glycosphingolipid receptor Gb₃ *in vitro* and *in vivo*. In contrast to the homologous human cells, Stx2 did not alter inflammatory kinase activity, cytokine release, or cell viability of the murine glomerular cells. However, murine renal cortical and medullary tubular cells expressed Gb₃ and responded to Stx2 by undergoing apoptosis. Stx2-induced loss of collecting ducts *in vivo* caused production of increased dilute urine, resulted in dehydration, and contributed to renal failure. Stx2 mediated renal dysfunction was ameliorated by administration of the non-selective caspase inhibitor Q-VD-OPH *in vivo*. Stx2 therefore targets the murine collecting duct and this Stx2 induced injury can be blocked by inhibitors of apoptosis *in vivo*.

Introduction

Shiga toxin producing *Escherichia coli* (STEC) is the principal etiologic agent of diarrhea-associated hemolytic uremic syndrome (D+HUS)^{31,50,83,439}. Renal disease is thought to be due to the combined action of Shiga toxins (Stx1, Stx2), the primary virulence factors of STEC, and bacterial LPS on the renal glomeruli and tubules⁴⁴⁴. Of these, Stx2 is most frequently associated with development of HUS^{31,83,439}. Shiga toxin enters susceptible cell types after binding to the cell surface receptor glycosphingolipid globotriaosylceramide (Gb₃), and specifically depurinates the 28S rRNA, thereby inhibiting protein synthesis^{115,328,329,343,349,455-457}. The damage initiates a ribotoxic stress response consisting of MAP kinase activation, and can be associated with cytokine release and cell death^{115,124}. This cell death is often caspase dependent apoptosis^{107,234,330,349,458,459}. Gb₃ is expressed by human glomerular endothelial cells, podocytes, and multiple tubular epithelial cell types, and damage markers for these cells can be detected in HUS patient urine^{37,195,460}. Shiga toxin binds to these cells in patient renal sections, and along with the typical fibrin rich glomerular microangiopathy, these sections demonstrate apoptosis of both glomerular and tubular cell types^{31,330}. However, despite the multiple distinct categories of renal damage, the primary mechanism leading to complete HUS is thought to be glomerular damage with dysregulation of coagulation^{187,412}.

Concomitant development of the most prominent features of HUS: anemia, thrombocytopenia, and renal failure, in the murine model requires both Shiga toxin and LPS^{187,412}. Nevertheless, our previous work also demonstrated that this renal failure is mediated exclusively by Stx2³⁹⁸. While it is established that Gb₃ is the unique Shiga toxin receptor^{94,116,398,435}, the current literature regarding the mechanism by which Shiga

toxin causes renal toxicity in the mouse is inconsistent. Even though Gb₃ has been localized to some murine renal tubules and tubular damage has been observed^{187,398,412}, glomerular abnormalities including platelet and fibrin deposition occur as well^{116,435}. Furthermore, although multiple groups have been unable to locate the Shiga toxin receptor Gb₃ in glomeruli on murine renal sections⁴⁶¹, one group has published that murine glomerular podocytes possess Gb₃ and respond to Stx2 *in vitro*³⁹⁸, and another that renal tubular capillaries express the receptor⁴⁶². We demonstrate here that murine glomerular endothelial cells and podocytes are unresponsive to Stx2 because they do not produce the glycosphingolipid receptor Gb₃ *in vitro* or *in vivo*, and that renal collecting duct apoptosis is responsible for Stx2 induced murine renal failure.

Methods

Shiga Toxin Purification

Shiga toxin 2 (Stx2) was purified by immunoaffinity chromatography from cell lysates (generously provided by Alison O'Brien) of *E. coli* DH5α containing the Stx2 producing pJES120 plasmid⁴⁶². Lysates were processed using 11E10 antibody⁴⁴³ immobilized with an AminoLink Plus Kit, and endotoxin was removed using De-toxi-Gel (Pierce Biotechnology, Rockford IL). Stx2 purity was assessed by SDS-PAGE, determined to be endotoxin free, and activity was measured in a Vero cell cytotoxicity assay. *E. coli* O55:B5 LPS purified by gel filtration chromatography and gamma irradiation was purchased from Sigma-Aldrich (St. Louis, MO).

Cell Lines

HUVEC purchased from VEC Technologies (Rensselaer, NY)³⁴⁹, and RPTEC purchased from Clonetics (San Diego, CA)⁴⁶³ were cultured as described. Conditionally immortalized human glomerular endothelial cells⁴⁶⁴, primary murine aortic endothelial cells graciously provided by Dr. Lynn Hedrick (University of Virginia, Charlottesville, VA)³⁴⁹, immortalized murine proximal tubular epithelial cells kindly provided by Dr. Mark Okusa (University of Virginia, Charlottesville, VA)⁴⁶⁵, conditionally immortalized human podocytes⁴⁶⁶⁻⁴⁶⁸, conditionally immortalized murine podocytes generously provided by Dr. John Sedor (Case Western Reserve University, Cleveland, OH), and conditionally immortalized murine glomerular endothelial cells from Dr. Michael Madaio (Temple University, Philadelphia, PA)^{463,465-467}, were all cultured as described. Briefly, conditionally immortalized cells lines were maintained at the permissive 33°C and considered undifferentiated. Undifferentiated cells were moved to the non-permissive 37°C two weeks prior to experimental use, after which point they were considered differentiated⁴⁶⁹. Cells were seeded at 5×10^5 per well in 6-well plates or 2×10^4 per well in 96-well plates. All experiments were performed on plates coated with rat tail collagen I (BD Biosciences, San Jose, CA) in serum-free RPMI (Mediatech, Herndon, VA). Except for cytotoxicity assays, cells were challenged with either: no toxin, Stx2, 1 µg/mL LPS, or Stx2 and LPS, with 1 pM and 1 nM Stx2 employed for human glomerular and murine glomerular cells, respectively.

Thin Layer Chromatography Shiga Toxin Overlay

Each cell type grown to confluency on one 75-cm² flask was trypsinized and neutral glycolipids were isolated⁴⁷⁰. For some studies, cells were incubated with 1 µg/mL LPS

(*E. coli* O55:B5, Sigma-Aldrich, St. Louis, MO) 24 hours prior. Gb₃ content was analyzed by thin-layer chromatography (TLC) with Stx1B overlay⁴⁷¹. Total neutral lipids on a duplicate plate were visualized using CuSO₄ along with neutral glycosphingolipid standards (Matreya LLC, Pleasant Gap, PA)⁴⁷². Images are representative of triplicate experiments.

Immunoblotting

Cells were incubated with toxins for 0.5-12 h. Cells were lysed in modified RIPA buffer²⁶⁷. Lysate protein was quantified with a BCA protein assay (Pierce). Total cell lysate was loaded at 5 µg per well, resolved by SDS-PAGE, transferred to PVDF membrane, and probed with the following: anti-p38 MAPK and anti-phospho-p38 antibodies (BD Biosciences), anti-mouse horseradish peroxidase (HRP)-tagged antibody (Amersham, Piscataway, NJ), anti-β-actin (Abcam, Cambridge, MA), and anti-SV40 T-antigen (Calbiochem, San Diego, CA). Bound HRP was detected by chemiluminescence (Perkin Elmer, Waltham, MA). Images are representative of triplicate experiments.

Cytotoxicity Assay

Cells were treated with between 1 fM and 10 nM Stx2 for 24 h. CCK-8 cell viability assays were performed to determine the CD₅₀ (Dojindo Molecular Technologies, Gaithersburg, MD). Co-incubation with 1 µg/mL LPS only enhanced HUVEC cytotoxicity⁴⁷³. Caspases were inhibited with 100 µM Q-VD-OPH (MP Biochemicals, Solon, OH) suspended in dimethyl sulfoxide (DMSO) for 1 h prior to, as well as

following, the addition of Stx2⁴⁷⁴. The final concentration of DMSO was 0.5%. Data are representative of quadruplicate experiments.

Extracellular Signaling Molecule Quantification

Cells were incubated with toxins for 12 h. Extracellular MCP-1, IL-6, VEGF, IL-8 and CXCL1/KC release was quantified using DuoSet ELISA kits (R&D Systems, Minneapolis, MN). Because mice do not produce IL-8, CXCL1/KC was used as the murine functional homolog¹⁸⁷. Extracellular proteins measured in pg/mL were normalized to values from control cells and expressed as percent change. Data are representative of triplicate experiments.

Caspase Activity Assay

Cells were challenged with toxins for 12 h. Lysates were collected as described above and tested for caspase activity with the Caspase 3/7 Assay Kit (Upstate, Lake Placid, NY) using the fluorogenic caspase substrate Ac-DEVD-AMC. Data are representative of triplicate experiments.

Murine Model of HUS

C57BL/6 and CD-1 male mice weighing 22-24 grams were purchased from Charles River (Wilmington, MA). C3H/HeJ and BALB/c mice were purchased from Jackson (Bar Harbor, ME). Food and water were provided ad libitum. Mice were injected intraperitoneally with 300 µg/kg LPS (O55:B5, Sigma-Aldrich, St. Louis, MO), 225 ng/kg Stx2, or both as described⁴⁷⁵. Mice were weighed every 12 hours after injection

and weight loss was expressed as percent change from the time 0. At 0, 24, 48, 60, and 72 h after injection mice were euthanized. For each mouse, kidneys, blood, and urine were collected. To prevent apoptosis *in vivo*, mice were intraperitoneally injected with two 18 mg/kg doses of Q-VD-OPH in 100 μ L 50% DMSO at 24 and 48 h after Stx2 plus LPS injection^{463,465-467}. In separate experiments, normal mice were dehydrated for 20 h by withholding access to water. All animal procedures were done in accordance with University of Virginia Animal Care and Use Committee policies (Charlottesville, VA).

Blood Analysis and Urinalysis

Blood was collected with heparinized capillary tubes (Fisher, Pittsburgh, PA) by retro-orbital bleed and centrifuged at 840 x g for 15 min at 4°C to collect the plasma layer. Blood urea nitrogen (BUN) was determined with VetScan (Idexx Corporation, Westbrook, ME). Urine was collected by direct bladder puncture, and osmolality was determined with the Vapro vapor pressure osmometer (Wescor, Logan UT). Each data point represents the average from 8 mice.

Immunohistochemistry

Control and Stx2 plus LPS challenged C57BL/6 mice and normal CD-1, BALB/c, C3H/HeN and C3H/HeJ mice were used. Kidney was fixed in 4% paraformaldehyde, processed in acetone for Gb₃ or ethanol for TUNEL staining, and embedded in paraffin as described³⁶⁹. Ethanol has been previously demonstrated to both remove endogenous Gb₃ and cause false positive Gb₃ staining³⁶⁹. Sections were incubated with anti-Gb₃/CD77 IgM (Beckman Coulter, Fullerton, CA) at 1:40 dilution, isotype-matched rat IgM

(Millipore, Billerica, MA), anti-activated caspase 3 (Cell Signaling, Danvers, MA) at 1:200 or isotype-matched rabbit IgG (Chemicon), and anti-rat IgM biotin conjugate (American Qualex, San Clemente, CA) at 1:500 dilution. Terminal deoxynucleotidyl transferase biotin-dUTP nick end labeling (TUNEL) was performed with the ApopTag Peroxidase *In Situ* Apoptosis Detection Kit (Chemicon, Temecula, CA), with post-weaning female rat mammary gland as a positive control. Immunoreactivity was detected using Vectastain ELITE ABC kit (VECTOR Laboratories, Burlingame, CA). Hematoxylin was the counterstain. Renal apoptosis was quantified by counting the number of apoptotic cell nuclei per sixteen 200x fields, and expressed as the average number of apoptotic nuclei per kidney. Each data point represents the average from 8 mice.

Immunofluorescence

Kidney tissue was isolated following perfusion fixation in 4% paraformaldehyde. Sections were blocked with anti-rat IgM or secondary antibody-matched normal sera, incubated with anti-Gb₃/CD77 at 1:100 dilution, anti-CD31 (BD Pharmingen) at 1:50, anti-aquaporin-1 (Chemicon) at 1:1000, anti-aquaporin-2 (Chemicon) at 1:800, or isotype control antibody (Chemicon) at the equivalent concentration in normal goat serum, washed, and incubated with fluorescent secondary antibodies (Invitrogen, Carlsbad, CA). Specimens were examined with an LSM 510 microscope (Zeiss, Thornwood, NY) and analyzed using LSM Image Browser software (Zeiss).

Statistics

All data are expressed as means \pm standard deviations. Statistics were performed using two sample Student's t-test assuming unequal variances. $P < 0.05$ was considered significant.

Results

Murine Glomerular Cells Do Not Express Gb₃

Human HUS is thought to result from glomerular damage by Shiga toxin. We began investigating the mechanism of renal failure in the mouse model by determining the sensitivity of murine glomerular filtration barrier cells to Stx2. Conditionally immortalized human and murine glomerular endothelial cells and podocytes have been described in detail^{465,466}. These cells grow indefinitely at 33°C. When differentiated at 37°C these cells express cell type specific markers and slow their proliferation. Whole cell lysates were derived from cells grown at permissive and non-permissive temperatures and analyzed by immunoblot (Figure 19a). These cells were compared to primary human umbilical vein endothelial cells (HUVEC) that do not express the temperature sensitive SV40 large T antigen. When incubated at non-permissive conditions all conditionally immortalized cell types appropriately degraded the transgene and slowed or stopped proliferation. Differentiated human and murine podocytes also developed typical arborizations (data not shown)^{234,458}.

To test the murine glomerular cells for the presence of the Stx2 receptor Gb₃, cellular lipids were isolated and separated by thin layer chromatography (TLC). Total neutral lipids were visualized on the TLC plate by staining with cupric sulfate (bottom, Figure 19b) and Gb₃ was specifically identified by overlay with Stx1B (top, Figure 19b).

Although the lipid profiles differed between cell types, similar loading was verified by the slow migrating glycolipid band at the bottom of the TLC plate. Human glomerular endothelial cells and podocytes expressed very high levels of Gb₃ consistent with previous reports, while murine glomerular endothelial cells, podocytes, and primary cells failed to express detectable Gb₃²⁶⁷. Only HUVEC produced more Gb₃ when incubated with LPS for 24 h (data not shown)^{115,328,329,343,455-457}.

Figure 19. Human and murine glomerular cell SV40 and Gb3 in vitro.

Human and murine glomerular cell expression of SV40 Large T Antigen and Gb₃. (a) Whole cell lysates from human glomerular cells and murine glomerular cells grown at permissive conditions (33°C), compared to human and murine glomerular cells grown at non-permissive conditions (37°C). Differentiated cells grown for two weeks at non-permissive conditions degraded the SV40 temperature sensitive large T antigen. HUVEC human primary endothelial cells were used as a control. (b) Top: thin-layer chromatography (TLC) of total neutral lipids with Stx1b overlay to specifically detect Gb₃. Bottom: total neutral lipids visualized by cupric sulfate to demonstrate similar loading. The glycosphingolipid standards included: CMH, ceramide monohexoside (glucosylceramide); CDH, ceramide dihexoside (lactosylceramide); Gb₃, Globotriaosylceramide; Gb₄, globotetraosylceramide.

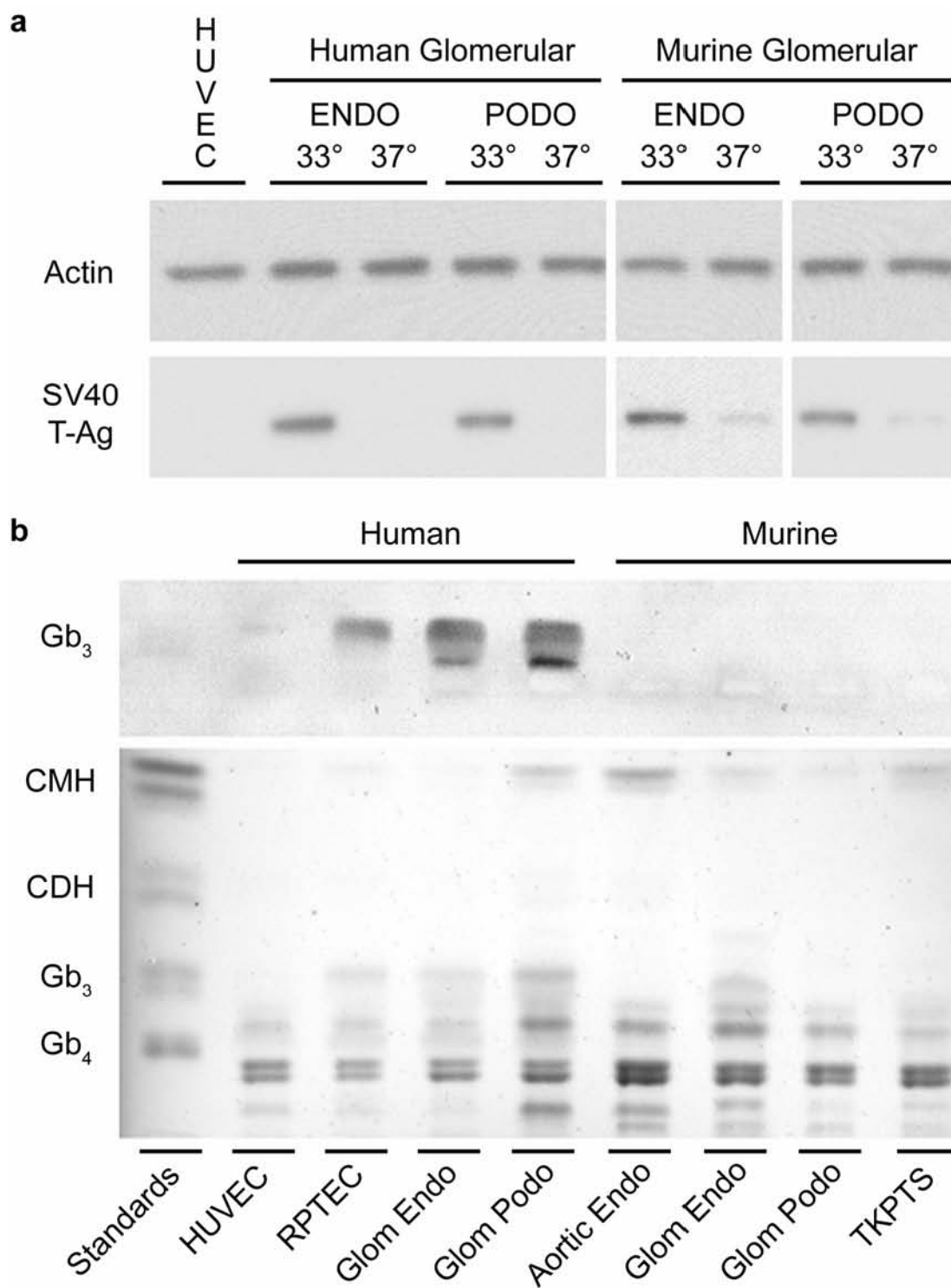


Figure 19. Human and murine glomerular cell SV40 and Gb₃ *in vitro*.

Murine Glomerular Cells are Insensitive to Stx2

Stx2 has been demonstrated to have multiple effects on susceptible cell types including initiation of inflammatory intracellular signaling, cytokine release, and cellular apoptosis^{267,349}. Table 5 summarizes the immortalization status and Stx2 induced 24 h 50% cytotoxic dose (CD₅₀), for the human and mouse cells used in this study. Human glomerular cells were extremely sensitive to the cytotoxic effects of Stx2, while murine glomerular cells were insensitive to Stx2, even at a dose of 10 nM. Primary cell lines from both species were used as controls for the conditional immortalization. Primary HUVECs and renal proximal tubule epithelial cells (RPTEC) were sensitive, as previously reported, while primary murine aortic endothelial cells were not^{115,456,457}. The sensitivities of cells to the cytotoxic effect of Stx2 generally correlated with their level of Gb₃ expression (Table 5, Figure 19b).

Table 5. The 24 hour LD50 for human and murine cell types.

The Stx2 24 hour 50% lethal dose (LD₅₀) and immortalization status for cell types used in this study.

^aInsensitive cells did not respond to the maximum dose of 10 nM Stx2 for 48 h.

Cell Type	Human Cells		Murine Cells	
	Cell Isolation	24 hour CD ₅₀	Cell Isolation	24 hour CD ₅₀
Glomerular Endothelium	Conditionally Immortalized	0.1 pM	Conditionally Immortalized	Insensitive ^a
Glomerular Podocytes	Conditionally Immortalized	0.5 pM	Conditionally Immortalized	Insensitive ^a
Proximal Tubules	Primary	10 pM	Immortalized	Insensitive ^a
Large Vessel Endothelium	Primary	1 nM	Primary	Insensitive ^a

Table 5. The 24 hour LD₅₀ for human and murine cell types

Stx2 increases inflammatory mediator release and MAP kinase activation in some cell types, even in the absence of cytotoxicity^{115,124}. Even though the murine cells were not sensitive to the cytotoxic effects of Stx2, they might respond by activating intracellular kinases or by releasing extracellular signaling molecules. To test this, whole cell lysates from human and murine glomerular cells were treated with Stx2 or LPS over a 12 hour time course, and immunoblotted for total and activated p38 MAP kinase (Figure 20) and JNK (data not shown). p38 was activated in the human cells by both LPS and 1 pM Stx2, though the kinetics were distinct. LPS caused a rapid increase in p38 activation from 1-2 hours, while Stx2 began to exert its effect by 2-6 hours and continued throughout the experiment. In contrast, the murine glomerular cells only responded to LPS, even at a Stx2 concentration of 1 nM (Figure 20). The murine glomerular cells were more sensitive than the human cells to the effects of LPS, showing a more rapid response between 0.5-2 h, but no significant increase in p38 phosphorylation was observed in response to Stx2. JNK activation due to Stx2 and LPS showed similar qualitative results as for p38 in all cell types (data not shown).

Figure 20. Western blots for p38 from human and murine glomerular cells.

Western immunoblots of activated and total p38 from differentiated human and murine glomerular cells over a 12 hour time course. Cells were incubated in media alone as a control, or challenged with Stx2, 1 $\mu\text{g}/\text{mL}$ LPS, or Stx2 plus LPS. For human cells 1 pM Stx2 was employed, while 1 nM Stx2 was used for the murine cells.

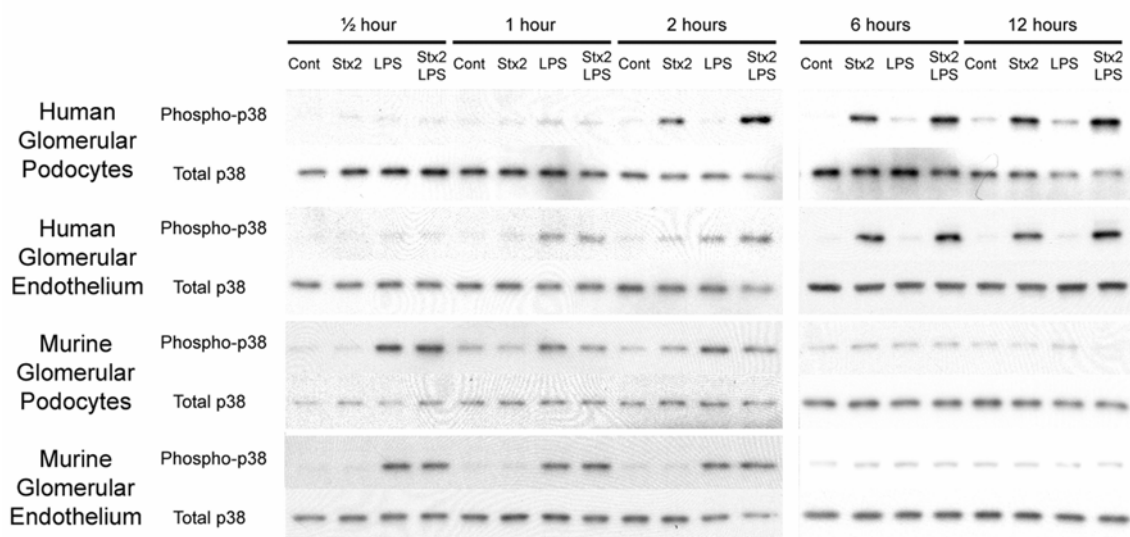


Figure 20. Western blots for p38 from human and murine glomerular cells.

Table 6. Extracellular signaling molecules altered by Stx2 or LPS in vitro.

Extracellular signaling molecule concentrations with significant fold change by ELISA compared to control media from human and murine glomerular cells. Control media cytokine values are presented in pg/mL, and cytokine concentrations for other treatments are reported as fold change from those control baseline values. ^aFold change only shown if $P < 0.05$ compared to control media values used as baseline; -, $P > 0.05$ and thus not significant; nt, not tested.

Cytokine	Human Glomerular Endothelium			Human Glomerular Podocytes			Murine Glomerular Endothelium			Murine Glomerular Podocytes						
	pg/mL baseline	Fold Change ^a			pg/mL baseline	Fold Change ^a			pg/mL baseline	Fold Change ^a			pg/mL baseline	Fold Change ^a		
		Stx	LPS	Stx + LPS		Stx	LPS	Stx + LPS		Stx	LPS	Stx + LPS		Stx	LPS	Stx + LPS
KC/ CXCL1	nt	nt	nt	nt	nt	nt	nt	nt	573 ± 65	-	5.2 ± 0.1	5.2 ± 0.1	491 ± 12	-	5.5 ± 0.1	5.7 ± 0.2
IL-8	152 ± 3	-	16 ± 0.3	5.3 ± 0.1	526 ± 27	-	1.9 ± 0.1	1.8 ± 0.1	nt	nt	nt	nt	nt	nt	nt	nt
IL-6	111 ± 4	-	100 ± 0.6	16 ± 1.2	903 ± 28	-	1.2 ± 0.1	1.2 ± 0.1	10 ± 1	-	1.8 ± 0.2	1.5 ± 0.1	10 ± 1	-	2.0 ± 0.1	2.3 ± 0.3
MCP-1	30 ± 4	-	31 ± 1.0	2.6 ± 0.2	177 ± 5	-	3.3 ± 0.1	3.0 ± 0.1	532 ± 65	-	2.1 ± 0.5	2.0 ± 0.2	999 ± 41	-	2.2 ± 0.1	2.2 ± 0.1
VEGF	< 10	-	-	-	62 ± 9	0.2 ± 0.3	5 ± 0.1	0.2 ± 0.1	< 10	-	-	-	53 ± 6	-	0.5 ± 0.1	0.6 ± 0.1

Table 6. Extracellular signaling molecules altered by Stx2 or LPS *in vitro*.

Presented in Table 6 is the relative fold change in extracellular signaling molecule release by human and murine glomerular cells in response to 12 h with Stx2 and LPS. LPS increased supernatant cytokine release by these cell types. In contrast, Stx2 only affected the Gb₃ expressing human cells, and did so by decreasing the signaling molecules released. Stx2 mediated 15±3% and 25±5% cytotoxicity on the human podocytes and endothelial cells, respectively, at this time point. Human glomerular cells incubated with the same dose of LPS but a 10-fold lower dose of Stx2 (100 fM) did not exhibit significantly decreased cell viability or LPS induced cytokine release by 12 h (data not shown). This suggested that the Stx2 inhibition of inflammatory mediator release was secondary to Stx2 mediated cell death.

Stx2 Mediates Caspase Dependent Apoptosis

It has been reported that Shiga toxin mediates caspase dependent apoptotic cell death in certain cell types⁴⁷⁶. Caspases are cytoplasmic cysteine proteases essential to the destructive phase of apoptosis¹⁸⁷. Thus, activity of the major effector caspase 3 was measured in lysates from cells treated for 12 h with Stx2, LPS, or the combination. Caspase activity was increased in human glomerular endothelial cells (Figure 21a) and podocytes (Figure 21b) in response to Stx2, but not in murine glomerular cells (data not shown). LPS did not have a significant impact on caspase 3 activity in any cell type (Figure 21a,b). In human cells, the non-selective caspase inhibitor Q-VD-OPH rescued 80% of the cytotoxic effect of Stx2 on endothelial cells (Figure 21c), and 100% of the effect on podocytes (Figure 21d). Although higher and lower concentrations of the

caspase inhibitor were tested, the dose reported provided the maximum non-toxic effect (data not shown).

Figure 21. Caspase 3 activity and apoptosis inhibition in human glomerular cells. Human glomerular cell caspase activity and cell death inhibition by the non-selective caspase inhibitor Q-VD-OPH. Lysates from human glomerular endothelial cells (a) and human glomerular podocytes (b) were treated with Stx2, LPS or Stx2 plus LPS for 12 h. Cell viability after incubation of human glomerular endothelial cells (c) and human glomerular podocytes (d) with Q-VD-OPH was compared to media alone or 0.5% DMSO vehicle. Controls for both Q-VD-OPH and Stx2 treatment are media alone. *, $P < 0.05$ compared to control unchallenged with Stx2; **, $P < 0.05$ compared to Stx2 challenge without Q-VD-OPH.

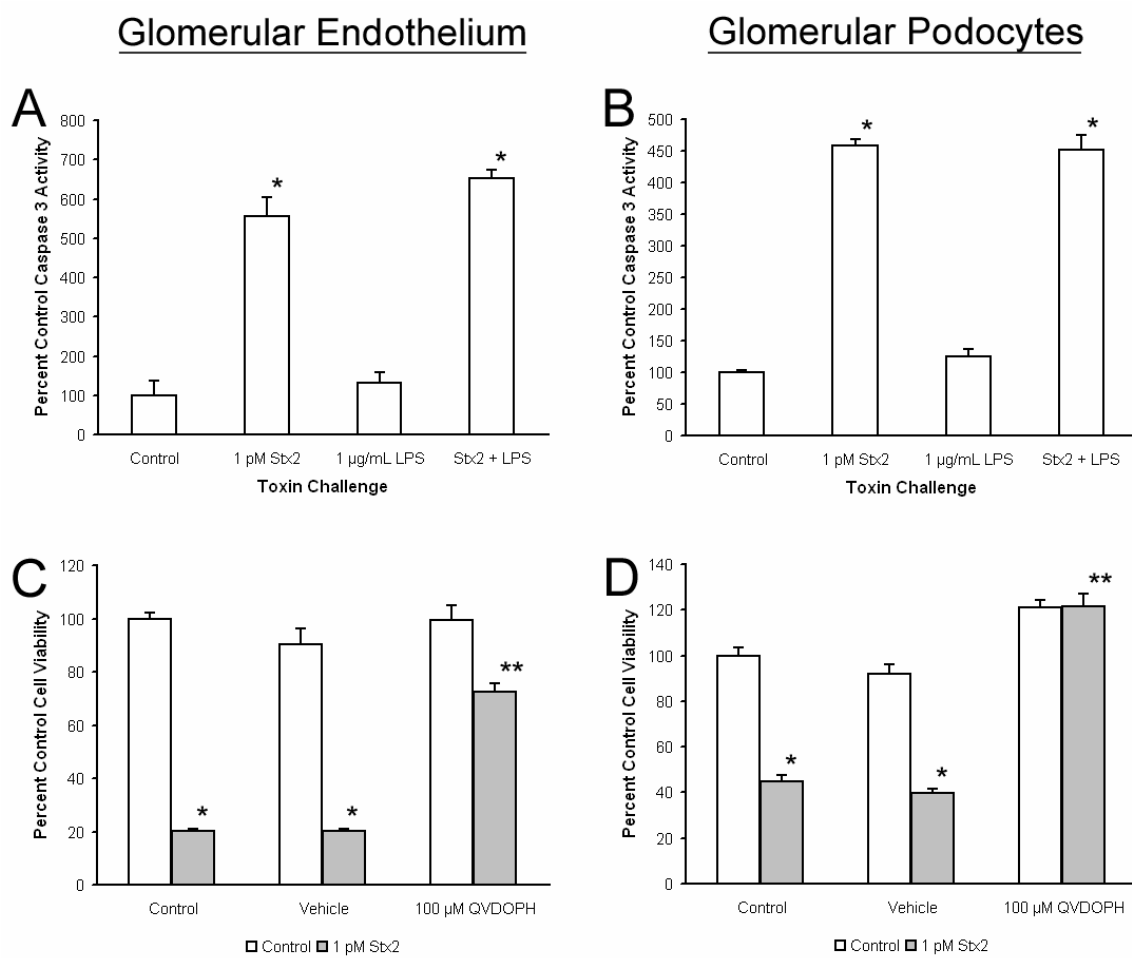


Figure 21. Caspase 3 activity and apoptosis inhibition in human glomerular cells.

Murine Renal Tubules Produce Gb₃

It has previously been shown that Stx2 causes murine renal failure¹¹. Having demonstrated that Stx2 does not directly affect the murine renal glomerular filtration barrier cells *in vitro*, we sought to determine the Stx2 target cells in the mouse kidney. Normal mouse renal tissue subjected to immunohistochemistry with anti-Gb₃ antibody demonstrated Gb₃ only on tubular cells, and not in glomeruli or blood vessels (Figure 22). Similar qualitative staining was observed in all mouse strains tested, including C57BL/6, CD-1, BALB/c, and C3H/HeJ mice (data not shown). Morphologically, Gb₃ appeared to strongly stain cells of the collecting duct, with some less robust staining of proximal tubules, distal tubules, and parts of the loop of Henle (Figure 22).

To confirm the identity of the most abundant Gb₃-positive cell types, immunofluorescence co-localization for Gb₃ and aquaporin-2 was performed¹¹. Aquaporin-2 is a specific collecting duct cytoplasmic and membrane protein that mediates water reabsorption from the tubular lumen¹¹. High power images of Gb₃ and aquaporin-2 showed co-localized staining, with Gb₃ on the outer membrane, consistent with antibody binding the outer carbohydrate moiety, and aquaporin-2 distributed both in the membrane and cytoplasm (Figure 23a). Low power images of the murine renal medulla stained for Gb₃, aquaporin-2, or both (Figure 23b), depicted almost all Gb₃ expressing medullary tubules to be collecting ducts. Gb₃ staining was not found to co-localize with the endothelial marker CD31 in the mouse kidney (data not shown).

Figure 22. Immunohistochemistry of Gb3 in mouse kidney.

Normal untreated mouse renal Gb3 localization by immunohistochemistry. Isotype control shows no renal staining. Sections from cortex, papilla, and medulla demonstrate anti-Gb3 staining of the collecting ducts, loops of Henle, and parts of the proximal and distal tubules by morphology. No staining was observed in glomeruli. Images are representative of 8 mice each and are at 200x magnification.

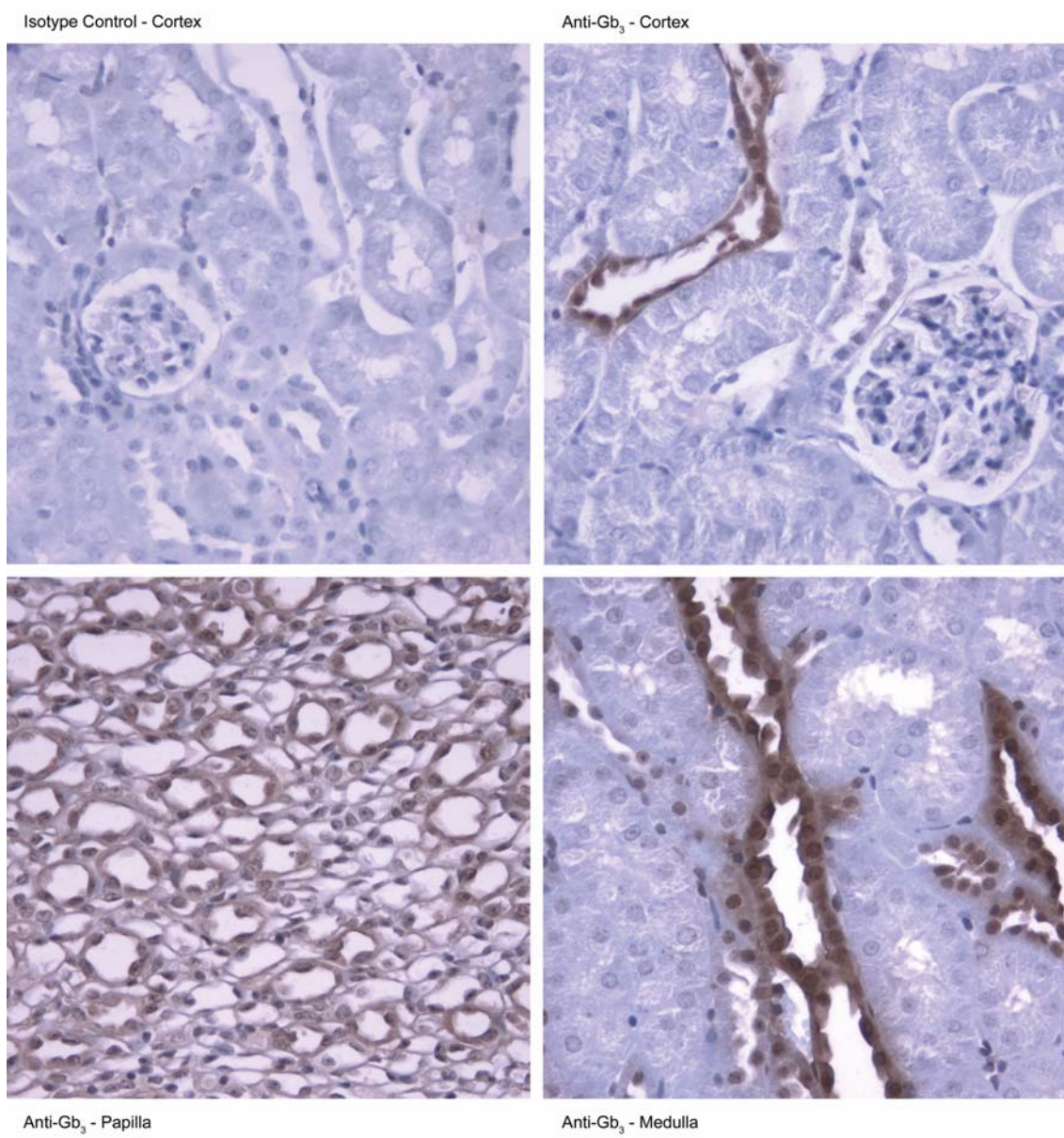


Figure 22. Immunohistochemistry of Gb₃ in mouse kidney.

Figure 23. Immunofluorescence of Gb₃ and aquaporin-2 in mouse kidney.

Immunofluorescence staining of normal mouse renal tissue for Gb₃ and aquaporin-2. (a) High power images of medullary tubules stained with anti-Gb₃, anti-aquaporin-2, and the merged image with overlap colored in yellow, and magnification of boxed region (inset). (b) Low power images of renal medulla stained with anti-Gb₃, anti-aquaporin-2, and the merged image. Bar measures 10 μm in (a) and 100 μm in (b).

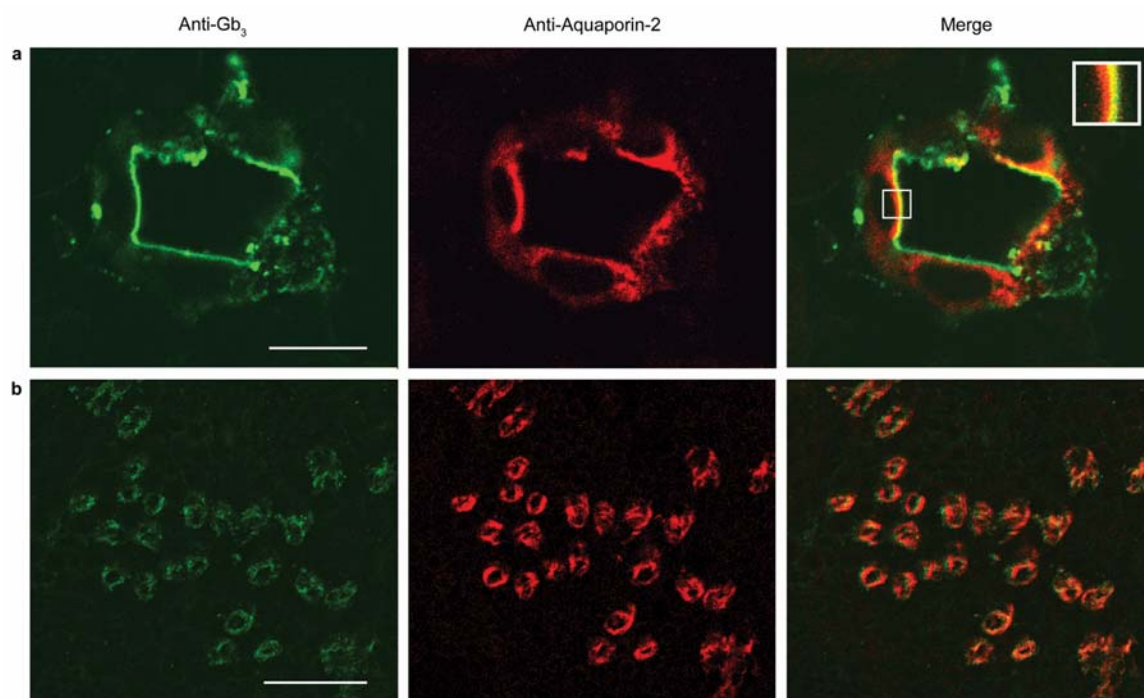


Figure 23. Immunofluorescence of Gb₃ and aquaporin-2 in mouse kidney.

Stx2 Causes Murine Tubular Apoptosis

To determine if the cells found to produce Gb₃ *in vivo* undergo apoptosis, TUNEL staining was performed on renal sections from mice 72 h after Stx2 plus LPS injection. Positive TUNEL stain was found only in tubular cell nuclei (Figure 24), and only rare TUNEL positive cells were observed in normal mouse renal sections. Consistent with the absence of Gb₃, there were no apoptotic cells visualized in the glomeruli or renal vasculature of Stx2 plus LPS challenged mice. Analysis of kidneys from mice between 0 and 72 h after Stx2 plus LPS injection demonstrated increased TUNEL positive cells at 60 and 72 h post injection (Figure 25a). LPS alone did not increase renal apoptosis above baseline (data not shown).

203

Figure 24. Renal apoptosis in Stx2 plus LPS challenged mice.

TUNEL peroxidase staining of renal sections from mice challenged with Stx2 plus LPS.

Mice were euthanized 72 hours after Stx2 plus LPS injection. Compared to control saline injected mouse cortical and medullary sections, cortical and medullary sections from Stx2 plus LPS injected mice demonstrated tubular apoptosis. Images are representative of 8 mice each and are at 200x magnification.

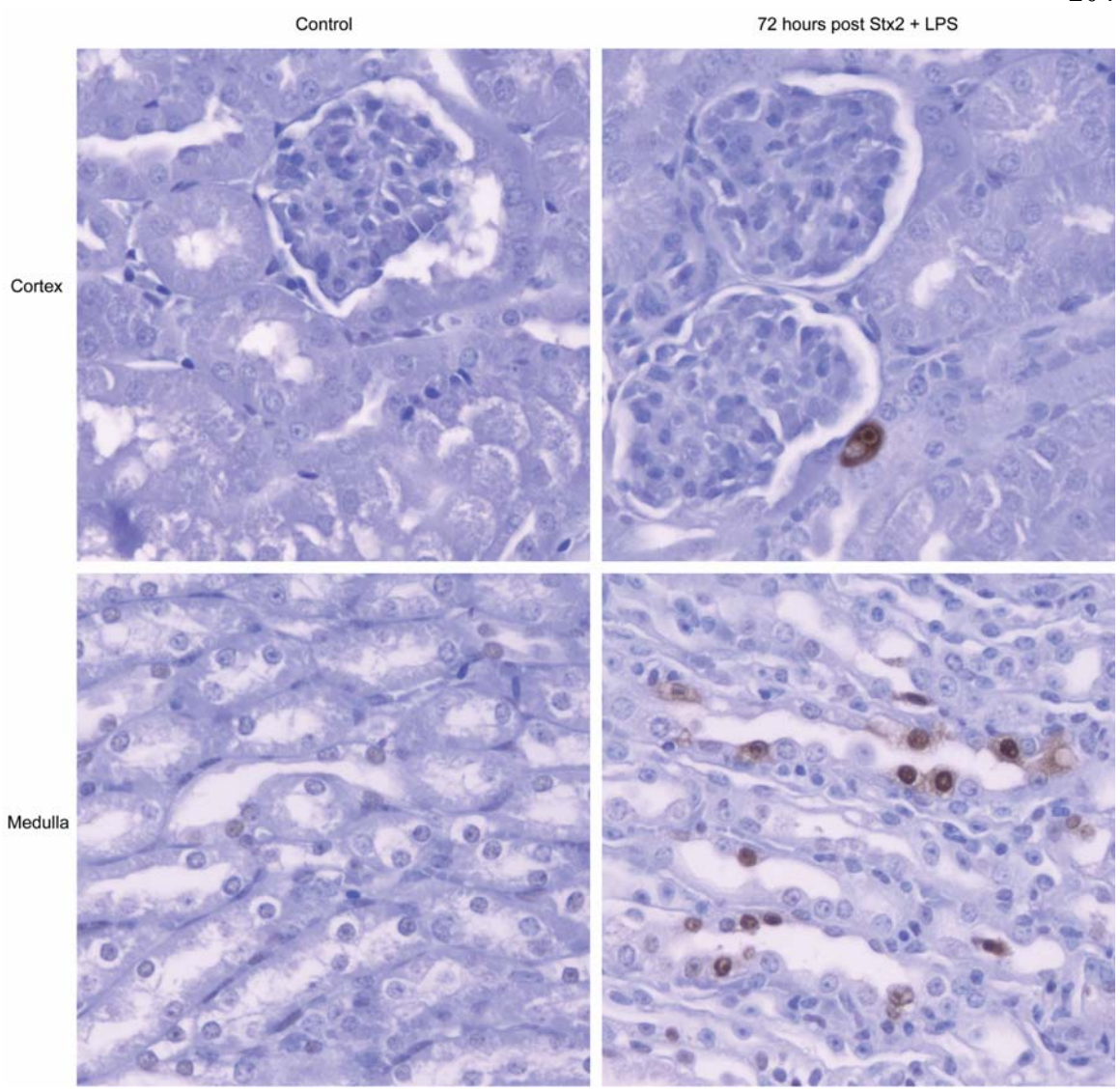


Figure 24. Renal apoptosis in Stx2 plus LPS challenged mice.

Renal Tubular Apoptosis Correlates with Renal Dysfunction

BUN values in Stx2 plus LPS injected mice increased with a time course similar to tubular apoptosis (Figure 25b). Because the collecting ducts are responsible for water reabsorption, we tested whether these mice had a defect in urine concentration¹⁸⁷. It had been previously shown that LPS mediated the initial 24 h weight loss and Stx2 the later weight loss in these mice⁴³⁷. Mice challenged with Stx2 plus LPS developed brief hyperuria during the first 24 h that led to a renal increase in urine osmolality when measured at 24 h post injection (Figure 25c). This initial increased urine osmolality was mimicked by injection with LPS alone (data not shown), and as published previously^{94,116,398,435}. Mice given Stx2 plus LPS, or Stx2 alone developed hyperuria and osmotically dilute urine between 48 and 72 h post injection (Figure 25c). Stx2 plus LPS challenged mice produced 2.7 ± 0.8 mL of urine between 48 and 72 h compared to 1.1 ± 0.5 mL urine for controls ($P < 0.05$). These osmotically dilute hyperuric events correlated with the weight loss and signs of dehydration observed in mice given Stx2 plus LPS (Figure 25d). This decreased urine osmolality is in contrast to normal mice dehydrated for 20 h by water restriction. Water restricted mice lost $10 \pm 0.5\%$ of their body weight and produced a minimal volume of urine, all of which was of high osmolality of 3485 ± 762 mmol/kg ($n=4$).

Figure 25. Timeline of renal dysfunction in Stx2 plus LPS challenged mice.

Quantification of renal apoptosis, renal failure, urine osmolality, and weight loss in mice injected with Stx2 plus LPS. (a) The total number of TUNEL stained nuclei were counted per sixteen 200x fields per tissue section and averaged. Renal apoptosis increased over the time course, and became significant starting at 60 hours after injection. (b) Increased BUN occurred over a similar time course as tubular apoptosis. (c) Urine osmolality was decreased late in the time course although these mice demonstrated an initial increase in urine solute concentration. (d) Mice lost substantial weight over the time course. *, $P < 0.05$ compared to control.

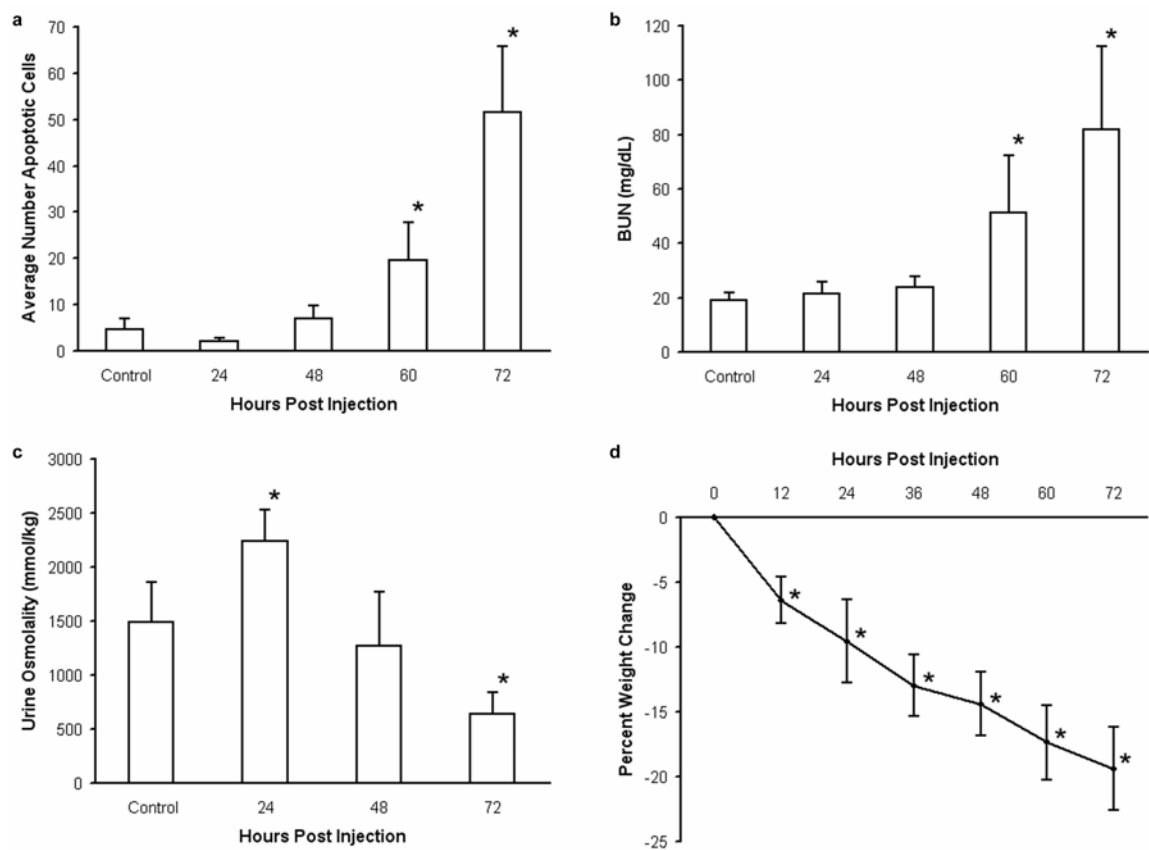


Figure 25. Timeline of renal dysfunction in Stx2 plus LPS challenged mice.

Renal Tubular Apoptosis Causes Renal Dysfunction

To test whether tubular apoptosis caused the renal dysfunction, Stx2 plus LPS injected mice were given two divided doses of the non-selective apoptosis inhibitor Q-VD-OPH at 24 and 48 h. At 72 h after Stx2 plus LPS injection these mice demonstrated significantly decreased numbers of renal tubular apoptotic cells, increased urine osmolality, and decreased BUN levels (Figure 26a-c). Although these mice developed the initial hyperuria and weight loss mediated by LPS, they exhibited a significant recovery in body weight during the time when Stx2 normally caused a loss in body weight (Figure 26d).

Discussion

Previous studies examining the location of murine renal Gb₃ have provided conflicting results^{94,116,369,398,435}. Our data support the conclusion that the primary Gb₃ producing structure and Stx2 target in the murine kidney is the tubular system. We did not detect Gb₃ expression by murine endothelial cells, and it is noteworthy that the previous study that reported murine renal endothelial production of Gb₃ did not perform direct co-localization³⁹⁸. Even though not all collecting duct cells appeared TUNEL positive at any single time point after Stx2 challenge, it is likely that more cells died than were visualized because apoptotic cells only stain with TUNEL for three hours⁴⁷⁷. Collecting duct dysfunction is in agreement with findings in other murine models of Stx mediated injury, and with microarray analysis in this model that revealed Stx2 mediated downregulation of collecting duct specific transcripts^{37,187,195,414,416,435}. LPS has been previously shown not to cause tubular damage when administered at similar doses over this time course^{187,402}. Although functional collecting duct damage in response to Stx

was postulated in prior reports ^{406,435}, it was probably not observed because little morphological change occurs. In support of our findings, production of dilute urine has recently been described in mice inoculated with STEC ⁴⁷⁸.

Figure 26. Caspase inhibition and renal dysfunction in Stx2 and LPS injected mice. Quantification of renal apoptosis, renal failure, urine osmolality, and weight loss in mice injected with Stx2 plus LPS and the non-selective caspase inhibitor Q-VD-OPH, or DMSO vehicle. Stx2 plus LPS challenged mice treated with the inhibitor demonstrated decreased numbers of apoptotic nuclei on TUNEL stained renal tissue sections (a), increased urine osmolality (b), decreased BUN (c), and less weight loss (d), than mice challenged with Stx2 plus LPS alone. *, $P < 0.05$ compared to control; **, $P < 0.05$ compared to Stx2 plus LPS challenge alone.

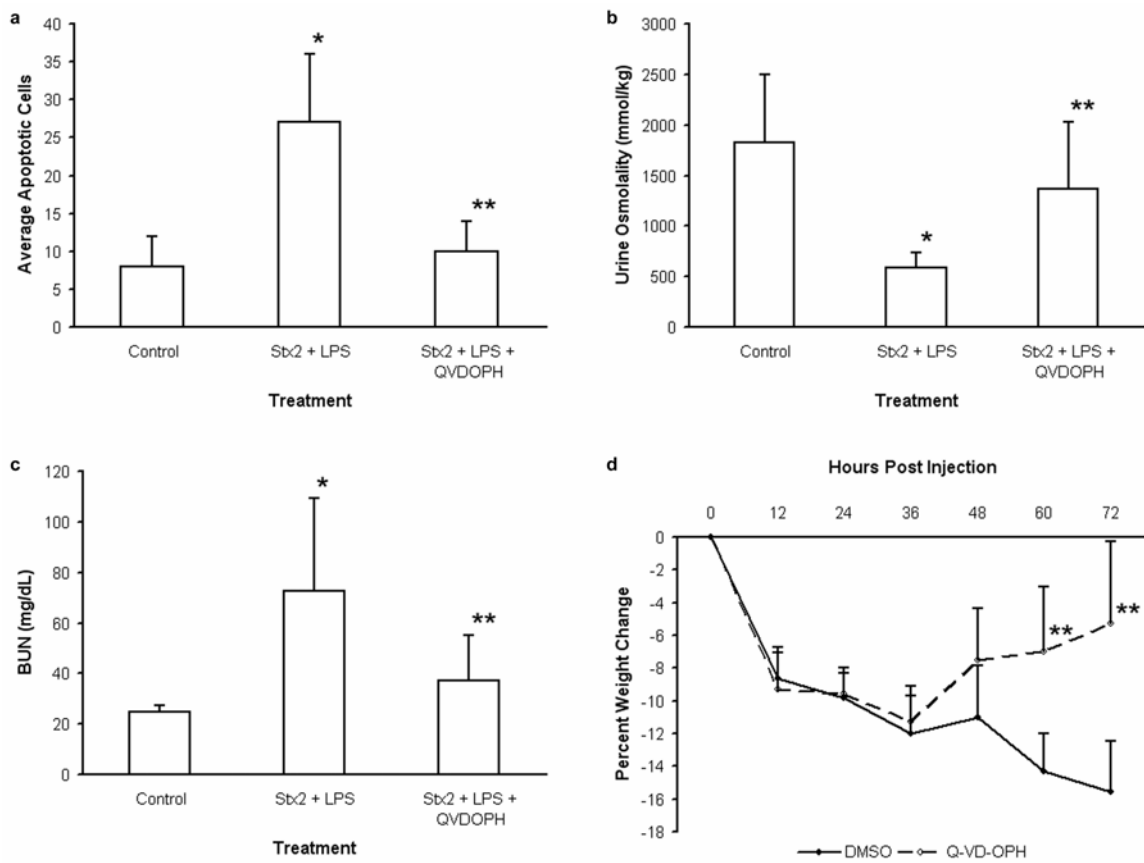


Figure 26. Caspase inhibition and renal dysfunction in Stx2 and LPS injected mice.

The present study confirmed that murine glomerular podocytes lack Gb₃ and are insensitive to Stx2. Even though identical conditionally immortalized mouse podocytes were previously reported to produce Gb₃ and respond to Stx2, we failed to detect Gb₃ by a more specific method, or to demonstrate a response to Stx2, even at 500 times the reported dose^{461,466}. These cells are known to express TLR4 and release cytokines in response to LPS⁴⁷⁹, and our cells responded to LPS by activating p38 in a time course similar to that detailed for Stx2⁴⁶¹. Additionally, we have demonstrated that these cells lack Gb₃ *in vivo*. Therefore the effects previously ascribed to Stx2 in murine podocytes may be due to a small contaminating dose of LPS. Furthermore, the murine glomerular endothelial cells displayed similar responses to LPS and insensitivity to Stx2, suggesting that murine models reporting glomerular damage are likely due to LPS or indirect effects of Stx2; only those models that use live STEC or Stx plus LPS injection observe glomerular defects^{187,399,400,407,478}. Although the Stx2 induced HUS mouse model lacks glomerular damage, we believe this difference from human disease does not preclude the utility of this system. Murine Stx2 plus LPS challenge results in anemia, leukocytosis, thrombocytopenia, and cytokine dependent fibrin deposition, and their relationships to HUS patient findings remain to be investigated^{187,188}.

The human glomerular cells studied here were exquisitely sensitive to the cytotoxic effects of Stx2. Whereas it was previously reported that human glomerular epithelial cells were sensitive to Shiga toxin *in vitro* at a only a much higher dose³⁴³, the cells used prior were likely to be glomerular parietal epithelial cells rather than podocytes. This supposition is supported by their isolation using a sieving procedure shown to create cultures of non-podocyte glomerular epithelial cells, their adoption of

cobblestone as opposed to arborized morphology, and their lack of expression of the podocyte marker WT-1^{466,480,481}.

Human tubular damage does occur in HUS patients, though the glomerular dysfunction appears to be predominant^{195,330}. We showed that Stx2 is more toxic to human glomerular compared to tubular cells. This supports studies that have failed to find cases of renal disease in the absence of microvascular and hemolytic symptoms following STEC bloody diarrhea^{482,483}. In contrast to the polyuria and dilute urine of the Stx2 plus LPS challenged mouse, most HUS patients are oligoanuric³¹. However, two case reports detail Stx mediated HUS associated with polyuria and persistent production of iso-osmotic urine^{460,484}. Thus direct tubular insult by Stx2 may participate in HUS associated renal failure, and we hypothesize that collecting duct damage may facilitate dehydration that contributes to worse outcome in some patients^{180,210}. Although not without technical difficulty³¹, testing prodromal HUS patients for urine concentrating defects may identify those with severe disease and at greater risk for dehydration with worse outcome.

The findings reported here have specific implications for understanding and treating human HUS. In contrast to the other human endothelial and epithelial cells described previously^{144,329,343,455,456}, the response of the human glomerular filtration barrier to Stx2 appeared distinctly non-inflammatory. Despite causing a ribotoxic stress response in the human glomerular cells, Shiga toxin did not increase release of the inflammatory mediators tested. This may explain why HUS patients often report a fever during the diarrheal prodrome, presumably due to increased circulating inflammatory mediators, but are afebrile upon HUS presentation^{31,144,168,169,457}. However, Stx2 mediated a decline in human podocyte VEGF release. As decreased podocyte VEGF has

been demonstrated to cause renal glomerular thrombotic microangiopathy in mice and in patients, this mechanism of Shiga toxin mediated reduction in VEGF may contribute to HUS clinically¹³. Finally, we have also described how blocking apoptosis can rescue direct Stx2 renal insult *in vivo*, and Stx2 induced human glomerular endothelial and podocyte apoptosis can be inhibited by the same anti-apoptotic agent *in vitro*. Thus a clinically approved caspase inhibitor may be able to block Shiga toxin mediated apoptosis in patients^{37,195,485}.

Supplemental Data

The following data supports the conclusions of Chapter 3, that Shiga toxin 2 induced tubular apoptosis causes renal failure in the murine model of the hemolytic uremic syndrome. Electron micrographs of collecting ducts from normal control mice and mice after 48 hours of Stx2 plus LPS demonstrate tubular cell destruction, absent tubular lumen, loss of normal undulated membrane morphology, membrane blebbing, and nuclear loss (Figure 27). This agrees with light microscopy of TUNEL positive collecting ducts following Stx2 treatment. Electron micrographs were obtained as previously described above¹⁸⁷. Furthermore, caspase 3 activation, visualized by immunohistochemistry of renal sections from control and 72 hour Stx2 plus LPS challenged mice (Figure 28), occurs in renal collecting ducts qualitatively similar to those positive for Gb₃ and TUNEL stained apoptosis (Figures 22,24). Activated caspase immunohistochemistry was performed as above with anti-cleaved caspase 3 antibody (Cell Signaling Technology, Danvers MA) followed by DAB staining²⁷. These Gb₃

positive murine renal tubules are not proximal tubules or loops of Henle, as they do not stain for the marker Aquaporin-1 (Figure 29). Finally, immunohistochemistry with the same antibodies on human cadaveric tissue from a 58 year old male reveals collecting duct Gb₃ positivity (Figure30).

Figure 27. Electron micrographs of murine renal tubular damage.

Electron micrographs of a renal collecting duct from a control mouse (A) and a mouse challenged for 48 hours with Stx2 plus LPS (B). Normal collecting ducts display a visible lumen "L," clear cell nuclei "N," and normal undulated luminal cell membranes. Toxin exposed collecting ducts display tubular cell destruction with membrane blebbing "B" with nuclear loss and lumen obliteration. Micrographs are representative of 3 mice each. Bars = 10 um.

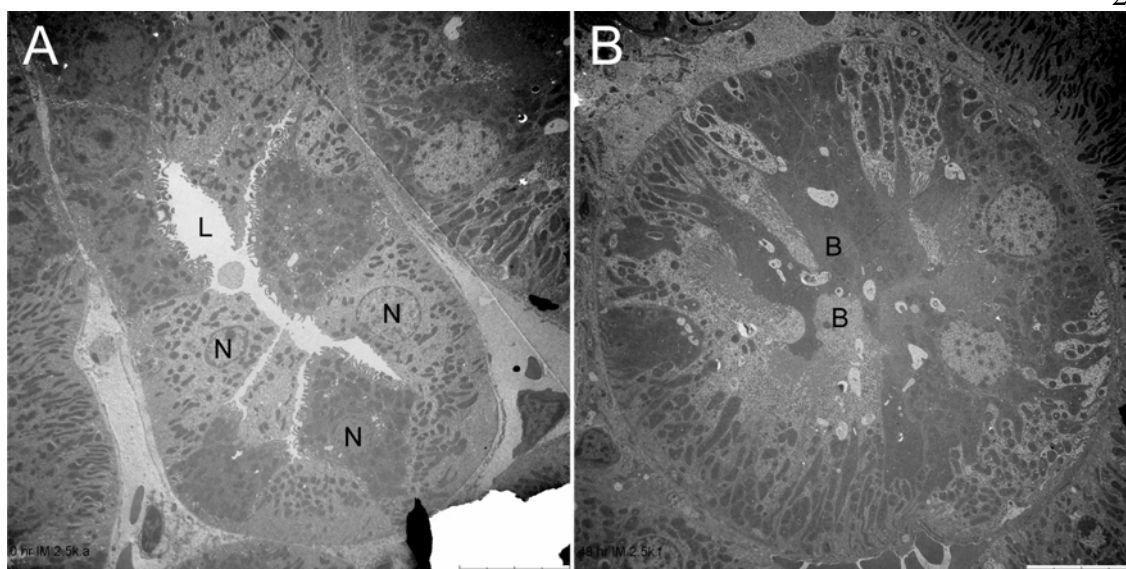


Figure 27. Electron micrographs of murine renal tubular damage.

Figure 28. Light micrograph of murine renal caspase 3 activation.

Activated caspase 3 immunohistochemistry from renal sections of cortex (A, B) and medulla (C, D) from control mice (A, C) and mice challenged for 72 hours with Stx2 plus LPS. Stx2 plus LPS exposed mice demonstrate brown-stained activated caspase 3 in tubular cells of the cortex and medulla, while none is present in control sections. Images are representative of 3 mice each, and at 200x magnification.

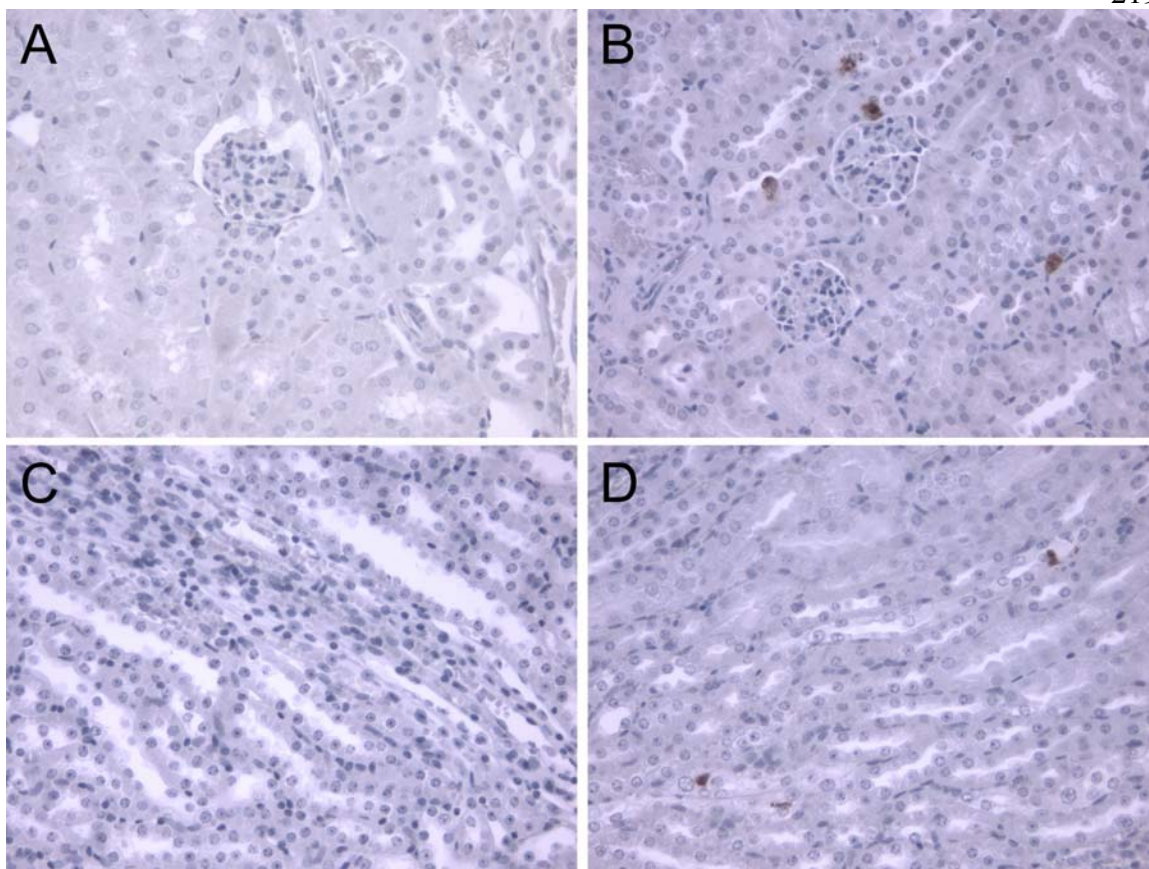


Figure 28. Light micrograph of murine renal caspase 3 activation.

Figure 29. Immunofluorescence of Gb₃ and aquaporin-1 in mouse kidney.

Immunofluorescence staining of normal mouse renal tissue for Gb₃ and aquaporin-1. (A) Cortical and (B) medullary tubules stained with anti-Gb₃, anti-aquaporin-1, and the merged image with overlap colored in yellow. Some cortical tubules express only aquaporin-1 (single arrow), some express only Gb₃ throughout (double arrow), while others express aquaporin-1 and Gb₃ in a punctuate pattern (arrowhead). Bar measures 20 μm .

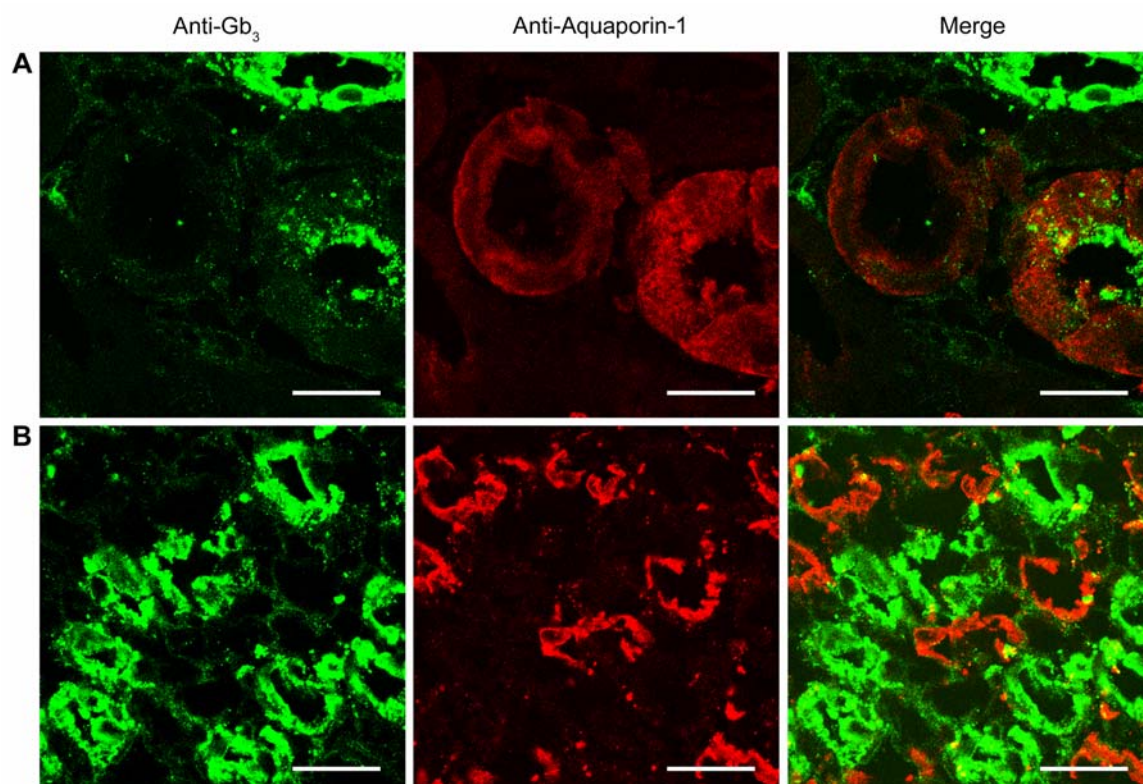


Figure 29. Immunofluorescence of Gb₃ and aquaporin-1 in mouse kidney.

Figure 30. Human kidney Gb3 and Aquaporin-2. Human renal medulla stained with isotype control for anti-aquaporin-2 (A), anti-aquaporin-2 (B), isotype control for anti-Gb₃ (C), and anti-Gb₃ (D) by immunohistochemistry. Morphologically similar structures in the human renal medulla stain for positive for Gb₃ and Aquaporin-2.

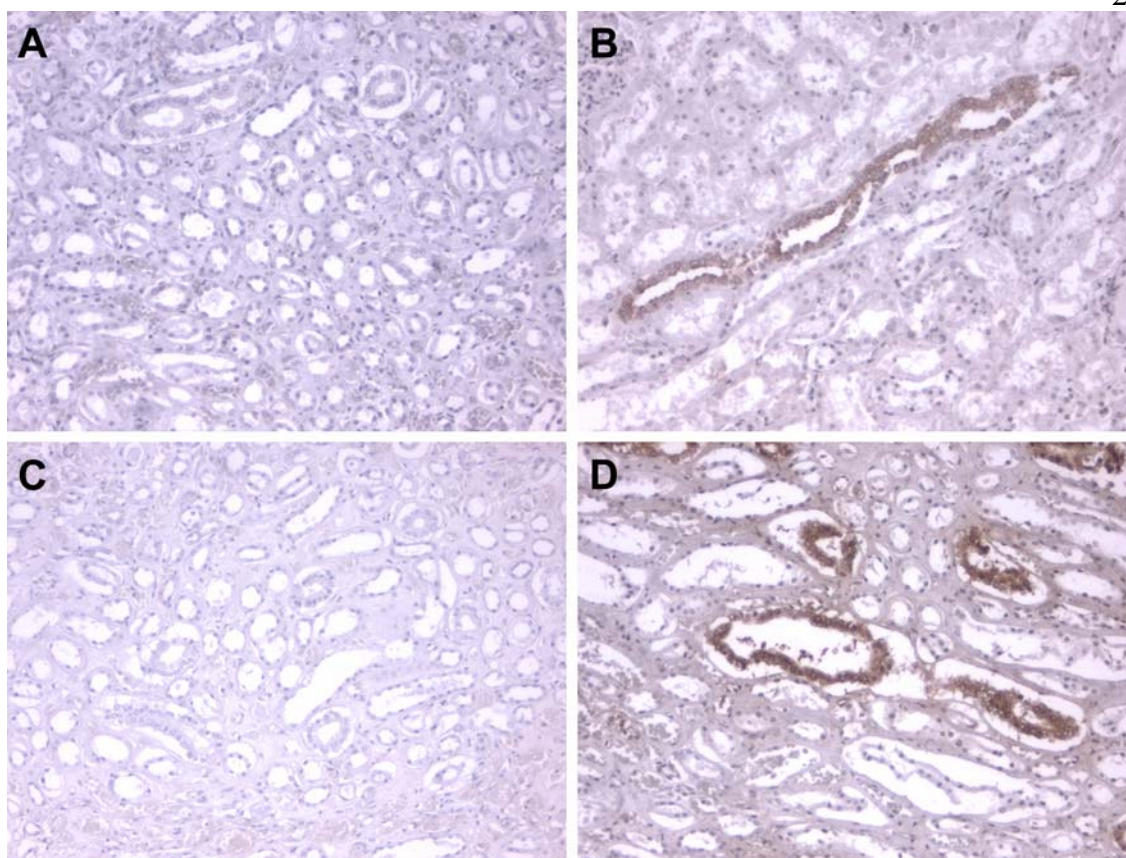


Figure 30. Human kidney Gb₃ and Aquaporin-2.

Chapter 4: Conclusions and Perspectives

The Future of the Mouse Model of Hemolytic Uremic Syndrome

Mice challenged with Stx2 with or without LPS become substantially dehydrated, and develop renal failure associated with early dilute polyuria and late anuria. Normally, two-thirds of mammalian body weight is composed solely of water, of which 66% percent is located intracellularly and 33% extracellularly⁴⁸⁶. Of the extracellular water, only 25% (8% of the total body water) is intravascular, which in the adult 24 gram mouse corresponds to 16 grams of total body water, 5.3 grams of extracellular water, and 1.3 grams intravascular water^{486,487}. When water is lost from the extracellular space, the increased extracellular tonicity forms an osmotic gradient. Body water then shifts from the intracellular to extracellular fluid to maintain equal osmolality in all of the main body fluid spaces⁴⁸⁶. As discussed earlier, the extracellular fluid volume is maintained at a level that allows adequate tissue perfusion. The acute loss of 10% of the extracellular fluid volume can cause tissue hypoperfusion, manifested by renal dysfunction and intense body water conservation with oliguria⁴⁸⁶. When extracellular fluid is lost, intracellular volume shifts to maintain intravascular volume and tissue perfusion in the face of increased osmolality inside and outside of cells⁴⁸⁶. Thus, to stably lose 10% of the extracellular fluid consisting of about 0.5 grams water, approximately 12 times that amount needs to be lost in total, or 6 grams of water weight⁴⁸⁶. Dehydration mediated by Stx2 destruction of the murine renal collecting ducts causes loss of approximately 20-25% of mouse body weight, or about 5-6 grams. Hence the dehydration that occurs in

Stx treated mice is mathematically severe enough to cause extracellular fluid depletion that impairs appropriate tissue perfusion and renal function, and this pre-renal failure could be the culprit in the mouse model.

However, the mouse appears to exhibit intrinsic tubular renal injury in addition to the subsequent pre-renal failure. Direct tubular injury can cause oliguria in some cases, although oliguria typically occurs when the damaged tubules are proximal compared to distal or collecting duct²². Nevertheless, because the time between diuresis and renal failure as measured by serum markers is brief, distinguishing the contribution to the renal failure mediated by these two mechanisms is difficult. There is some evidence that physical tubular blockage in Stx challenged mice may be responsible for the decreased urine output (Figure 27). Other data even suggest that the intrinsic renal injury is dominant. First, ischemic (prerenal) injury usually affects cells of the proximal tubule, while mice challenged with Stx2 demonstrate apoptosis in collecting ducts¹⁹. This reinforces the idea that the collecting duct apoptosis is caused by direct toxin action rather than ischemia, and the lack of proximal tubule apoptosis argues that whatever ischemia exists is not severe. Second, in mice that were dehydrated by water restriction, only slight increases in BUN were found even after 20% of their weight had been lost. Dehydration alone is therefore not sufficient to mediate the renal failure observed in these Stx2 challenged mice.

Although the effect of arginine vasopressin (AVP) appears mostly blocked during Stx2 mediated dehydration, partial urine concentrating ability is still present as the urine osmolality does not decrease below normal a plasma osmolality of about 300 mOsm/kg H₂O. These data demonstrate that some collecting ducts still function normally, and that

even though the underlying cause of the renal failure is the collecting duct apoptosis, the combination of the direct tubular blockage and resulting polyuric dehydration with decreased perfusion probably together cause the murine renal failure. The renal dysfunction is likely due to the combination of the pre-renal effect and the direct tubular damage, and possibly even some additional undiscovered mechanism.

It is significant that these mice eventually become anuric, as humans and mice that are affected with mutant aquaporin-2 do not become dehydrated to the point of anuria unless water restricted⁴⁸⁸. This dysfunctional mutation of aquaporin-2, a disease called nephrogenic diabetes insipidus in which absolutely no aquaporin-2 is present, prohibits the concentration of urine above 300 mOsm/kg H₂O⁴⁸⁸. However normally increased water intake can prevent dehydration in these people. Because the mice challenged with Stx2 have unlimited access to water, it seems likely that the dehydration and anuria is due to some decreased water intake as well. This decline in water intake, due to lethargy or paralysis could be the additional factor that combines with renal collecting duct urine concentrating defect to facilitate renal failure and anuria.

In spite of the uncertain mechanism, dehydration is a significant finding in the mouse model of HUS as it probably contributes to the decline in renal function. Clinically, as dehydration is associated with worse outcomes in humans with HUS, collecting duct damage with polyuria may contribute to this process in patients. Abnormal neurologic findings can result from acute renal failure or from direct Stx2 insult, including encephalopathy, seizure, and coma, and these may form part of a deadly feedback loop that drives the mice further and further into dehydration through a mix of polyuria and adipsia^{187,188}. With regards to the relevance of the mouse model to human

disease, the role of the collecting duct dysfunction, with possible resulting polyuria and dehydration should be more closely investigated in HUS patients. Testing patients in the prodrome or during the acute phase of HUS for production of hypotonic urine may allow better classification of patients who require more aggressive volume expansion and rehydration to prevent the worse outcomes associated with dehydration. Whether the typical neurologic dysfunction found in Stx2 treated animals is due to direct toxin damage or the resulting dehydration and azotemia also remains to be investigated.

The inflammation present in the mouse model, both in terms of inflammatory cell infiltrates and tubular production of inflammatory mediators, does not appear to alter the renal function as measured by serum markers, or be specific to Stx mediated damage. However, the relevance of the murine renal fibrin deposition to the human disease remains incompletely understood. Both the LPS and Stx2 cause variable renal fibrin deposition in the mouse, both in the glomeruli and interstitium. Subsequent experiments have demonstrated that fibrin deposition in these mice up until 48 hours is dependent on renal tubular cytokine production. Injection of specific cytokine neutralizing antibodies prior to and concurrent with Stx2 and LPS prevents the deposition of fibrin by 48 hours¹⁸⁸. Even though the cytokines MCP-1, MIP-1 α , and RANTES, are responsible for the fibrin deposition in early the mouse model, no observations from these mice exist at 72 hours, when the most robust fibrin deposition occurs. No effect is observed from these neutralizing antibodies on the degree of renal dysfunction either, suggesting that the fibrin deposition is an independent process from the renal failure. Additionally, the main inducer of these chemokines appears to be LPS, though Stx2 can extend and increase their release⁴⁸⁹. Thus these changes are not specific to Stx2 mediated HUS and similar to

other changes in the mouse kidney following Stx2 plus LPS injection, are dominated by the actions of LPS (Figure 18, Table 2). Analogously, only LPS and not Stx2 causes tubular release of the neutrophil chemokines KC and JE and neutrophil influx into the murine kidney^{392,393}. Thus, the coagulation abnormalities and inflammation observed in the mouse model appear to be very distinct from those observed in humans, and due to a process disconnected from the Stx2 mediated renal failure.

The fibrin deposition visible in the LPS plus Stx2 murine model may be explained by the combinatorial effect of LPS and Stx2 action on coagulation factors and platelets. The inflammatory cytokines demonstrated to induce fibrin deposition during the first 48 hours of the time course may act either in an autocrine or endocrine manner. These cytokines can signal either to the tubular cells that produce them, to other cells of the nephron, or to circulating cell types. Because anti-inflammatory adenosine receptor agonism also blocks this renal fibrin deposition, it is predicted that platelets, which express high levels of adenosine receptors are the target cell type (T.R. Keepers, unpublished observations). The only way to definitively prove this hypothesis is to create bone marrow transplanted mice between wild type and adenosine receptor knockout mice. If platelets are the underlying agent in the fibrin deposition, then mice with adenosine receptor on all the renal tissue but no circulating cell types should still deposit renal fibrin when challenged with Stx2 plus LPS and co-treated with adenosine agonists. Additionally, if platelets are the underlying cause, then bone marrow transplant of adenosine receptor positive circulating cells into adenosine receptor negative mice should allow adenosine agonists to still block Stx2 plus LPS mediated renal fibrin deposition. If platelets and any other circulating bone marrow derived cell type are not responsible for

the fibrin deposition, then the above bone marrow transplants will generate opposite results.

Despite the data that link tubular cytokine production with renal fibrin deposition, other reports have implicated LPS alteration of clotting and fibrinolytic factor expression in the murine production of renal fibrin. Murine challenge with LPS alone causes a large increase in PAI-1 expression as demonstrated by microarray (Table 4), and also causes increased tissue factor mRNA expression⁴⁹⁰. These changes occur within the first 8 hours after LPS administration⁴⁹⁰. PAI-1 is normally undetectable in kidney, and LPS induced expression occurs in the glomeruli and peritubular endothelial cells⁴⁹⁰. TF mRNA is also undetectable in control kidneys but upregulated in cortical tubular epithelial cells when treated with LPS⁴⁹⁰. In contrast uPA is normally highly expressed by medullary tubular epithelial cells and downregulated there by LPS⁴⁹⁰. In these publications, fibrin deposition is only found in the kidneys and adrenals, and its deposition correlates with changes in uPA but not tPA mRNA and activity⁴⁹⁰. Furthermore, no fibrin deposition occurs when PAI-1 deficient mice are given LPS^{490,491}. Renal fibrin formation in these animals is transient, peaking at 8 hours and disappearing by 24 hours, and correlates with changes in coagulant molecule expression⁴⁹⁰. Thus, from these data it seems that murine fibrin deposition in response to LPS occurs because of combined increases in PAI-1 and TF, with a decrease in uPA^{490,491}. Fibrinolytic antagonism in these mice by treating with the plasminogen inhibitor epsilon-aminocaproic acid causes increased fibrin deposition in tissues in addition to the kidney, and extends the duration of the deposition⁴⁹⁰. Thus a completely distinct mechanism of murine renal fibrin deposition in response to LPS has

been delineated, and resolution of the relative roles of LPS mediated and cytokine induced fibrin formation will require further experimentation.

With regards to the role of Stx2 in murine renal fibrin deposition, the data from LPS induced coagulation changes offer some insight. Combining the information that fibrinolysis inhibition can prolong LPS mediated induction of fibrin deposition, that uPA is produced by the renal tubules, and that the renal tubules are the targets of Stx2 in the mouse model, it seems plausible that the increased late fibrin expression with Stx2 and LPS is due to Stx2 inhibition of fibrinolysis^{490,491}. To determine if this is the cause of the observed fibrin 72 hour time point deposition, the protein levels and activity of the fibrinolysis proteins uPA, tPA, and PAI-1 should be measured by western blot and immunohistochemistry, and correlated to the degree of fibrin deposition in the Stx2 plus LPS injected mice. Furthermore, if Stx2 increases renal fibrin by blocking tubular fibrinolytic enzyme production, then plasmin inhibitors should further increase Stx2 mediated fibrin deposition, and exogenous fibrinolytic enzymes administered to the kidney should be able to rescue the Stx2 mediated fibrin defect. To determine the role of Stx2 in causing murine renal fibrin production, these experiments should be performed.

Regardless of the fibrin deposition, an appropriate small animal model is still needed to allow pathophysiologic and therapeutic testing of the renal damage of HUS. Because the current mouse models do not properly recapitulate human HUS, new model systems are required. Neither the rat nor the commonly used rabbit have renal Gb₃ expression that is similar to humans, and like the mouse, the rat appears to only express Gb₃ on renal tubular cells^{85,392-394,403,414-425}. Although it expresses Gb₃ intestinally and cerebrally, and develops colitis in response to Stx2, the commonly used New Zealand

White rabbit does not express any Gb₃ in the kidney⁴⁸⁴. Thus, the rabbit is only a good model for the intestinal and cerebral aspects of the disease, while the mouse and rat mimic only the tubular damage and possibly the direct neurological insult by Stx. Recently, the Dutch Belted strain of rabbit has been reported to develop renal disease in response to Shiga toxin, however the details of the renal Stx sensitivity and Gb₃ expression have not been elucidated^{423,424}. Because only bacterial infection and not Stx injection causes renal pathology similar to the human in the Dutch Belted rabbit model, it should be regarded as incomplete until the details of renal Gb₃ and purified Stx mediated renal pathology can be shown. To date, only the canine and primate models of Stx induced HUS properly recapitulate the human disease, yet they remain expensive and unfeasible to perform mechanistic and therapeutic evaluations³⁹²⁻³⁹⁷.

Despite its current failings, the mouse may still offer a viable source of experimentation in the field of Stx mediated HUS. Given the detailed description of the murine response to Stx2 and LPS reported here, genetic manipulation to create a humanized Gb₃ mouse should be feasible. Although the control of Gb₃ production is complicated because it is not a protein and not encoded by a single gene, altering the activity and expression of the anabolic and catabolic enzymes in the Gb₃ synthesis pathway (Figure 3) should allow murine renal Gb₃ expression. This humanized Gb₃ mouse would be able to definitively prove that Stx mediated renal vascular destruction of Gb₃ positive cells causes HUS, and should provide a proper model for in depth deconstruction of pathophysiology and development of new therapies. Nevertheless, with at least four enzymes directly controlling the cellular levels of Gb₃, further research must be performed to determine the optimal manipulation. The unique ability of a mouse

with humanized glomerular endothelium to definitively prove the endothelial derived etiology of Shiga toxin mediated HUS makes pursuing this valuable goal worthwhile.

The available Fabry mouse model may help the development of the humanized endothelial Gb₃ mouse, as it already bears Gb₃ on some endothelial cells. Although normal murine aortic endothelial cells lack detectable Gb₃ (Figure 19), aortic endothelial cells isolated from α -galactosidase deficient Fabry mice produce significant Gb₃^{122,492}. Whether these cells are sensitive to the cytotoxic effects of Stx, or whether the produced Gb₃ is sequestered into a nonfunctional compartment with regards to Stx, remains to be tested. Because these Fabry mice are still sensitive to the lethal effects of Stx, albeit at a much increased dose compared to wild type mice, it may be worth investigating whether the pathology of Stx mediated damage is similar to that in wild type mice¹²². Fabry mice die when dosed with 20 times the Stx dose needed to kill normal mice, though the renal pathology has not been investigated¹¹⁹. It may be that in these Fabry mice glomerular endothelial and podocyte Gb₃ production is restored, and even though the rest of the system has increased Gb₃ as well, different pathology may develop than in wild type mice^{119,122}.

In the current flawed mouse model system, significant valuable information regarding the actions of Stx in a mammalian setting can still be obtained. An important question that remains to be fully answered is why there is a long time delay between Stx administration in the murine model and evidence of pathogenic dysfunction. This question is clinically relevant because the same delay occurs in HUS patients between the diarrheal prodrome, when Shiga toxin can be found shed in feces, and the onset of frank HUS, when Stx is usually undetectable from the intestinal contents. In contrast to LPS

injection into animals, after which glomerular fibrotic pathology and systemic changes occur within two hours, Stx causes most detectable changes after 48-72 hours (Figure 18). Furthermore, this delay occurs in spite of evidence that injected Stx is rapidly cleared within minutes from the circulation, presumably to target tissues^{392,414,435}.

Some insight into the delay process comes from microarray data in the mouse model, where Stx injection alone alters the expression of a small subset of renal gene transcripts after 12 hours (Appendix I). These proteins include Cyr61, c-Jun, BTG-2, ATF-3, and GDF-15 (Appendix I, Table 7). Other gene transcripts changed by Stx challenge in the mouse model do not demonstrate significant departure from normal values until 24-48 hours post challenge. Cyr61 is a defined marker of renal injury in multiple systems^{22,493,494}. Although these data strongly suggest that this small set of transcripts might determine the cellular response to Stx, isolated investigation into the role of one of these genes proved uninformative (Appendix I). Nevertheless, the observed transcriptional response of these genes 12 hours after Stx administration indicates that Stx reaches the tissue far more rapidly than it causes significant pathological effects. Thus, the lag between Stx toxemia and renal pathology may be due to the time it takes for Stx to cause enough dysfunction on the cellular level for it to be visible on the tissue, organ, and whole animal level. In this way therapeutics directed specifically at the enzymatic activity of Stx, such as with the few competitive rRNA mimics that are currently being investigated, may provide the best opportunity to deter tissue damage during this window of opportunity^{495,496}. Even so, proper delivery of these inhibitors at adequate tissue concentrations probably represents a large hurdle to clinical implementation.

The route of Stx transport in the renal vasculature can also be addressed by the current mouse model system. Although Stx is thought to primarily travel in the vasculature, Stx mediated damage to human and murine renal tubules demonstrates that in some circumstances Stx exits the circulation^{37,195,239,330,350,460,484,497}. In the human, Stx vascular exit may occur following vascular endothelial damage, detachment, and death, allowing Stx access to the underlying tissue. However this mechanism cannot function in mice where the vascular endothelium is insensitive to Stx. Additionally, Stx has been detected in human patients bound to the tubular luminal surface^{37,195,239}. Combined with the murine data, these findings suggest that Stx is able to pass through the glomerular filtration barrier into the tubular filtrate. This conclusion is not completely surprising as the Stx size of 70 kDa is at the typically conceived size cutoff for the glomerular filtration barrier. Furthermore, some researchers argue that large amounts of protein of this size pass through the filtration barrier regularly³⁻¹². Stx passage through the filtration barrier can be tested in the mouse by either using labeled Stx and looking for its appearance in the urine after injection, or by injecting normal Stx and analyzing urine collected at various time points afterwards by western immunoblot⁴⁴³.

In conclusion, the data presented here demonstrate clearly that the mouse is not an adequate model of human hemolytic uremic syndrome even though it still may have valuable information to offer. Although Stx2 plus LPS administration to the mouse results in the traditional diagnostic triad of thrombocytopenia, anemia, and acute renal failure, the mechanism is distinct from HUS in human STEC infected patients. In contrast to the high sensitivity of the human glomerular filtration barrier cells to the cytotoxic effects of Stx, the corresponding mouse cells lack Gb₃ and are insensitive to

Stx. The only cell types in the mouse kidney that can be shown to respond to Stx and possess Gb₃ are tubular, thus indicating that the mouse model of Stx induced renal failure primarily consists of parenchymal rather than vascular injury. Nonetheless these findings in the mouse model demonstrate that Stx induced tubular injury alone is detrimental enough to cause serious systemic dysfunction and lethality. Although the reportedly rare tubular injury visible in patients may still be secondary to decreased renal blood flow and tissue ischemia, these data prove that Stx has the capacity to mediate severe tubular damage *in vivo* by means of a direct cytotoxic effect.

Ribotoxic Stress and Apoptosis

The ribotoxic stress response has been demonstrated to occur in various cell types in response to ribosomal stresses including Stx and ricin intoxication, however the importance of this effect is unresolved. The ribotoxic stress response typically consists of inflammatory MAPK activation and signaling molecule release, though here it is demonstrated that this response is not consistent^{135,140,141,143-145}. Although the intracellular component of the ribotoxic stress response is induced by Stx challenge of human glomerular endothelial cells and podocytes, no increased inflammatory mediator release occurs (Figure 20, Table 4). This lack of extracellular inflammation is consistent with the caspase activation and apoptotic death initiated in these cells. This disconnect may be evidence of some further control on the system, because intracellular MAPK activation is not sufficient for inflammatory molecule release. Alternatively the production of inflammatory mediators may be cell type dependent, as this lack of effect is only observed in human cells of the glomerular filtration barrier. In this system the non-

inflammatory apoptotic response is dominant over the previously described inflammatory response of Stx challenge. The anti-inflammatory effect does not appear to be a matter of dose, because at lower concentrations of Stx no increased inflammatory mediator release is detected, and at higher doses the cells die even more rapidly. As mentioned above this non-inflammatory response may help explain the lack of fever in HUS patients during the acute phase of disease. Additionally, because the anti-inflammatory aspect of apoptosis is typically considered to be beneficial, it may be that the balance between inflammation and apoptosis partially determines the outcome in HUS, or both may be counterproductive. Future studies should try to determine which of these inflammatory or non-inflammatory processes occur *in vivo* in human kidney cells affected by Stx.

The importance of the ribotoxic stress response is further undermined by experiments detailing that p38 and JNK inhibition do not block Stx2 induced apoptosis by human glomerular cells *in vitro* (Appendix III). When preincubated with either the p38 inhibitor SB203580 or the JNK inhibitor SP600125, neither human glomerular endothelial cells nor podocytes demonstrate more than 20% reduced cytotoxicity in response to Stx2 (Figures 36,37,38,39). Furthermore, combining these two drugs only increases their own direct cellular cytotoxicity and does not augment their ability to rescue Stx2 mediated damage (data not shown). Using these same inhibitors *in vivo* at concentrations comparable to the published literature did not show any effect in the mouse model either (Appendix IV). Mice pretreated with SB203580 or SP600125 did not demonstrate any consistent rescue from the lethal effects of Stx2 intoxication, even when the inhibitors were used in combination (Figures 40,41,42). Additionally, a

collaborator has demonstrated that treatment of human colonic epithelial cells with the inhibitor DHP-2, a compound that blocks activation of the kinase MLK7 that is upstream of p38 and JNK, only exhibits moderate 15% rescue of Stx induced cytotoxicity⁴⁹⁸. Thus while the intracellular component of the ribotoxic stress response occurs in multiple cellular contexts, its role in activating inflammatory or apoptotic processes *in vitro* or *in vivo* is dubious and requires further investigation.

Following either the ribotoxic stress pathway or another mechanism, the primary outcome of Stx intoxication is apoptosis, therefore new therapeutics that antagonize the role of apoptosis in this disease should be investigated. Both glomerular and tubular cell types respond to Stx2 challenge with apoptosis, and the initial endothelial detachment leading to vascular activation of coagulation may derive from this apoptotic response. Although the compounds normally utilized *in vitro* are not available for clinical testing, one non-selective caspase inhibitor is being used in clinical trials. IDN-6556 is an anti-apoptotic non-selective caspase inhibitor that has so far demonstrated few detrimental side effects, is able to decrease liver damage in patients with chronic hepatitis, and can be administered orally⁴⁹⁹⁻⁵⁰¹. The ability of this compound to inhibit Stx2 induced apoptosis should be investigated *in vitro* and *in vivo* in the mouse, and if successful, may be tried in the baboon model system to ameliorate Stx2 induced injury. Given that this compound has already been demonstrated safe and effective in some human clinical trials, the likelihood of using it for successful intervention is increased compared to other clinically untested compounds.

Shiga Toxin Targets: Vascular and Parenchymal Cells

Most D+HUS research focuses on the role of the vasculature in mediating HUS associated pathology. Whether the mechanism of vascular dysfunction derives from primarily endothelial, leukocyte, platelet, or non-cellular coagulation defects, the effect on tissue and organ function is thought to follow from vascular occlusion and tissue ischemia. Given the diverse and voluminous data regarding these effects, it is likely that vascular damage is a causative lesion in HUS patients, and successive vascular blockage and tissue ischemia generate improper organ activity²²². However, animal models and some findings in clinical studies suggest that direct parenchymal targeting by Shiga toxin or LPS also cause significant organ dysfunction^{37,222,350}. In the case of the renal tubular system, the data presented here clearly confirm the devastating effect Stx induced epithelial damage alone can have in mice, and other non-vascular cell types likely share similar fates during the course of human HUS. Clinical data suggest that the human pancreas, heart, and intestinal cells participate in a similar toxic fate. Though largely ignored, direct parenchymal effects of STEC mediated toxemia may contribute substantially to the clinical dysfunction that takes place during hemolytic uremic syndrome development, as well as the persistence of long term morbid features.

Numerous studies demonstrate that human renal tubular epithelial cells are sensitive to the cytotoxic and inflammatory effects of Shiga toxin *in vitro*, however the role this toxicity plays in the etiology of human disease remains unclear. Human proximal tubular epithelial cells produce Gb₃, and Stx1 and Stx2 cause apoptosis of these cells in a dose and time dependent fashion (Figure 19)^{341,342,349,455,502-506}. Human proximal tubular cells also release cytokines in response to Stx1 and Stx2 incubation,

increasing TNF- α and interleukins at both the mRNA and protein levels^{455,507}.

Interestingly, although Stx increases many cytokine mRNAs significantly, IL-6 mRNA and protein levels do not increase, and in some cases decrease in response to Stx challenge^{455,507}. This effect may be related to the global anti-inflammatory outcome of Stx2 challenge on human cells of the glomerular filtration barrier. Nevertheless the *in vitro* response of other human renal tubular cell types to the effects of Stx and LPS remain to be investigated, including the cells of the loop of Henle, distal tubule and collecting duct. In human cadaveric samples, renal collecting ducts stain positive for Gb₃ suggesting they may be sensitive to Stx *in vivo* (Figure 30).

Sparse clinical data indicate that renal tubular damage specifically to the collecting duct does occur in some HUS patients. There are four reported cases of STEC confirmed HUS associated with increased urine output and decreased urine osmolality⁴⁸⁴. The first, a 67 year old woman, presented to the hospital with acute renal failure and a history of increasing urinary frequency. On subsequent sequential urinalyses she demonstrated iso-osmotic urine with plasma of 309 mOsm/kg H₂O on two occasions, consistent with a persistent urine concentrating defect⁴⁸⁴. Also observed in this case were muddy brown casts in the urine. These granular casts are found with tubular injury. Though there was typical HUS glomerular injury, with fibrin deposition and some fibrinoid necrosis, the tubules demonstrated localized acute injury consistent with the urine concentrating defect⁴⁸⁴. *E. coli* O157:H7 infection was confirmed by the presence of specific anti-LPS IgM and not IgG antibodies during the acute phase of the disease⁴⁸⁴. The second case, a 7 year old boy with Stx2 mediated HUS demonstrated nonoliguric acute renal failure, increased urinary levels of tubular specific enzymes *N*-acetyl

glucosaminidase and β_2 -microglobulin, and decreased urine concentrating ability⁴⁶⁰.

Stx2 was found bound primarily to his tubular cells along with tubular cell apoptosis, and though he displayed proteinuria, hematuria, and schistocytosis, he never became oliguric and persistently produced dilute urine less than 300 mOsm/kg H₂O⁴⁶⁰. Two additional case studies identified patients who presented with a period of polyuria prior to the onset of HUS, suggestive of tubular dysfunction similar to that observed in the mouse model³¹³. These patients also demonstrated the normal hemolytic anemia, thrombocytopenia, and renal failure demonstrating that they did not constitute alternative forms of the disease³¹³. These four case reports prove that although Stx toxemia typically targets the renal vasculature, cases of renal tubular damage similar to that visible in the mouse model can occur.

There exists some additional evidence of tubular damage in the acute phase of human HUS. Although polyuria is an uncommon finding in most STEC mediated HUS cases, medullary hemorrhagic necrosis found in some patients is not normally associated with nearby arteriolar thrombosis, and thus likely represents non-ischemic parenchymal injury³². Tubular atrophy with tubulointerstitial nephritis that is observed in biopsy specimens from some HUS cases may constitute the pathologic change accompanied by direct tubular Stx mediated toxicity³⁵⁰. Markers of renal tubular epithelial damage, specifically β_2 -microglobulin and *N*-acetyl glucosaminidase, have been found in the urine from many HUS patients during the acute phase of the disease, suggesting that tubular damage generally does occur^{330,497}. Unfortunately, these studies do not distinguish the etiology of the tubular damage, and it may follow from either ischemic insult or direct Stx cytotoxicity.

Shiga toxin association with and binding to human renal tubular epithelial cells on patient biopsies has been demonstrated as well^{37,195,239}. Tissue from patients demonstrate signs of focal tubular necrosis and tissue regeneration, with visible mitotic cells²³⁹. Tubules with the greatest pathology also bind the most Stx detected by anti-Stx antibody, and Stx binding to the tubular epithelial cells in these patients occurs primarily on the apical side^{37,239}. The binding of Stx correlates with the expression of human tubular Gb₃, and renal apoptosis takes place both in the glomeruli and tubules of STEC mediated HUS patients, suggesting that Stx causes both effects *in vivo*^{195,239}. These data provide evidence that Stx is able to reach and cause toxicity directly at the human tubular epithelium, specifically the collecting duct, and suggest that this injury happens clinically. Nonetheless evidence of renal concentrating defects and polyuria during the acute phase of HUS provide the strongest proof that direct tubular injury occurs in this disease, as they demonstrate that the nephron is not completely ischemic even though it is dysfunctional. These findings should be monitored in future clinical HUS investigations in order to determine their prevalence and relevance to the overall clinical picture and patient prognosis.

Unlike glomeruli, tubular epithelial cells have great potential to regenerate injured tissue, and therefore no long term tubular specific damage exists except secondary to glomerular loss^{27-29,508}. If HUS patients do develop a renal concentrating defect during the acute phase, it is typically repaired after two years of recovery²⁰⁰. Prior HUS patients have been demonstrated to produce normally concentrated urine, and respond to exogenously administered vasopressin by appropriately increasing urine osmolality in most studies²⁰⁰. Increased glomerulosclerosis and tubular degeneration following acute

glomerular loss most likely cause the progressive decrease in vasopressin stimulated urine concentrating ability in some patients²²³. Again, because urine osmolality is not typically assessed in HUS patients in the acute phase, the true prevalence of tubular concentrating function and relation to subsequent outcome in this disease is currently unknown. Nevertheless, dehydration mediated by a renal tubular concentrating defect may be an unrecognized pathogenic mechanism in this disease^{235,236,363}. It has been demonstrated in retrospective analyses that dehydration and hemoconcentration are associated with worse outcomes in HUS patients, and the tubular damage may add to dehydration caused by the prodromal diarrhea^{31,33,36,177-180}. Stx2 induced direct tubular injury may also contribute to worse later prognosis by synergizing with other mechanisms of tissue and organ dysfunction. Further clinical studies are needed to determine the validity of these hypotheses.

Future studies involving the renal tubular response to Shiga toxin and LPS in the context of HUS should employ human and mouse cell types *in vitro*, as well as additional human HUS case data. A large variety of cultured renal tubular cells exist that can be used to determine if the observations and hypotheses made from murine models hold true *in vitro*⁵⁰⁹. As the human proximal tubular response has already been described in detail, cell lines that represent the human ascending and descending loops of Henle, distal convoluted tubules, cortical collecting ducts, and outer and inner medullary collecting ducts should be investigated⁵⁰⁹. Specifically, both human and murine collecting duct cell lines have been isolated and should be used to determine Gb₃ content as well as cytotoxic, inflammatory, and pro-coagulant responses to Stx and LPS⁵⁰⁹. In order to demonstrate the presence of this type of tubular damage in HUS patients, urine sample

from these individuals should be tested for abnormal dilution, and these findings should be correlated with the time when they occur during the acute phase, as well as with overall outcome of the patient. As it is non-invasive and simple, urine collection and osmolality testing should be relatively easy to perform and may offer valuable insight into the severity of renal damage and need for atypical treatment in some patients. For instance, those patients who demonstrate a renal concentrating defect may be at higher risk of dehydration, a finding known to associate with worse risk of developing HUS as well as long term morbidity and mortality^{31,33,36,177-180}.

In addition to the tubular epithelium, Stx direct effects on glomerular podocytes may also play an important pathogenic role. Although essentially part of the renal glomerular vasculature, the role of the podocytes in mediating thrombosis and as an Stx target is underappreciated and under investigated^{151,350}. Markers of increased podocyte sloughing from glomeruli are found in the urine of children with HUS, demonstrating that podocyte damage occurs *in vivo* in human patients⁴⁵⁹. Glomerular podocyte pathology has been observed in the acute phase of HUS patients on biopsy specimens¹⁵¹. Furthermore, histopathologic damage consistent with the development of focal segmental glomerulosclerosis (FSGS) following HUS also intimates podocyte injury^{222,350}. Because dysregulated podocytes are the key component of FSGS pathology, and because the data contained here demonstrate that human podocytes can be directly injured by Stx and LPS, it is possible that podocyte damage during the acute phase leads to later FSGS in HUS patients. This pathology is in addition to hyperfiltration and hyperperfusion injury that follows destruction of some glomeruli. Thus, although the loss of glomerular podocytes

may occur in response to glomerular endothelial injury or hypoperfusion, Stx can have a direct cytotoxic effect on podocytes, and this likely happens in HUS patients.

Future work regarding the roles of glomerular podocytes in the pathogenesis of HUS should involve *in vivo* animal models. Creating mice with cell type specific production of Gb₃ in glomerular podocytes or endothelium, the humanized Gb₃ mice, should allow testing of the hypothesis that glomerular podocyte Stx mediated toxicity contributes to the endothelial dysfunction in STEC mediated HUS. As described above, the mouse currently represents the vascular Gb₃ null state, with no vascular expression of Gb₃ and thus complete insensitivity to its toxic effects. As the future of the mouse model ideally consists of engineering knock-in mice that appropriately express Gb₃ on endothelial cell types, a corollary to this is to create mice that specifically express Gb₃ on podocytes. Podocyte specific promoter elements exist that allow targeting of genetic constructs to the podocytes alone, and should allow murine podocyte specific Gb₃ expression^{13,510,511}. Thus the research of the immediate future should focus on discerning the necessary genetic modifications necessary for appropriate glycosphingolipid enzyme production of Gb₃ in murine cell types that do not normally express it. If podocyte specific expression of Gb₃ can be accomplished, these mice can be challenged with Stx, and investigated for the development of vascular pathology. Furthermore, the vascular pathology and coagulation defects in these mice can be contrasted to mice with Gb₃ only on vascular endothelial cells to determine the relative roles of the podocyte and endothelial toxicity in causing overall vascular dysfunction.

A Current Model of Shiga Toxin Mediated Hemolytic Uremic Syndrome

Based on the available evidence, a current pathophysiological mechanism of Shiga toxin mediated HUS can be described. Gastrointestinal infection with STEC and intestinal adherence causes watery diarrhea followed by Stx release into the intestinal lumen. This Stx causes apoptosis of parts of the intestinal epithelium, and allows access of Stx and LPS to the intestinal substratum and vasculature. Both this initial intestinal destruction and the subsequent intestinal vascular thrombotic microangiopathy probably contribute to the clinically observed hemorrhagic colitis. The immune response to the bacterial damage and LPS entrance into the circulation ignites a strong inflammatory response consisting of cytokine release, fever, and leukocytosis. Increased leukocyte traffic spurred by cytokine release throughout the intestine and systemic vasculature may expedite the spread of Stx and LPS²³⁵. Although incompletely characterized, Stx likely circulates bound to both blood cells and plasma proteins³⁶³. Dehydration and intravascular volume depletion due to the watery and bloody diarrhea concentrate the LPS and Stx that enter the systemic circulation.

Circulating LPS and other cytokines appear to increase the sensitivity of the vascular endothelium and parenchymal cells of many organ systems to the cytotoxic effects of Stx. These effects are probably mediated by increasing the expression of Gb₃. Stx primarily encounters the vascular endothelium prior to parenchymal cells, as it is the barrier to all other tissues except in the kidney and brain. In these two regions, fenestrated endothelia exist, allowing Stx and LPS contact with cerebral neurons and astrocytes, and renal podocytes and tubular epithelium⁵¹². Additionally, the cerebral and renal vasculatures receive comparatively large volumes of the systemic blood supply and

are theoretically exposed to the most Stx and LPS molecules. The fenestrated endothelium and the large relative blood supplies to these two organs probably dictate at least part of why they are the most affected by Stx and LPS toxemia. The delay between the initiation of Stx and LPS systemic toxemia and clinically detectable tissue and organ dysfunction likely occurs while the toxin mediated tissue destruction reaches critical mass. This is similar to the delay between STEC infection with watery diarrhea and the development of bloody diarrhea during the prodrome. A certain percentage of endothelial and parenchymal cells likely need to be damaged before normal homeostasis cannot be maintained and overt sickness is observed. The changes in coagulation observed prior to the onset of complete HUS support a growing vascular abnormality proceeding vascular failure.

Organ specific dysfunction likely results from both vascular thrombotic microangiopathy with associated ischemia, and direct parenchymal damage by the toxins. Affected organs may include the spleen, liver, pancreas (leading to increased risk of subsequent diabetes), skin (petechial hemorrhages), cerebrum, and the kidney. Renal damage is likely caused by a combination of direct endothelial and podocyte cytotoxicity, which effectively delivers a double hit to the glomerular endothelium. Stx causes both direct glomerular endothelial death, and endothelial death secondary to decreasing the release of glomerular podocyte VEGF. This endothelial damage allows abnormal activation of the coagulation system, with the formation of pervasive fibrin rich clots and platelet activation leading to thrombocytopenia. Passing red blood cells through the high pressure glomerular vasculature in the presence of this extensive fibrin network causes the shredding, and the production of schistocytes.

Resolution of the vascular and parenchymal damage probably occurs when the Stx and LPS finally degrade, are destroyed by phagocyte ingestion and lysosomal degradation of apoptotic cells, or are expelled in the urine. Abnormal erythrocytes are captured and removed by the reticuloendothelial system of the spleen, and new erythrocytes and platelets are generated and released by the bone marrow. Macrophages and fibroblasts along with endothelial cell precursors help remove abnormal fibrin clots and reconstruct the vasculature in many tissues. Renal tubular epithelial cells dedifferentiate and repopulate the renal tubules so they regain normal function. However, tissue that has infarcted from severe ischemia, or cells that are unable to replicate like glomerular podocytes, enter a process characterized by fibrosis and scarring. Sufficiently damaged glomeruli are thus rendered obsolete and will never function again, with some partially injured glomeruli segmentally sclerosing and leading to FSGS or MPGN. Finally, hyperfiltration injury in the remaining glomeruli pushes these kidneys down a rapid slope of functional decline, culminating in early chronic renal failure.

Hemolytic Uremic Syndrome: Current Problems and Future Investigations

The difference between patients who progress to HUS following STEC bloody diarrhea and those who do not is of critical importance for the field, as improved understanding of the determinants of disease progression may allow clinical prevention of HUS following STEC infection. Based on the available evidence, it seems that progression from the hemorrhagic colitis to HUS occurs on a continuum of vascular and

renal injury. Whether the primary abnormality in HUS patients is thrombotic or vasculitic, altered coagulation factors, inflammatory mediators and markers of tissue damage are found to dose dependently correlate with progression from colitis to fulminant HUS. Thus it appears that there is a threshold of vascular or parenchymal injury that must be surpassed before clinical disease is manifest, and those who pass this barrier are considered to have HUS, while those who do not pass the threshold develop only sub-clinical disease. The level of the threshold is probably determined by how much of the vasculature needs to be thrombosed before significant ischemia results, how many glomeruli must be nonfunctional before renal failure is visible, how many clots need to be produced before observable changes in platelet numbers or erythrocyte fragmentation occurs, and how much tissue damage and brain edema needs to proceed before neurological or nonoliguric renal symptoms develop. For instance, STEC colitis is accompanied by at least some microvascular thrombosis, however when limited it resolves without evolving into HUS¹⁹⁶. It seems sensible that this etiology is what has allowed significant strides to be made in preventing morbidity and mortality in this disease simply by improving supportive care measures for these patients: lessening the patient burden of disease decreases their risk of progressing to complete severe HUS.

The underlying cause of the HUS disease continuum may be a matter of Stx and LPS dose, as well as the baseline responsiveness of the patient to these toxins. These attributes may determine where on the disease spectrum an individual falls⁴⁴. Patients also likely differ in the load of the initial bacterial inoculum, the amount of Stx produced by the specific bacterial strain, and their baseline health⁴⁴. Unfortunately the level of Stx production by different STEC strains, and the amount of Stx present in stool, only rarely

correlates well with their disease burden or virulence, and more research needs to be performed in this area^{44,357}. Although they have been investigated, no genetic signatures have been uniformly detected in patients who develop HUS compared to those who only present with colitis and resolve. Alterations in common prothrombotic mediators including factor V Leiden, the PAI-1 promoter, thrombin, changes in methylene tetrahydrofolate reductase, and mutations in PAF acetylhydrolase have demonstrated no increased frequency of mutation in HUS patients^{319,513}. Nevertheless, it seems likely that more complicated interactions of inflammatory gene expression, glycosphingolipid metabolism, and environmental factors contribute to development of HUS after STEC gastrointestinal infection.

Cytokine and leukocyte levels may correlate with the development of HUS because increased inflammation is a marker of increased intestinal barrier disruption, and thus increased entrance of the intestinal contents including Stx into the systemic vasculature²³⁷. In support of this, increased circulating Stx has been correlated with some cases of severe HUS^{383,384}. The inability of oral corticosteroids to modify the acute HUS disease course argues for the lack of direct involvement of inflammatory mediators³⁷⁸. Alternatively, increased inflammation may identify patients who are more susceptible to toxin induced damage, or who are more prone to produce inflammatory cytokines that may be causative in the disease process²⁵¹. Systemic volume expansion thus may function to ameliorate the development and severity of HUS by both diluting the intravascular Stx, and by decreasing the vascular stasis associated with diarrheal dehydration.

The mechanism that initiates abnormal intravascular coagulation remains to be definitively proven. Endothelial damage followed by detachment and exposure of the procoagulant basement membrane, with coincident loss of the anticoagulant normal endothelial surface, is the most likely pathogenic process. However, direct activation of the coagulation cascade, inflammatory modulation of anticoagulant endothelial function, and some currently undescribed mechanism all persist as viable alternative options. Although the prothrombotic abnormalities precede the development of complete HUS, no biopsies have been taken from these patients so the source of the dysfunction remains unknown. The most plausible theory is that the initial coagulopathy originates with subclinical endothelial damage. In this way, only when enough endothelial damage occurs such that the overall balance of the system tilts towards coagulation and platelet consumption does detectable microvascular hemolytic anemia and thrombocytopenia result. Although some studies have documented the ability of HUS patient plasma to activate platelet coagulation directly, the effect is weak and only indirect^{318,337}. The platelet activating activity in the plasma also does not correlate with disease severity, indicating that it is unlikely to be pathophysiologically significant, and probably is rather due to tissue and cell destruction with release of normally intracellular constituents into the vascular space³¹⁸. Thus, in spite of some weak arguments to the contrary, it seems most likely that the primary abnormality that occurs in HUS is the endothelial vascular damage, which causes and is followed by the coagulopathy, platelet consumption, erythrocyte shearing, and end organ damage. Nonetheless, in spite of these assessments, proof is needed of the true irreducible antecedent of human STEC mediated HUS.

The non-vascular injury caused by circulating LPS and Stx probably also occurs on a continuum, with a threshold between clinically detectable and undetectable parenchymal organ injury. While each type of tissue likely has its own response curve to these circulating toxins, with increasing doses causing increasing tissue damage, the overall progression from only vascular damage to severe extrarenal involvement probably depends on a variety of additional factors. In the current framework the vascular endothelial cells are the most sensitive cells to Stx and LPS, and are exposed to the highest circulating doses, making them the first and most vigorous to respond. Extensive thrombosis likely contributes to extravascular damage, though multiple non-vascular cells respond to Stx and LPS as well, synergizing with the vascular ischemic injury to cause tissue and organ failure. In this way, the most severe HUS cases can be conceptualized as being exposed to the highest doses of Stx and LPS, with the most vascular damage, the greatest extent of tissue ischemia, and the most severe direct tissue injury, leading to major extrarenal symptoms and pathology.

The most important technological advance to properly evaluate these hypotheses would be to develop a method to detect the circulating concentration of Stx in HUS patients. Currently it is undetermined if Stx or LPS dose correlate with increased disease, and what the local concentration of Stx is to which various human cell types are exposed. Because the response to both Stx and LPS by most cell types is extremely dependent on dose, this is a crucial piece of knowledge critical for the advancement of the HUS field. The concentrations of Stx used in the published literature may be completely irrelevant to those that occur in the course of the human disease, as they may be many-fold different. However, accomplishing this technological advance will be difficult, as Stx likely

circulates at extraordinarily low concentrations consistent with its very low toxic dosing *in vitro*. Methods that might be attempted to overcome these limitations include ELISAs that utilize multiple levels of signal amplification, assays that can use whole blood to detect the level of Stx enzymatic activity, or incubation of whole blood with Stx sensitive cell types to measure cytotoxic effect and correlate that with Stx dose. Thus far, similar techniques have been unsuccessful, though the importance of this information to the progression of the field indicates that continued attempts are necessary and worthwhile.

The mechanistic explanation of vascular and parenchymal damage on a continuum of Stx mediated HUS has implications for its treatment. Although the best means to prevent the development of HUS is still to prevent ingestion of STEC, future treatment modalities will likely take advantage of the above mechanisms of damage. Dilution of the systemic toxemia by intravascular volume expansion is currently the only effective treatment that utilizes these findings. Anti-Stx antibody administration has entered clinical trials, and these antibodies may be able to decrease the circulating dose of Stx in the window of opportunity between diarrhea and HUS attainment³⁶¹. Alternatively, increased HuSAP given by injection may be able to dilute and sequester Stx in the serum, functionally diluting the toxin^{499-501,514}. On a different tact, anti-apoptotic pharmacological intervention may become feasible, as non-selective caspase inhibitors have entered clinical trials⁵¹⁵. Although not currently testable in a relevant small animal model, these caspase inhibitors may be able to deter the dysregulated coagulation and endothelial damage of HUS. Finally, administration of exogenous VEGF to the renal vasculature may be able to partially prevent some of the glomerular

endothelial damage by replenishing VEGF normally produced by podocytes. In support of this, VEGF administration helped to protect rats from immune mediated glomerular thrombotic microangiopathy⁸².

However, there are inherent problems with developing new therapeutics for a disease that normally affects young children and is uncommon. First, because infection with STEC is relatively rare and sporadic, large cohorts of patients and multinational multicenter consortiums that require vast oversight and administration are needed to generate statistically significant clinical data^{31,216,516}. Second, efforts aimed at preventing the transformation of hemorrhagic colitis to fulminant HUS are severely limited because many patients do not present to their physician until they have significant intestinal damage, and theoretically at this time have high levels of LPS and Stx toxemia³¹. Third, an additional group of patients do not present to their physicians until they have succumbed to renal failure, making prevention of colitis to HUS transition impossible³¹. Fourth, although the best chance for therapeutic intervention may be in preventing severe morbidity and mortality during and following the HUS acute phase, because the event rate of these adverse clinical outcomes is only 12% (for death or end stage renal disease), thousands of patients will be required to generate adequate statistical power to show benefits for any therapy²¹⁶. Fifth, because the majority of D+HUS patients recover normally without significant sequelae, any therapeutic will have to demonstrate extremely low toxicity and assuage any fear in parents of making the disease outcome worse. When combined, these considerations suggest that the best course for developing new therapeutics is to target the renal vascular or parenchymal pathology using an appropriate model system, and with better understanding of the etiology derived therein

test novel therapies with good side effect profiles already clinically approved for other diseases.

STEC and HUS are products of our current national food production, processing and delivery systems, and the prevalence of this condition will continue to increase unless substantial changes are made⁵⁵. Factors that identify increased risk of STEC infection include eating at a table service restaurant and eating undercooked (pink) hamburger meat^{55,166}. Even though strides have been made to decrease STEC contamination of crops and of meat at slaughter, its increasing presence worldwide and ability to cripple our network of consumables necessitates continued diagnostic and therapeutic research⁵⁵. Though the mouse currently can only provide limited insight into the disease, careful modification should allow the development of mice that can propel HUS research rapidly forward. Until that time however, meat and vegetables should be purchased locally to decrease cross contamination and long distance STEC spread by the national and global food supply systems, they should be well washed and cooked thoroughly, a thermometer should be used for cooking, and those handling the food should wash their hands well after touching raw meat¹⁶⁶. Children and adults presenting with bloody diarrhea should be rushed to a hospital where they can be rapidly diagnosed, quarantined from susceptible siblings, and cared for to prevent the dire consequences of hemolytic uremic syndrome^{55,73,80,170}.

References

1. Knepper MA, Gamba G. Urine Concentration and Dilution. In: Brenner B, ed. Brenner & Rector's The Kidney. 7 ed. Philadelphia: Saunders, 2004: 599-636.
2. Madsen KM, Tisher CC. Anatomy of the Kidney. In: Brenner B, ed. Brenner & Rector's The Kidney. 7 ed. Philadelphia: Saunders, 2004: 3-72.
3. Russo LM, Sandoval RM, McKee M, Osicka TM, Collins AB, Brown D, Molitoris BA, Comper WD. The normal kidney filters nephrotic levels of albumin retrieved by proximal tubule cells: retrieval is disrupted in nephrotic states. *Kidney Int* 2007;**71**(6):504-13.
4. Russo LM, Sandoval RM, Brown D, Molitoris BA, Comper WD. Response to 'Albumin concentration in the Bowman's capsule: Multiphoton microscopy vs micropuncture technique'. *Kidney Int* 2007;**72**(11):1411.
5. Russo LM, Sandoval RM, Brown D, Molitoris BA, Comper WD. Response to 'On the origin of albuminuria'. *Kidney Int* 2007;**72**(11):1409-10.
6. Russo LM, Sandoval RM, Brown D, Molitoris BA, Comper WD. Controversies in nephrology: response to 'renal albumin handling, facts, and artifacts'. *Kidney Int* 2007;**72**(10):1195-7.
7. Gekle M. Renal albumin handling: a look at the dark side of the filter. *Kidney Int* 2007;**71**(6):479-81.
8. Christensen EI, Birn H, Rippe B, Maunsbach AB. Controversies in nephrology: renal albumin handling, facts, and artifacts! *Kidney Int* 2007;**72**(10):1192-4.

9. Remuzzi A, Sangalli F, Fassi A, Remuzzi G. Albumin concentration in the Bowman's capsule: multiphoton microscopy vs micropuncture technique. *Kidney Int* 2007;**72**(11):1410-1; author reply 1411.
10. de Borst MH. On the origin of albuminuria. *Kidney Int* 2007;**72**(11):1409; author reply 1409-10.
11. Fenton RA, Knepper MA. Mouse models and the urinary concentrating mechanism in the new millennium. *Physiol Rev* 2007;**87**(4):1083-112.
12. Maddox DA, Brenner BM. Glomerular Ultrafiltration. In: Brenner B, ed. Brenner & Rector's The Kidney. 7 ed. Philadelphia: Saunders, 2004: 353-412.
13. Eremina V, Jefferson JA, Kowalewska J, Hochster H, Haas M, Weisstuch J, Richardson C, Kopp JB, Kabir MG, Backx PH, Gerber HP, Ferrara N, Barisoni L, Alpers CE, Quaggin SE. VEGF inhibition and renal thrombotic microangiopathy. *N Engl J Med* 2008;**358**(11):1129-36.
14. Kone BC. The Metabolic Basis of Solute Transport. In: Brenner B, ed. Brenner & Rector's The Kidney. 7 ed. Philadelphia: Saunders, 2004: 231-260.
15. Dworkin LD, Brenner BM. The Renal Circulations. In: Brenner B, ed. Brenner & Rector's The Kidney. 7 ed. Philadelphia: Saunders, 2004: 309-352.
16. Meyer TW, Hostetter TH. Uremia. *N Engl J Med* 2007;**357**(13):1316-25.
17. Hediger MA, Mount DB, Rolfs A, Romero MF. The Molecular Basis of Solute Transport. In: Brenner B, ed. Brenner & Rector's The Kidney. 7 ed. Philadelphia: Saunders, 2004: 261-308.

18. Moe OW, Baum M, Berry CA, Rector FCJ. Renal Transport of Glucose, Amino Acids, Sodium, Chloride, and Water. In: Brenner B, ed. Brenner & Rector's The Kidney. 7 ed. Philadelphia: Saunders, 2004: 413-452.
19. Toto RD. Approach to the Patient with Kidney Disease. In: Brenner B, ed. Brenner & Rector's The Kidney. 7 ed. Philadelphia: Saunders, 2004: 1079-1106.
20. Ake JA, Jelacic S, Ciol MA, Watkins SL, Murray KF, Christie DL, Klein EJ, Tarr PI. Relative nephroprotection during Escherichia coli O157:H7 infections: association with intravenous volume expansion. *Pediatrics* 2005;**115**(6):e673-80.
21. Brady HR, Clarkson MR, Lieberthal W. Acute Renal Failure. In: Brenner B, ed. Brenner & Rector's The Kidney. 7 ed. Philadelphia: Saunders, 2004: 1215-1292.
22. Kellum JA. Acute kidney injury. *Crit Care Med* 2008;**36**(4 Suppl):S141-5.
23. Abuelo JG. Normotensive ischemic acute renal failure. *N Engl J Med* 2007;**357**(8):797-805.
24. Silkensen JR, and Kasiske, B.L. Laboratory Assessment of Kidney Disease: Clearance, Urinalysis, and Kidney Biopsy. In: Brenner B, ed. Brenner & Rector's The Kidney. 7 ed. Philadelphia: Saunders, 2004: 1107-1150.
25. Himmelfarb J, Joannidis M, Molitoris B, Schietz M, Okusa MD, Warnock D, Laghi F, Goldstein SL, Prielipp R, Parikh CR, Pannu N, Lobo SM, Shah S, D'Intini V, Kellum JA. Evaluation and Initial Management of Acute Kidney Injury. *Clin J Am Soc Nephrol* 2008.
26. Wan L, Bagshaw SM, Langenberg C, Saotome T, May C, Bellomo R. Pathophysiology of septic acute kidney injury: what do we really know? *Crit Care Med* 2008;**36**(4 Suppl):S198-203.

27. Bonventre JV. Dedifferentiation and proliferation of surviving epithelial cells in acute renal failure. *J Am Soc Nephrol* 2003;**14 Suppl 1**:S55-61.
28. Witzgall R, Brown D, Schwarz C, Bonventre JV. Localization of proliferating cell nuclear antigen, vimentin, c-Fos, and clusterin in the postischemic kidney. Evidence for a heterogeneous genetic response among nephron segments, and a large pool of mitotically active and dedifferentiated cells. *J Clin Invest* 1994;**93**(5):2175-88.
29. Witzgall R, Obermuller N, Bolitz U, Calvet JP, Cowley BD, Jr., Walker C, Kriz W, Gretz N, Bonventre JV. Kid-1 expression is high in differentiated renal proximal tubule cells and suppressed in cyst epithelia. *Am J Physiol* 1998;**275**(6 Pt 2):F928-37.
30. Van Biljon G. Causes, Prognostic Factors and Treatment Results of Acute Renal Failure in Children Treated in a Tertiary Hospital in South Africa. *J Trop Pediatr* 2008.
31. Tarr PI, Gordon CA, Chandler WL. Shiga-toxin-producing *Escherichia coli* and haemolytic uraemic syndrome. *Lancet* 2005;**365**(9464):1073-86.
32. Gianantonio CA, Vitacco M, Mendilaharsu F, Gallo GE, Sojo ET. The hemolytic-uremic syndrome. *Nephron* 1973;**11**(2):174-92.
33. Dundas S, Todd WT, Stewart AI, Murdoch PS, Chaudhuri AK, Hutchinson SJ. The central Scotland *Escherichia coli* O157:H7 outbreak: risk factors for the hemolytic uremic syndrome and death among hospitalized patients. *Clin Infect Dis* 2001;**33**(7):923-31.

34. Karch H, Bielaszewska M, Bitzan M, Schmidt H. Epidemiology and diagnosis of Shiga toxin-producing *Escherichia coli* infections. *Diagn Microbiol Infect Dis* 1999;**34**(3):229-43.
35. Serna At, Boedeker EC. Pathogenesis and treatment of Shiga toxin-producing *Escherichia coli* infections. *Curr Opin Gastroenterol* 2008;**24**(1):38-47.
36. Tserenpuntsag B, Chang HG, Smith PF, Morse DL. Hemolytic uremic syndrome risk and *Escherichia coli* O157:H7. *Emerg Infect Dis* 2005;**11**(12):1955-7.
37. Chaisri U, Nagata M, Kurazono H, Horie H, Tongtawe P, Hayashi H, Watanabe T, Tapchaisri P, Chongsa-nguan M, Chaicumpa W. Localization of Shiga toxins of enterohaemorrhagic *Escherichia coli* in kidneys of paediatric and geriatric patients with fatal haemolytic uraemic syndrome. *Microb Pathog* 2001;**31**(2):59-67.
38. Carter AO, Borczyk AA, Carlson JA, Harvey B, Hockin JC, Karmali MA, Krishnan C, Korn DA, Lior H. A severe outbreak of *Escherichia coli* O157:H7--associated hemorrhagic colitis in a nursing home. *N Engl J Med* 1987;**317**(24):1496-500.
39. Caletti MG, Gallo G, Gianantonio CA. Development of focal segmental sclerosis and hyalinosis in hemolytic uremic syndrome. *Pediatr Nephrol* 1996;**10**(6):687-92.
40. Lou-Meda R, Oakes RS, Gilstrap JN, Williams CG, Siegler RL. Prognostic significance of microalbuminuria in postdiarrheal hemolytic uremic syndrome. *Pediatr Nephrol* 2007;**22**(1):117-20.
41. Nataro JP, Kaper JB. Diarrheagenic *Escherichia coli*. *Clin Microbiol Rev* 1998;**11**(1):142-201.
42. Kaper JB, Nataro JP, Mobley HL. Pathogenic *Escherichia coli*. *Nat Rev Microbiol* 2004;**2**(2):123-40.

43. Milford D. The Hemolytic Uremic Syndromes in the United Kingdom. In: Kaplan BS, Trompeter, R.S., Moake, J.L., ed. Hemolytic Uremic Syndrome and Thrombotic Thrombocytopenic Purpura. 1 ed. New York: Marcel Dekker, Inc., 1992: 39-59.
44. Orth D, Grif K, Khan AB, Naim A, Dierich MP, Wurzner R. The Shiga toxin genotype rather than the amount of Shiga toxin or the cytotoxicity of Shiga toxin in vitro correlates with the appearance of the hemolytic uremic syndrome. *Diagn Microbiol Infect Dis* 2007;**59**(3):235-42.
45. Bielaszewska M, Kock R, Friedrich AW, von Eiff C, Zimmerhackl LB, Karch H, Mellmann A. Shiga toxin-mediated hemolytic uremic syndrome: time to change the diagnostic paradigm? *PLoS ONE* 2007;**2**(10):e1024.
46. Bielaszewska M, Prager R, Kock R, Mellmann A, Zhang W, Tschape H, Tarr PI, Karch H. Shiga toxin gene loss and transfer in vitro and in vivo during enterohemorrhagic Escherichia coli O26 infection in humans. *Appl Environ Microbiol* 2007;**73**(10):3144-50.
47. Banatvala N, Griffin PM, Greene KD, Barrett TJ, Bibb WF, Green JH, Wells JG. The United States National Prospective Hemolytic Uremic Syndrome Study: microbiologic, serologic, clinical, and epidemiologic findings. *J Infect Dis* 2001;**183**(7):1063-70.
48. Gianviti A, Tozzi AE, De Petris L, Caprioli A, Rava L, Edefonti A, Ardissino G, Montini G, Zacchello G, Ferretti A, Pecoraro C, De Palo T, Caringella A, Gaido M, Coppo R, Perfumo F, Miglietti N, Ratsche I, Penza R, Capasso G, Maringhini S, Li Volti S, Setzu C, Pennesi M, Bettinelli A, Peratoner L, Pela I, Salvaggio E,

- Lama G, Maffei S, Rizzoni G. Risk factors for poor renal prognosis in children with hemolytic uremic syndrome. *Pediatr Nephrol* 2003;**18**(12):1229-35.
49. Caprioli A, Morabito S, Brugere H, Oswald E. Enterohaemorrhagic Escherichia coli: emerging issues on virulence and modes of transmission. *Vet Res* 2005;**36**(3):289-311.
50. Bitzan M, Moebius E, Ludwig K, Muller-Wiefel DE, Heesemann J, Karch H. High incidence of serum antibodies to Escherichia coli O157 lipopolysaccharide in children with hemolytic-uremic syndrome. *J Pediatr* 1991;**119**(3):380-5.
51. Kaplan BS, de Chadarevian JP. Hemolytic-uremic syndrome. *Can Med Assoc J* 1977;**117**(11):1246-7.
52. Rangel JM, Sparling PH, Crowe C, Griffin PM, Swerdlow DL. Epidemiology of Escherichia coli O157:H7 outbreaks, United States, 1982-2002. *Emerg Infect Dis* 2005;**11**(4):603-9.
53. Doane CA, Pangloli P, Richards HA, Mount JR, Golden DA, Draughon FA. Occurrence of Escherichia coli O157:H7 in diverse farm environments. *J Food Prot* 2007;**70**(1):6-10.
54. Hilborn ED, Mermin JH, Mshar PA, Hadler JL, Voetsch A, Wojtkunski C, Swartz M, Mshar R, Lambert-Fair MA, Farrar JA, Glynn MK, Slutsker L. A multistate outbreak of Escherichia coli O157:H7 infections associated with consumption of mesclun lettuce. *Arch Intern Med* 1999;**159**(15):1758-64.
55. DuPont HL. The growing threat of foodborne bacterial enteropathogens of animal origin. *Clin Infect Dis* 2007;**45**(10):1353-61.

56. Tuttle J, Gomez T, Doyle MP, Wells JG, Zhao T, Tauxe RV, Griffin PM. Lessons from a large outbreak of Escherichia coli O157:H7 infections: insights into the infectious dose and method of widespread contamination of hamburger patties. *Epidemiol Infect* 1999;**122**(2):185-92.
57. Honish L, Preedy G, Hislop N, Chui L, Kowalewska-Grochowska K, Trottier L, Kreplin C, Zazulak I. An outbreak of E. coli O157:H7 hemorrhagic colitis associated with unpasteurized gouda cheese. *Can J Public Health* 2005;**96**(3):182-4.
58. Paunio M, Pebody R, Keskimaki M, Kokki M, Ruutu P, Oinonen S, Vuotari V, Siitonen A, Lahti E, Leinikki P. Swimming-associated outbreak of Escherichia coli O157:H7. *Epidemiol Infect* 1999;**122**(1):1-5.
59. Iijima K, Kamioka I, Nozu K. Management of diarrhea-associated hemolytic uremic syndrome in children. *Clin Exp Nephrol* 2008.
60. Fukushima H, Hashizume T, Morita Y, Tanaka J, Azuma K, Mizumoto Y, Kaneno M, Matsuura M, Konma K, Kitani T. Clinical experiences in Sakai City Hospital during the massive outbreak of enterohemorrhagic Escherichia coli O157 infections in Sakai City, 1996. *Pediatr Int* 1999;**41**(2):213-7.
61. Keene WE, Hedberg K, Herriott DE, Hancock DD, McKay RW, Barrett TJ, Fleming DW. A prolonged outbreak of Escherichia coli O157:H7 infections caused by commercially distributed raw milk. *J Infect Dis* 1997;**176**(3):815-8.
62. Brandt JR, Fouser LS, Watkins SL, Zelikovic I, Tarr PI, Nazar-Stewart V, Avner ED. Escherichia coli O 157:H7-associated hemolytic-uremic syndrome after ingestion of contaminated hamburgers. *J Pediatr* 1994;**125**(4):519-26.

63. Raffaelli RM, Paladini M, Hanson H, Kornstein L, Agasan A, Slavinski S, Weiss D, Fennelly GJ, Flynn JT. Child care-associated outbreak of Escherichia coli O157:H7 and hemolytic uremic syndrome. *Pediatr Infect Dis J* 2007;**26**(10):951-3.
64. Cody SH, Glynn MK, Farrar JA, Cairns KL, Griffin PM, Kobayashi J, Fyfe M, Hoffman R, King AS, Lewis JH, Swaminathan B, Bryant RG, Vugia DJ. An outbreak of Escherichia coli O157:H7 infection from unpasteurized commercial apple juice. *Ann Intern Med* 1999;**130**(3):202-9.
65. Williams RC, Isaacs S, Decou ML, Richardson EA, Buffett MC, Slinger RW, Brodsky MH, Ciebin BW, Ellis A, Hockin J. Illness outbreak associated with Escherichia coli O157:H7 in Genoa salami. E. coli O157:H7 Working Group. *Cmaj* 2000;**162**(10):1409-13.
66. Vogt RL, Dippold L. Escherichia coli O157:H7 outbreak associated with consumption of ground beef, June-July 2002. *Public Health Rep* 2005;**120**(2):174-8.
67. Cieslak PR, Noble SJ, Maxson DJ, Empey LC, Ravenholt O, Legarza G, Tuttle J, Doyle MP, Barrett TJ, Wells JG, McNamara AM, Griffin PM. Hamburger-associated Escherichia coli O157:H7 infection in Las Vegas: a hidden epidemic. *Am J Public Health* 1997;**87**(2):176-80.
68. Shefer AM, Koo D, Werner SB, Mintz ED, Baron R, Wells JG, Barrett TJ, Ginsberg M, Bryant R, Abbott S, Griffin PM. A cluster of Escherichia coli O157:H7 infections with the hemolytic-uremic syndrome and death in California. A mandate for improved surveillance. *West J Med* 1996;**165**(1-2):15-9.

69. Bell BP, Goldoft M, Griffin PM, Davis MA, Gordon DC, Tarr PI, Bartleson CA, Lewis JH, Barrett TJ, Wells JG, et al. A multistate outbreak of Escherichia coli O157:H7-associated bloody diarrhea and hemolytic uremic syndrome from hamburgers. The Washington experience. *Jama* 1994;**272**(17):1349-53.
70. Currie A, MacDonald J, Ellis A, Siushansian J, Chui L, Charlebois M, Peermohamed M, Everett D, Fehr M, Ng LK. Outbreak of Escherichia coli O157:H7 infections associated with consumption of beef donair. *J Food Prot* 2007;**70**(6):1483-8.
71. Hilborn ED, Mshar PA, Fiorentino TR, Dembek ZF, Barrett TJ, Howard RT, Cartter ML. An outbreak of Escherichia coli O157:H7 infections and haemolytic uraemic syndrome associated with consumption of unpasteurized apple cider. *Epidemiol Infect* 2000;**124**(1):31-6.
72. Besser RE, Lett SM, Weber JT, Doyle MP, Barrett TJ, Wells JG, Griffin PM. An outbreak of diarrhea and hemolytic uremic syndrome from Escherichia coli O157:H7 in fresh-pressed apple cider. *Jama* 1993;**269**(17):2217-20.
73. Mead PS, Finelli L, Lambert-Fair MA, Champ D, Townes J, Hutwagner L, Barrett T, Spitalny K, Mintz E. Risk factors for sporadic infection with Escherichia coli O157:H7. *Arch Intern Med* 1997;**157**(2):204-8.
74. Ackers ML, Mahon BE, Leahy E, Goode B, Damrow T, Hayes PS, Bibb WF, Rice DH, Barrett TJ, Hutwagner L, Griffin PM, Slutsker L. An outbreak of Escherichia coli O157:H7 infections associated with leaf lettuce consumption. *J Infect Dis* 1998;**177**(6):1588-93.

75. Ostroff SM, Griffin PM, Tauxe RV, Shipman LD, Greene KD, Wells JG, Lewis JH, Blake PA, Kobayashi JM. A statewide outbreak of *Escherichia coli* O157:H7 infections in Washington State. *Am J Epidemiol* 1990;**132**(2):239-47.
76. Wang G, Zhao T, Doyle MP. Fate of enterohemorrhagic *Escherichia coli* O157:H7 in bovine feces. *Appl Environ Microbiol* 1996;**62**(7):2567-70.
77. te Loo DM, Heuvelink AE, de Boer E, Nauta J, van der Walle J, Schroder C, van Hinsbergh VW, Chart H, van de Kar NC, van den Heuvel LP. Vero cytotoxin binding to polymorphonuclear leukocytes among households with children with hemolytic uremic syndrome. *J Infect Dis* 2001;**184**(4):446-50.
78. Pavia AT, Nichols CR, Green DP, Tauxe RV, Mottice S, Greene KD, Wells JG, Siegler RL, Brewer ED, Hannon D, et al. Hemolytic-uremic syndrome during an outbreak of *Escherichia coli* O157:H7 infections in institutions for mentally retarded persons: clinical and epidemiologic observations. *J Pediatr* 1990;**116**(4):544-51.
79. Ahn CK, Klein E, Tarr PI. Isolation of patients acutely infected with *Escherichia coli* O157:H7: low-tech, highly effective prevention of hemolytic uremic syndrome. *Clin Infect Dis* 2008;**46**(8):1197-9.
80. Werber D, Mason BW, Evans MR, Salmon RL. Preventing household transmission of Shiga toxin-producing *Escherichia coli* O157 infection: promptly separating siblings might be the key. *Clin Infect Dis* 2008;**46**(8):1189-96.
81. Silvestro L, Caputo M, Blancato S, Decastelli L, Fioravanti A, Tozzoli R, Morabito S, Caprioli A. Asymptomatic carriage of verocytotoxin-producing *Escherichia coli* O157 in farm workers in Northern Italy. *Epidemiol Infect* 2004;**132**(5):915-9.

82. Paton JC, Paton AW. Pathogenesis and diagnosis of Shiga toxin-producing *Escherichia coli* infections. *Clin Microbiol Rev* 1998;**11**(3):450-79.
83. Noris M, Remuzzi G. Hemolytic uremic syndrome. *J Am Soc Nephrol* 2005;**16**(4):1035-50.
84. Riley LW, Remis RS, Helgerson SD, McGee HB, Wells JG, Davis BR, Hebert RJ, Olcott ES, Johnson LM, Hargrett NT, Blake PA, Cohen ML. Hemorrhagic colitis associated with a rare *Escherichia coli* serotype. *N Engl J Med* 1983;**308**(12):681-5.
85. Ritchie JM, Thorpe CM, Rogers AB, Waldor MK. Critical roles for stx2, eae, and tir in enterohemorrhagic *Escherichia coli*-induced diarrhea and intestinal inflammation in infant rabbits. *Infect Immun* 2003;**71**(12):7129-39.
86. Karmali MA, Steele BT, Petric M, Lim C. Sporadic cases of haemolytic-uraemic syndrome associated with faecal cytotoxin and cytotoxin-producing *Escherichia coli* in stools. *Lancet* 1983;**1**(8325):619-20.
87. Proulx F, Seidman E, Mariscalco MM, Lee K, Carroll S. Increased circulating levels of lipopolysaccharide binding protein in children with *Escherichia coli* O157:H7 hemorrhagic colitis and hemolytic uremic syndrome. *Clin Diagn Lab Immunol* 1999;**6**(5):773.
88. Koster F, Levin J, Walker L, Tung KS, Gilman RH, Rahaman MM, Majid MA, Islam S, Williams RC, Jr. Hemolytic-uremic syndrome after shigellosis. Relation to endotoxemia and circulating immune complexes. *N Engl J Med* 1978;**298**(17):927-33.

89. van Wieringen PM, Monnens LA, Bakkeren JA. Hemolytic-uremic syndrome: absence of circulating endotoxin. *Pediatrics* 1976;**58**(4):561-3.
90. O'Loughlin EV, Robins-Browne RM. Effect of Shiga toxin and Shiga-like toxins on eukaryotic cells. *Microbes Infect* 2001;**3**(6):493-507.
91. Kawano K, Okada M, Haga T, Maeda K, Goto Y. Relationship between pathogenicity for humans and stx genotype in Shiga toxin-producing *Escherichia coli* serotype O157. *Eur J Clin Microbiol Infect Dis* 2008;**27**(3):227-32.
92. Ostroff SM, Kobayashi JM, Lewis JH. Infections with *Escherichia coli* O157:H7 in Washington State. The first year of statewide disease surveillance. *Jama* 1989;**262**(3):355-9.
93. Ostroff SM, Tarr PI, Neill MA, Lewis JH, Hargrett-Bean N, Kobayashi JM. Toxin genotypes and plasmid profiles as determinants of systemic sequelae in *Escherichia coli* O157:H7 infections. *J Infect Dis* 1989;**160**(6):994-8.
94. Tesh VL, Burris JA, Owens JW, Gordon VM, Wadolkowski EA, O'Brien AD, Samuel JE. Comparison of the relative toxicities of Shiga-like toxins type I and type II for mice. *Infect Immun* 1993;**61**(8):3392-402.
95. Samuel JE, Perera LP, Ward S, O'Brien AD, Ginsburg V, Krivan HC. Comparison of the glycolipid receptor specificities of Shiga-like toxin type II and Shiga-like toxin type II variants. *Infect Immun* 1990;**58**(3):611-8.
96. Chart H, Scotland SM, Rowe B. Serum antibodies to *Escherichia coli* serotype O157:H7 in patients with hemolytic uremic syndrome. *J Clin Microbiol* 1989;**27**(2):285-90.

97. Chart H, Smith HR, Scotland SM, Rowe B, Milford DV, Taylor CM. Serological identification of *Escherichia coli* O157:H7 infection in haemolytic uraemic syndrome. *Lancet* 1991;**337**(8734):138-40.
98. Chart H, Rowe B, vd Kar N, Monnens LA. Serological identification of *Escherichia coli* O157 as cause of haemolytic uraemic syndrome in Netherlands. *Lancet* 1991;**337**(8738):437.
99. Sherman P, Soni R, Yeger H. Characterization of flagella purified from enterohemorrhagic, vero-cytotoxin-producing *Escherichia coli* serotype O157:H7. *J Clin Microbiol* 1988;**26**(7):1367-72.
100. Reymond D, Johnson RP, Karmali MA, Petric M, Winkler M, Johnson S, Rahn K, Renwick S, Wilson J, Clarke RC, Spika J. Neutralizing antibodies to *Escherichia coli* Vero cytotoxin 1 and antibodies to O157 lipopolysaccharide in healthy farm family members and urban residents. *J Clin Microbiol* 1996;**34**(9):2053-7.
101. Tsutsumi R, Ichinohe N, Shimooki O, Obata F, Takahashi K, Inada K, Sasaki M, Sato S, Chida S. Homologous and heterologous antibody responses to lipopolysaccharide after enterohemorrhagic *Escherichia coli* infection. *Microbiol Immunol* 2004;**48**(1):27-38.
102. Stahl AL, Svensson M, Morgelin M, Svanborg C, Tarr PI, Mooney JC, Watkins SL, Johnson R, Karpman D. Lipopolysaccharide from enterohemorrhagic *Escherichia coli* binds to platelets through TLR4 and CD62 and is detected on circulating platelets in patients with hemolytic uremic syndrome. *Blood* 2006;**108**(1):167-76.

103. Alves-Rosa F, Vulcano M, Beigier-Bompadre M, Fernandez G, Palermo M, Isturiz MA. Interleukin-1beta induces in vivo tolerance to lipopolysaccharide in mice. *Clin Exp Immunol* 2002;**128**(2):221-8.
104. Bannerman DD, Goldblum SE. Mechanisms of bacterial lipopolysaccharide-induced endothelial apoptosis. *Am J Physiol Lung Cell Mol Physiol* 2003;**284**(6):L899-914.
105. Ouyang DY, Wang YY, Zheng YT. Activation of c-Jun N-terminal kinases by ribotoxic stresses. *Cell Mol Immunol* 2005;**2**(6):419-25.
106. Niyogi SK. Shigellosis. *J Microbiol* 2005;**43**(2):133-43.
107. Chark D, Nutikka A, Trusevych N, Kuzmina J, Lingwood C. Differential carbohydrate epitope recognition of globotriaosyl ceramide by verotoxins and a monoclonal antibody. *Eur J Biochem* 2004;**271**(2):405-17.
108. Lingwood CA, Law H, Richardson S, Petric M, Brunton JL, De Grandis S, Karmali M. Glycolipid binding of purified and recombinant Escherichia coli produced verotoxin in vitro. *J Biol Chem* 1987;**262**(18):8834-9.
109. Lindberg AA, Brown JE, Stromberg N, Westling-Ryd M, Schultz JE, Karlsson KA. Identification of the carbohydrate receptor for Shiga toxin produced by Shigella dysenteriae type 1. *J Biol Chem* 1987;**262**(4):1779-85.
110. Jacewicz MS, Mobassaleh M, Gross SK, Balasubramanian KA, Daniel PF, Raghavan S, McCluer RH, Keusch GT. Pathogenesis of Shigella diarrhea: XVII. A mammalian cell membrane glycolipid, Gb3, is required but not sufficient to confer sensitivity to Shiga toxin. *J Infect Dis* 1994;**169**(3):538-46.

111. Chong DC, Paton JC, Thorpe CM, Paton AW. Clathrin-dependent trafficking of subtilase cytotoxin, a novel AB(5) toxin that targets the endoplasmic reticulum chaperone BiP. *Cell Microbiol* 2007.
112. Obrig TG, Moran TP, Brown JE. The mode of action of Shiga toxin on peptide elongation of eukaryotic protein synthesis. *Biochem J* 1987;**244**(2):287-94.
113. Jacewicz MS, Acheson DW, Binion DG, West GA, Lincicome LL, Fiocchi C, Keusch GT. Responses of human intestinal microvascular endothelial cells to Shiga toxins 1 and 2 and pathogenesis of hemorrhagic colitis. *Infect Immun* 1999;**67**(3):1439-44.
114. Cherla RP, Lee SY, Tesh VL. Shiga toxins and apoptosis. *FEMS Microbiol Lett* 2003;**228**(2):159-66.
115. Smith WE, Kane AV, Campbell ST, Acheson DW, Cochran BH, Thorpe CM. Shiga toxin 1 triggers a ribotoxic stress response leading to p38 and JNK activation and induction of apoptosis in intestinal epithelial cells. *Infect Immun* 2003;**71**(3):1497-504.
116. Fujii Y, Numata S, Nakamura Y, Honda T, Furukawa K, Urano T, Wiels J, Uchikawa M, Ozaki N, Matsuo S, Sugiura Y. Murine glycosyltransferases responsible for the expression of globo-series glycolipids: cDNA structures, mRNA expression, and distribution of their products. *Glycobiology* 2005;**15**(12):1257-67.
117. Sillence DJ. New insights into glycosphingolipid functions--storage, lipid rafts, and translocators. *Int Rev Cytol* 2007;**262**:151-89.

118. Lahiri S, Futerman AH. The metabolism and function of sphingolipids and glycosphingolipids. *Cell Mol Life Sci* 2007;**64**(17):2270-84.
119. Cilmi SA, Karalius BJ, Choy W, Smith RN, Butterton JR. Fabry disease in mice protects against lethal disease caused by Shiga toxin-expressing enterohemorrhagic *Escherichia coli*. *J Infect Dis* 2006;**194**(8):1135-40.
120. Clarke JT. Narrative review: Fabry disease. *Ann Intern Med* 2007;**146**(6):425-33.
121. Sessa A, Meroni M, Battini G, Maglio A, Brambilla PL, Bertella M, Nebuloni M, Pallotti F, Giordano F, Bertagnolio B, Tosoni A. Renal pathological changes in Fabry disease. *J Inherit Metab Dis* 2001;**24 Suppl 2**:66-70; discussion 65.
122. Ohshima T, Murray GJ, Swaim WD, Longenecker G, Quirk JM, Cardarelli CO, Sugimoto Y, Pastan I, Gottesman MM, Brady RO, Kulkarni AB. alpha-Galactosidase A deficient mice: a model of Fabry disease. *Proc Natl Acad Sci U S A* 1997;**94**(6):2540-4.
123. Williams JM, Lea N, Lord JM, Roberts LM, Milford DV, Taylor CM. Comparison of ribosome-inactivating proteins in the induction of apoptosis. *Toxicol Lett* 1997;**91**(2):121-7.
124. Fujii J, Matsui T, Heatherly DP, Schlegel KH, Lobo PI, Yutsudo T, Ciruolo GM, Morris RE, Obrig T. Rapid apoptosis induced by Shiga toxin in HeLa cells. *Infect Immun* 2003;**71**(5):2724-35.
125. Kiyokawa N, Taguchi T, Mori T, Uchida H, Sato N, Takeda T, Fujimoto J. Induction of apoptosis in normal human renal tubular epithelial cells by *Escherichia coli* Shiga toxins 1 and 2. *J Infect Dis* 1998;**178**(1):178-84.

126. Danielsen AJ, Maihle NJ. The EGF/ErbB receptor family and apoptosis. *Growth Factors* 2002;**20**(1):1-15.
127. Henson ES, Gibson SB. Surviving cell death through epidermal growth factor (EGF) signal transduction pathways: implications for cancer therapy. *Cell Signal* 2006;**18**(12):2089-97.
128. Jones NL, Islur A, Haq R, Mascarenhas M, Karmali MA, Perdue MH, Zanke BW, Sherman PM. Escherichia coli Shiga toxins induce apoptosis in epithelial cells that is regulated by the Bcl-2 family. *Am J Physiol Gastrointest Liver Physiol* 2000;**278**(5):G811-9.
129. Erwert RD, Eiting KT, Tupper JC, Winn RK, Harlan JM, Bannerman DD. Shiga toxin induces decreased expression of the anti-apoptotic protein Mcl-1 concomitant with the onset of endothelial apoptosis. *Microb Pathog* 2003;**35**(2):87-93.
130. Suzuki A, Doi H, Matsuzawa F, Aikawa S, Takiguchi K, Kawano H, Hayashida M, Ohno S. Bcl-2 antiapoptotic protein mediates verotoxin II-induced cell death: possible association between bcl-2 and tissue failure by E. coli O157:H7. *Genes Dev* 2000;**14**(14):1734-40.
131. Erwert RD, Winn RK, Harlan JM, Bannerman DD. Shiga-like toxin inhibition of FLICE-like inhibitory protein expression sensitizes endothelial cells to bacterial lipopolysaccharide-induced apoptosis. *J Biol Chem* 2002;**277**(43):40567-74.
132. Wilson C, Foster GH, Bitzan M. Silencing of Bak ameliorates apoptosis of human proximal tubular epithelial cells by Escherichia coli-derived Shiga toxin 2. *Infection* 2005;**33**(5-6):362-7.

133. Ching JC, Jones NL, Ceponis PJ, Karmali MA, Sherman PM. Escherichia coli shiga-like toxins induce apoptosis and cleavage of poly(ADP-ribose) polymerase via in vitro activation of caspases. *Infect Immun* 2002;**70**(8):4669-77.
134. Bhattacharjee RN, Park KS, Uematsu S, Okada K, Hoshino K, Takeda K, Takeuchi O, Akira S, Iida T, Honda T. Escherichia coli verotoxin 1 mediates apoptosis in human HCT116 colon cancer cells by inducing overexpression of the GADD family of genes and S phase arrest. *FEBS Lett* 2005;**579**(29):6604-10.
135. Brigotti M, Carnicelli D, Ravanelli E, Vara AG, Martinelli C, Alfieri RR, Petronini PG, Sestili P. Molecular damage and induction of proinflammatory cytokines in human endothelial cells exposed to Shiga toxin 1, Shiga toxin 2, and alpha-sarcin. *Infect Immun* 2007;**75**(5):2201-7.
136. Brigotti M, Alfieri R, Sestili P, Bonelli M, Petronini PG, Guidarelli A, Barbieri L, Stirpe F, Sperti S. Damage to nuclear DNA induced by Shiga toxin 1 and ricin in human endothelial cells. *Faseb J* 2002;**16**(3):365-72.
137. Brigotti M, Accorsi P, Carnicelli D, Rizzi S, Gonzalez Vara A, Montanaro L, Sperti S. Shiga toxin 1: damage to DNA in vitro. *Toxicon* 2001;**39**(2-3):341-8.
138. Iordanov MS, Pribnow D, Magun JL, Dinh TH, Pearson JA, Chen SL, Magun BE. Ribotoxic stress response: activation of the stress-activated protein kinase JNK1 by inhibitors of the peptidyl transferase reaction and by sequence-specific RNA damage to the alpha-sarcin/ricin loop in the 28S rRNA. *Mol Cell Biol* 1997;**17**(6):3373-81.
139. Cameron P, Bingham D, Paul A, Pavelka M, Cameron S, Rotondo D, Plevin R. Essential role for verotoxin in sustained stress-activated protein kinase and

- nuclear factor kappa B signaling, stimulated by Escherichia coli O157:H7 in Vero cells. *Infect Immun* 2002;**70**(10):5370-80.
140. Foster GH, Armstrong CS, Sakiri R, Tesh VL. Shiga toxin-induced tumor necrosis factor alpha expression: requirement for toxin enzymatic activity and monocyte protein kinase C and protein tyrosine kinases. *Infect Immun* 2000;**68**(9):5183-9.
141. Foster GH, Tesh VL. Shiga toxin 1-induced activation of c-Jun NH(2)-terminal kinase and p38 in the human monocytic cell line THP-1: possible involvement in the production of TNF-alpha. *J Leukoc Biol* 2002;**71**(1):107-14.
142. Yamasaki C, Natori Y, Zeng XT, Ohmura M, Yamasaki S, Takeda Y. Induction of cytokines in a human colon epithelial cell line by Shiga toxin 1 (Stx1) and Stx2 but not by non-toxic mutant Stx1 which lacks N-glycosidase activity. *FEBS Lett* 1999;**442**(2-3):231-4.
143. Zoja C, Angioletti S, Donadelli R, Zanchi C, Tomasoni S, Binda E, Imberti B, te Loo M, Monnens L, Remuzzi G, Morigi M. Shiga toxin-2 triggers endothelial leukocyte adhesion and transmigration via NF-kappaB dependent up-regulation of IL-8 and MCP-1. *Kidney Int* 2002;**62**(3):846-56.
144. Thorpe CM, Smith WE, Hurley BP, Acheson DW. Shiga toxins induce, superinduce, and stabilize a variety of C-X-C chemokine mRNAs in intestinal epithelial cells, resulting in increased chemokine expression. *Infect Immun* 2001;**69**(10):6140-7.
145. Thorpe CM, Hurley BP, Lincicome LL, Jacewicz MS, Keusch GT, Acheson DW. Shiga toxins stimulate secretion of interleukin-8 from intestinal epithelial cells. *Infect Immun* 1999;**67**(11):5985-93.

146. Yamasaki C, Nishikawa K, Zeng XT, Katayama Y, Natori Y, Komatsu N, Oda T. Induction of cytokines by toxins that have an identical RNA N-glycosidase activity: Shiga toxin, ricin, and modeccin. *Biochim Biophys Acta* 2004;**1671**(1-3):44-50.
147. Matussek A, Lauber J, Bergau A, Hansen W, Rohde M, Dittmar KE, Gunzer M, Mengel M, Gatzlaff P, Hartmann M, Buer J, Gunzer F. Molecular and functional analysis of Shiga toxin-induced response patterns in human vascular endothelial cells. *Blood* 2003;**102**(4):1323-32.
148. Stricklett PK, Hughes AK, Ergonul Z, Kohan DE. Molecular basis for up-regulation by inflammatory cytokines of Shiga toxin 1 cytotoxicity and globotriaosylceramide expression. *J Infect Dis* 2002;**186**(7):976-82.
149. Copelovitch L, Kaplan BS. The thrombotic microangiopathies. *Pediatr Nephrol* 2007.
150. Gautier E, and Siebenmann, R.E. The Birth of the Hemolytic Uremic Syndrome. In: Kaplan BS, Trompeter, R.S., Moake, J.L., ed. Hemolytic Uremic Syndrome and Thrombotic Thrombocytopenic Purpura. 1 ed. New York: Marcel Dekker, Inc., 1992: 1-18.
151. Habib R. Pathology of the Hemolytic Uremic Syndrome. In: Kaplan BS, Trompeter RS, Moake JL, eds. Hemolytic Uremic Syndrome and Thrombotic Thrombocytopenic Purpura. New York: Marcel Dekker, Inc., 1992: 315-353.
152. Lieberman E, Heuser E, Donnell GN, Landing BH, Hammond GD. Hemolytic-uremic syndrome. Clinical and pathological considerations. *N Engl J Med* 1966;**275**(5):227-36.

153. Kaplan BS. Another step forward in our understanding of the hemolytic uremic syndromes: tying up some loose ends. *Pediatr Nephrol* 1995;**9**(1):30-2.
154. Moake JL. Moschcowitz, multimers, and metalloprotease. *N Engl J Med* 1998;**339**(22):1629-31.
155. Konowalchuk J, Speirs JJ, Stavric S. Vero response to a cytotoxin of *Escherichia coli*. *Infect Immun* 1977;**18**(3):775-9.
156. Wade WG, Thom BT, Evans N. Cytotoxic enteropathogenic *Escherichia coli*. *Lancet* 1979;**2**(8154):1235-6.
157. Sharpstone P, Evans RG, O'Shea M, Alexander L, Lee HA. Haemolytic-uraemic syndrome: survival after prolonged oliguria. *Arch Dis Child* 1968;**43**(232):711-6.
158. van Wieringen PM, Monnens LA, Schretlen ED. Haemolytic-uraemic syndrome. Epidemiological and clinical study. *Arch Dis Child* 1974;**49**(6):432-7.
159. O'Brien AO, Lively TA, Chen ME, Rothman SW, Formal SB. *Escherichia coli* O157:H7 strains associated with haemorrhagic colitis in the United States produce a *Shigella dysenteriae* 1 (SHIGA) like cytotoxin. *Lancet* 1983;**1**(8326 Pt 1):702.
160. O'Brien AD, Lively TA, Chang TW, Gorbach SL. Purification of *Shigella dysenteriae* 1 (Shiga)-like toxin from *Escherichia coli* O157:H7 strain associated with haemorrhagic colitis. *Lancet* 1983;**2**(8349):573.
161. Taylor CM, Howie AJ, Williams JM. No common final pathogenetic pathway in haemolytic uraemic syndromes. *Nephrol Dial Transplant* 1999;**14**(5):1100-2.
162. Hosler GA, Cusumano AM, Hutchins GM. Thrombotic thrombocytopenic purpura and hemolytic uremic syndrome are distinct pathologic entities. A review of 56 autopsy cases. *Arch Pathol Lab Med* 2003;**127**(7):834-9.

163. Inward CD, Howie AJ, Fitzpatrick MM, Rafaat F, Milford DV, Taylor CM.
Renal histopathology in fatal cases of diarrhoea-associated haemolytic uraemic syndrome. British Association for Paediatric Nephrology. *Pediatr Nephrol* 1997;**11**(5):556-9.
164. Nolasco LH, Turner NA, Bernardo A, Tao Z, Cleary TG, Dong JF, Moake JL.
Hemolytic uremic syndrome-associated Shiga toxins promote endothelial-cell secretion and impair ADAMTS13 cleavage of unusually large von Willebrand factor multimers. *Blood* 2005;**106**(13):4199-209.
165. Desch K, Motto D. Is there a shared pathophysiology for thrombotic thrombocytopenic purpura and hemolytic-uremic syndrome? *J Am Soc Nephrol* 2007;**18**(9):2457-60.
166. Rivas M, Sosa-Estani S, Rangel J, Caletti MG, Valles P, Roldan CD, Balbi L, Marsano de Mollar MC, Amoedo D, Miliwebsky E, Chinen I, Hoekstra RM, Mead P, Griffin PM. Risk factors for sporadic Shiga toxin-producing *Escherichia coli* infections in children, Argentina. *Emerg Infect Dis* 2008;**14**(5):763-71.
167. Kaplan BS, Drummond KN. The hemolytic-uremic syndrome is a syndrome. *N Engl J Med* 1978;**298**(17):964-6.
168. Proulx F, Toledano B, Phan V, Clermont MJ, Mariscalco MM, Seidman EG.
Circulating granulocyte colony-stimulating factor, C-X-C, and C-C chemokines in children with *Escherichia coli* O157:H7 associated hemolytic uremic syndrome. *Pediatr Res* 2002;**52**(6):928-34.

169. Litalien C, Proulx F, Mariscalco MM, Robitaille P, Turgeon JP, Orrbine E, Rowe PC, McLaine PN, Seidman E. Circulating inflammatory cytokine levels in hemolytic uremic syndrome. *Pediatr Nephrol* 1999;**13**(9):840-5.
170. Kaplan BS, Meyers KE, Schulman SL. The pathogenesis and treatment of hemolytic uremic syndrome. *J Am Soc Nephrol* 1998;**9**(6):1126-33.
171. Gallo EG, Gianantonio CA. Extrarenal involvement in diarrhoea-associated haemolytic-uraemic syndrome. *Pediatr Nephrol* 1995;**9**(1):117-9.
172. Cavagnaro F, Gana JC, Lagomarsino E, Vogel A, Gederlini A. [Hemolytic uremic syndrome: the experience of a pediatric center]. *Rev Med Chil* 2005;**133**(7):781-7.
173. Siegler RL. Spectrum of extrarenal involvement in postdiarrheal hemolytic-uremic syndrome. *J Pediatr* 1994;**125**(4):511-8.
174. Starr M, Bennett-Wood V, Bigham AK, de Koning-Ward TF, Bordun AM, Lightfoot D, Bettelheim KA, Jones CL, Robins-Browne RM. Hemolytic-uremic syndrome following urinary tract infection with enterohemorrhagic *Escherichia coli*: case report and review. *Clin Infect Dis* 1998;**27**(2):310-5.
175. Wells JG, Davis BR, Wachsmuth IK, Riley LW, Remis RS, Sokolow R, Morris GK. Laboratory investigation of hemorrhagic colitis outbreaks associated with a rare *Escherichia coli* serotype. *J Clin Microbiol* 1983;**18**(3):512-20.
176. Vitacco M, Sanchez Avalos J, Gianantonio CA. Heparin therapy in the hemolytic-uremic syndrome. *J Pediatr* 1973;**83**(2):271-5.
177. Joishy M, Jauhari P, Mathew AA, Rangarajan T. Can we predict the development of haemolytic uraemic syndrome in the early stage of *Escherichia coli* O157 infection? *Arch Dis Child* 2008;**93**(2):180-1.

178. Fernandez GC, Gomez SA, Ramos MV, Bentancor LV, Fernandez-Brando RJ, Landoni VI, Lopez L, Ramirez F, Diaz M, Alduncin M, Grimoldi I, Exeni R, Isturiz MA, Palermo MS. The functional state of neutrophils correlates with the severity of renal dysfunction in children with hemolytic uremic syndrome. *Pediatr Res* 2007;**61**(1):123-8.
179. Walters MD, Matthei IU, Kay R, Dillon MJ, Barratt TM. The polymorphonuclear leucocyte count in childhood haemolytic uraemic syndrome. *Pediatr Nephrol* 1989;**3**(2):130-4.
180. Oakes RS, Siegler RL, McReynolds MA, Pysher T, Pavia AT. Predictors of fatality in postdiarrheal hemolytic uremic syndrome. *Pediatrics* 2006;**117**(5):1656-62.
181. Hunt BJ, Lammle B, Nevard CH, Haycock GB, Furlan M. von Willebrand factor-cleaving protease in childhood diarrhoea-associated haemolytic uraemic syndrome. *Thromb Haemost* 2001;**85**(6):975-8.
182. Sasseti B, Vizcarguenaga MI, Zanaro NL, Silva MV, Kordich L, Florentini L, Diaz M, Vitacco M, Sanchez Avalos JC. Hemolytic uremic syndrome in children: platelet aggregation and membrane glycoproteins. *J Pediatr Hematol Oncol* 1999;**21**(2):123-8.
183. Proesmans W. The role of coagulation and fibrinolysis in the pathogenesis of diarrhea-associated hemolytic uremic syndrome. *Semin Thromb Hemost* 2001;**27**(3):201-5.
184. Dhaliwal G, Cornett PA, Tierney LM, Jr. Hemolytic anemia. *Am Fam Physician* 2004;**69**(11):2599-606.

185. Monnens L, van Aken W, de Jong M. "Active" intravascular coagulation in the epidemic form of hemolytic-uremic syndrome. *Clin Nephrol* 1982;**17**(6):284-7.
186. Kaplan BS, Katz J, Krawitz S, Lurie A. An analysis of the results of therapy in 67 cases of the hemolytic-uremic syndrome. *J Pediatr* 1971;**78**(3):420-5.
187. Keepers TR, Psocka MA, Gross LK, Obrig TG. A Murine Model of HUS: Shiga Toxin with Lipopolysaccharide Mimics the Renal Damage and Physiologic Response of Human Disease. *J Am Soc Nephrol* 2006;**17**(12):3404-14.
188. Keepers TR, Gross LK, Obrig TG. Monocyte chemoattractant protein 1, macrophage inflammatory protein 1 alpha, and RANTES recruit macrophages to the kidney in a mouse model of hemolytic-uremic syndrome. *Infect Immun* 2007;**75**(3):1229-36.
189. Murata A, Shimazu T, Yamamoto T, Taenaka N, Nagayama K, Honda T, Sugimoto H, Monden M, Matsuura N, Okada S. Profiles of circulating inflammatory- and anti-inflammatory cytokines in patients with hemolytic uremic syndrome due to *E. coli* O157 infection. *Cytokine* 1998;**10**(7):544-8.
190. Corrigan JJ, Jr., Boineau FG. Hemolytic-uremic syndrome. *Pediatr Rev* 2001;**22**(11):365-9.
191. Proulx F, Litalien C, Turgeon JP, Mariscalco MM, Seidman E. Circulating levels of transforming growth factor-beta1 and lymphokines among children with hemolytic uremic syndrome. *Am J Kidney Dis* 2000;**35**(1):29-34.
192. Aihara Y, Nakamura T, Unayama T, Yoshida Y, Yokota S. Usefulness of serum fibrinogen degradation product-E in sporadic cases of classical hemolytic uremic syndrome. *Pediatr Int* 2000;**42**(5):523-7.

193. Vitsky BH, Suzuki Y, Strauss L, Churg J. The hemolytic-uremic syndrome: a study of renal pathologic alterations. *Am J Pathol* 1969;**57**(3):627-47.
194. Richardson SE, Karmali MA, Becker LE, Smith CR. The histopathology of the hemolytic uremic syndrome associated with verocytotoxin-producing *Escherichia coli* infections. *Hum Pathol* 1988;**19**(9):1102-8.
195. Karpman D, Hakansson A, Perez MT, Isaksson C, Carlemalm E, Caprioli A, Svanborg C. Apoptosis of renal cortical cells in the hemolytic-uremic syndrome: in vivo and in vitro studies. *Infect Immun* 1998;**66**(2):636-44.
196. Tsai HM, Chandler WL, Sarode R, Hoffman R, Jelacic S, Habeeb RL, Watkins SL, Wong CS, Williams GD, Tarr PI. von Willebrand factor and von Willebrand factor-cleaving metalloprotease activity in *Escherichia coli* O157:H7-associated hemolytic uremic syndrome. *Pediatr Res* 2001;**49**(5):653-9.
197. Karpman D, Andreasson A, Thysell H, Kaplan BS, Svanborg C. Cytokines in childhood hemolytic uremic syndrome and thrombotic thrombocytopenic purpura. *Pediatr Nephrol* 1995;**9**(6):694-9.
198. Nesmith JD, Ellis E. Childhood hemolytic uremic syndrome is associated with adolescent-onset diabetes mellitus. *Pediatr Nephrol* 2007;**22**(2):294-7.
199. Appiani AC, Edefonti A, Bettinelli A, Cossu MM, Paracchini ML, Rossi E. The relationship between plasma levels of the factor VIII complex and platelet release products (beta-thromboglobulin and platelet factor 4) in children with the hemolytic-uremic syndrome. *Clin Nephrol* 1982;**17**(4):195-9.
200. van Setten PA, van Hinsbergh VW, van den Heuvel LP, Preyers F, Dijkman HB, Assmann KJ, van der Velden TJ, Monnens LA. Monocyte chemoattractant

- protein-1 and interleukin-8 levels in urine and serum of patents with hemolytic uremic syndrome. *Pediatr Res* 1998;**43**(6):759-67.
201. Upadhyaya K, Barwick K, Fishaut M, Kashgarian M, Siegel NJ. The importance of nonrenal involvement in hemolytic-uremic syndrome. *Pediatrics* 1980;**65**(1):115-20.
202. Piastra M, Ruggiero A, Langer A, Caresta E, Chiaretti A, Pulitano S, Polidori G, Riccardi R. Pulmonary hemorrhage complicating a typical hemolytic-uremic syndrome. *Respiration* 2004;**71**(5):537-41.
203. Thayu M, Chandler WL, Jelacic S, Gordon CA, Rosenthal GL, Tarr PI. Cardiac ischemia during hemolytic uremic syndrome. *Pediatr Nephrol* 2003;**18**(3):286-9.
204. Suri RS, Clark WF, Barrowman N, Mahon JL, Thiessen-Philbrook HR, Rosas-Arellano MP, Zarnke K, Garland JS, Garg AX. Diabetes during diarrhea-associated hemolytic uremic syndrome: a systematic review and meta-analysis. *Diabetes Care* 2005;**28**(10):2556-62.
205. Casteels K, Van Damme-Lombaerts R. Recurrence of diabetes after diarrhea-associated hemolytic uremic syndrome. *Diabetes Care* 2006;**29**(4):947-8.
206. Fitzpatrick MM, Shah V, Trompeter RS, Dillon MJ, Barratt TM. Long term renal outcome of childhood haemolytic uraemic syndrome. *Bmj* 1991;**303**(6801):489-92.
207. Eriksson KJ, Boyd SG, Tasker RC. Acute neurology and neurophysiology of haemolytic-uraemic syndrome. *Arch Dis Child* 2001;**84**(5):434-5.
208. Kelles A, Van Dyck M, Proesmans W. Childhood haemolytic uraemic syndrome: long-term outcome and prognostic features. *Eur J Pediatr* 1994;**153**(1):38-42.

209. Yasuhara A, Araki A, Ochi A, Kobayashi Y. Magnetic resonance imaging of brain lesions of a patient with hemolytic uremic syndrome following *Escherichia coli* O157 infection. *Pediatr Int* 2000;**42**(3):302-5.
210. Havens PL, O'Rourke PP, Hahn J, Higgins J, Walker AM. Laboratory and clinical variables to predict outcome in hemolytic-uremic syndrome. *Am J Dis Child* 1988;**142**(9):961-4.
211. Caletti MG, Lejarraga H, Kelmansky D, Missoni M. Two different therapeutic regimes in patients with sequelae of hemolytic-uremic syndrome. *Pediatr Nephrol* 2004;**19**(10):1148-52.
212. Bassani CE, Ferraris J, Gianantonio CA, Ruiz S, Ramirez J. Renal transplantation in patients with classical haemolytic-uraemic syndrome. *Pediatr Nephrol* 1991;**5**(5):607-11.
213. Garg AX, Salvadori M, Okell JM, Thiessen-Philbrook HR, Suri RS, Filler G, Moist L, Matsell D, Clark WF. Albuminuria and estimated GFR 5 years after *Escherichia coli* O157 hemolytic uremic syndrome: an update. *Am J Kidney Dis* 2008;**51**(3):435-44.
214. Siegler RL, Pavia AT, Cook JB. Hemolytic-uremic syndrome in adolescents. *Arch Pediatr Adolesc Med* 1997;**151**(2):165-9.
215. Cobenas CJ, Alconcher LF, Spizzirri AP, Rahman RC. Long-term follow-up of Argentinean patients with hemolytic uremic syndrome who had not undergone dialysis. *Pediatr Nephrol* 2007;**22**(9):1343-7.
216. Garg AX, Suri RS, Barrowman N, Rehman F, Matsell D, Rosas-Arellano MP, Salvadori M, Haynes RB, Clark WF. Long-term renal prognosis of diarrhea-

- associated hemolytic uremic syndrome: a systematic review, meta-analysis, and meta-regression. *Jama* 2003;**290**(10):1360-70.
217. Huseman D, Gellermann J, Vollmer I, Ohde I, Devaux S, Ehrich JH, Filler G. Long-term prognosis of hemolytic uremic syndrome and effective renal plasma flow. *Pediatr Nephrol* 1999;**13**(8):672-7.
218. Ogborn MR, Hamiwka L, Orrbine E, Newburg DS, Sharma A, McLaine PN, Orr P, Rowe P. Renal function in Inuit survivors of epidemic hemolytic-uremic syndrome. *Pediatr Nephrol* 1998;**12**(6):485-8.
219. Dieguez S, Ayuso S, Brindo M, Osinde E, Canepa C. Renal functional reserve evolution in children with a previous episode of hemolytic uremic syndrome. *Nephron Clin Pract* 2004;**97**(3):c118-22.
220. Oakes RS, Kirkham JK, Nelson RD, Siegler RL. Duration of oliguria and anuria as predictors of chronic renal-related sequelae in post-diarrheal hemolytic uremic syndrome. *Pediatr Nephrol* 2008.
221. Garg AX, Clark WF, Salvadori M, Thiessen-Philbrook HR, Matsell D. Absence of renal sequelae after childhood Escherichia coli O157:H7 gastroenteritis. *Kidney Int* 2006;**70**(4):807-12.
222. Moghal NE, Ferreira MA, Howie AJ, Milford DV, Raafat E, Taylor CM. The late histologic findings in diarrhea-associated hemolytic uremic syndrome. *J Pediatr* 1998;**133**(2):220-3.
223. de Jong M, Monnens L. Haemolytic-uraemic syndrome: a 10-year follow-up study of 73 patients. *Nephrol Dial Transplant* 1988;**3**(4):379-82.

224. Perelstein EM, Grunfield BG, Simsolo RB, Gimenez MI, Gianantonio CA.
Renal functional reserve compared in haemolytic uraemic syndrome and single kidney. *Arch Dis Child* 1990;**65**(7):728-31.
225. Burns JC, Berman ER, Fagre JL, Shikes RH, Lum GM. Pancreatic islet cell necrosis: association with hemolytic-uremic syndrome. *J Pediatr* 1982;**100**(4):582-4.
226. Sagripanti A, Carpi A. Antithrombotic and prothrombotic activities of the vascular endothelium. *Biomed Pharmacother* 2000;**54**(2):107-11.
227. Tesfamariam B, DeFelice AF. Endothelial injury in the initiation and progression of vascular disorders. *Vascul Pharmacol* 2007;**46**(4):229-37.
228. Pries AR, Secomb TW, Gaehtgens P. The endothelial surface layer. *Pflugers Arch* 2000;**440**(5):653-66.
229. Boos CJ, Goon PK, Lip GY. The endothelium, inflammation, and coagulation in sepsis. *Clin Pharmacol Ther* 2006;**79**(1):20-2.
230. Ballermann BJ. Endothelial cell activation. *Kidney Int* 1998;**53**(6):1810-26.
231. Yamamoto T, Nagayama K, Satomura K, Honda T, Okada S. Increased serum IL-10 and endothelin levels in hemolytic uremic syndrome caused by *Escherichia coli* O157. *Nephron* 2000;**84**(4):326-32.
232. Hastings NE, Simmers MB, McDonald OG, Wamhoff BR, Blackman BR.
Atherosclerosis-prone hemodynamics differentially regulates endothelial and smooth muscle cell phenotypes and promotes pro-inflammatory priming. *Am J Physiol Cell Physiol* 2007;**293**(6):C1824-33.

233. Nevard CH, Blann AD, Jurd KM, Haycock GB, Hunt BJ. Markers of endothelial cell activation and injury in childhood haemolytic uraemic syndrome. *Pediatr Nephrol* 1999;**13**(6):487-92.
234. Ergonul Z, Clayton F, Fogo AB, Kohan DE. Shigatoxin-1 binding and receptor expression in human kidneys do not change with age. *Pediatr Nephrol* 2003;**18**(3):246-53.
235. Tazzari PL, Ricci F, Carnicelli D, Caprioli A, Tozzi AE, Rizzoni G, Conte R, Brigotti M. Flow cytometry detection of Shiga toxins in the blood from children with hemolytic uremic syndrome. *Cytometry* 2004;**61B**(1):40-4.
236. Brigotti M, Caprioli A, Tozzi AE, Tazzari PL, Ricci F, Conte R, Carnicelli D, Procaccino MA, Minelli F, Ferretti AV, Paglialonga F, Edefonti A, Rizzoni G. Shiga toxins present in the gut and in the polymorphonuclear leukocytes circulating in the blood of children with hemolytic-uremic syndrome. *J Clin Microbiol* 2006;**44**(2):313-7.
237. Te Loo DM, van Hinsbergh VW, van den Heuvel LP, Monnens LA. Detection of verocytotoxin bound to circulating polymorphonuclear leukocytes of patients with hemolytic uremic syndrome. *J Am Soc Nephrol* 2001;**12**(4):800-6.
238. Griener TP, Mulvey GL, Marcato P, Armstrong GD. Differential binding of Shiga toxin 2 to human and murine neutrophils. *J Med Microbiol* 2007;**56**(Pt 11):1423-30.
239. Uchida H, Kiyokawa N, Horie H, Fujimoto J, Takeda T. The detection of Shiga toxins in the kidney of a patient with hemolytic uremic syndrome. *Pediatr Res* 1999;**45**(1):133-7.

240. Kaplan BS, Koornhof HJ. Haemolytic-uraemic syndrome: failure to demonstrate circulating endotoxin. *Lancet* 1969;**2**(7635):1424-5.
241. Vilcek J. The Cytokines: an Overview. In: Thomson AW, Lotze MT, eds. The Cytokine Handbook. San Diego: Academic Press, 2003: 3-18.
242. Charo IF, Ransohoff RM. The many roles of chemokines and chemokine receptors in inflammation. *N Engl J Med* 2006;**354**(6):610-21.
243. Ramos MV, Fernandez GC, Patey N, Schierloh P, Exeni R, Grimoldi I, Vallejo G, Elias-Costa C, Del Carmen Sasiain M, Trachtman H, Combadiere C, Proulx F, Palermo MS. Involvement of the fractalkine pathway in the pathogenesis of childhood hemolytic uremic syndrome. *Blood* 2007;**109**(6):2438-45.
244. Coad NA, Marshall T, Rowe B, Taylor CM. Changes in the postenteropathic form of the hemolytic uremic syndrome in children. *Clin Nephrol* 1991;**35**(1):10-6.
245. Buteau C, Proulx F, Chaibou M, Raymond D, Clermont MJ, Mariscalco MM, Lebel MH, Seidman E. Leukocytosis in children with Escherichia coli O157:H7 enteritis developing the hemolytic-uremic syndrome. *Pediatr Infect Dis J* 2000;**19**(7):642-7.
246. Forsyth KD, Simpson AC, Fitzpatrick MM, Barratt TM, Levinsky RJ. Neutrophil-mediated endothelial injury in haemolytic uraemic syndrome. *Lancet* 1989;**2**(8660):411-4.
247. van de Kar NC, Sauerwein RW, Demacker PN, Grau GE, van Hinsbergh VW, Monnens LA. Plasma cytokine levels in hemolytic uremic syndrome. *Nephron* 1995;**71**(3):309-13.

248. Proulx F, Turgeon JP, Litalien C, Mariscalco MM, Robitaille P, Seidman E. Inflammatory mediators in Escherichia coli O157:H7 hemorrhagic colitis and hemolytic-uremic syndrome. *Pediatr Infect Dis J* 1998;**17**(10):899-904.
249. Inward CD, Varagunam M, Adu D, Milford DV, Taylor CM. Cytokines in haemolytic uraemic syndrome associated with verocytotoxin-producing Escherichia coli infection. *Arch Dis Child* 1997;**77**(2):145-7.
250. Masri C, Proulx F, Toledano B, Clermont MJ, Mariscalco MM, Seidman EG, Carcillo J. Soluble Fas and soluble Fas-ligand in children with Escherichia coli O157:H7-associated hemolytic uremic syndrome. *Am J Kidney Dis* 2000;**36**(4):687-94.
251. Westerholt S, Hartung T, Tollens M, Gustrau A, Oberhoffer M, Karch H, Klare B, Pfeffer K, Emmrich P, Oberhoffer R. Inflammatory and immunological parameters in children with haemolytic uremic syndrome (HUS) and gastroenteritis-pathophysiological and diagnostic clues. *Cytokine* 2000;**12**(6):822-7.
252. Shiraishi M, Ichiyama T, Matsushige T, Iwaki T, Iyoda K, Fukuda K, Makata H, Matsubara T, Furukawa S. Soluble tumor necrosis factor receptor 1 and tissue inhibitor of metalloproteinase-1 in hemolytic uremic syndrome with encephalopathy. *J Neuroimmunol* 2008.
253. Lopez EL, Contrini MM, Devoto S, de Rosa MF, Grana MG, Genero MH, Canepa C, Gomez HF, Cleary TG. Tumor necrosis factor concentrations in hemolytic uremic syndrome patients and children with bloody diarrhea in Argentina. *Pediatr Infect Dis J* 1995;**14**(7):594-8.

254. Wada H, Saitoh M, Tamaki S, Masuya M, Morita K, Tabata M, Tanigawa M, Kageyama S, Tsuzi K, Ohta C, et al. [Clinical analysis on thrombotic thrombocytopenic purpura and hemolytic uremic syndrome, with plasma level of cytokine]. *Rinsho Ketsueki* 1990;**31**(9):1537-43.
255. Maroeska Te Loo D, Bosma N, Van Hinsbergh V, Span P, De Waal R, Clarijs R, Sweep C, Monnens L, Van Den Heuvel L. Elevated levels of vascular endothelial growth factor in serum of patients with D+ HUS. *Pediatr Nephrol* 2004;**19**(7):754-60.
256. Inward CD, Pall AA, Adu D, Milford DV, Taylor CM. Soluble circulating cell adhesion molecules in haemolytic uraemic syndrome. *Pediatr Nephrol* 1995;**9**(5):574-8.
257. Simmons EM, Himmelfarb J, Sezer MT, Chertow GM, Mehta RL, Paganini EP, Soroko S, Freedman S, Becker K, Spratt D, Shyr Y, Ikizler TA. Plasma cytokine levels predict mortality in patients with acute renal failure. *Kidney Int* 2004;**65**(4):1357-65.
258. van der Poll T, Barber AE, Coyle SM, Lowry SF. Hypercortisolemia increases plasma interleukin-10 concentrations during human endotoxemia--a clinical research center study. *J Clin Endocrinol Metab* 1996;**81**(10):3604-6.
259. Lever A, Mackenzie I. Sepsis: definition, epidemiology, and diagnosis. *Bmj* 2007;**335**(7625):879-83.
260. Bozza FA, Salluh JI, Japiassu AM, Soares M, Assis EF, Gomes RN, Bozza MT, Castro-Faria-Neto HC, Bozza PT. Cytokine profiles as markers of disease severity in sepsis: a multiplex analysis. *Crit Care* 2007;**11**(2):R49.

261. Schnyder-Candrian S, Walz A. Neutrophil-activating protein ENA-78 and IL-8 exhibit different patterns of expression in lipopolysaccharide- and cytokine-stimulated human monocytes. *J Immunol* 1997;**158**(8):3888-94.
262. Kuhns DB, Alvord WG, Gallin JI. Increased circulating cytokines, cytokine antagonists, and E-selectin after intravenous administration of endotoxin in humans. *J Infect Dis* 1995;**171**(1):145-52.
263. Miyamoto Y, Iimura M, Kaper JB, Torres AG, Kagnoff MF. Role of Shiga toxin versus H7 flagellin in enterohaemorrhagic Escherichia coli signalling of human colon epithelium in vivo. *Cell Microbiol* 2006;**8**(5):869-79.
264. Kim DC, Reitz B, Carmichael DF, Bloedow DC. Kidney as a major clearance organ for recombinant human interleukin-1 receptor antagonist. *J Pharm Sci* 1995;**84**(5):575-80.
265. Chiu PJ, Radwanski E, Tetiloff G, Monge A, Swanson SJ. Interleukin-10 pharmacokinetics in intact and nephrectomized mice. *Eur Cytokine Netw* 1996;**7**(1):67-9.
266. Gruskin AB. Mediators, markers, and modulators in the hemolytic uremic syndrome. *Am J Kidney Dis* 2000;**36**(4):859-62.
267. Stone MK, Kolling GL, Lindner MH, Obrig TG. p38 mitogen-activated protein kinase mediates lipopolysaccharide and tumor necrosis factor alpha induction of shiga toxin 2 sensitivity in human umbilical vein endothelial cells. *Infect Immun* 2008;**76**(3):1115-21.

268. Hughes AK, Ergonul Z, Stricklett PK, Kohan DE. Molecular basis for high renal cell sensitivity to the cytotoxic effects of shigatoxin-1: upregulation of globotriaosylceramide expression. *J Am Soc Nephrol* 2002;**13**(9):2239-45.
269. Stricklett PK, Hughes AK, Kohan DE. Inhibition of p38 Mitogen-Activated Protein Kinase Ameliorates Cytokine Up-Regulated Shigatoxin-1 Toxicity in Human Brain Microvascular Endothelial Cells. *J Infect Dis* 2005;**191**(3):461-71.
270. Thorpe CM, Hurley BP, Acheson DW. Shiga toxin interactions with the intestinal epithelium. *Methods Mol Med* 2003;**73**:263-73.
271. van de Kar NC, Monnens LA, Karmali MA, van Hinsbergh VW. Tumor necrosis factor and interleukin-1 induce expression of the verocytotoxin receptor globotriaosylceramide on human endothelial cells: implications for the pathogenesis of the hemolytic uremic syndrome. *Blood* 1992;**80**(11):2755-64.
272. Van de Kar NC, Monnens LA, Van Hinsbergh VW. Tumor necrosis factor and interleukin 1 induce expression of the glycolipid verotoxin receptor in human endothelial cells. Implications for the pathogenesis of the haemolytic uraemic syndrome. *Behring Inst Mitt* 1993(92):202-9.
273. van de Kar NC, Kooistra T, Vermeer M, Lesslauer W, Monnens LA, van Hinsbergh VW. Tumor necrosis factor alpha induces endothelial galactosyl transferase activity and verocytotoxin receptors. Role of specific tumor necrosis factor receptors and protein kinase C. *Blood* 1995;**85**(3):734-43.
274. Kaye SA, Louise CB, Boyd B, Lingwood CA, Obrig TG. Shiga toxin-associated hemolytic uremic syndrome: interleukin-1 beta enhancement of Shiga toxin

- cytotoxicity toward human vascular endothelial cells in vitro. *Infect Immun* 1993;**61**(9):3886-91.
275. Louise CB, Obrig TG. Shiga toxin-associated hemolytic-uremic syndrome: combined cytotoxic effects of Shiga toxin, interleukin-1 beta, and tumor necrosis factor alpha on human vascular endothelial cells in vitro. *Infect Immun* 1991;**59**(11):4173-9.
276. Louise CB, Obrig TG. Shiga toxin-associated hemolytic uremic syndrome: combined cytotoxic effects of shiga toxin and lipopolysaccharide (endotoxin) on human vascular endothelial cells in vitro. *Infect Immun* 1992;**60**(4):1536-43.
277. Louise CB, Obrig TG. Human renal microvascular endothelial cells as a potential target in the development of the hemolytic uremic syndrome as related to fibrinolysis factor expression, in vitro. *Microvasc Res* 1994;**47**(3):377-87.
278. Louise CB, Kaye SA, Boyd B, Lingwood CA, Obrig TG. Shiga toxin-associated hemolytic uremic syndrome: effect of sodium butyrate on sensitivity of human umbilical vein endothelial cells to Shiga toxin. *Infect Immun* 1995;**63**(7):2766-9.
279. Louise CB, Tran MC, Obrig TG. Sensitization of human umbilical vein endothelial cells to Shiga toxin: involvement of protein kinase C and NF-kappaB. *Infect Immun* 1997;**65**(8):3337-44.
280. van Setten PA, van Hinsbergh VW, van der Velden TJ, van de Kar NC, Vermeer M, Mahan JD, Assmann KJ, van den Heuvel LP, Monnens LA. Effects of TNF alpha on verocytotoxin cytotoxicity in purified human glomerular microvascular endothelial cells. *Kidney Int* 1997;**51**(4):1245-56.

281. Nash MC, Wade AM, Shah V, Dillon MJ. Normal levels of soluble E-selectin, soluble intercellular adhesion molecule-1 (sICAM-1), and soluble vascular cell adhesion molecule-1 (sVCAM-1) decrease with age. *Clin Exp Immunol* 1996;**103**(1):167-70.
282. Liu J, Akahoshi T, Sasahana T, Kitasato H, Namai R, Sasaki T, Inoue M, Kondo H. Inhibition of neutrophil apoptosis by verotoxin 2 derived from Escherichia coli O157:H7. *Infect Immun* 1999;**67**(11):6203-5.
283. Liu J, He T, He Y, Zhang Z, Akahoshi T, Kondo H, Zhong S. Prolongation of functional life-span of neutrophils by recombinant verotoxin 2. *Chin Med J (Engl)* 2002;**115**(6):900-3.
284. Morigi M, Micheletti G, Figliuzzi M, Imberti B, Karmali MA, Remuzzi A, Remuzzi G, Zoja C. Verotoxin-1 promotes leukocyte adhesion to cultured endothelial cells under physiologic flow conditions. *Blood* 1995;**86**(12):4553-8.
285. Walport MJ. Complement. First of two parts. *N Engl J Med* 2001;**344**(14):1058-66.
286. Caprioli J, Castelletti F, Bucchioni S, Bettinaglio P, Bresin E, Pianetti G, Gamba S, Brioschi S, Daina E, Remuzzi G, Noris M. Complement factor H mutations and gene polymorphisms in haemolytic uraemic syndrome: the C-257T, the A2089G and the G2881T polymorphisms are strongly associated with the disease. *Hum Mol Genet* 2003;**12**(24):3385-95.
287. Manuelian T, Hellwage J, Meri S, Caprioli J, Noris M, Heinen S, Jozsi M, Neumann HP, Remuzzi G, Zipfel PF. Mutations in factor H reduce binding affinity to C3b and heparin and surface attachment to endothelial cells in hemolytic uremic syndrome. *J Clin Invest* 2003;**111**(8):1181-90.

288. Noris M, Brioschi S, Caprioli J, Todeschini M, Bresin E, Porrati F, Gamba S, Remuzzi G. Familial haemolytic uraemic syndrome and an MCP mutation. *Lancet* 2003;**362**(9395):1542-7.
289. Noris M, Remuzzi G. Familial and recurrent forms of hemolytic uremic syndrome/thrombotic thrombocytopenic purpura. *Contrib Nephrol* 2001(136):125-39.
290. Zipfel PF, Skerka C, Caprioli J, Manuelian T, Neumann HH, Noris M, Remuzzi G. Complement factor H and hemolytic uremic syndrome. *Int Immunopharmacol* 2001;**1**(3):461-8.
291. Zipfel PF, Skerka C, Hellwage J, Jokiranta ST, Meri S, Brade V, Kraiczy P, Noris M, Remuzzi G. Factor H family proteins: on complement, microbes and human diseases. *Biochem Soc Trans* 2002;**30**(Pt 6):971-8.
292. Kaplan BS, Thomson PD, MacNab GM. Letter: Serum-complement levels in haemolytic-uraemic syndrome. *Lancet* 1973;**2**(7844):1505-6.
293. Robson WL, Leung AK, Fick GH, McKenna AI. Hypocomplementemia and leukocytosis in diarrhea-associated hemolytic uremic syndrome. *Nephron* 1992;**62**(3):296-9.
294. Stassen JM, Arnout J, Deckmyn H. The hemostatic system. *Curr Med Chem* 2004;**11**(17):2245-60.
295. Monroe DM, Hoffman M. What does it take to make the perfect clot? *Arterioscler Thromb Vasc Biol* 2006;**26**(1):41-8.

296. Pysher TJ, Siegler RL, Tesh VL, Taylor FB, Jr. von Willebrand Factor expression in a Shiga toxin-mediated primate model of hemolytic uremic syndrome. *Pediatr Dev Pathol* 2002;**5**(5):472-9.
297. Weisel JW. Fibrinogen and fibrin. *Adv Protein Chem* 2005;**70**:247-99.
298. Gear AR, Camerini D. Platelet chemokines and chemokine receptors: linking hemostasis, inflammation, and host defense. *Microcirculation* 2003;**10**(3-4):335-50.
299. Maly MA, Tomasov P, Hajek P, Blasko P, Hrachovinova I, Salaj P, Veselka J. The role of tissue factor in thrombosis and hemostasis. *Physiol Res* 2007;**56**(6):685-95.
300. Mosesson MW. Fibrinogen and fibrin structure and functions. *J Thromb Haemost* 2005;**3**(8):1894-904.
301. Van Geet C, Proesmans W, Arnout J, Vermeylen J, Declerck PJ. Activation of both coagulation and fibrinolysis in childhood hemolytic uremic syndrome. *Kidney Int* 1998;**54**(4):1324-30.
302. Lippi G, Franchini M, Montagnana M, Guidi GC. Coagulation testing in pediatric patients: the young are not just miniature adults. *Semin Thromb Hemost* 2007;**33**(8):816-20.
303. Toh CH, Downey C. Back to the future: testing in disseminated intravascular coagulation. *Blood Coagul Fibrinolysis* 2005;**16**(8):535-42.
304. Brozna JP. Shwartzman reaction. *Semin Thromb Hemost* 1990;**16**(4):326-32.
305. Cotran RS, Pober JS. Cytokine-endothelial interactions in inflammation, immunity, and vascular injury. *J Am Soc Nephrol* 1990;**1**(3):225-35.

306. Avalos JS, Vitacco M, Molinas F, Penalver J, Gianantonio C. Coagulation studies in the hemolytic-uremic syndrome. *J Pediatr* 1970;**76**(4):538-48.
307. Fong JS, King-Hrycaj BD. Impaired and exhausted platelets in modified generalized Shwartzman reaction: an analogue of hemolytic uremic syndrome associated with endotoxemia. *J Lab Clin Med* 1983;**102**(6):847-57.
308. Slofstra SH, ten Cate H, Spek CA. Low dose endotoxin priming is accountable for coagulation abnormalities and organ damage observed in the Shwartzman reaction. A comparison between a single-dose endotoxemia model and a double-hit endotoxin-induced Shwartzman reaction. *Thromb J* 2006;**4**:13.
309. Remick DG. Pathophysiology of sepsis. *Am J Pathol* 2007;**170**(5):1435-44.
310. Cosio FG, Eddy A, Mentser MI, Bergstein JM. Decreased plasma fibronectin levels in children with hemolytic-uremic syndrome. *Am J Med* 1985;**78**(4):549-54.
311. Katz J, Lurie A, Kaplan BS, Krawitz S, Metz J. Coagulation findings in the hemolytic-uremic syndrome of infancy: similarity to hyperacute renal allograft rejection. *J Pediatr* 1971;**78**(3):426-34.
312. Grabowski EF. The hemolytic-uremic syndrome--toxin, thrombin, and thrombosis. *N Engl J Med* 2002;**346**(1):58-61.
313. Kaplan BS, Fong JS. Reduced platelet aggregation in hemolytic-uremic syndrome. *Thromb Haemost* 1980;**43**(2):154-7.
314. Fong JS, Kaplan BS. Impairment of platelet aggregation in hemolytic uremic syndrome: evidence for platelet "exhaustion". *Blood* 1982;**60**(3):564-70.
315. Bolande RP, Kaplan BS. Experimental studies on the hemolytic-uremic syndrome. *Nephron* 1985;**39**(3):228-36.

316. Katayama M, Handa M, Araki Y, Ambo H, Kawai Y, Watanabe K, Ikeda Y. Soluble P-selectin is present in normal circulation and its plasma level is elevated in patients with thrombotic thrombocytopenic purpura and haemolytic uraemic syndrome. *Br J Haematol* 1993;**84**(4):702-10.
317. Galli M, Grassi A, Barbui T. Platelet-derived microvesicles in thrombotic thrombocytopenic purpura and hemolytic uremic syndrome. *Thromb Haemost* 1996;**75**(3):427-31.
318. Walters MD, Levin M, Smith C, Nokes TJ, Hardisty RM, Dillon MJ, Barratt TM. Intravascular platelet activation in the hemolytic uremic syndrome. *Kidney Int* 1988;**33**(1):107-15.
319. Smith JM, Jones F, Ciol MA, Jelacic S, Boster DR, Watkins SL, Williams GD, Tarr PI, Henderson WR, Jr. Platelet-activating factor and Escherichia coli O157:H7 infections. *Pediatr Nephrol* 2002;**17**(12):1047-52.
320. Benigni A, Boccardo P, Noris M, Remuzzi G, Siegler RL. Urinary excretion of platelet-activating factor in haemolytic uraemic syndrome. *Lancet* 1992;**339**(8797):835-6.
321. Karpman D, Papadopoulou D, Nilsson K, Sjogren AC, Mikaelsson C, Lethagen S. Platelet activation by Shiga toxin and circulatory factors as a pathogenetic mechanism in the hemolytic uremic syndrome. *Blood* 2001;**97**(10):3100-8.
322. Cooling LL, Walker KE, Gille T, Koerner TA. Shiga toxin binds human platelets via globotriaosylceramide (Pk antigen) and a novel platelet glycosphingolipid. *Infect Immun* 1998;**66**(9):4355-66.

323. Thorpe CM, Flaumenhaft R, Hurley B, Jacewicz M, Acheson DW, Keusch GT. Shiga toxins do not directly stimulate alpha-granule secretion or enhance aggregation of human platelets. *Acta Haematol* 1999;**102**(1):51-5.
324. Viisoreanu D, Polanowska-Grabowska R, Suttitanamongkol S, Obrig TG, Gear AR. Human platelet aggregation is not altered by Shiga toxins 1 or 2. *Thromb Res* 2000;**98**(5):403-10.
325. Ghosh SA, Polanowska-Grabowska RK, Fujii J, Obrig T, Gear AR. Shiga toxin binds to activated platelets. *J Thromb Haemost* 2004;**2**(3):499-506.
326. Yoshimura K, Fujii J, Yutsudo T, Kikuchi R, Soejima T, Shirahata S, Yoshida S. No direct effects of Shiga toxin 1 and 2 on the aggregation of human platelets in vitro. *Thromb Haemost* 1998;**80**(3):529-30.
327. Leytin V, Shakoor S, Mody M, Allen D, Garvey B, Freedman J. Sepsis- and endotoxemia-generated cytokines do not trigger activation of human platelets. *Crit Care Med* 2002;**30**(12):2771-3.
328. Guessous F, Marcinkiewicz M, Polanowska-Grabowska R, Keepers TR, Obrig T, Gear AR. Shiga toxin 2 and lipopolysaccharide cause monocytic THP-1 cells to release factors which activate platelet function. *Thromb Haemost* 2005;**94**(5):1019-27.
329. Guessous F, Marcinkiewicz M, Polanowska-Grabowska R, Kongkhum S, Heatherly D, Obrig T, Gear AR. Shiga toxin 2 and lipopolysaccharide induce human microvascular endothelial cells to release chemokines and factors that stimulate platelet function. *Infect Immun* 2005;**73**(12):8306-16.

330. Chandler WL, Jelacic S, Boster DR, Ciol MA, Williams GD, Watkins SL, Igarashi T, Tarr PI. Prothrombotic coagulation abnormalities preceding the hemolytic-uremic syndrome. *N Engl J Med* 2002;**346**(1):23-32.
331. Kisker CT, Rush RA. Absence of intravascular coagulation in the hemolytic-uremic syndrome. *Am J Dis Child* 1975;**129**(2):223-6.
332. Hotchkiss RS, Nicholson DW. Apoptosis and caspases regulate death and inflammation in sepsis. *Nat Rev Immunol* 2006;**6**(11):813-22.
333. Sutor AH, Thomas KB, Prufer FH, Grohmann A, Brandis M, Zimmerhackl LB. Function of von Willebrand factor in children with diarrhea-associated hemolytic-uremic syndrome (D+ HUS). *Semin Thromb Hemost* 2001;**27**(3):287-92.
334. Moake JL, Byrnes JJ, Troll JH, Rudy CK, Weinstein MJ, Colannino NM, Hong SL. Abnormal VIII: von Willebrand factor patterns in the plasma of patients with the hemolytic-uremic syndrome. *Blood* 1984;**64**(3):592-8.
335. Proesmans W, Geet CV. Fibrinolysis in the hemolytic uremic syndrome. *Pediatr Nephrol* 2002;**17**(10):871-2; author reply 873-4.
336. Shibata T, Magari Y, Mizunaga S, Ishii T, Tomo T, Yasumori R, Nasu M, Taguchi T. Urinary fibrin/fibrinogen degradation product E (FDP-E) measured by a highly sensitive ELISA method in renal diseases. *Nephron* 1998;**79**(4):494-5.
337. Rose PE, Armour JA, Williams CE, Hill FG. Verotoxin and neuraminidase induced platelet aggregating activity in plasma: their possible role in the pathogenesis of the haemolytic uraemic syndrome. *J Clin Pathol* 1985;**38**(4):438-41.
338. Camerer E, Kolsto AB, Prydz H. Cell biology of tissue factor, the principal initiator of blood coagulation. *Thromb Res* 1996;**81**(1):1-41.

339. Medcalf RL. Fibrinolysis, inflammation, and regulation of the plasminogen activating system. *J Thromb Haemost* 2007;**5 Suppl 1**:132-42.
340. Obrig TG, Louise CB, Lingwood CA, Boyd B, Barley-Maloney L, Daniel TO. Endothelial heterogeneity in Shiga toxin receptors and responses. *J Biol Chem* 1993;**268**(21):15484-8.
341. Taguchi T, Uchida H, Kiyokawa N, Mori T, Sato N, Horie H, Takeda T, Fujimoto J. Verotoxins induce apoptosis in human renal tubular epithelium derived cells. *Kidney Int* 1998;**53**(6):1681-8.
342. Hughes AK, Stricklett PK, Kohan DE. Cytotoxic effect of Shiga toxin-1 on human proximal tubule cells. *Kidney Int* 1998;**54**(2):426-37.
343. Hughes AK, Stricklett PK, Schmid D, Kohan DE. Cytotoxic effect of Shiga toxin-1 on human glomerular epithelial cells. *Kidney Int* 2000;**57**(6):2350-9.
344. Scoville DH, Sato T, He XC, Li L. Current view: intestinal stem cells and signaling. *Gastroenterology* 2008;**134**(3):849-64.
345. Schuller S, Heuschkel R, Torrente F, Kaper JB, Phillips AD. Shiga toxin binding in normal and inflamed human intestinal mucosa. *Microbes Infect* 2007;**9**(1):35-9.
346. Schuller S, Frankel G, Phillips AD. Interaction of Shiga toxin from *Escherichia coli* with human intestinal epithelial cell lines and explants: Stx2 induces epithelial damage in organ culture. *Cell Microbiol* 2004;**6**(3):289-301.
347. Bjork S, Breimer ME, Hansson GC, Karlsson KA, Leffler H. Structures of blood group glycosphingolipids of human small intestine. A relation between the expression of fucolipids of epithelial cells and the ABO, Le and Se phenotype of the donor. *J Biol Chem* 1987;**262**(14):6758-65.

348. Holgersson J, Jovall PA, Breimer ME. Glycosphingolipids of human large intestine: detailed structural characterization with special reference to blood group compounds and bacterial receptor structures. *J Biochem* 1991;**110**(1):120-31.
349. Williams JM, Boyd B, Nutikka A, Lingwood CA, Barnett Foster DE, Milford DV, Taylor CM. A comparison of the effects of verocytotoxin-1 on primary human renal cell cultures. *Toxicol Lett* 1999;**105**(1):47-57.
350. Meyers KE, Kaplan BS. Many cell types are Shiga toxin targets. *Kidney Int* 2000;**57**(6):2650-1.
351. Simon M, Cleary TG, Hernandez JD, Abboud HE. Shiga toxin 1 elicits diverse biologic responses in mesangial cells. *Kidney Int* 1998;**54**(4):1117-27.
352. Robinson LA, Hurley RM, Lingwood C, Matsell DG. Escherichia coli verotoxin binding to human paediatric glomerular mesangial cells. *Pediatr Nephrol* 1995;**9**(6):700-4.
353. Van Setten PA, van Hinsbergh VW, Van den Heuvel LP, van der Velden TJ, van de Kar NC, Krebbers RJ, Karmali MA, Monnens LA. Verocytotoxin inhibits mitogenesis and protein synthesis in purified human glomerular mesangial cells without affecting cell viability: evidence for two distinct mechanisms. *J Am Soc Nephrol* 1997;**8**(12):1877-88.
354. Moyer MP, Dixon PS, Rothman SW, Brown JE. Cytotoxicity of Shiga toxin for primary cultures of human colonic and ileal epithelial cells. *Infect Immun* 1987;**55**(6):1533-5.

355. Hurley BP, Jacewicz M, Thorpe CM, Lincicome LL, King AJ, Keusch GT, Acheson DW. Shiga toxins 1 and 2 translocate differently across polarized intestinal epithelial cells. *Infect Immun* 1999;**67**(12):6670-7.
356. Hurley BP, Thorpe CM, Acheson DW. Shiga toxin translocation across intestinal epithelial cells is enhanced by neutrophil transmigration. *Infect Immun* 2001;**69**(10):6148-55.
357. Cornick NA, Jelacic S, Ciol MA, Tarr PI. Escherichia coli O157:H7 infections: discordance between filterable fecal shiga toxin and disease outcome. *J Infect Dis* 2002;**186**(1):57-63.
358. Kimura T, Tani S, Matsumoto Yi Y, Takeda T. Serum amyloid P component is the Shiga toxin 2-neutralizing factor in human blood. *J Biol Chem* 2001;**276**(45):41576-9.
359. Marcato P, Vander Helm K, Mulvey GL, Armstrong GD. Serum amyloid P component binding to Shiga toxin 2 requires both a subunit and B pentamer. *Infect Immun* 2003;**71**(10):6075-8.
360. Kimura T, Tani S, Motoki M, Matsumoto Y. Role of Shiga toxin 2 (Stx2)-binding protein, human serum amyloid P component (HuSAP), in Shiga toxin-producing Escherichia coli infections: assumption from in vitro and in vivo study using HuSAP and anti-Stx2 humanized monoclonal antibody TMA-15. *Biochem Biophys Res Commun* 2003;**305**(4):1057-60.
361. Armstrong GD, Mulvey GL, Marcato P, Griener TP, Kahan MC, Tennent GA, Sabin CA, Chart H, Pepys MB. Human serum amyloid P component protects against

- Escherichia coli O157:H7 Shiga toxin 2 in vivo: therapeutic implications for hemolytic-uremic syndrome. *J Infect Dis* 2006;**193**(8):1120-4.
362. Geelen JM, van der Velden TJ, Te Loo DM, Boerman OC, van den Heuvel LP, Monnens LA. Lack of specific binding of Shiga-like toxin (verocytotoxin) and non-specific interaction of Shiga-like toxin 2 antibody with human polymorphonuclear leucocytes. *Nephrol Dial Transplant* 2007;**22**(3):749-55.
363. Fernandez GC, Gomez SA, Rubel CJ, Bentancor LV, Barrionuevo P, Alduncin M, Grimoldi I, Exeni R, Isturiz MA, Palermo MS. Impaired neutrophils in children with the typical form of hemolytic uremic syndrome. *Pediatr Nephrol* 2005;**20**(9):1306-14.
364. Bitzan M, Richardson S, Huang C, Boyd B, Petric M, Karmali MA. Evidence that verotoxins (Shiga-like toxins) from Escherichia coli bind to P blood group antigens of human erythrocytes in vitro. *Infect Immun* 1994;**62**(8):3337-47.
365. Trof RJ, Di Maggio F, Leemreis J, Groeneveld AB. Biomarkers of acute renal injury and renal failure. *Shock* 2006;**26**(3):245-53.
366. Fleck RA, Rao LV, Rapaport SI, Varki N. Localization of human tissue factor antigen by immunostaining with monospecific, polyclonal anti-human tissue factor antibody. *Thromb Res* 1990;**59**(2):421-37.
367. Drake TA, Morrissey JH, Edgington TS. Selective cellular expression of tissue factor in human tissues. Implications for disorders of hemostasis and thrombosis. *Am J Pathol* 1989;**134**(5):1087-97.
368. Lingwood CA. Verotoxin-binding in human renal sections. *Nephron* 1994;**66**(1):21-8.

369. Kolling GL, Obata F, Gross LK, Obrig TG. Immunohistologic techniques for detecting the glycolipid Gb(3) in the mouse kidney and nervous system. *Histochem Cell Biol* 2008.
370. Turi S, Nemeth I, Vargha I, Matkovics B. Oxidative damage of red blood cells in haemolytic uraemic syndrome. *Pediatr Nephrol* 1994;**8**(1):26-9.
371. Fitzpatrick MM, Shah V, Filler G, Dillon MJ, Barratt TM. Neutrophil activation in the haemolytic uraemic syndrome: free and complexed elastase in plasma. *Pediatr Nephrol* 1992;**6**(1):50-3.
372. Milford D, Taylor CM, Rafaat F, Halloran E, Dawes J. Neutrophil elastases and haemolytic uraemic syndrome. *Lancet* 1989;**2**(8672):1153.
373. Robson WL, Fick GH, Wilson PC. Prognostic factors in typical postdiarrhea hemolytic-uremic syndrome. *Child Nephrol Urol* 1988;**9**(4):203-7.
374. Malnic G, Bailey, M.A., and Giebisch, G. Control of Renal Potassium Excretion. In: Brenner B, ed. Brenner & Rector's The Kidney. 7 ed. Philadelphia: Saunders, 2004: 453-495.
375. Zipfel PF, Misselwitz J, Licht C, Skerka C. The role of defective complement control in hemolytic uremic syndrome. *Semin Thromb Hemost* 2006;**32**(2):146-54.
376. Schulman SL, Kaplan BS. Management of patients with hemolytic uremic syndrome demonstrating severe azotemia but not anuria. *Pediatr Nephrol* 1996;**10**(5):671-4.
377. Exeni RA. [Hemolytic uremic syndrome]. *Medicina (B Aires)* 1996;**56**(2):197-8.
378. Perez N, Spizzirri F, Rahman R, Suarez A, Larrubia C, Lasarte P. Steroids in the hemolytic uremic syndrome. *Pediatr Nephrol* 1998;**12**(2):101-4.

379. Wong CS, Jelacic S, Habeeb RL, Watkins SL, Tarr PI. The risk of the hemolytic-uremic syndrome after antibiotic treatment of *Escherichia coli* O157:H7 infections. *N Engl J Med* 2000;**342**(26):1930-6.
380. Safdar N, Said A, Gangnon RE, Maki DG. Risk of hemolytic uremic syndrome after antibiotic treatment of *Escherichia coli* O157:H7 enteritis: a meta-analysis. *Jama* 2002;**288**(8):996-1001.
381. Cimolai N. Treatment of Shiga-like toxin-producing *Escherichia coli* infection. *Clin Infect Dis* 2006;**42**(12):1804-5.
382. Tzipori S, Sheoran A, Akiyoshi D, Donohue-Rolfe A, Trachtman H. Antibody therapy in the management of shiga toxin-induced hemolytic uremic syndrome. *Clin Microbiol Rev* 2004;**17**(4):926-41, table of contents.
383. Sheoran AS, Chapman S, Singh P, Donohue-Rolfe A, Tzipori S. Stx2-specific human monoclonal antibodies protect mice against lethal infection with *Escherichia coli* expressing Stx2 variants. *Infect Immun* 2003;**71**(6):3125-30.
384. Sheoran AS, Chapman-Bonofiglio S, Harvey BR, Mukherjee J, Georgiou G, Donohue-Rolfe A, Tzipori S. Human antibody against shiga toxin 2 administered to piglets after the onset of diarrhea due to *Escherichia coli* O157:H7 prevents fatal systemic complications. *Infect Immun* 2005;**73**(8):4607-13.
385. Dowling TC, Chavaillaz PA, Young DG, Melton-Celsa A, O'Brien A, Thuning-Roberson C, Edelman R, Tacket CO. Phase 1 safety and pharmacokinetic study of chimeric murine-human monoclonal antibody c alpha Stx2 administered intravenously to healthy adult volunteers. *Antimicrob Agents Chemother* 2005;**49**(5):1808-12.

386. Bagshaw SM, Bellomo R, Kellum JA. Oliguria, volume overload, and loop diuretics. *Crit Care Med* 2008;**36**(4 Suppl):S172-8.
387. Tarr P. Shiga toxin-induced thrombotic microangiopathy: a thrombin-dependent process? *Thromb Haemost* 2004;**92**(2):227-8.
388. Stuart J, Winterborn MH, White RH, Flinn RM. Thrombolytic therapy in haemolytic--uraemic syndrome. *Br Med J* 1974;**3**(925):217-21.
389. Van Damme-Lombaerts R, Proesmans W, Van Damme B, Eeckels R, Binda ki Muaka P, Mercieca V, Vlietinck R, Vermeylen J. Heparin plus dipyridamole in childhood hemolytic-uremic syndrome: a prospective, randomized study. *J Pediatr* 1988;**113**(5):913-8.
390. Van Dyck M, Proesmans W. Renoprotection by ACE inhibitors after severe hemolytic uremic syndrome. *Pediatr Nephrol* 2004;**19**(6):688-90.
391. Loirat C, Niaudet P. The risk of recurrence of hemolytic uremic syndrome after renal transplantation in children. *Pediatr Nephrol* 2003;**18**(11):1095-101.
392. Richardson SE, Rotman TA, Jay V, Smith CR, Becker LE, Petric M, Olivieri NF, Karmali MA. Experimental verocytotoxemia in rabbits. *Infect Immun* 1992;**60**(10):4154-67.
393. Zoja C, Corna D, Farina C, Sacchi G, Lingwood C, Doyle MP, Padhye VV, Abbate M, Remuzzi G. Verotoxin glycolipid receptors determine the localization of microangiopathic process in rabbits given verotoxin-1. *J Lab Clin Med* 1992;**120**(2):229-38.
394. Ren J, Utsunomiya I, Taguchi K, Ariga T, Tai T, Ihara Y, Miyatake T. Localization of verotoxin receptors in nervous system. *Brain Res* 1999;**825**(1-2):183-8.

395. Raife T, Friedman KD, Fenwick B. Lepirudin prevents lethal effects of Shiga toxin in a canine model. *Thromb Haemost* 2004;**92**(2):387-93.
396. Hertzke DM, Cowan LA, Schoning P, Fenwick BW. Glomerular ultrastructural lesions of idiopathic cutaneous and renal glomerular vasculopathy of greyhounds. *Vet Pathol* 1995;**32**(5):451-9.
397. Cowan LA, Hertzke DM, Fenwick BW, Andreasen CB. Clinical and clinicopathologic abnormalities in greyhounds with cutaneous and renal glomerular vasculopathy: 18 cases (1992-1994). *J Am Vet Med Assoc* 1997;**210**(6):789-93.
398. Okuda T, Tokuda N, Numata S, Ito M, Ohta M, Kawamura K, Wiels J, Urano T, Tajima O, Furukawa K. Targeted disruption of Gb3/CD77 synthase gene resulted in the complete deletion of globo-series glycosphingolipids and loss of sensitivity to verotoxins. *J Biol Chem* 2006;**281**(15):10230-5.
399. Shimizu K, Tanaka K, Akatsuka A, Endoh M, Koga Y. Induction of glomerular lesions in the kidneys of mice infected with vero toxin-producing *Escherichia coli* by lipopolysaccharide injection. *J Infect Dis* 1999;**180**(4):1374-7.
400. Sugatani J, Igarashi T, Munakata M, Komiyama Y, Takahashi H, Komiyama N, Maeda T, Takeda T, Miwa M. Activation of coagulation in C57BL/6 mice given verotoxin 2 (VT2) and the effect of co-administration of LPS with VT2. *Thromb Res* 2000;**100**(1):61-72.
401. Sugatani J, Igarashi T, Shimura M, Yamanaka T, Takeda T, Miwa M. Disorders in the immune responses of T- and B-cells in mice administered intravenous verotoxin 2. *Life Sci* 2000;**67**(9):1059-72.

402. Harel Y, Silva M, Giroir B, Weinberg A, Cleary TB, Beutler B. A reporter transgene indicates renal-specific induction of tumor necrosis factor (TNF) by shiga-like toxin. Possible involvement of TNF in hemolytic uremic syndrome. *J Clin Invest* 1993;**92**(5):2110-6.
403. Barrett TJ, Potter ME, Wachsmuth IK. Bacterial endotoxin both enhances and inhibits the toxicity of Shiga-like toxin II in rabbits and mice. *Infect Immun* 1989;**57**(11):3434-7.
404. Palermo MS, Alves Rosa MF, Van Rooijen N, Isturiz MA. Depletion of liver and splenic macrophages reduces the lethality of Shiga toxin-2 in a mouse model. *Clin Exp Immunol* 1999;**116**(3):462-7.
405. Alves-Rosa F, Beigier-Bompadre M, Fernandez G, Barrionuevo P, Mari L, Palermo M, Isturiz M. Tolerance to lipopolysaccharide (LPS) regulates the endotoxin effects on Shiga toxin-2 lethality. *Immunol Lett* 2001;**76**(2):125-31.
406. Palermo M, Alves-Rosa F, Rubel C, Fernandez GC, Fernandez-Alonso G, Alberto F, Rivas M, Isturiz M. Pretreatment of mice with lipopolysaccharide (LPS) or IL-1beta exerts dose-dependent opposite effects on Shiga toxin-2 lethality. *Clin Exp Immunol* 2000;**119**(1):77-83.
407. Ikeda M, Ito S, Honda M. Hemolytic uremic syndrome induced by lipopolysaccharide and Shiga-like toxin. *Pediatr Nephrol* 2004;**19**(5):485-9.
408. Suzuki K, Tateda K, Matsumoto T, Gondaira F, Tsujimoto S, Yamaguchi K. Effects of interaction between Escherichia coli verotoxin and lipopolysaccharide on cytokine induction and lethality in mice. *J Med Microbiol* 2000;**49**(10):905-10.

409. Kita E, Yunou Y, Kurioka T, Harada H, Yoshikawa S, Mikasa K, Higashi N. Pathogenic mechanism of mouse brain damage caused by oral infection with Shiga toxin-producing *Escherichia coli* O157:H7. *Infect Immun* 2000;**68**(3):1207-14.
410. Kurioka T, Yunou Y, Kita E. Enhancement of susceptibility to Shiga toxin-producing *Escherichia coli* O157:H7 by protein calorie malnutrition in mice. *Infect Immun* 1998;**66**(4):1726-34.
411. Aiba Y, Ishikawa H, Shimizu K, Noda S, Kitada Y, Sasaki M, Koga Y. Role of internalization in the pathogenicity of Shiga toxin-producing *Escherichia coli* infection in a gnotobiotic murine model. *Microbiol Immunol* 2002;**46**(11):723-31.
412. Karpman D, Connell H, Svensson M, Scheutz F, Alm P, Svanborg C. The role of lipopolysaccharide and Shiga-like toxin in a mouse model of *Escherichia coli* O157:H7 infection. *J Infect Dis* 1997;**175**(3):611-20.
413. Wadolkowski EA, Sung LM, Burris JA, Samuel JE, O'Brien AD. Acute renal tubular necrosis and death of mice orally infected with *Escherichia coli* strains that produce Shiga-like toxin type II. *Infect Immun* 1990;**58**(12):3959-65.
414. Sugatani J, Komiyama N, Mochizuki T, Hoshino M, Miyamoto D, Igarashi T, Hoshi S, Miwa M. Urinary concentrating defect in rats given Shiga toxin: elevation in urinary AQP2 level associated with polyuria. *Life Sci* 2002;**71**(2):171-89.
415. Yamamoto ET, Mizuno M, Nishikawa K, Miyazawa S, Zhang L, Matsuo S, Natori Y. Shiga toxin 1 causes direct renal injury in rats. *Infect Immun* 2005;**73**(11):7099-106.

416. Shibolet O, Shina A, Rosen S, Cleary TG, Brezis M, Ashkenazi S. Shiga toxin induces medullary tubular injury in isolated perfused rat kidneys. *FEMS Immunol Med Microbiol* 1997;**18**(1):55-60.
417. Barrett TJ, Potter ME, Wachsmuth IK. Continuous peritoneal infusion of Shiga-like toxin II (SLT II) as a model for SLT II-induced diseases. *J Infect Dis* 1989;**159**(4):774-7.
418. Yamada Y, Fujii J, Murasato Y, Nakamura T, Hayashida Y, Kinoshita Y, Yutsudo T, Matsumoto T, Yoshida S. Brainstem mechanisms of autonomic dysfunction in encephalopathy-associated Shiga toxin 2 intoxication. *Ann Neurol* 1999;**45**(6):716-23.
419. Mizuguchi M, Tanaka S, Fujii I, Tanizawa H, Suzuki Y, Igarashi T, Yamanaka T, Takeda T, Miwa M. Neuronal and vascular pathology produced by verocytotoxin 2 in the rabbit central nervous system. *Acta Neuropathol* 1996;**91**(3):254-62.
420. Chopra P, Verma D, Khullar M, Sapru S, Mahmood S. Shiga toxin exposure modulates intestinal brush border membrane functional proteins in rabbit ileum. *Mol Cell Biochem* 2006;**283**(1-2):85-92.
421. Takahashi K, Funata N, Ikuta F, Sato S. Neuronal apoptosis and inflammatory responses in the central nervous system of a rabbit treated with Shiga toxin-2. *J Neuroinflammation* 2008;**5**(1):11.
422. Sherman P, Soni R, Karmali M. Attaching and effacing adherence of Vero cytotoxin-producing *Escherichia coli* to rabbit intestinal epithelium in vivo. *Infect Immun* 1988;**56**(4):756-61.

423. Garcia A, Marini RP, Feng Y, Vitsky A, Knox KA, Taylor NS, Schauer DB, Fox JG. A naturally occurring rabbit model of enterohemorrhagic *Escherichia coli*-induced disease. *J Infect Dis* 2002;**186**(11):1682-6.
424. Garcia A, Bosques CJ, Wishnok JS, Feng Y, Karalius BJ, Butterton JR, Schauer DB, Rogers AB, Fox JG. Renal injury is a consistent finding in Dutch Belted rabbits experimentally infected with enterohemorrhagic *Escherichia coli*. *J Infect Dis* 2006;**193**(8):1125-34.
425. Pai CH, Kelly JK, Meyers GL. Experimental infection of infant rabbits with verotoxin-producing *Escherichia coli*. *Infect Immun* 1986;**51**(1):16-23.
426. Garcia A, Marini RP, Catalfamo JL, Knox KA, Schauer DB, Rogers AB, Fox JG. Intravenous Shiga toxin 2 promotes enteritis and renal injury characterized by polymorphonuclear leukocyte infiltration and thrombosis in Dutch Belted rabbits. *Microbes Infect* 2008.
427. Wolski VM, Soltyk AM, Brunton JL. Tumour necrosis factor alpha is not an essential component of verotoxin 1-induced toxicity in mice. *Microb Pathog* 2002;**32**(6):263-71.
428. Tesh VL, Samuel JE, Burris JA, Owens JW, Taylor FB, Siegler RL. Quantitation and localization of shiga toxin/shiga-like toxin-binding glycolipid receptors in human and baboon tissues. In: Karmali MA, Goglio AG, eds. *Recent Advances in Verocytotoxin-Producing *Escherichia coli* Infections*. Bergamo, Italy: Elsevier Science BV, 1994: 189-192.
429. Taylor FB, Jr., Tesh VL, DeBault L, Li A, Chang AC, Kosanke SD, Pysker TJ, Siegler RL. Characterization of the baboon responses to Shiga-like toxin:

- descriptive study of a new primate model of toxic responses to Stx-1. *Am J Pathol* 1999;**154**(4):1285-99.
430. Siegler RL, Pysher TJ, Tesh VL, Taylor FB, Jr. Response to single and divided doses of Shiga toxin-1 in a primate model of hemolytic uremic syndrome. *J Am Soc Nephrol* 2001;**12**(7):1458-67.
431. Siegler RL, Obrig TG, Pysher TJ, Tesh VL, Denkers ND, Taylor FB. Response to Shiga toxin 1 and 2 in a baboon model of hemolytic uremic syndrome. *Pediatr Nephrol* 2003;**18**(2):92-6.
432. Siegler RL, Pysher TJ, Lou R, Tesh VL, Taylor FB, Jr. Response to Shiga toxin-1, with and without lipopolysaccharide, in a primate model of hemolytic uremic syndrome. *Am J Nephrol* 2001;**21**(5):420-5.
433. Clayton F, Pysher TJ, Lou R, Kohan DE, Denkers ND, Tesh VL, Taylor FB, Jr., Siegler RL. Lipopolysaccharide upregulates renal shiga toxin receptors in a primate model of hemolytic uremic syndrome. *Am J Nephrol* 2005;**25**(6):536-40.
434. Siegler RL, Pysher TJ, Tesh VL, Denkers ND, Taylor FB. Prophylactic heparinization is ineffective in a primate model of hemolytic uremic syndrome. *Pediatr Nephrol* 2002;**17**(12):1053-8.
435. Rutjes NW, Binnington BA, Smith CR, Maloney MD, Lingwood CA. Differential tissue targeting and pathogenesis of verotoxins 1 and 2 in the mouse animal model. *Kidney Int* 2002;**62**(3):832-45.
436. Taylor CM, Williams JM, Lote CJ, Howie AJ, Thewles A, Wood JA, Milford DV, Raafat F, Chant I, Rose PE. A laboratory model of toxin-induced hemolytic uremic syndrome. *Kidney Int* 1999;**55**(4):1367-74.

437. Fu XJ, Iijima K, Nozu K, Hamahira K, Tanaka R, Oda T, Yoshikawa N, Matsuo M. Role of p38 MAP kinase pathway in a toxin-induced model of hemolytic uremic syndrome. *Pediatr Nephrol* 2004;**19**(8):844-52.
438. Korcheva V, Wong J, Corless C, Iordanov M, Magun B. Administration of ricin induces a severe inflammatory response via nonredundant stimulation of ERK, JNK, and P38 MAPK and provides a mouse model of hemolytic uremic syndrome. *Am J Pathol* 2005;**166**(1):323-39.
439. Siegler R, Oakes R. Hemolytic uremic syndrome; pathogenesis, treatment, and outcome. *Curr Opin Pediatr* 2005;**17**(2):200-4.
440. Mead PS, Griffin PM. Escherichia coli O157:H7. *Lancet* 1998;**352**(9135):1207-12.
441. Cleary TG. The role of Shiga-toxin-producing Escherichia coli in hemorrhagic colitis and hemolytic uremic syndrome. *Semin Pediatr Infect Dis* 2004;**15**(4):260-5.
442. Melton-Celsa AR, and O'Brien, A. D. Shiga toxins of *Shigella dysenteriae* and *Escherichia coli*. In: Aktories K, and Just, I., ed. Handbook of Experimental Pharmacology: Springer, Freiburg, 2000: 385-406.
443. Perera LP, Marques LR, O'Brien AD. Isolation and characterization of monoclonal antibodies to Shiga-like toxin II of enterohemorrhagic Escherichia coli and use of the monoclonal antibodies in a colony enzyme-linked immunosorbent assay. *J Clin Microbiol* 1988;**26**(10):2127-31.
444. O'Brien AD, Tesh VL, Donohue-Rolfe A, Jackson MP, Olsnes S, Sandvig K, Lindberg AA, Keusch GT. Shiga toxin: biochemistry, genetics, mode of action, and role in pathogenesis. *Curr Top Microbiol Immunol* 1992;**180**:65-94.

445. Pusey W, Edwards CA. A modification of the martius yellow-scarlet red-aniline blue method for fibrin. *Stain Technol* 1978;**53**(1):58-9.
446. Artoni A, Li J, Mitchell B, Ruan J, Takagi J, Springer TA, French DL, Collier BS. Integrin beta3 regions controlling binding of murine mAb 7E3: implications for the mechanism of integrin alphaIIb beta3 activation. *Proc Natl Acad Sci U S A* 2004;**101**(36):13114-20.
447. Li C, Wong WH. Model-based analysis of oligonucleotide arrays: expression index computation and outlier detection. *Proc Natl Acad Sci U S A* 2001;**98**(1):31-6.
448. Tusher VG, Tibshirani R, Chu G. Significance analysis of microarrays applied to the ionizing radiation response. *Proc Natl Acad Sci U S A* 2001;**98**(9):5116-21.
449. Reich M, Ohm K, Angelo M, Tamayo P, Mesirov JP. GeneCluster 2.0: an advanced toolset for bioarray analysis. *Bioinformatics* 2004;**20**(11):1797-8.
450. Litalien C, Proulx F, Mariscalco MM, Robitaille P, Turgeon JP, Orrbine E, Rowe PC, McLaine PN, Seidman E. Circulating inflammatory cytokine levels in hemolytic uremic syndrome. *Pediatr Nephrol* 1999;**13**(9):840-5.
451. Bishop DF, Johansson A, Phelps R, Shady AA, Ramirez MCM, Yasuda M, Caro A, Desnick RJ. Uroporphyrinogen III Synthase Knock-In Mice Have the Human Congenital Erythropoietic Porphyria Phenotype, Including the Characteristic Light-Induced Cutaneous Lesions. *Am J Hum Genet* 2006;**78**(4):645-658.
452. Peters LL, Lane PW, Andersen SG, Gwynn B, Barker JE, Beutler E. Downeast Anemia (dea), a New Mouse Model of Severe Nonspherocytic Hemolytic Anemia Caused by Hexokinase (HKI) Deficiency. *Blood Cells, Molecules, and Diseases* 2001;**27**(5):850-860.

453. Chaisri U, Nagata M, Kurazono H, Horie H, Tongtawe P, Hayashi H, Watanabe T, Tapchaisri P, Chongsa-nguan M, Chaicumpa W. Localization of Shiga toxins of enterohaemorrhagic *Escherichia coli* in kidneys of paediatric and geriatric patients with fatal haemolytic uraemic syndrome. *Microb Pathog* 2001;**31**(2):59-67.
454. Palermo MS, Alves Rosa MF, Van Rooijen N, Isturiz MA. Depletion of liver and splenic macrophages reduces the lethality of Shiga toxin-2 in a mouse model. *Clin Exp Immunol* 1999;**116**(3):462-7.
455. Hughes AK, Stricklett PK, Kohan DE. Shiga toxin-1 regulation of cytokine production by human proximal tubule cells. *Kidney Int* 1998;**54**(4):1093-106.
456. Hughes AK, Stricklett PK, Kohan DE. Shiga toxin-1 regulation of cytokine production by human glomerular epithelial cells. *Nephron* 2001;**88**(1):14-23.
457. Tesh VL, Ramegowda B, Samuel JE. Purified Shiga-like toxins induce expression of proinflammatory cytokines from murine peritoneal macrophages. *Infect Immun* 1994;**62**(11):5085-94.
458. Pijpers AH, van Setten PA, van den Heuvel LP, Assmann KJ, Dijkman HB, Pennings AH, Monnens LA, van Hinsbergh VW. Verocytotoxin-induced apoptosis of human microvascular endothelial cells. *J Am Soc Nephrol* 2001;**12**(4):767-78.
459. De Petris L, Patrick J, Christen E, Trachtman H. Urinary podocyte mRNA excretion in children with D+HUS: a potential marker of long-term outcome. *Ren Fail* 2006;**28**(6):475-82.

460. Kaneko K, Kiyokawa N, Ohtomo Y, Nagaoka R, Yamashiro Y, Taguchi T, Mori T, Fujimoto J, Takeda T. Apoptosis of renal tubular cells in Shiga-toxin-mediated hemolytic uremic syndrome. *Nephron* 2001;**87**(2):182-5.
461. Morigi M, Buelli S, Zanchi C, Longaretti L, Macconi D, Benigni A, Moioli D, Remuzzi G, Zoja C. Shigatoxin-induced endothelin-1 expression in cultured podocytes autocrinally mediates actin remodeling. *Am J Pathol* 2006;**169**(6):1965-75.
462. Melton-Celsa AR, and O'Brien, A. D. In: Aktories K, and Just, I., ed. Handbook of Experimental Pharmacology: Springer, Freiburg, 2000: 385-406.
463. Satchell SC, Tasman CH, Singh A, Ni L, Geelen J, von Ruhland CJ, O'Hare MJ, Saleem MA, van den Heuvel LP, Mathieson PW. Conditionally immortalized human glomerular endothelial cells expressing fenestrations in response to VEGF. *Kidney Int* 2006;**69**(9):1633-40.
464. Bolick DT, Orr AW, Whetzel A, Srinivasan S, Hatley ME, Schwartz MA, Hedrick CC. 12/15-lipoxygenase regulates intercellular adhesion molecule-1 expression and monocyte adhesion to endothelium through activation of RhoA and nuclear factor-kappaB. *Arterioscler Thromb Vasc Biol* 2005;**25**(11):2301-7.
465. Saleem MA, O'Hare MJ, Reiser J, Coward RJ, Inward CD, Farren T, Xing CY, Ni L, Mathieson PW, Mundel P. A conditionally immortalized human podocyte cell line demonstrating nephrin and podocin expression. *J Am Soc Nephrol* 2002;**13**(3):630-8.
466. Mundel P, Reiser J, Zuniga Mejia Borja A, Pavenstadt H, Davidson GR, Kriz W, Zeller R. Rearrangements of the cytoskeleton and cell contacts induce process

- formation during differentiation of conditionally immortalized mouse podocyte cell lines. *Exp Cell Res* 1997;**236**(1):248-58.
467. Akis N, Madaio MP. Isolation, culture, and characterization of endothelial cells from mouse glomeruli. *Kidney Int* 2004;**65**(6):2223-7.
468. Awad AS, Rouse M, Liu L, Vergis AL, Rosin DL, Linden J, Sedor JR, Okusa MD. Activation of adenosine 2A receptors preserves structure and function of podocytes. *J Am Soc Nephrol* 2008;**19**(1):59-68.
469. Rose HG, Oklander M. Improved Procedure for the Extraction of Lipids from Human Erythrocytes. *J Lipid Res* 1965;**6**:428-31.
470. Nutikka A, Binnington-Boyd B, Lingwood CA. Methods for the identification of host receptors for Shiga toxin. *Methods Mol Med* 2003;**73**:197-208.
471. Abe A, Gregory S, Lee L, Killen PD, Brady RO, Kulkarni A, Shayman JA. Reduction of globotriaosylceramide in Fabry disease mice by substrate deprivation. *J Clin Invest* 2000;**105**(11):1563-71.
472. Schrecengost RS, Riggins RB, Thomas KS, Guerrero MS, Bouton AH. Breast cancer antiestrogen resistance-3 expression regulates breast cancer cell migration through promotion of p130Cas membrane localization and membrane ruffling. *Cancer Res* 2007;**67**(13):6174-82.
473. Caserta TM, Smith AN, Gultice AD, Reedy MA, Brown TL. Q-VD-OPh, a broad spectrum caspase inhibitor with potent antiapoptotic properties. *Apoptosis* 2003;**8**(4):345-52.

474. Lee J, Cacalano G, Camerato T, Toy K, Moore MW, Wood WI. Chemokine binding and activities mediated by the mouse IL-8 receptor. *J Immunol* 1995;**155**(4):2158-64.
475. Melnikov VY, Faubel S, Siegmund B, Lucia MS, Ljubanovic D, Edelstein CL. Neutrophil-independent mechanisms of caspase-1- and IL-18-mediated ischemic acute tubular necrosis in mice. *J Clin Invest* 2002;**110**(8):1083-91.
476. Taylor RC, Cullen SP, Martin SJ. Apoptosis: controlled demolition at the cellular level. *Nat Rev Mol Cell Biol* 2008;**9**(3):231-41.
477. Gavrieli Y, Sherman Y, Ben-Sasson SA. Identification of programmed cell death in situ via specific labeling of nuclear DNA fragmentation. *J Cell Biol* 1992;**119**(3):493-501.
478. Eaton KA, Friedman DI, Francis GJ, Tyler JS, Young VB, Haeger J, Abu-Ali G, Whittam TS. The Pathogenesis of Renal Disease Due to Enterohemorrhagic *Escherichia coli* in Germ Free Mice. *Infect Immun* 2008.
479. Banas MC, Banas B, Hudkins KL, Wietecha TA, Iyoda M, Bock E, Hauser P, Pippin JW, Shankland SJ, Smith KD, Stoelcker B, Liu G, Grone HJ, Kramer BK, Alpers CE. TLR4 Links Podocytes with the Innate Immune System to Mediate Glomerular Injury. *J Am Soc Nephrol* 2008.
480. Yaoita E, Kurihara H, Sakai T, Ohshiro K, Yamamoto T. Phenotypic modulation of parietal epithelial cells of Bowman's capsule in culture. *Cell Tissue Res* 2001;**304**(3):339-49.
481. Yaoita E, Yoshida Y. Polygonal epithelial cells in glomerular cell culture: Podocyte or parietal epithelial origin? *Microsc Res Tech* 2002;**57**(4):212-6.

482. Lopez EL, Contrini MM, Devoto S, de Rosa MF, Grana MG, Aversa L, Gomez HF, Genero MH, Cleary TG. Incomplete hemolytic-uremic syndrome in Argentinean children with bloody diarrhea. *J Pediatr* 1995;**127**(3):364-7.
483. Rowe PC, Orrbine E, Lior H, Wells GA, Yetisir E, Clulow M, McLaine PN. Risk of hemolytic uremic syndrome after sporadic Escherichia coli O157:H7 infection: results of a Canadian collaborative study. Investigators of the Canadian Pediatric Kidney Disease Research Center. *J Pediatr* 1998;**132**(5):777-82.
484. Scully RE, Mark EJ, McNeely WF, Ebeling SH, Phillips LD. Case records of the Massachusetts General Hospital. Weekly clinicopathological exercises. Case 17-1997. A 67-year-old woman with vomiting, bloody diarrhea, and azotemia. *N Engl J Med* 1997;**336**(22):1587-94.
485. Valentino KL, Gutierrez M, Sanchez R, Winship MJ, Shapiro DA. First clinical trial of a novel caspase inhibitor: anti-apoptotic caspase inhibitor, IDN-6556, improves liver enzymes. *Int J Clin Pharmacol Ther* 2003;**41**(10):441-9.
486. Mange K, Matsuura D, Cizman B, Soto H, Ziyadeh FN, Goldfarb S, Neilson EG. Language guiding therapy: the case of dehydration versus volume depletion. *Ann Intern Med* 1997;**127**(9):848-53.
487. Cheek DB, Holt AB. Growth and body composition of the mouse. *Am J Physiol* 1963;**205**(5):913-8.
488. Sands JM, Bichet DG. Nephrogenic diabetes insipidus. *Ann Intern Med* 2006;**144**(3):186-94.
489. Roche JK, Keepers TR, Gross LK, Seaner RM, Obrig TG. CXCL1/KC and CXCL2/MIP-2 are critical effectors and potential targets for therapy of

- Escherichia coli O157:H7-associated renal inflammation. *Am J Pathol* 2007;**170**(2):526-37.
490. Yamamoto K, Loskutoff DJ. Fibrin deposition in tissues from endotoxin-treated mice correlates with decreases in the expression of urokinase-type but not tissue-type plasminogen activator. *J Clin Invest* 1996;**97**(11):2440-51.
491. Moll S, Schifferli JA, Huarte J, Lemoine R, Vassalli JD, Sappino AP. LPS induces major changes in the extracellular proteolytic balance in the murine kidney. *Kidney Int* 1994;**45**(2):500-8.
492. Shu L, Murphy HS, Cooling L, Shayman JA. An in vitro model of Fabry disease. *J Am Soc Nephrol* 2005;**16**(9):2636-45.
493. Muramatsu Y, Tsujie M, Kohda Y, Pham B, Perantoni AO, Zhao H, Jo SK, Yuen PS, Craig L, Hu X, Star RA. Early detection of cysteine rich protein 61 (CYR61, CCN1) in urine following renal ischemic reperfusion injury. *Kidney Int* 2002;**62**(5):1601-10.
494. Sawai K, Mori K, Mukoyama M, Sugawara A, Suganami T, Koshikawa M, Yahata K, Makino H, Nagae T, Fujinaga Y, Yokoi H, Yoshioka T, Yoshimoto A, Tanaka I, Nakao K. Angiogenic protein Cyr61 is expressed by podocytes in anti-Thy-1 glomerulonephritis. *J Am Soc Nephrol* 2003;**14**(5):1154-63.
495. Sturm MB, Roday S, Schramm VL. Circular DNA and DNA/RNA hybrid molecules as scaffolds for ricin inhibitor design. *J Am Chem Soc* 2007;**129**(17):5544-50.
496. Miller DJ, Ravikumar K, Shen H, Suh JK, Kerwin SM, Robertus JD. Structure-based design and characterization of novel platforms for ricin and shiga toxin inhibition. *J Med Chem* 2002;**45**(1):90-8.

497. Takeda T, Dohi S, Igarashi T, Yamanaka T, Yoshiya K, Kobayashi N. Impairment by verotoxin of tubular function contributes to the renal damage seen in haemolytic uraemic syndrome. *J Infect* 1993;**27**(3):339-41.
498. Jandhyala DM, Ahluwalia A, Obrig T, Thorpe CM. ZAK: a MAP3Kinase that transduces Shiga toxin- and ricin-induced proinflammatory cytokine expression. *Cell Microbiol* 2008.
499. Hoglen NC, Chen LS, Fisher CD, Hirakawa BP, Groessl T, Contreras PC. Characterization of IDN-6556 (3-[2-(2-tert-butyl-phenylaminoxy)amino]-propionylamino]-4-oxo-5-(2,3,5,6-tetrafluoro-phenoxy)-pentanoic acid): a liver-targeted caspase inhibitor. *J Pharmacol Exp Ther* 2004;**309**(2):634-40.
500. Pockros PJ, Schiff ER, Shiffman ML, McHutchison JG, Gish RG, Afdhal NH, Makhviladze M, Huyghe M, Hecht D, Oltersdorf T, Shapiro DA. Oral IDN-6556, an antiapoptotic caspase inhibitor, may lower aminotransferase activity in patients with chronic hepatitis C. *Hepatology* 2007;**46**(2):324-9.
501. Baskin-Bey ES, Washburn K, Feng S, Oltersdorf T, Shapiro D, Huyghe M, Burgart L, Garrity-Park M, van Vilsteren FG, Oliver LK, Rosen CB, Gores GJ. Clinical Trial of the Pan-Caspase Inhibitor, IDN-6556, in Human Liver Preservation Injury. *Am J Transplant* 2007;**7**(1):218-25.
502. Creydt VP, Silberstein C, Zotta E, Ibarra C. Cytotoxic effect of Shiga toxin-2 holotoxin and its B subunit on human renal tubular epithelial cells. *Microbes Infect* 2006;**8**(2):410-9.

503. Hughes AK, Schmid DI, Kohan DE. Sex steroids do not affect shigatoxin cytotoxicity on human renal tubular or glomerular cells. *BMC Nephrol* 2002;**3**(1):6.
504. Bitzan M, Bickford BB, Foster GH. Verotoxin (shiga toxin) sensitizes renal epithelial cells to increased heme toxicity: possible implications for the hemolytic uremic syndrome. *J Am Soc Nephrol* 2004;**15**(9):2334-43.
505. Nestoridi E, Kushak RI, Duguerre D, Grabowski EF, Ingelfinger JR. Up-regulation of tissue factor activity on human proximal tubular epithelial cells in response to Shiga toxin. *Kidney Int* 2005;**67**(6):2254-66.
506. Kodama T, Nagayama K, Yamada K, Ohba Y, Akeda Y, Honda T. Induction of apoptosis in human renal proximal tubular epithelial cells by Escherichia coli verocytotoxin 1 in vitro. *Med Microbiol Immunol (Berl)* 1999;**188**(2):73-8.
507. Lee JE, Kim JS, Choi IH, Tagawa M, Kohsaka T, Jin DK. Cytokine expression in the renal tubular epithelial cells stimulated by Shiga toxin 2 of Escherichia coli O157:H7. *Ren Fail* 2002;**24**(5):567-75.
508. Morooka H, Bonventre JV, Pombo CM, Kyriakis JM, Force T. Ischemia and reperfusion enhance ATF-2 and c-Jun binding to cAMP response elements and to an AP-1 binding site from the c-jun promoter. *J Biol Chem* 1995;**270**(50):30084-92.
509. Bens M, Vandewalle A. Cell models for studying renal physiology. *Pflugers Arch* 2008.
510. Eremina V, Sood M, Haigh J, Nagy A, Lajoie G, Ferrara N, Gerber HP, Kikkawa Y, Miner JH, Quaggin SE. Glomerular-specific alterations of VEGF-A expression

- lead to distinct congenital and acquired renal diseases. *J Clin Invest* 2003;**111**(5):707-16.
511. Eremina V, Cui S, Gerber H, Ferrara N, Haigh J, Nagy A, Ema M, Rossant J, Jothy S, Miner JH, Quaggin SE. Vascular endothelial growth factor a signaling in the podocyte-endothelial compartment is required for mesangial cell migration and survival. *J Am Soc Nephrol* 2006;**17**(3):724-35.
512. Pries AR, Kuebler WM. Normal endothelium. *Handb Exp Pharmacol* 2006(176 Pt 1):1-40.
513. Sprouse JT, Wong CS, Chandler WL, Williams GD, Watkins SL, Tarr PI. Thrombogenic alleles, Escherichia coli O157:H7 infections, and hemolytic uremic syndrome. *Blood Coagul Fibrinolysis* 2001;**12**(4):283-8.
514. Linton SD, Aja T, Armstrong RA, Bai X, Chen LS, Chen N, Ching B, Contreras P, Diaz JL, Fisher CD, Fritz LC, Gladstone P, Groessl T, Gu X, Herrmann J, Hirakawa BP, Hoglen NC, Jahangiri KG, Kalish VJ, Karanewsky DS, Kodandapani L, Krebs J, McQuiston J, Meduna SP, Nalley K, Robinson ED, Sayers RO, Sebring K, Spada AP, Ternansky RJ, Tomaselli KJ, Ullman BR, Valentino KL, Weeks S, Winn D, Wu JC, Yeo P, Zhang CZ. First-in-class pan caspase inhibitor developed for the treatment of liver disease. *J Med Chem* 2005;**48**(22):6779-82.
515. Suga S, Kim YG, Joly A, Puchacz E, Kang DH, Jefferson JA, Abraham JA, Hughes J, Johnson RJ, Schreiner GF. Vascular endothelial growth factor (VEGF121) protects rats from renal infarction in thrombotic microangiopathy. *Kidney Int* 2001;**60**(4):1297-308.

516. Klein EJ, Boster DR, Stapp JR, Wells JG, Qin X, Clausen CR, Swerdlow DL, Braden CR, Tarr PI. Diarrhea etiology in a Children's Hospital Emergency Department: a prospective cohort study. *Clin Infect Dis* 2006;**43**(7):807-13.
517. van Deventer SJ, Buller HR, ten Cate JW, Sturk A, Pauw W. Endotoxaemia: an early predictor of septicaemia in febrile patients. *Lancet* 1988;**1**(8586):605-9.
518. Montrucchio G, Bosco O, Del Sorbo L, Fascio Pecetto P, Lupia E, Goffi A, Omede P, Emanuelli G, Camussi G. Mechanisms of the priming effect of low doses of lipopoly-saccharides on leukocyte-dependent platelet aggregation in whole blood. *Thromb Haemost* 2003;**90**(5):872-81.
519. Sheu JR, Hung WC, Kan YC, Lee YM, Yen MH. Mechanisms involved in the antiplatelet activity of Escherichia coli lipopolysaccharide in human platelets. *Br J Haematol* 1998;**103**(1):29-38.
520. Triantafilou M, Brandenburg K, Gutschmann T, Seydel U, Triantafilou K. Innate recognition of bacteria: engagement of multiple receptors. *Crit Rev Immunol* 2002;**22**(4):251-68.
521. Hirschfeld M, Ma Y, Weis JH, Vogel SN, Weis JJ. Cutting edge: repurification of lipopolysaccharide eliminates signaling through both human and murine toll-like receptor 2. *J Immunol* 2000;**165**(2):618-22.
522. Lau LF, Lam SC. The CCN family of angiogenic regulators: the integrin connection. *Exp Cell Res* 1999;**248**(1):44-57.
523. Hartman MG, Lu D, Kim ML, Kociba GJ, Shukri T, Buteau J, Wang X, Frankel WL, Guttridge D, Prentki M, Grey ST, Ron D, Hai T. Role for activating

- transcription factor 3 in stress-induced beta-cell apoptosis. *Mol Cell Biol* 2004;**24**(13):5721-32.
524. Whitmore MM, Iparraguirre A, Kubelka L, Weninger W, Hai T, Williams BR. Negative regulation of TLR-signaling pathways by activating transcription factor-3. *J Immunol* 2007;**179**(6):3622-30.
525. Khuu CH, Barrozo RM, Hai T, Weinstein SL. Activating transcription factor 3 (ATF3) represses the expression of CCL4 in murine macrophages. *Mol Immunol* 2007;**44**(7):1598-605.
526. Nemetski SM, Gardner LB. Hypoxic regulation of Id-1 and activation of the unfolded protein response are aberrant in neuroblastoma. *J Biol Chem* 2007;**282**(1):240-8.
527. Brown SL, Sekhar KR, Rachakonda G, Sasi S, Freeman ML. Activating transcription factor 3 is a novel repressor of the nuclear factor erythroid-derived 2-related factor 2 (Nrf2)-regulated stress pathway. *Cancer Res* 2008;**68**(2):364-8.
528. Xu J, Kimball TR, Lorenz JN, Brown DA, Bauskin AR, Klevitsky R, Hewett TE, Breit SN, Molkentin JD. GDF15/MIC-1 functions as a protective and antihypertrophic factor released from the myocardium in association with SMAD protein activation. *Circ Res* 2006;**98**(3):342-50.
529. Zimmers TA, Jin X, Hsiao EC, Perez EA, Pierce RH, Chavin KD, Koniaris LG. Growth differentiation factor-15: induction in liver injury through p53 and tumor necrosis factor-independent mechanisms. *J Surg Res* 2006;**130**(1):45-51.

530. Zimmers TA, Jin X, Hsiao EC, McGrath SA, Esquela AF, Koniaris LG. Growth differentiation factor-15/macrophage inhibitory cytokine-1 induction after kidney and lung injury. *Shock* 2005;**23**(6):543-8.
531. Subramaniam S, Strelau J, Unsicker K. Growth differentiation factor-15 prevents low potassium-induced cell death of cerebellar granule neurons by differential regulation of Akt and ERK pathways. *J Biol Chem* 2003;**278**(11):8904-12.
532. Noorali S, Kurita T, Woolcock B, de Algara TR, Lo M, Paralkar V, Hoodless P, Vielkind J. Dynamics of expression of growth differentiation factor 15 in normal and PIN development in the mouse. *Differentiation* 2007;**75**(4):325-36.
533. Hsiao EC, Koniaris LG, Zimmers-Koniaris T, Sebald SM, Huynh TV, Lee SJ. Characterization of growth-differentiation factor 15, a transforming growth factor beta superfamily member induced following liver injury. *Mol Cell Biol* 2000;**20**(10):3742-51.
534. Vogt PK, Bader AG. Jun: stealth, stability, and transformation. *Mol Cell* 2005;**19**(4):432-3.
535. Ashida R, Tominaga K, Sasaki E, Watanabe T, Fujiwara Y, Oshitani N, Higuchi K, Mitsuyama S, Iwao H, Arakawa T. AP-1 and colorectal cancer. *Inflammopharmacology* 2005;**13**(1-3):113-25.
536. Canzoniere D, Farioli-Vecchioli S, Conti F, Ciotti MT, Tata AM, Augusti-Tocco G, Mattei E, Lakshmana MK, Krizhanovsky V, Reeves SA, Giovannoni R, Castano F, Servadio A, Ben-Arie N, Tirone F. Dual control of neurogenesis by PC3 through cell cycle inhibition and induction of Math1. *J Neurosci* 2004;**24**(13):3355-69.

537. Park S, Lee YJ, Lee HJ, Seki T, Hong KH, Park J, Beppu H, Lim IK, Yoon JW, Li E, Kim SJ, Oh SP. B-cell translocation gene 2 (Btg2) regulates vertebral patterning by modulating bone morphogenetic protein/smad signaling. *Mol Cell Biol* 2004;**24**(23):10256-62.
538. Lee SW, Kwak HB, Lee HC, Lee SK, Kim HH, Lee ZH. The anti-proliferative gene TIS21 is involved in osteoclast differentiation. *J Biochem Mol Biol* 2002;**35**(6):609-14.
539. Ryu MS, Lee MS, Hong JW, Hahn TR, Moon E, Lim IK. TIS21/BTG2/PC3 is expressed through PKC-delta pathway and inhibits binding of cyclin B1-Cdc2 and its activity, independent of p53 expression. *Exp Cell Res* 2004;**299**(1):159-70.
540. Kireeva ML, Mo FE, Yang GP, Lau LF. Cyr61, a product of a growth factor-inducible immediate-early gene, promotes cell proliferation, migration, and adhesion. *Mol Cell Biol* 1996;**16**(4):1326-34.
541. Kireeva ML, Latinkic BV, Kolesnikova TV, Chen CC, Yang GP, Abler AS, Lau LF. Cyr61 and Fisp12 are both ECM-associated signaling molecules: activities, metabolism, and localization during development. *Exp Cell Res* 1997;**233**(1):63-77.
542. Kireeva ML, Lam SC, Lau LF. Adhesion of human umbilical vein endothelial cells to the immediate-early gene product Cyr61 is mediated through integrin alphavbeta3. *J Biol Chem* 1998;**273**(5):3090-6.
543. Jedsadayanmata A, Chen CC, Kireeva ML, Lau LF, Lam SC. Activation-dependent adhesion of human platelets to Cyr61 and Fisp12/mouse connective tissue growth

factor is mediated through integrin alpha(IIb)beta(3). *J Biol Chem*

1999;**274**(34):24321-7.

544. Lau LF, Nathans D. Expression of a set of growth-related immediate early genes in BALB/c 3T3 cells: coordinate regulation with c-fos or c-myc. *Proc Natl Acad Sci U S A* 1987;**84**(5):1182-6.
545. O'Brien TP, Yang GP, Sanders L, Lau LF. Expression of *cyr61*, a growth factor-inducible immediate-early gene. *Mol Cell Biol* 1990;**10**(7):3569-77.
546. Bain J, Plater L, Elliott M, Shpiro N, Hastie CJ, McLauchlan H, Klevernic I, Arthur JS, Alessi DR, Cohen P. The selectivity of protein kinase inhibitors: a further update. *Biochem J* 2007;**408**(3):297-315.

Appendix I: Direct Interactions of Platelets with Stx2 and LPS

Background

In HUS, microthrombi are found in the small vasculature (arterioles and capillaries) of the kidney, brain, skin, pancreas, spleen and adrenals⁵¹⁷. These thrombi are composed of platelets and fibrin, yet their etiology remains unknown. Platelet dysfunction in the context of bacterial sepsis may offer some insight into HUS. Septic patients have thrombocytopenia with some renal dysfunction, usually oliguria. The principal harmful substance in sepsis is bacterial endotoxin produced by bacteria growing in the bloodstream⁸². In contrast, HUS is a toxemia where toxin-producing *E. coli* do not actively invade the gastrointestinal mucosa, and thus the entirety of the disease process can be attributed to bacterial products that disseminate via the circulation. The main two products that enter the blood are LPS and Shiga toxin³²⁵. It is therefore likely that one or both of these is responsible for platelet dysfunction in HUS.

Shiga toxin appears to bind to a subpopulation of activated platelets, however it probably does not interact with resting platelets^{323,324,326}. Furthermore there seems to be no direct *in vitro* effect of Stx on platelet aggregation⁵¹⁸. These data suggest that LPS (either alone or in conjunction with Shiga toxin) may cause the platelet activation and microthrombus formation in HUS. There exists a wide body of literature that describes the interaction of LPS with platelets, however the data is conflicting. It has been published that LPS alone has no effect on platelet function⁵¹⁹. However, other reports use high dose LPS (100-300 µg/mL) and demonstrate a dose dependent inhibition of platelet function⁵¹⁷. This latter study is in agreement with older studies employing high dose

LPS, however it does not reflect physiologic concentrations of LPS found in endotoxemic patients. Most endotoxemic patients have less than 0.5 ng/mL LPS in the bloodstream⁵²⁰. We sought to determine the effect of lower dose LPS on platelet function.

Molecular recognition of LPS by cells normally requires CD14, LPS Binding Protein (LBP), and Toll-Like Receptor 4 (TLR4). CD14 exists as both a GPI-anchored protein and a soluble molecule (sCD14) that likely performs the primary binding of LPS. LBP is present only as a serum protein, and is upregulated in inflammatory states. TLR4 is the transmembrane signal transducer of the LPS signal to the cell interior⁵²¹. Together these molecules transducer the inflammatory LPS signal to the cell interior.

Methods

Preparation of Washed Human Platelets

Fresh human whole blood was obtained and anticoagulated with acid-citrate-dextrose (ACD). Platelet Rich Plasma (PRP) was isolated by centrifugation at 350g for 3, 3, and 5 minute cycles in the presence of ACD. Washed platelets were isolated from PRP by centrifugation twice at 620g for 20 minutes in a solution of ACD, apyrase, indomethacin and prostacyclin. Platelets were then washed with ACD-containing apyrase, and finally resuspended in a modified Eagles buffer without fibrinogen at a concentration of 4 x 10⁸/ml. Platelets were stored at room temperature until use.

CD14 Depletion

Platelets in solution with ACD, apyrase, indomethacin and prostacyclin were rotated for 30 minutes at 25°C with 2×10^8 α -CD14 antibody coated M-450 Dynabeads (DynaL Biotech ASA, Oslo, Norway) per 10^{10} platelets. Beads were removed with a magnet. Where used, recombinant sCD14 (R&D Systems, Minneapolis, MN) was replaced at a concentration of .5 μ g/mL.

Aggregometry

Platelets at a concentration of 4×10^8 /ml were used in a volume of 250 μ L on a dual-sample Chronolog Aggregometer. Platelet aggregation was measured as an increase in light transmission as small platelet clumps fell out of solution. All samples were incubated at 37°C for 30 minutes prior to activation. Those samples with LPS or Lipid A were incubated with platelets for 30 minutes. 100 ng/mL LPS O55:B5 (Alexis, San Diego, CA) was used, either directly suspended in 1x PBS or Phenol-purified and suspended in 1x PBS. Phenol purification was performed according to Hirschfeld et al¹⁰². Lipid A (Sigma, St. Louis, MO) was also used at 100 ng/mL in 1x PBS, with 0.1% Triethylamine.

Flow Cytometry

Washed platelets were diluted to a concentration of 1×10^8 /ml. Unfixed platelets were labeled with PE-Cy5 conjugated anti-CD41a antibody (BD Biosciences Pharmingen, San Diego, CA) and incubated with 100 ng/mL Alexa Fluor conjugated LPS O55:B5 (Molecular Probes). Incubation for 30 minutes at 37°C. For negative control 100x excess LPS O55:B5 was added. Samples were then fixed and stored overnight in 1%

paraformaldehyde, after which they were resuspended in 1x PBS. Analysis by flow cytometry using a FACS-Calibur flow cytometer and Cell Quest software (Beckton Dickinson, Mountain View, CA)

Results

Bacterial LPS, specifically Lipid A, potentiates platelet aggregation by traditional platelet mediators (Figure 26). 5-100 ng/mL LPS increased platelet reactivity to ADP (Figure 26) and thrombin (data not shown). Eliminating soluble CD14 (sCD14) with anti-CD14 antibody beads blocked this induction (Figure 27), demonstrating that platelets recognize LPS by a similar mechanism as other inflammatory cells. Because re-introduction of sCD14 rescues potentiation of CD14 depleted platelets, we have demonstrated our effect to be specific, and not due to depletion of contaminating inflammatory cells. This data implies that platelet dysfunction in HUS and other diseases may be due to a direct response to bacterial LPS. In agreement with previous data, Stx2 incubation demonstrated no effect on platelet reactivity in response to ADP or thrombin, with or without the additional presence of LPS (data not shown).

Discussion

This work demonstrates that at least in some cases, LPS can participate in activating human platelets. This conclusion is justified by a report demonstrating that STEC O157 LPS binds to platelets in HUS patients, and that LPS mediated platelet exposure of

adhesion molecules occurs *in vitro*⁵²². These data should encourage further research into the role of circulating LPS in causing direct platelet changes in HUS.

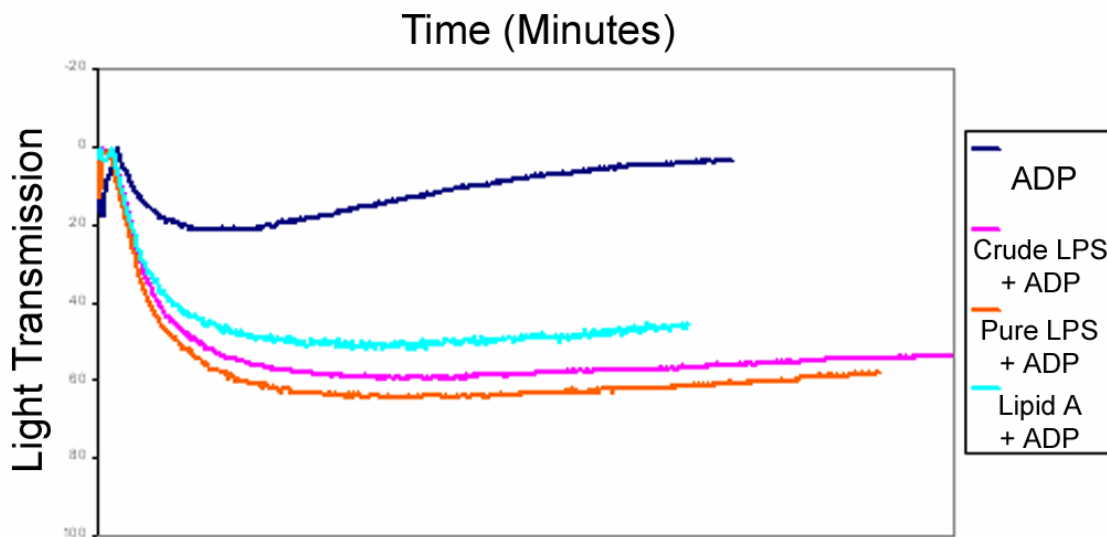


Figure 31. Aggregometry of platelets incubated with LPS and ADP.

Platelet aggregometry after treatment with ADP and either no co-treatment, crude LPS preparation, purified LPS, or isolated Lipid A. *Figure in collaboration with M. Marcinkiewicz.*

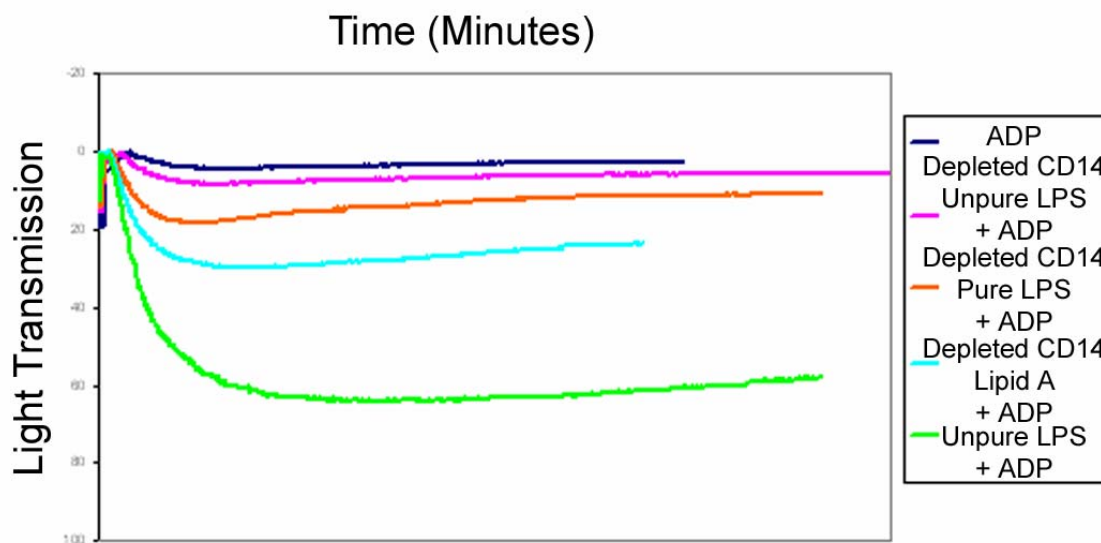


Figure 32. Aggregometry of platelets incubated with LPS and ADP without CD14.

Platelet aggregometry after treatment with ADP and with antibody mediated depletion of CD14 and either no co-treatment, crude LPS preparation, purified LPS, or isolated Lipid A.

A. Figure in collaboration with M. Marcinkiewicz.

Appendix II: The Role of Cyr61 in Stx2 Mediated Cell Death

Background

A limited number of murine renal gene transcripts are initially altered after Stx2 challenge (Table 7). These include the *c-jun*, *cyr61*, *atf-3*, *btg-2*, and *gdf15*. ATF-3 is an immediate early transcriptional repressor induced in response to stress by NF- κ B, JNK signaling, LPS induced TLR signaling, and the unfolded protein response⁵²³⁻⁵²⁶.

ATF-3 (activating transcription factor 3) regulates the cellular response to toxins and stress, and can determine whether apoptosis and inflammation result from cell insult^{523-525,527}. ATF-3 knockout mice and cells demonstrate significantly increased inflammation and apoptosis in response to tissue damage⁵²⁵.

GDF-15 (growth differentiation factor 15) is a secreted autocrine and endocrine factor that can be induced by both TNF- α and p53 dependent and independent pathways^{528,529}. GDF-15 is induced following many types of tissue injury, and is an early mediator of injury response in a variety of tissues, however the particular response to its expression is cell type dependent⁵³⁰⁻⁵³². Unfortunately, GDF-15 knockout mice behave identically to wild type mice after liver injury even though it is highly upregulated during that injury, suggesting that its role in injury response is redundant⁵³³.

Jun is an oncogenic transcription factor that controls target gene transcription by homodimerization and heterodimerization with c-Fos, these dimers are called AP-1^{534,535}. Jun is regulated by JNK and glycogen synthase kinase 3 (GSK-3), and AP-1 dimers control the transcription of numerous factors involved in proliferation, differentiation and apoptosis^{534,535}.

Btg-2 (B-cell translocation gene 2) is a molecular target of p53 and protein kinase C (PKC) that controls cell differentiation and cell cycle progression as an intracellular adaptor molecule⁵³⁶⁻⁵³⁸. Btg-2 knockout mice exhibit vertebral patterning defects likely through Btg-2 interaction with bone morphogenic proteins (BMP)⁵³⁷. Btg-2 mediates cell cycle arrest at G2/M, and can induce apoptosis when overexpressed⁵³⁹.

Cysteine rich protein 61 (Cyr61, CCN1) is a secreted extracellular matrix associated protein that has been demonstrated to influence diverse cellular actions, including adhesion, migration, mitogenesis, differentiation, angiogenesis, tumorigenesis, wound healing and survival⁵⁴⁰⁻⁵⁴³. The pro-angiogenic and pro-repair protein Cyr61 mediates signals between the extracellular matrix and various cell types by binding to multiple varieties of integrins. 42 kDa Cyr61 is secreted by epithelial, endothelial and mesenchymal cell types, and seems to be able to direct responses in any cell type with appropriate integrin expression. Cyr61 can mediate adhesion of multiple cell types to culture plates. Initially discovered to allow HUVEC and 3T3 cell attachment to culture dishes and fibronectin, it also permits attachment by fibroblasts and human platelets⁵⁴³. Platelets however only adhere when activated⁵²².

The CCN family of genes are upregulated by growth factors and other stimuli in an immediate-early time course, meaning they are among the genes rapidly upregulated (within 30 minutes) without additional protein synthesis⁵⁴⁴. Expression of *cyr61* and other immediate early genes have been previously discovered to be modulated by protein synthesis inhibition. Although the half-life of *cyr61* mRNA is only 10-20 minutes, degradation of the mRNA is blocked by the protein synthesis inhibitor cycloheximide⁵⁴⁵. Cyr61 expression is cell cycle dependent. Transcriptional upregulation occurs at the

transition of G0 to G1 phase, and during logarithmic growth *cyr61* levels are maintained at a consistent level¹⁸⁷.

Methods

Microarray Analysis

Microarray samples and analysis were performed as described previously, with four mice per time point per treatment group⁵⁴⁵.

Transfection

The Amaxa Nucleofector 2 (Amaxa, Gaithersburg, MD) was used for electroporation of primary RPTEC (Clonetics) according to the manufacturer's instructions. RPTEC were grown as above. Human IMAGE clone 3454581 (MGC-5081) of full length *Cyr61* cDNA in a pCMV-SPORT6 vector was used to transfect in *cyr61*. pmax-GFP plasmid (Amaxa) was used as a transfection control and evaluated by flow cytometry.

siGENOME SMARTpool siRNA for human *Cyr61* was purchased from Dharmacon (Lafayette, CO). Nucleofector program "U-30" and the Primary Mammalian Epithelial Cell Kit (Amaxa) was used for all experiments. 1 µg of pmax-GFP, 1 µg of pCMV-*Cyr61*-SPORT6, 1.5 µg siRNA were used per reaction. Under these conditions, 66% of the transfected cells died during the procedure, however 90.5% of the remaining cells demonstrated robust GFP expression by flow cytometry (data not shown). siRNA knockdown of *Cyr61* expression was validated by Western Blot as described above, using rabbit anti-*Cyr61* generated by Biosynthesis Incorporated (Lewisville, TX).

Recombinant Cyr61

Recombinant GST-tagged Cyr61 was purchased from Abnova Corporation (Taipei City, Taiwan) and used at a concentration of 1 µg/mL in RPTEC media.

Results

Cyr61 is differentially expressed in the mouse kidney in response to Stx2 and LPS intraperitoneal administration (Figure 26). The earliest genes upregulated by Stx include the growth promoting genes *jun* and *cyr61*, as well as the growth inhibiting gene *btg-2*, the transcriptional repressor *atf-3*, and the apoptotic gene *gdf-15* (*mic-1*, *nag-1*) (Table 7). These genes demonstrate the initiation of both an apoptotic and a repair response in the murine renal tissue in response to Stx2 administration. *cyr61* expression occurs relatively rapidly following intraperitoneal injection: at 8 hours with combination treatment, and 12 hours with Stx alone. Notably *cyr61* also displays an increased effect, both in terms of time of induction and level of induction, in response to LPS plus Stx compared to Stx alone (3-5 fold increase compared to 5-8 fold increase). Compared to the extensive list of other immediate early genes upregulated by LPS and Stx in our model system, including *c-jun*, *c-fos*, *c-myc*, *junB*, *egr-1*, *egr-2*, and the cytokines KC (CXCL1 homolog) and JE (CCL2 homolog)¹¹⁵, *cyr61* expression is specifically induced by Stx and relatively uninduced by LPS alone.

Confluent RPTEC challenged for 24 hours with Stx2 displayed a CD₅₀ of 10 pM Stx2 (Figure 27). These cells were then used to determine if altering the dose of Cyr61

would have an effect on Stx2 mediated cytotoxicity. Transfection mediated siRNA knockdown of RPTEC Cyr61 only slightly synergized with Stx2 induced cytotoxicity (Figure 28), and RPTEC incubation with recombinant Cyr61 at a dose of 1 $\mu\text{g}/\text{mL}$ did not cause any discernable effect either alone or in combination with Stx2 (Figure 29). Finally, transfection with the Cyr61 expressing plasmid also caused increased Stx2 cytotoxicity (Figure 30). Overall, the data is inconclusive, and suggests that Cyr61 does not significantly modulate Stx2 mediated RPTEC cytotoxicity.

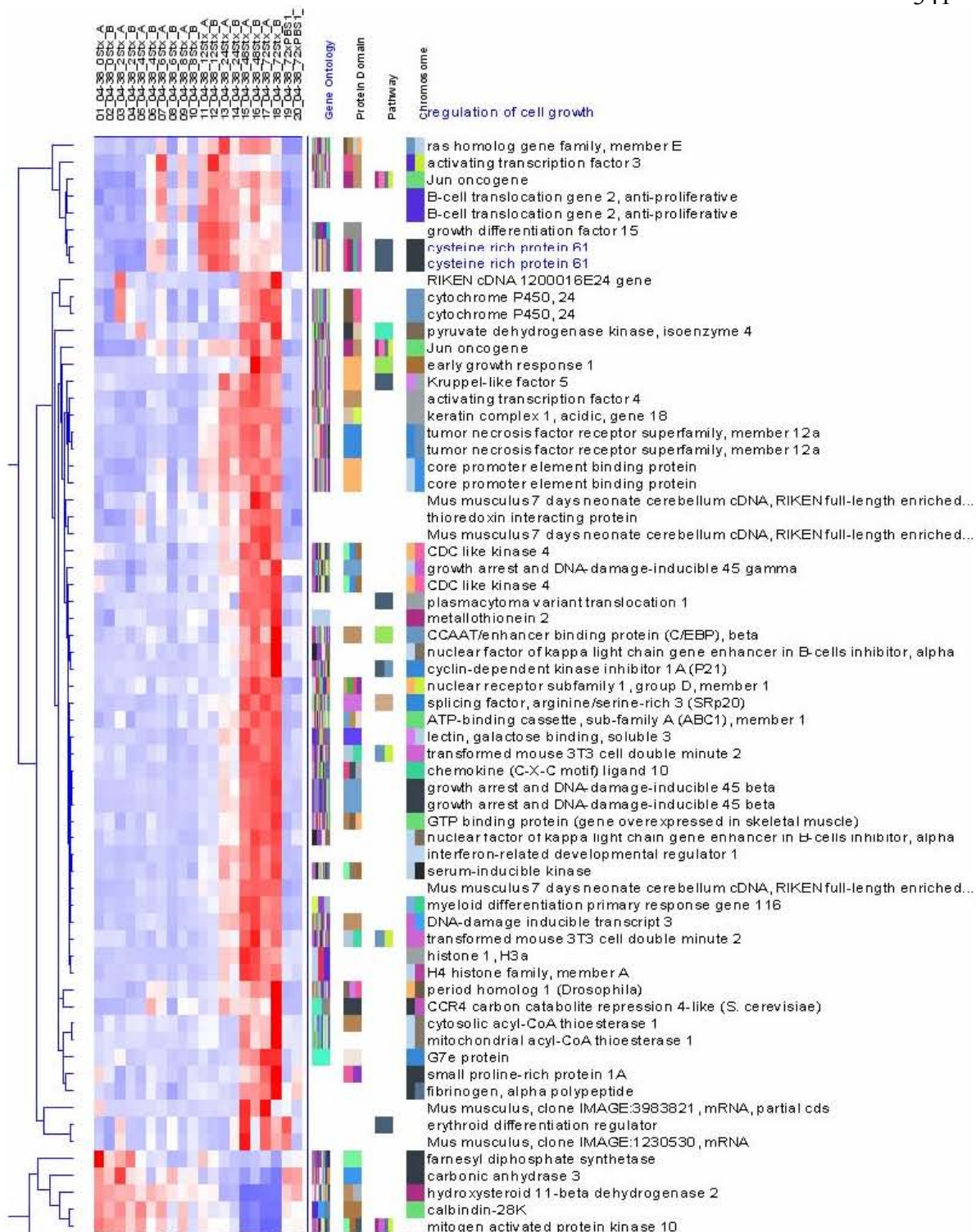


Figure 33. Heatmap of murine renal transcripts altered by Stx2 injection.

Downregulation (blue) and upregulation (red) of transcripts by Stx2 administration.

Gene	Accession	Fold Increase	Function	Ref
activating transcription factor 3 (ATF3)	BC019946	11.3	Transcription repressor, regulator of cellular stress response, inflammation, and apoptosis	523-527
growth differentiation factor 15 (GDF15, MIC1, NAG1)	NM_011819	9.2	Secreted immediate early protein in response to tissue injury	528-533
c-Jun	BC002081	4.3	Transcription activator involved in numerous processes including proliferation, differentiation, and apoptosis	534,535
cysteine rich protein 61 (Cyr61)	BM202770	3.7	Secreted extracellular matrix associated mediator of repair, adhesion, and survival	540-545
B-cell translocation gene 2 (Btg2, PC3, TIS21)	BG965405	3.2	Anti-proliferative apoptotic signaling molecule that controls cell cycle progression	536-539

Table 7. Murine renal transcripts rapidly upregulated by Stx2 challenge.

Murine renal gene transcripts rapidly upregulated by Stx2 challenge. These are the only transcripts significantly upregulated by Stx2 within the first 12 hours post Stx2 administration.

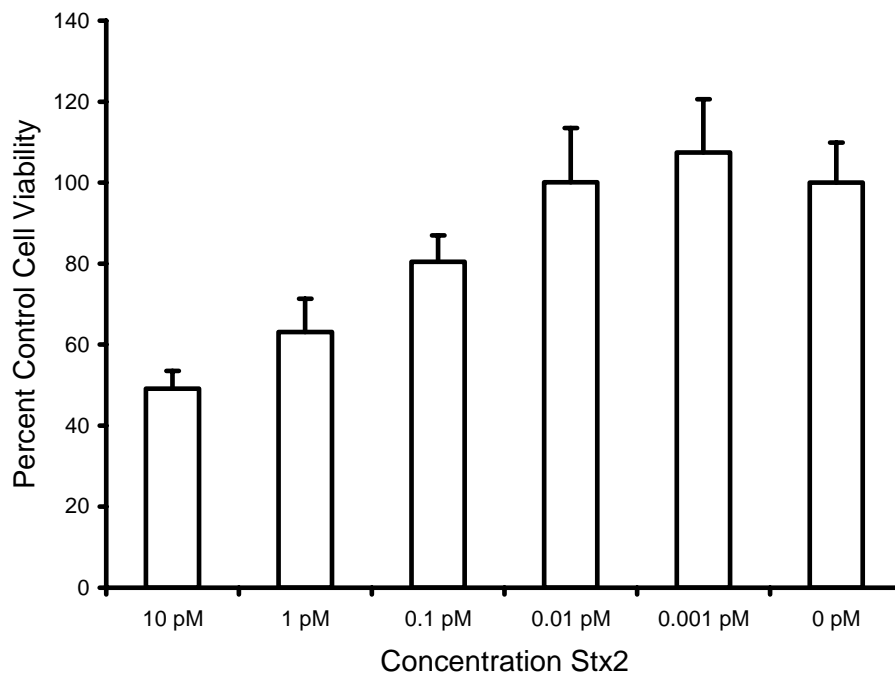


Figure 34. RPTEC 24 hour Stx2 mediated cytotoxicity.

Stx2 24 hour cytotoxicity for primary human RPTEC grown to confluence.

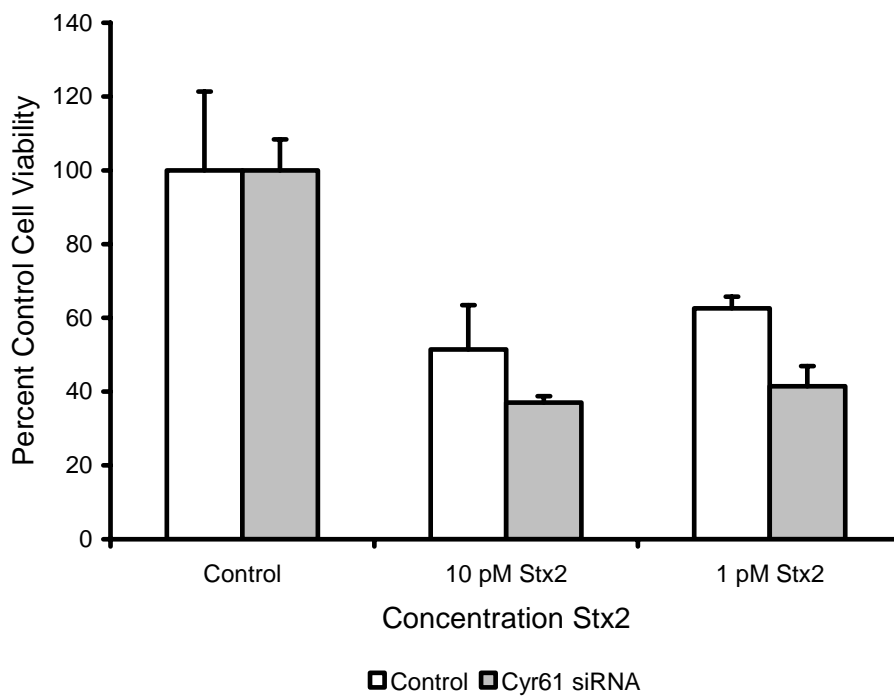


Figure 35. Cyr61 siRNA effect on Stx2 mediated RPTEC cytotoxicity.

Stx2 mediated 24 hour RPTEC cytotoxicity after Cyr61 siRNA administration by electroporation 48 hours prior. Cyr61 siRNA knockdown marginally increased Stx2 mediated cell cytotoxicity.

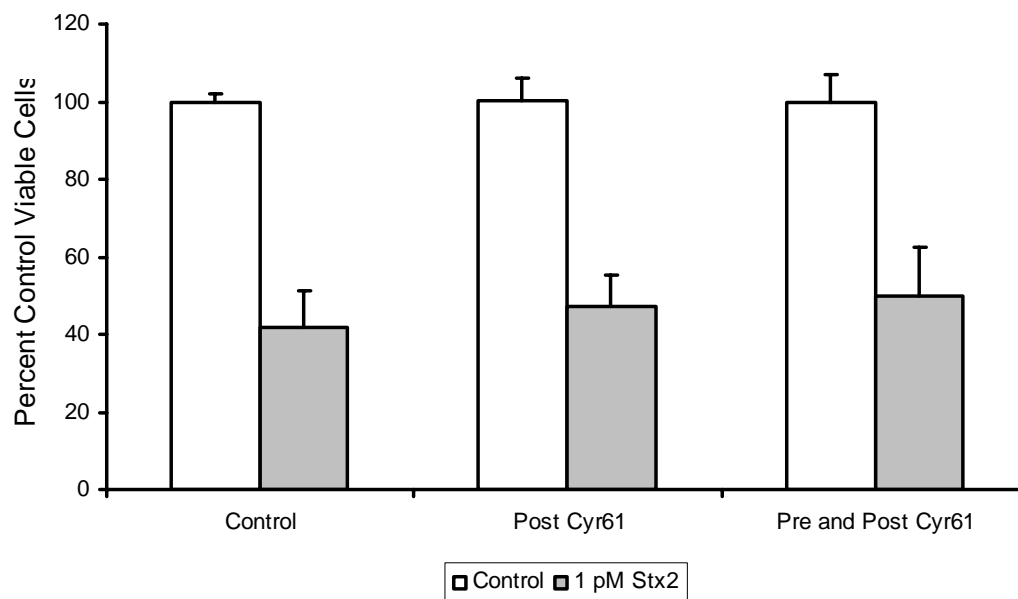


Figure 36. Recombinant Cyr61 effect on Stx2 mediated RPTEC cytotoxicity.

Stx2 mediated cytotoxicity of RPTEC treated with recombinant Cyr61 either concurrent with Stx2 administration (post Cyr61) or treated with Cyr61 prior to and concurrent with Stx2 administration (pre and post Cyr61). Recombinant Cyr61 incubation did not affect Stx2 mediated RPTEC cytotoxicity. Results are representative of quadruplicate experiments.

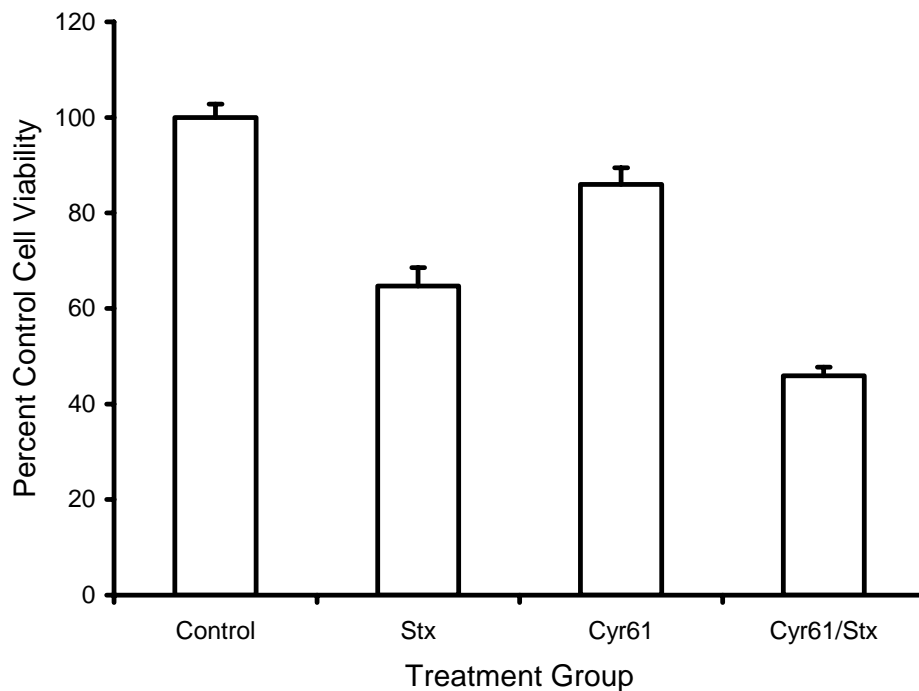


Figure 37. Cyr61 overexpression effect on Stx2 mediated RPTEC cytotoxicity.

1 pM Stx2 24 hour cytotoxicity following electroporation with the Cyr61-expressing pCMV-SPORT6 plasmid. Increased Cyr61 expression did not increase cell viability, and transfection with the plasmid alone caused cell cytotoxicity. Control cells were untreated, Stx cells were incubated with Stx2, Cyr61 cells were transfected with the Cyr61 plasmid, and Cyr61/Stx cells were transfected with the Cyr61 plasmid and 24 hours later incubated with Stx2.

Discussion

Altering the expression levels of Cyr61 in human RPTECs demonstrated no functional effect on Stx2 mediated cytotoxicity. Thus, the role of Cyr61 upregulation in this setting remains undefined. Nevertheless, Cyr61 is becoming a recognized damage marker for the kidney in many experimental and clinical settings^{22,493,494}. It appears that in this way, as a detectable sign of intrinsic renal damage, the increase in Cyr61 mRNA in response to Stx2 challenge expresses the time course of damage in the murine kidney.

Appendix III: The Role of p38 and JNK MAP Kinases in Stx2 Mediated

Apoptosis

Background

JNK and p38 MAP kinases are activated in some cell types in response to Shiga toxin⁵⁴⁶. Small molecule inhibitors for these MAPK pathways can be used to inhibit their activity and determine the roles of p38 and JNK in Stx2 induced cell death.

Methods

The JNK inhibitor SP600125 and the p38 inhibitor SB203580 were purchased from EMD Biosciences (La Jolla, CA). SP600125 was resuspended in 100% DMSO and diluted in media. SB203580 hydrochloride was resuspended in sterile pyrogen free water and diluted in media. Inhibitors were incubated with differentiated human glomerular endothelial cells and podocytes for 1 hour prior to challenge with Stx2.

Results

Each inhibitor alone rescued 10-20% of the Stx2 cytotoxicity in the human glomerular endothelial cells (Figures 31 and 32), however they were not able to completely rescue the cell death, even in combination (data not shown). This data suggests that both JNK and p38 are involved in Stx2 mediated glomerular endothelial cell death, however other signaling pathways are also utilized. In contrast, neither inhibitor provided any rescue from Stx2 induced cell death in the human glomerular podocytes (Figures 33 and 34), even in combination (data not shown). Nevertheless, neither inhibitor is completely

specific for these signaling pathways, and less broad inhibition is needed to clarify the roles of p38 and JNK in Stx2 mediated human glomerular cell death¹¹⁵.

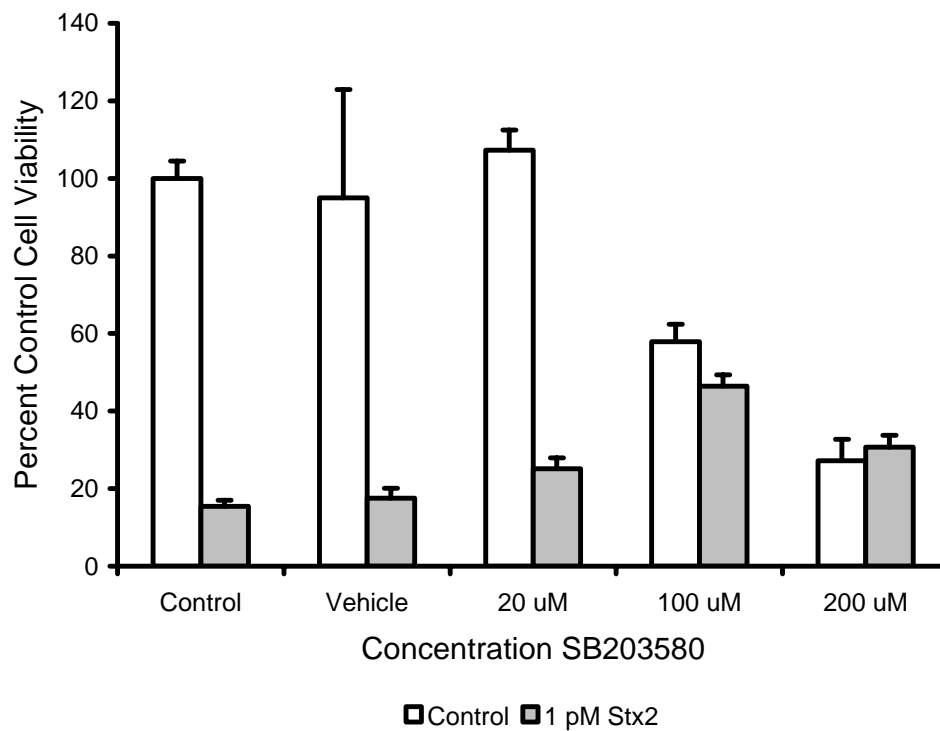


Figure 38. Effect of p38 inhibition on glomerular endothelial cytotoxicity.

Stx2 24 hour human glomerular endothelial cytotoxicity in the presence of the p38 inhibitor SB203580. p38 inhibition in this assay does not block Stx2 cytotoxicity.

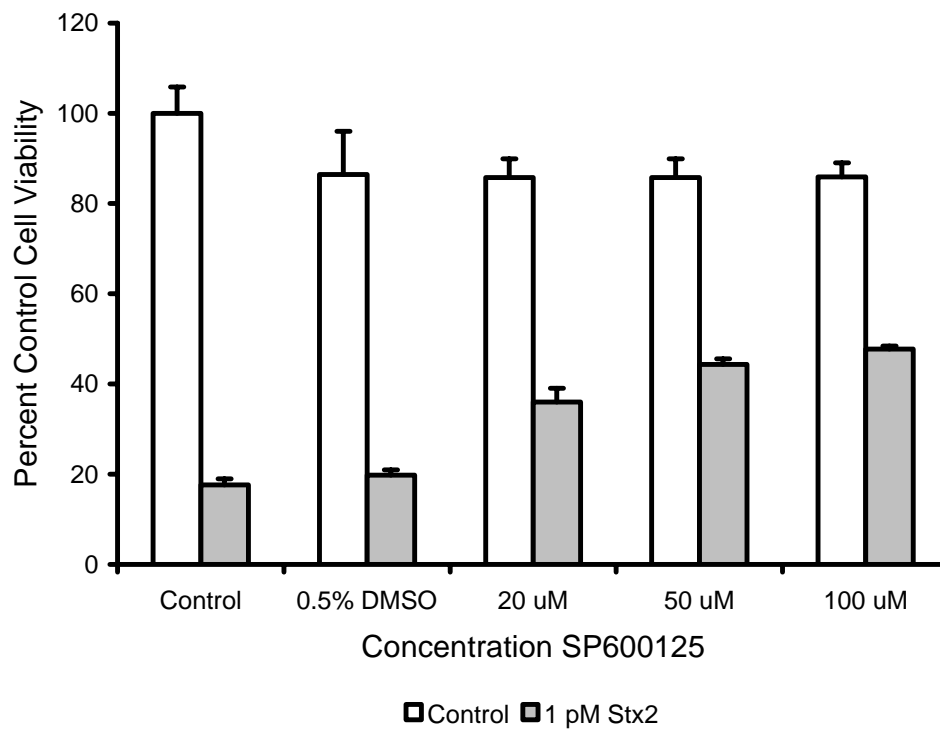


Figure 39. Effect of JNK inhibition on glomerular endothelial cytotoxicity.

Stx2 24 hour human glomerular endothelial cytotoxicity in the presence of the JNK inhibitor SP600125. JNK inhibition in this assay partially blocks Stx2 cytotoxicity, though it also causes some independent direct cytotoxicity.

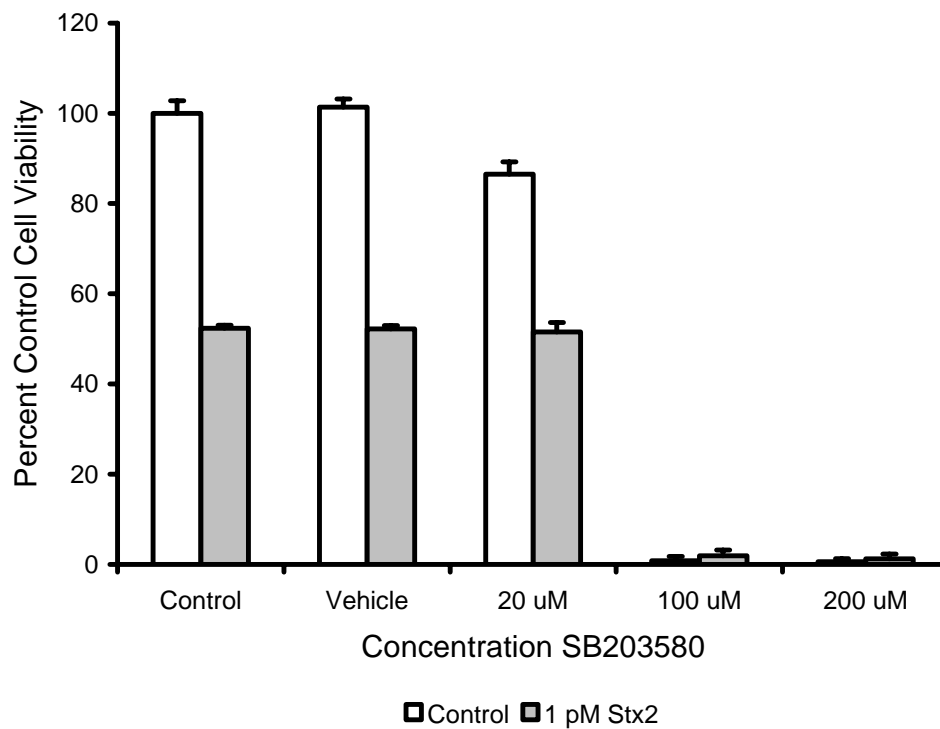


Figure 40. Effect of p38 inhibition on glomerular podocyte cytotoxicity.

Stx2 24 hour human glomerular podocyte cytotoxicity in the presence of the p38 inhibitor SB203580. p38 inhibition in this assay does not block Stx2 cytotoxicity without causing independent cytotoxicity.

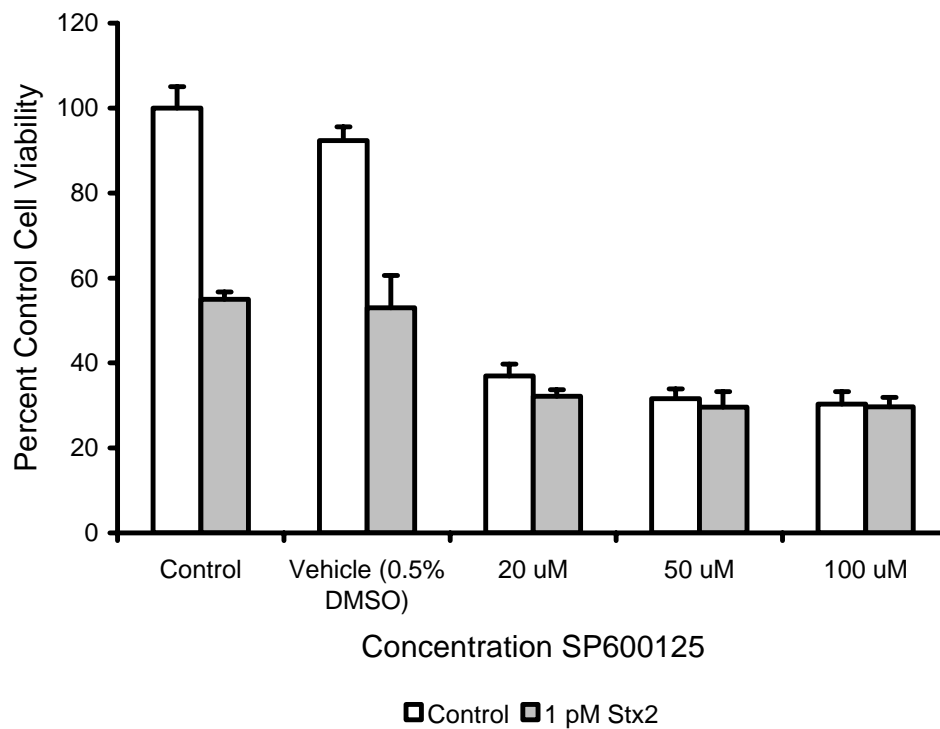


Figure 41. Effect of JNK inhibition on glomerular podocyte cytotoxicity.

Stx2 24 hour human glomerular podocyte cytotoxicity in the presence of the JNK inhibitor SP600125. JNK inhibition in this assay does not block Stx2 cytotoxicity, and it causes some independent direct cytotoxicity.

Appendix IV: The Therapeutic Role of p38 and JNK MAP Kinase Inhibitors SB203580 and SP600125 in the Mouse Model of HUS

Background

JNK and p38 MAP kinases are activated in some cell types in response to Shiga toxin¹⁸⁷. Small molecule inhibitors for these MAPK pathways can be used to inhibit their activity and determine the roles of p38 and JNK in Stx2 plus LPS induced murine death⁴³⁷. In a ricin mediated model of rat HUS, the p38 MAPK inhibitor FR167652 reduced serum cytokine levels, renal failure, and microangiopathy induced by intravenous ricin administration¹⁸⁷. If effective, these p38 inhibiting compounds may be useful as therapeutics for human HUS.

Methods

The JNK inhibitor SP600125 and the p38 inhibitor SB203580 were purchased from EMD Biosciences (La Jolla, CA). SP600125 was resuspended in 100% DMSO and diluted to 30% DMSO in water. SB203580 hydrochloride was resuspended in sterile pyrogen free water. Mice were injected with Stx2 and LPS as previously described. Mice were pretreated with the inhibitors for 24 hours prior to the administration of Stx2 plus LPS, and given 9 mg/kg SB203580 every 24 hours and 15 mg/kg SP600125 every 12 hours. Injections were 100 μ L total volume for each inhibitor.

Results

Neither inhibitor alone or in combination had any effect on the lethality observed following Stx2 plus LPS administration to the mice (Figures 35, 36, and 37).

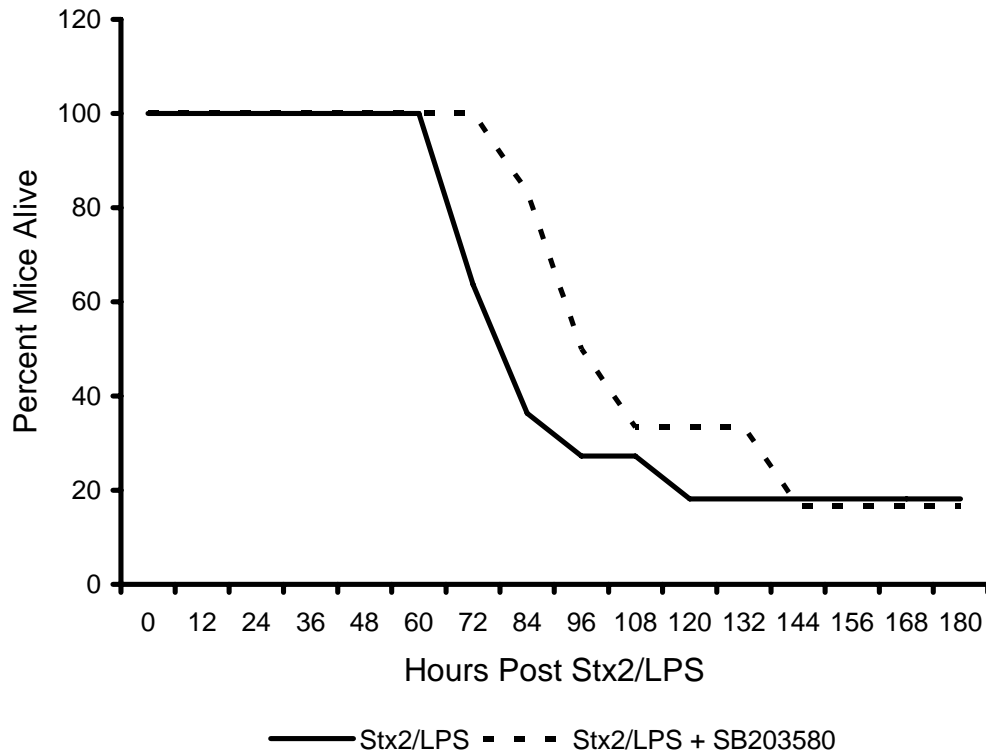


Figure 42. Effect of p38 inhibition on Stx2 plus LPS mouse lethality.

Stx2 plus LPS induced murine lethality with co-administration of 9 mg/kg/day SB203580. Very little difference in timing, and no difference in overall lethality was observed compared to water control.

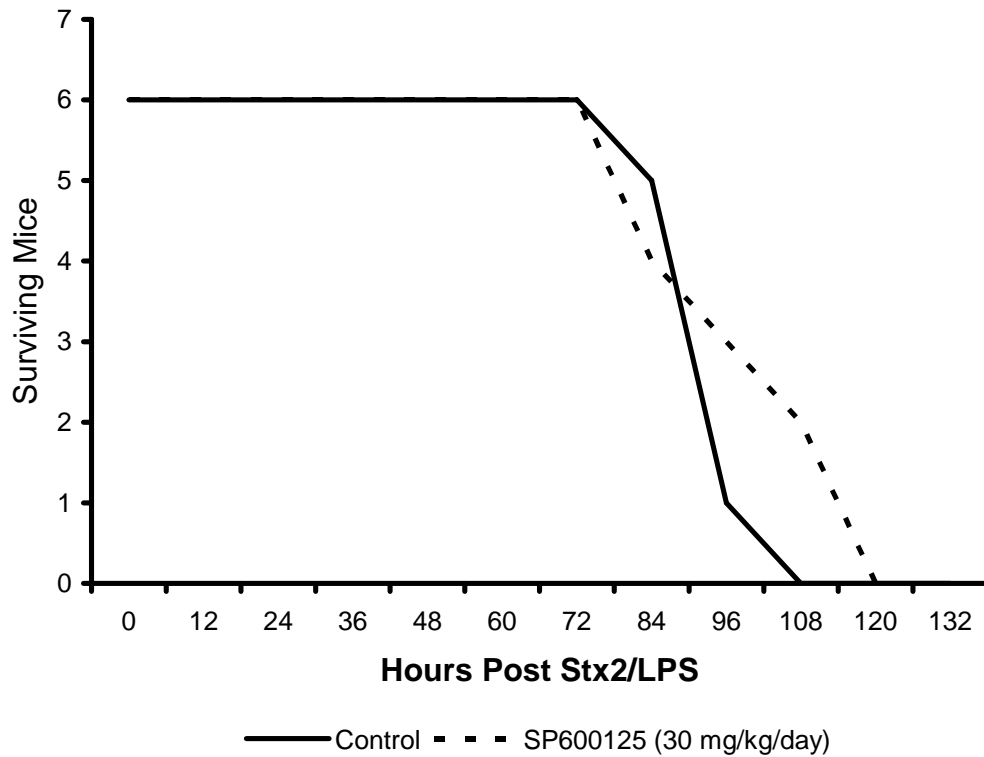


Figure 43. Effect of JNK inhibition on Stx2 plus LPS mouse lethality.

Stx2 plus LPS induced murine lethality with co-administration of 30 mg/kg/day SP600125. Very little difference in timing, and no difference in overall lethality was observed compared to DMSO control.

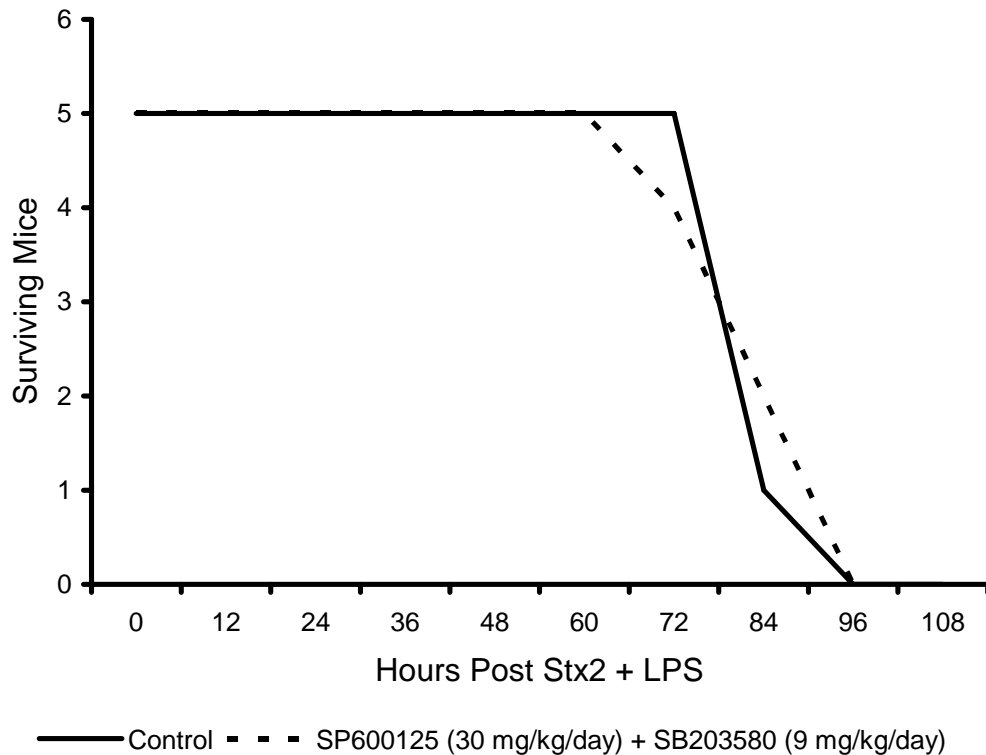


Figure 44. Effect of p38 and JNK inhibition on Stx2 plus LPS mouse lethality.

Stx2 plus LPS induced murine lethality with co-administration of 30 mg/kg/day SP600125 and 9 mg/kg/day SB203580. Very little difference in time to death, and no difference in overall lethality was observed compared to DMSO and water controls.

The End